frontiers | Research Topics

Resistance to third-generation tetracyclines

Edited by
Eun-Jeong Yoon, Seok Hoon Jeong and Rustam Aminov

Published in
Frontiers in Microbiology

ISSN 1664-8714
ISBN 978-2-83251-467-2
DOI 10.3389/978-2-83251-467-2

About Frontiers

Frontiers is more than just an open access publisher of scholarly articles: it is a pioneering approach to the world of academia, radically improving the way scholarly research is managed. The grand vision of Frontiers is a world where all people have an equal opportunity to seek, share and generate knowledge. Frontiers provides immediate and permanent online open access to all its publications, but this alone is not enough to realize our grand goals.

Frontiers journal series

The Frontiers journal series is a multi-tier and interdisciplinary set of open-access, online journals, promising a paradigm shift from the current review, selection and dissemination processes in academic publishing. All Frontiers journals are driven by researchers for researchers; therefore, they constitute a service to the scholarly community. At the same time, the *Frontiers journal series* operates on a revolutionary invention, the tiered publishing system, initially addressing specific communities of scholars, and gradually climbing up to broader public understanding, thus serving the interests of the lay society, too.

Dedication to quality

Each Frontiers article is a landmark of the highest quality, thanks to genuinely collaborative interactions between authors and review editors, who include some of the world's best academicians. Research must be certified by peers before entering a stream of knowledge that may eventually reach the public - and shape society; therefore, Frontiers only applies the most rigorous and unbiased reviews. Frontiers revolutionizes research publishing by freely delivering the most outstanding research, evaluated with no bias from both the academic and social point of view. By applying the most advanced information technologies, Frontiers is catapulting scholarly publishing into a new generation.

What are Frontiers Research Topics?

Frontiers Research Topics are very popular trademarks of the *Frontiers journals series*: they are collections of at least ten articles, all centered on a particular subject. With their unique mix of varied contributions from Original Research to Review Articles, Frontiers Research Topics unify the most influential researchers, the latest key findings and historical advances in a hot research area.

Find out more on how to host your own Frontiers Research Topic or contribute to one as an author by contacting the Frontiers editorial office: frontiersin.org/about/contact

Resistance to third-generation tetracyclines

Topic editors

Eun-Jeong Yoon — Division of Antimicrobial Resistance, Center for Infectious Disease Research, Korea National Institute of Health, Republic of Korea

Seok Hoon Jeong — Yonsei University, Republic of Korea

Rustam Aminov — University of Aberdeen, United Kingdom

Citation

Yoon, E.-J., Jeong, S. H., Aminov, R., eds. (2023). *Resistance to third-generation tetracyclines*. Lausanne: Frontiers Media SA. doi: 10.3389/978-2-83251-467-2

Table of contents

frontiers | Frontiers in Microbiology

TYPE Editorial
PUBLISHED 12 January 2023
DOI 10.3389/fmicb.2022.1114660

OPEN ACCESS

EDITED AND REVIEWED BY
Chang-Wei Lei,
Sichuan University, China

*CORRESPONDENCE
Rustam Aminov
✉ rustam.aminov@abdn.ac.uk

SPECIALTY SECTION
This article was submitted to Antimicrobials, Resistance and Chemotherapy, a section of the journal Frontiers in Microbiology

RECEIVED 02 December 2022
ACCEPTED 29 December 2022
PUBLISHED 12 January 2023

CITATION
Yoon E-J, Jeong SH and Aminov R (2023) Editorial: Resistance to third-generation tetracyclines. *Front. Microbiol.* 13:1114660. doi: 10.3389/fmicb.2022.1114660

Editorial: Resistance to third-generation tetracyclines

Eun-Jeong Yoon[1,2], Seok Hoon Jeong[2] and Rustam Aminov[3]*

[1]Korea National Institute of Health, Korea Disease Control and Prevention Agency, Cheongju-si, Republic of Korea, [2]Department of Laboratory Medicine, Research Institute of Bacterial Resistance, Yonsei University College of Medicine, Seoul, Republic of Korea, [3]The School of Medicine, Medical Sciences and Nutrition, University of Aberdeen, Aberdeen, United Kingdom

KEYWORDS

third-generation tetracyclines, glycylcyclines, fluorocyclines, animals, environment, One Health

Editorial on the Research Topic
Resistance to third-generation tetracyclines

Discovery and development of many antimicrobials have followed the common route that begins from the isolation and characterization of an antimicrobial agent from a natural source, and then the original molecule is modified through several iterations to broaden the spectrum of pathogens targeted, improve its pharmacokinetic and pharmacodynamic properties, and, most importantly, to overcome bacterial antimicrobial resistance (AMR), which inevitably emerges and propagates among bacterial pathogens (Aminov, 2017). In this respect, the tetracycline family of antimicrobials is not an exception. The first natural tetracyclines were discovered in the 1940s and shortly thereafter introduced into the clinical and agricultural practices. They demonstrated excellent efficacy against a broad range of bacterial pathogens, with little side effects, and thus were widely used in human and veterinary medicine as well as in many areas of agriculture for metaphylaxis and growth-promoting purposes. The growing resistance problem, however, prompted the development of the second generation tetracyclines such as doxycycline and minocycline in the 1960s. Once again, their efficacy was compromised by bacterial resistance and the development of the third-generation of tetracyclines (3GT), glycylcyclines and fluorocyclines, was commenced in the late 1990s. The currently available drugs of this generation include glycylcycline, eravacycline, omadacycline, and sarecycline, which were approved in the mid-2000 to the late 2010s.

In the beginning of the antimicrobial era, there have been almost no monitoring efforts directed at detection and analysis of AMR. Thus, we have a very limited understanding of the processes in the past that led to the acquisition and spread of resistance to "older" antimicrobials. The introduction of novel antimicrobials such as the 3GT offers unique opportunities in this regard and may allow to discern the mechanisms by which bacteria become resistant. Besides, developments in genomics and metagenomics allow rapid and large-scale analyses of bacterial samples of various origin carrying suspected AMR genes and mobile genetic elements (MGEs) associated with them. Concerning resistance toward 3GT, the (meta)genomic data available at the time suggested that one of the most likely mechanism of resistance to emerge could be *via* the acquisition and dissemination of *tet*(X) genes, which encode flavin-containing monooxygenases that are capable of degrading 3GT (Aminov, 2009, 2013). One of the contributing factors to this process could be the use of "older" tetracyclines in agriculture, which selects for *tet*(X) as well (Aminov, 2021).

Indeed, as demonstrated by papers in this Research Topic, microbiota from agricultural settings display a range of the *tet*(X) genes that are located on MGEs such as plasmids. Wang J. et al. isolated 49 *Escherichia coli* strains from pigs, and six of them were resistantt toward tigecycline. The resistance was encoded by the *tet*(X4) gene, which was located on a IncFIA18/IncFIB(K)/IncX1 hybrid plasmid. The *tet*(X4)-carrying *E. coli* ST761 lineage seems frequent in different areas in China, with a high risk of further

dissemination. As demonstrated by Li et al., Enterobacterales (*Citrobacter* spp., *E. coli*, *Enterobacter hormaechei*, and *Providencia alcalifaciens*) and *Acinetobacter* spp. (*A. variabilis*, *A. lwoffii*, and *A. baumannii)* isolates from chicken farms also carry a range of the *tet*(X) genes, with the dominance of *tet*(X4). Within the extended One Health framework, Chen et al. analyzed plasmid-encoded diversity of the *tet*(X) genes in *Acinetobacter* spp. isolates of different origin, ranging from humans to agricultural animals to migratory birds and the environment. GR31 group of plasmids, which carried different variants of *tet*(X), seems to be prevalent among *Acinetobacter* spp. isolates. Thus, within the One Health context, the extensive diversity of mobile *tet*(X) variants in different ecological compartments should be considered as a risk factor and measures have to be taken to reduce this risk.

Implementation of potential risk-reduction strategies, however, requires a better understanding of underlying biological processes that drive the selection and maintenance of resistance to 3GT. The most obvious factor is the selection of resistance to 3GT by "older" tetracyclines (Aminov, 2021). Once selected, however, the fitness cost of carrying a *tet*(X)-containing IncFII plasmid by a bacterial host could be substantial (Xiao et al.). Location of *tet*(X) on other plasmids may ameliorate this cost though. For example, the mechanism of stable maintenance of the *tet*(X) genes in bacterial populations could be aided by their location on IncX1 plasmids, since these plasmids encode a histone-like nucleoid-structuring protein, which reduces the fitness cost of plasmid carriage by bacterial hosts and contributes to the stable plasmid inheritance (Cai et al.).

Other mechanisms of resistance toward 3GT are present in clinical isolates, and these are mainly mediated by efflux pumps. As demonstrated by Hao et al., the drug efflux mechanism is implicated in tigecycline resistance in a clinical *Klebsiella pneumoniae* isolate. Wang Y. et al. established that in other species of *Klebsiella* such as *K. variicola*, *K. quasipneumoniae* and *K. michiganensis*, resistance to tygecycline is mediated by resistance-nodulation-division- (RND) type efflux pumps (TMexCD2-TOprJ2 clusters) and these are located on IncHI1B type plasmids. The RND-type efflux pump-mediated tigecycline resistance also operates in *A. pittii* (Ding et al.). In *Staphylococcus aureus* isolates, resistance to 3GT is mainly conferredby mutations in the genes encoding MepRAB efflux pumps and 30S ribosomal subunits, while overexpression of other efflux pump genes such as *tet*(38), *tet*(K) and *tet*(L) is also noted in several tigecycline-resistant strains (Zeng et al.). Thus the current mechanisms of resistance to 3GT in clinical isolates is *via* the mutations that up-regulate the expression of efflux pumps. These mechanisms are presumably generated during the therapy, and they are species-specific, which makes the dissemination to various pathogens unlikely.

Presently, plasmid-encoded *tet*(X) and especially the *tet*(X4) variant are widely distributed in various ecological compartments in China as demonstrated by papers in this Research Topic as well as by publications elsewhere (Sun et al., 2019; Li et al., 2021; Feng et al., 2022; Zhang et al., 2022). Geographical boundaries for plasmid-encoded *tet*(X4) seems to be expanding with its detection in Pakistan (Mohsin et al., 2021) and Turkey (Kürekci et al., 2022). Moreover, plasmid-encoded *tet*(X4) seems to be emerging in clinical settings (Zhai et al., 2022). These concerning developments may pose a significant risk for public health and must be dealt with promptly.

Author contributions

All authors listed have made a substantial, direct, and intellectual contribution to the work and approved it for publication.

Conflict of interest

The authors declare that the research was conducted in the absence of any commercial or financial relationships that could be construed as a potential conflict of interest.

Publisher's note

All claims expressed in this article are solely those of the authors and do not necessarily represent those of their affiliated organizations, or those of the publisher, the editors and the reviewers. Any product that may be evaluated in this article, or claim that may be made by its manufacturer, is not guaranteed or endorsed by the publisher.

References

Aminov, R. (2017). History of antimicrobial drug discovery: major classes and health impact. *Biochem. Pharmacol.* 133, 4–19. doi: 10.1016/j.bcp.2016.10.001

Aminov, R. (2021). Acquisition and spread of antimicrobial resistance: a *tet*(X) case study. *Int. J. Mol. Sci.* 22, 3905. doi: 10.3390/ijms22083905

Aminov, R. I. (2009). The role of antibiotics and antibiotic resistance in nature. *Environ. Microbiol.* 11, 2970–2988. doi: 10.1111/j.1462-2920.2009.01972.x

Aminov, R. I. (2013). Evolution in action: dissemination of *tet*(X) into pathogenic microbiota. *Front. Microbiol.* 4, 192. doi: 10.3389/fmicb.2013.00192

Feng, J., Su, M., Li, K., Ma, J., Li, R., Bai, L., et al. (2022). Extensive spread of *tet*(X4) in multidrug-resistant *Escherichia coli* of animal origin in western China. *Vet. Microbiol.* 269, 109420. doi: 10.1016/j.vetmic.2022.109420

Kürekci, C., Lu, X., Celil, B. G., Disli, H. B., Mohsin, M., Wang, Z., et al. (2022). Emergence and characterization of tigecycline resistance gene *tet*(X4) in ST609 *Escherichia coli* isolates from wastewater in Turkey. *Microbiol. Spectr.* 10, e0073222. doi: 10.1128/spectrum.00732-22

Li, R., Li, Y., Peng, K., Yin, Y., Liu, Y., He, T., et al. (2021). comprehensive genomic investigation of tigecycline resistance gene *tet*(X4)-bearing strains expanding among different settings. *Microbiol. Spectr.* 9, e0163321. doi: 10.1128/spectrum.01633-21

Mohsin, M., Hassan, B., Martins, W. M. B. S., Li, R., Abdullah, S., Sands, K., et al. (2021). Emergence of plasmid-mediated tigecycline resistance *tet*(X4) gene in *Escherichia coli* isolated from poultry, food and the environment in South Asia. *Sci. Total Environ.* 787, 147613. doi: 10.1016/j.scitotenv.2021.147613

Sun, J., Chen, C., Cui, C. Y., Zhang, Y., Liu, X., Cui, Z. H., et al. (2019). Plasmid-encoded *tet*(X) genes that confer high-level tigecycline resistance in *Escherichia coli*. *Nat. Microbiol.* 4, 1457–1464. doi: 10.1038/s41564-019-0496-4

Zhai, W., Tian, Y., Lu, M., Zhang, M., Song, H., Fu, Y., et al. (2022). Presence of mobile tigecycline resistance gene *tet*(X4) in clinical *Klebsiella pneumoniae*. *Microbiol. Spectr.* 10, e0108121. doi: 10.1128/spectrum.01081-21

Zhang, S., Wen, J., Wang, Y., Wang, M., Jia, R., Chen, S., et al. (2022). Dissemination and prevalence of plasmid-mediated high-level tigecycline resistance gene *tet*(X4). *Front. Microbiol.* 13, 969769. doi: 10.3389/fmicb.2022.969769

frontiers in Microbiology

ORIGINAL RESEARCH
published: 06 October 2021
doi: 10.3389/fmicb.2021.759208

Characterization of IncHI1B Plasmids Encoding Efflux Pump *TmexCD2-ToprJ2* in Carbapenem-Resistant *Klebsiella variicola*, *Klebsiella quasipneumoniae*, and *Klebsiella michiganensis* Strains

Yujiao Wang[1†], Bo Zhu[2†], Min Liu[3†], Xiutao Dong[1], Jianping Ma[1], Xiaofeng Li[1], Fang Cheng[1], Jianzhuang Guo[1], Sumei Lu[1], Furong Wan[1], Yingying Hao[4], Wanshan Ma[1], Mingju Hao[1]* and Liang Chen[5,6]*

[1]Department of Clinical Laboratory Medicine, The First Affiliated Hospital of Shandong First Medical University & Shandong Provincial Qianfoshan Hospital, Shandong Medicine and Health Key Laboratory of Laboratory Medicine, Jinan, China, [2]Xiamen Key Laboratory of Genetic Testing, Department of Laboratory Medicine, The First Affiliated Hospital of Xiamen University, Xiamen, China, [3]Department of Clinical Laboratory, Jinan Dermatosis Prevention and Control Hospital, Jinan, China, [4]Department of Clinical Laboratory, Shandong Provincial Hospital Affiliated to Shandong First Medical University, Jinan, China, [5]Center for Discovery and Innovation, Hackensack Meridian Health, Nutley, NJ, United States, [6]Department of Medical Sciences, Hackensack Meridian School of Medicine, Nutley, NJ, United States

OPEN ACCESS

Edited by:
Seok Hoon Jeong,
Yonsei University, South Korea

Reviewed by:
Martijn Zwama,
Osaka University, Japan
Dokyun Kim,
Gangnam Severance Hospital, South Korea
Catherine Llanes,
University of Franche-Comté, France

***Correspondence:**
Mingju Hao
haomingju@163.com
Wanshan Ma
ws_ma@126.com

[†]These authors have contributed equally to this work

Specialty section:
This article was submitted to Antimicrobials, Resistance and Chemotherapy, a section of the journal Frontiers in Microbiology

Received: 16 August 2021
Accepted: 10 September 2021
Published: 06 October 2021

Citation:
Wang Y, Zhu B, Liu M, Dong X, Ma J, Li X, Cheng F, Guo J, Lu S, Wan F, Hao Y, Ma W, Hao M and Chen L (2021) Characterization of IncHI1B Plasmids Encoding Efflux Pump TmexCD2-ToprJ2 in Carbapenem-Resistant Klebsiella variicola, Klebsiella quasipneumoniae, and Klebsiella michiganensis Strains. Front. Microbiol. 12:759208. doi: 10.3389/fmicb.2021.759208

Tigecycline serves as one of the last-resort antibiotics to treat severe infections caused by carbapenem-resistant Enterobacterales. Recently, a novel plasmid-mediated resistance-nodulation-division (RND)-type efflux pump gene cluster, *TmexCD1-ToprJ1*, and its variants, *TmexCD2-ToprJ2* and *TmexCD3-ToprJ3*, encoding tetracyclines and tigecycline resistance, were revealed. In this study, we reported three *TmexCD2-ToprJ2*-harboring *Klebsiella* species strains, collected from two teaching tertiary hospitals in China, including one *K. quasipneumoniae*, one *K. variicola*, and one *K. michiganensis*. The three strains were characterized by antimicrobial susceptibility testing (AST), conjugation assay, WGS, and bioinformatics analysis. AST showed that *K. variicola* and *K. quasipneumoniae* strains were resistant to tigecycline with MIC values of 4 μg/ml, whereas the *K. michiganensis* was susceptible to tigecycline with an MIC value of 1 μg/ml. The *TmexCD2-ToprJ2* clusters were located on three similar IncHI1B plasmids, of which two co-harbored the metallo-β-lactamase gene bla_{NDM-1}. Conjugation experiments showed that all three plasmids were capable of self-transfer *via* conjugation. Our results showed, for the first time, that this novel plasmid-mediated tigecycline resistance mechanism *TmexCD2-ToprJ2* has spread into different *Klebsiella* species, and clinical susceptibility testing may fail to detect. The co-occurrence of bla_{NDM-1} and *TmexCD2-ToprJ2* in the same plasmid is of particular public health concern as the convergence of "mosaic" plasmids can confer both tigecycline and carbapenem resistance. Its further spread into other clinical high-risk *Klebsiella* clones will likely exacerbate the antimicrobial resistance crisis. A close monitoring of the dissemination of *TmexCD-ToprJ* encoding resistance should be considered.

Keywords: *TmexCD2-ToprJ2*, carbapenem resistance, bla_{NDM-1}, bla_{NDM-5}, *Klebsiella variicola*, *Klebsiella quasipneumoniae*, *Klebsiella michiganensis*, tigecycline resistance

INTRODUCTION

Tigecycline is one of the last-resort antibiotics used to treat severe infections caused by carbapenem-resistant Enterobacterales (Cheng et al., 2020). However, increasing studies reported the emergence of tigecycline resistance in clinical settings, which is frequently caused by the overexpression of non-specific active efflux pumps [*tet*(A) and *tet*(K)] or mutations within the drug-binding site in the ribosome [*tet*(M); Grossman, 2016; Linkevicius et al., 2016]. In *Klebsiella pneumoniae*, tigecycline resistance is also frequently associated with the overexpression of *ramA*, which can directly regulate multidrug resistance efflux pumps AcrAB and OqxAB (Ruzin et al., 2005, 2008). These tigecycline resistances are primarily mediated by chromosome-encoding mechanisms thus could not be easily transferred horizontally. The newly emerging mobile tigecycline resistance mechanism is of particular public health concern (He et al., 2019; Lv et al., 2020). The enzymatic modification gene variants [tet(X)] are highly transferable between species (Linkevicius et al., 2016; He et al., 2019; Sun et al., 2019).

Recently, a novel plasmid-mediated resistance-nodulation-division (RND)-type efflux pump gene cluster, *TmexCD1-ToprJ1*, has been identified in *K. pneumoniae* (Lv et al., 2020). This gene cluster was first identified in animal isolates but soon later was also found in clinical isolates (Sun et al., 2020). *TmexCD1-ToprJ1* was initially reported in China, but it has now been found in clinical *K. pneumoniae* isolates outside of China (Hirabayashi et al., 2021), suggesting this resistance has started to spread into other global regions. Two homologous variants, *TmexCD2-ToprJ2* (Wang et al., 2021a) and *TmexCD3-ToprJ3* (Wang et al., 2021b), have also been identified in *Raoultella ornithinolytica* and *Proteus mirabilis*, displaying similar tigecycline resistance profiles. Worrisomely, the mobile tigecycline gene clusters have also been found in clinical carbapenem-resistant *K. pneumoniae* strains (Chiu et al., 2017). Here, we reported the identifications of three clinical *TmexCD2-ToprJ2*-encoding Klebsiella strains, including two carbapenem-resistant strains co-harboring $bla_{\text{VIM-8/NDM-5}}$ or $bla_{\text{NDM-1}}$.

MATERIALS AND METHODS

Bacterial Strains

Klebsiella variicola strain JNQH579 was recovered from a sputum sample of a 64-year male patient in intensive care units (ICUs) at a tertiary hospital in Jinan City, Shandong Province, in March 2021, who had been hospitalized for 17 days due to severe pneumoniae and renal failure. The patient had received tigecycline treatment for 7 days at a dosage of 100 mg (IV) q12h before the isolation of the strain. Based on the antibiotic susceptibility testing results, antibiotic therapy was switched to aztreonam 0.5 g (IV) q8h in combination with tigecycline. The respiratory symptoms improved after antibiotic treatment and the patient continued to be hospitalized for 3 months due to cardiovascular and renal disease. *Klebsiella quasipneumoniae* strain JNQH473 was recovered from a urine sample of a 1-month-old infant with sepsis at a tertiary hospital in Xiamen City, Fujian Province, in August 2019, who was hospitalized at the department of pediatrics for 7 days. During her hospitalization, the neonate received multiple antimicrobial treatments, including cefotaxime, vancomycin, and ceftazidime. The patient was fully recovered after antimicrobial and supportive treatment and was discharged on hospital day 13. *Klebsiella michiganensis* strain JNQH491 was recovered from a blood culture of a 48-year male patient at the department of oncology, who had received chemotherapy due to nasopharyngeal carcinoma in the same hospital as JNQH473. The patient was discharged home after a cycle of chemotherapy on hospital day 11. The overall strain features of the three strains are listed in **Table 1**. All the patients reported no recent travel abroad.

Antibiotic Susceptibility Testing

Antibiotic susceptibility testing (AST) was performed using the VITEK 2 (bioMérieux, Nürtingen, Germany) system. Minimum inhibitory concentrations (MICs) for tigecycline were performed by broth microdilution according to the Clinical and Laboratory Standards Institute (CLSI) guidelines. ATCC 25922 (*Escherichia coli*) and ATCC 27853 (*Pseudomonas aeruginosa*) were used as quality control strains for susceptibility testing. All the tests were performed in duplicate in different days. The breakpoints were interpreted according to CLSI guidelines except for tigecycline, of which the EUCAST epidemiological cutoff value >2 μg/ml (for *K. pneumoniae*) was used.[1]

Whole-Genome Sequencing, Assembly, and Annotation

The combination Oxford Nanopore (MinION system) and Illumina sequencing (NovaSeq) were used to achieve a high-quality genome assembly. First, we derived fastq read

[1]https://eucast.org/clinical_breakpoints/

TABLE 1 | Overall strain features of JNQH473, JNQH491, and JNQH579.

Characteristics	JNQH473	JNQH491	JNQH579
Species	*Klebsiella quasipneumoniae*	*Klebsiella michiganensis*	*Klebsiella variicola*
Isolation location	Xiamen	Xiamen	Jinan
Sector	Department of pediatrics	Department of oncology	Intensive care units
Host disease	Urinary infection, septic	Nasopharyngeal carcinoma	Pneumonia, renal failure
Isolation site	Urine	Blood	Sputum
Antimicrobial treatment before isolation	Cefotaxime, vancomycin, ceftazidime	–	Tigecycline
Collection time	2019.08	2020.08	2021.03
MLST	ST571	ST109	ST2013
K locus	KL64	ND	ND
O locus	O5	ND	OL103

MLST, multilocus sequence typing; K locus, Klebsiella pneumoniae species complex capsule locus; O locus, K. pneumoniae species complex LPS locus; ND, not determined.

sequences from MinION raw electric signal fast5 files using guppy 3.2.2 with the high accuracy flip-flop algorithm. Adapters were trimmed out with Porechop.[2] Low-quality reads were filtered out using trimmomatic 0.38 (Bolger et al., 2014). The filtered nanopore reads were *de novo* assembled with Flye 2.8.3 (Kolmogorov et al., 2019). Then, the obtained assemblies were polished using Nanopore reads by Racon 1.4.3 (1–4 iterations; Vaser et al., 2017). Next, the polished sequences were additionally corrected using Illumina reads by Pilon 1.23 until no changes occur (Walker et al., 2014). The whole-genome sequences were annotated by Prokka (Seemann, 2014) and RAST (Brettin et al., 2015), followed by manually curations.

Genomic Analysis

The *in silico* multilocus sequence typing (MLST) was carried out using MLST v. 2.19.0,[3] and antibiotic resistance/plasmid replicon gene detections were carried out using ABRicate v. 0.9.9[4] using CARD (Jia et al., 2017) and PlasmidFinder (Carattoli et al., 2014) database, respectively. The intrinsic variants of *oqxAB*, chromosomal *ampH* and *fosA*, which confer resistance to quinolones, β-lactams and fosfomycin, respectively, in Enterobacterales rather than *Klebsiella* species, are therefore not reported (Henderson et al., 1997; Lam et al., 2021). Kleborate v. 1.0.0 (Lam et al., 2021) was used for *Klebsiella* K locus and O locus typing. The comparative analysis of *TmexCD2-ToprJ2* harboring plasmids was done by BLASTn and illustrated using CGView Server (Grant and Stothard, 2008). Easyfig (Sullivan et al., 2011) was used to visualize the genetic context comparisons. Selected plasmids were compared with Mauve 2.3.1 (Darling et al., 2010), followed by visualization using genoPlotR (Guy et al., 2010). Plasmid distance trees were generated using Mashtree (Katz et al., 2019). Alignment between three *TmexCD-ToprJ* variants was done by Clustal Omega (Madeira et al., 2019). ISFinder[5] was used to identify ISs. Tn number was identified using Tn Number Registry (Roberts et al., 2008). In order to examine the distribution and relationships of *TmexCD2-ToprJ2* and its variants (*TmexCD1-ToprJ1*, *TmexCD2-ToprJ2*), plasmid sequences were downloaded from NCBI[6] and compared.

Conjugation Experiment

Conjugation experiments were performed by plate mating using *E. coli* J53 (AziR) as the recipient as described in our previous study (Hao et al., 2021). Briefly, overnight cultures of the donor strains and the recipient strain *E. coli* J53 were mixed (1:1) and applied onto an LB agar plate, followed by overnight culture at 37°C. Transconjugants were selected on Mueller-Hinton (MH) agar containing sodium azide (200 μg/ml) and tigecycline (0.5 μg/ml). The presence of *TmexCD2-ToprJ2* and IncHI1B replicons, as well as $bla_{\text{NDM-1}}$ and *sul1* resistance genes in transconjugants, was confirmed by PCR (**Supplementary Table S1**). Conjugation frequency was calculated by dividing the number of transconjugants by the number of recipient cells. AST of the *E. coli* J53 transconjugants was performed as described above.

[2]https://github.com/rrwick/Porechop
[3]https://github.com/tseemann/mlst
[4]https://github.com/tseemann/abricate
[5]https://isfinder.biotoul.fr/
[6]https://ftp.ncbi.nlm.nih.gov/refseq/release/plasmid, latest update on July 15, 2021.

RESULTS

Susceptibility of Three *Klebsiella* Isolates

The MICs for JNQH473, JNQH491, and JNQH579 were shown in **Table 2**. The MICs of tigecycline in JNQH473 and JNQH579 were both 4 μg/ml. However, JNQH491 was susceptible to tigecycline with a MIC value of 1 μg/ml. These strains were resistant to almost all tested β-lactam antibiotics except that JNQH491 and JNQH579 were susceptible to aztreonam. All the strains were susceptible to amikacin with an MIC value of less than 2 μg/ml.

Characterization of Carbapenem-Resistant *Klebsiella variicola* Isolate JNQH473

Strain JNQH473 was classified as sequence type 571 (ST571) based on the *in silico* MLST, and it belonged to KL64 capsule and O5 lipopolysaccharide serotypes (**Table 1**). It harbored a 5.39-Mb chromosome and four plasmids, designated pJNQH473-1 (229.2-Kb), pJNQH473-2 (70.9-Kb), pJNQH473-3 (297.9-Kb), and pJNQH473-4 (46.1-Kb), respectively (**Table 3**). Two metallo-β-lactamase (bla_{MBL}) genes, $bla_{\text{IMP-8}}$ and $bla_{\text{NDM-5}}$, were located on incompatible FIB type plasmid pJNQH473-1 and IncX3 type plasmid pJNQH473-4, respectively. $bla_{\text{IMP-8}}$ was located in class 1 integron In*655* carrying the gene cassette of $bla_{\text{IMP-8}}$-*aacA4* (Jiang et al., 2017), and $bla_{\text{NDM-5}}$ was located in an ΔTn*125*-like region containing ble_{MBL} and IS*26* genes downstream and IS*3000*, IS*30*, and IS*5* family transposase genes upstream. The *TmexCD2-ToprJ2* gene cluster was located on an IncHI1B type plasmid, pJNQH473-3. In addition to *TmexCD2-ToprJ2* genes, nine antimicrobial resistance genes were found on the same plasmid, including two copies of sulfonamide resistance gene *sul1* and single copy of aminoglycoside resistance gene *aac(3)-IId* and *aadA16*, quinolone-resistant gene *qnrS1*, macrolides resistance gene *mphA*, trimethoprim resistance gene *dfrA27*, the β-lactamase gene $bla_{\text{TEM-1D}}$, and rifampicin resistance ribosyltransferase gene *arr-3*.

Characterization of Carbapenem-Resistant *Klebsiella michiganensis* Isolate JNQH491

Strain JNQH491 belonged to ST109 type (**Table 1**). The K and O locus could not be classified according to the currently available K and O loci database. The genome contained a 6.04-Mb chromosome and two plasmids, pJNQH491-1 (205.5-Kb) and pJNQH491-2 (307.4-Kb; **Table 3**). The *TmexCD2-ToprJ2* gene cluster was located on pJNQH491-2, which is an IncHI1B type plasmid, co-harboring multiple resistant genes, including the bla_{MBL} and $bla_{\text{NDM-1}}$ (**Figure 1**). The pJNQH491-1 plasmid had an IncFIB replicon and did not carry any known resistance genes.

TABLE 2 | Minimum inhibitory concentration (MIC) profiles of parental strains and trans-conjugants (μg/ml).

Strains	β-lactams								Aminoglycosides			Quinolones		Tetracycline	Others	
	AMP	AMC	PIPC/TAZ	FOX	CRO	FEP	ATM	ETP	IMP	AK	GEN	TOB	CIP	LEV	TIG	NFT	SMZ/TMP
JNQH473	≥32	≥32	≥128	≥64	≥64	≥64	16	≥8	≥16	≤2	≥16	8	2	1	4	128	≥320
JNQH491	≥32	≥32	≥128	≥64	≥64	16	≤1	≥8	8	≤2	≥16	2	1	1	1	64	≥320
JNQH579	≥32	≥32	≥128	≥64	≥64	≥64	≤1	≥8	≥16	≤2	≤1	8	2	1	4	32	≥320
Escherichia coli J53	8	4	<4	8	≤1	≤1	≤1	≤0.5	≤1	≤2	≤1	≤1	≤0.25	≤0.25	0.125	≤16	≤20
***E. coli* J53 transconjugants**																	
pJNQH473-3	**≥32**	**16**	≤4	**32**	≤1	≤1	≤1	≤0.5	≤1	≤2	**≥16**	≤1	**≥4**	**4**	**1**	≤16	**≥320**
pJNQH491-2	**≥32**	**≥32**	**≥128**	**≥64**	**≥64**	**≥64**	≤1	**≥8**	**≥16**	≤2	**≥16**	≤1	**≥4**	**4**	**1**	≤16	**≥320**
pJNQH579-2	**≥32**	**≥32**	**≥128**	**≥64**	**≥64**	**≥64**	≤1	**≥8**	**≥16**	≤2	≤1	≤1	**≥4**	**4**	**1**	≤16	**≥320**

AMP, ampicillin; AMC, Amoxicillin-clavulanate; PIPC/TAZ, piperacillin/tazobactam; TIG, tigecycline; FOX, cefoxitin; FEP, cefepime; CIP, ciprofloxacin; CRO, ceftriaxone; ATM, aztreonam; IMP, imipenem; ETP, ertapenem; AK, amikacin; TOB, tobramycin; GEN, gentamycin; LEV, levofloxacin; NFT, nitrofurantoin, SMZ/TMP, sulfamethoxazole/trimethoprim. MICs of tigecycline were determined by microdilution and of other antibiotics were performed using VITEK2 system. All tests were performed in duplicate, and each test included three biological replicates. Changed MIC values in the E. coli J53 transconjugants relative to E. coli J53 itself were highlighted in bold.

Characterization of Carbapenem-Resistant *Klebsiella quasipneumoniae* Isolate JNQH579

Strain JNQH579 belonged to ST2013 and harbored an OL103 serotype (**Table 1**). The genome included a 5.58-Mb chromosome and two plasmids, designated pJNQH579-1 (197.4-Kb) and pJNQH579-2 (369.3-Kb), respectively (**Table 3**). The *TmexCD2-ToprJ2* gene cluster was carried by a 34,827 bp mobile region, which was located on pJNQH579-2 plasmid (**Figure 2**). pJNQH579-2 is also an IncHI1B type plasmid, co-harboring multiple resistance genes [*aac(6′)-Ib*, *aadA16*, *qnrS1*, *mphE*, *msrE*, *catB3*, *catII.2*, *arr-3*, *sul1*, *dfrA27*, $bla_{\text{OXA-1}}$, and $bla_{\text{NDM-1}}$; **Table 3**]. Notably, the $bla_{\text{NDM-1}}$ carbapenem-resistant gene was co-existed with *TmexCD2-ToprJ2* in pJNQH579-2 plasmid. $bla_{\text{NDM-1}}$ was found within a truncated transposon Tn*125* (**Figure 3**), with the structure of "Δ*ISAba125*-$bla_{\text{NDM-1}}$-ble_{MBL}-*tat-dvt-groESL- tnpAISCR21*" (Poirel et al., 2012). The pJNQH579-1 plasmid had an IncFIB replicon but did not carry any known resistance genes.

Comparative Genomic Analysis of HI1B Plasmids Carrying *TmexCD2-ToprJ2*

The *TmexCD2-ToprJ2* cluster in the three strains had almost 100% nucleotide identities to the cluster of the originally reported *TmexCD2-ToprJ2* (Wang et al., 2021a). Plasmid sequence comparison demonstrated that pJNQH473-3 and pJNQH491-2 had highly conserved plasmid synteny and structure, with over 99.9% nucleotide identities (**Figure 3**). pJNQH491-2 had a blast query coverage of 74% and over 99% nucleotide identities with pJNQH579-2. Further plasmid BLAST query against GenBank database showed that pJNQH473-3 and pJNQH491-2 were closely related to plasmid pKOX-R1 (NC018107), isolated from Taiwan in *K. michiganensis* E718 (**Figure 3**). In comparison with pKOX-R1, a 16,846 bp region, containing the *TmexCD2-ToprJ2*, was inserted into the *umuC* gene of pJNQH473-3, generated a 3 bp (CAT) direct repeats (**Figure 2**). The three pJNQH plasmids contain the same *TmexCD2-ToprJ2* structure of "*hp1-hp2-tnpA-tnfxB2-IS881-TmexCD2-ToprJ2*," with an average GC content of 42.3%. pJNQH579-2 was found to be closely related to plasmid pC2315-2-NDM (CP039829). The putative "*hp1-hp2-tnpA-tnfxB2-IS881-TmexCD2-ToprJ2*" transposon was surrounded by *XerC*, *XerD*, and additional hypothetical genes. This region was also inserted into the *umuC* gene therefore constituted a putative larger transposon unit of 34,827 bp (**Figure 2**).

Sequence Comparison of Three *TmexCD-ToprJ* Gene Clusters

TmexCD2-ToprJ2 cluster shares a high similarity to *TmexCD1-ToprJ1*, of which the variants of *TmexC*, *TmexD*, and *ToprJ* genes had 98.02, 96.75, and 99.93% nucleotide identities and 97.67, 97.61, and 99.79% amino acid identities between each other. Compared with *TmexCD3-ToprJ3*, the variants of *TmexC*, *TmexD*, and *ToprJ* genes shared 94, 96.72, and 99.86% nucleotide identities and 97.12, 98.08, and 99.79% amino acid identities. *ToprJ* gene shares the highest similarity at the amino acid

TABLE 3 | Chromosome and plasmid features of strains in this study.

Strains	Chromosome or plasmid	Size (bp)	Plasmid type	Acquired AMR genes
K. quasipneumoniae JNQH473	Chromosome	5,390,886	–	$bla_{OKP-A-3}$
	pJNQH473-1	229,265	IncFIB	*aac(6')-Ib4*,$bla_{CTX-M-14}$,bla_{IMP-8}
	pJNQH473-2	70,940	FII(pBK30683)	–
	pJNQH473-3*	297,981	IncHI1B	*aac(3)-IId;aadA16,qnrS1,mphA,arr-3,sul1,tmexCD2-toprJ2,dfrA27*,bla_{TEM-1D}
	pJNQH473-4	46,166	IncX3_1	bla_{NDM-5}
K. michiganensis JNQH491	Chromosome	6,039,729	–	$bla_{OXY-1-3}$
	pJNQH491-1	205,582	IncFIB	–
	pJNQH491-2*	307,464	IncHI1B	*aac(3)-IId,qnrS1,mphA,sul1,tmexCD2-toprJ2,dfrB4*,bla_{TEM-1D}, bla_{NDM-1}
K. variicola JNQH579	Chromosome	5,583,188	–	$bla_{OXY-1-3}$
	pJNQH579-1	197,434	IncFIB	–
	pJNQH579-2*	369,339	IncHI1B	*aac(6')-Ib,aadA16,qnrS1,mphE,msrE,catB3,catII.2,arr-3,sul1,tmexCD2-toprJ2,dfrA27*,bla_{OXA-1},bla_{NDM-1}

**TmexCD2-ToprJ2 harboring plasmid.*

level among the three variants, of which *ToprJ2* differs from *ToprJ1* and *ToprJ3* by a single amino acid substitution (Ala47Thr; **Supplementary Figure S1**).

Genomic Analysis of Plasmids Harboring *TmexCD-ToprJ* Variants

The analysis of plasmid database revealed that a total of 43 plasmids carried *TMexCD1-ToprJ1* ($n = 23$), *TmexCD2-ToprJ2* ($n = 8$), and *TmexCD3-ToprJ3* ($n = 12$) gene clusters (with 100% gene coverage and over 99.97% identity), which were distributed mainly in *Enterobacteriaceae* and *P. aeruginosa* (**Figure 4**). *TmexCD1-ToprJ1* and *TmexCD2-ToprJ2* were mostly identified in *K. pneumoniae*, whereas *TmexCD3-ToprJ3* was more frequently found in *P. aeruginosa*. In addition to *Klebsiella*, the *TmexCD2-ToprJ2* harboring plasmids were also found in *R. ornithinolytica* ($n = 1$), *Citrobacter freundii* ($n = 1$). Most *TmexCD2-toprJ2* gene clusters were associated with IncFII ($n = 3$), IncHI1B ($n = 3$), and IncQ ($n = 2$) plasmids. Of note, six *TmexCD2-ToprJ2* harboring plasmids also co-harbored carbapenem-resistant genes, including four bla_{NDM-1} and two bla_{KPC-1} genes.

Transfer of *TmexCD2-ToprJ2* Harboring Plasmids *via* Conjugation

The *TmexCD2-ToprJ2* harboring IncHI1B plasmids were successfully transferred into *E. coli* J53 from three JNQH strains. Further PCRs confirmed that other plasmids in the donor strains were not co-transferred along with the *TmexCD2-ToprJ2* harboring IncHI1B plasmids into the recipient *E. coli* J53 strain (**Supplementary Figure S2**). The conjugation frequency was 10^{-6}, 10^{-6}, and 10^{-5} for JNQH473, JNQH491, and JNQH579 per recipient cell, respectively. The MICs for the *E.coli* J53 transconjugants are shown in **Table 2**. The MICs of tigecycline against *E. coli* J53 transconjugants were 1 μg/ml, which were 8-fold higher than that of the *E. coli* J53 itself. In addition, the transfer of bla_{NDM-1} together with the *TmexCD2-ToprJ2* genes for JNQH491 and JNQH579 in the *E. coli* J53 transconjugants conferred resistance to all tested β-lactams (ampicillin, amoxicillin-clavulanate, piperacillin/tazobactam, cefoxitin, ceftriaxone, cefepime, imipenem, and ertapenem) except for aztreonam. All transconjugants exhibited resistance to quinolones (ciprofloxacin and levofloxacin, ≥4 μg/ml), which was likely due to the combinational effects of both quinolone resistance determinant *qnrS1* and the *TmexCD2-ToprJ2*. Further, *E.coli* J53 transconjugants for JNQH491 and JNQH579 exhibited resistance to gentamycin, while it was susceptible for JNQH473. *Aac(3)-IId* is likely the main source of the disparity on the basis that *aac(3)-IId* was co-harbored with *TmexCD2-ToprJ2* in the same plasmids for JNQH473 and JNQH491 strains, while it was absent on the pJNQH579-2 plasmid.

DISCUSSION

TmexCD1-ToprJ1 is the first reported plasmid-encoded RND efflux pump, conferring resistance to multiple drugs including tigecycline (Lv et al., 2020). More recently, a variant of *TmexCD2-ToprJ2* was identified in a clinical *R. ornithinolytica* strain NC189, which demonstrated similar tigecycline resistance as the *TmexCD1-ToprJ1* (Wang et al., 2021a). In comparison with *TmexCD1-ToprJ1*, most of which were detected in *K. pneumoniae* (**Figure 2**), *TmexCD2-ToprJ2* was identified among a variety of *Enterobacteriaceae* species, including *R. ornithinolytica*, *C. freundii*, *Aeromonas hydrophila*, and *K. pneumoniae* (Wang et al., 2021a). Our study demonstrated that the *TmexCD2-ToprJ2* had spread into carbapenem-resistant *K. pneumoniae* species complex (KpSC), which is an emerging pathogenic species and frequently detected clinically (Wyres et al., 2020). The highly conserved synteny and structure of the *TmexCD2-ToprJ2* harboring plasmids suggested the likelihood of horizontal transfer of a highly similar plasmid between different *Klebsiella* species. We also found the co-existence of *TmexCD2-ToprJ2* and bla_{NDM-1} genes in pJNQH491-2 and pJNQH579-2, confirmed by the resistance profile of the transconjugants. The co-transfer of bla_{NDM-1} with *TmexCD2-ToprJ2* for JNQH491 and JNQH579 in the *E. coli*

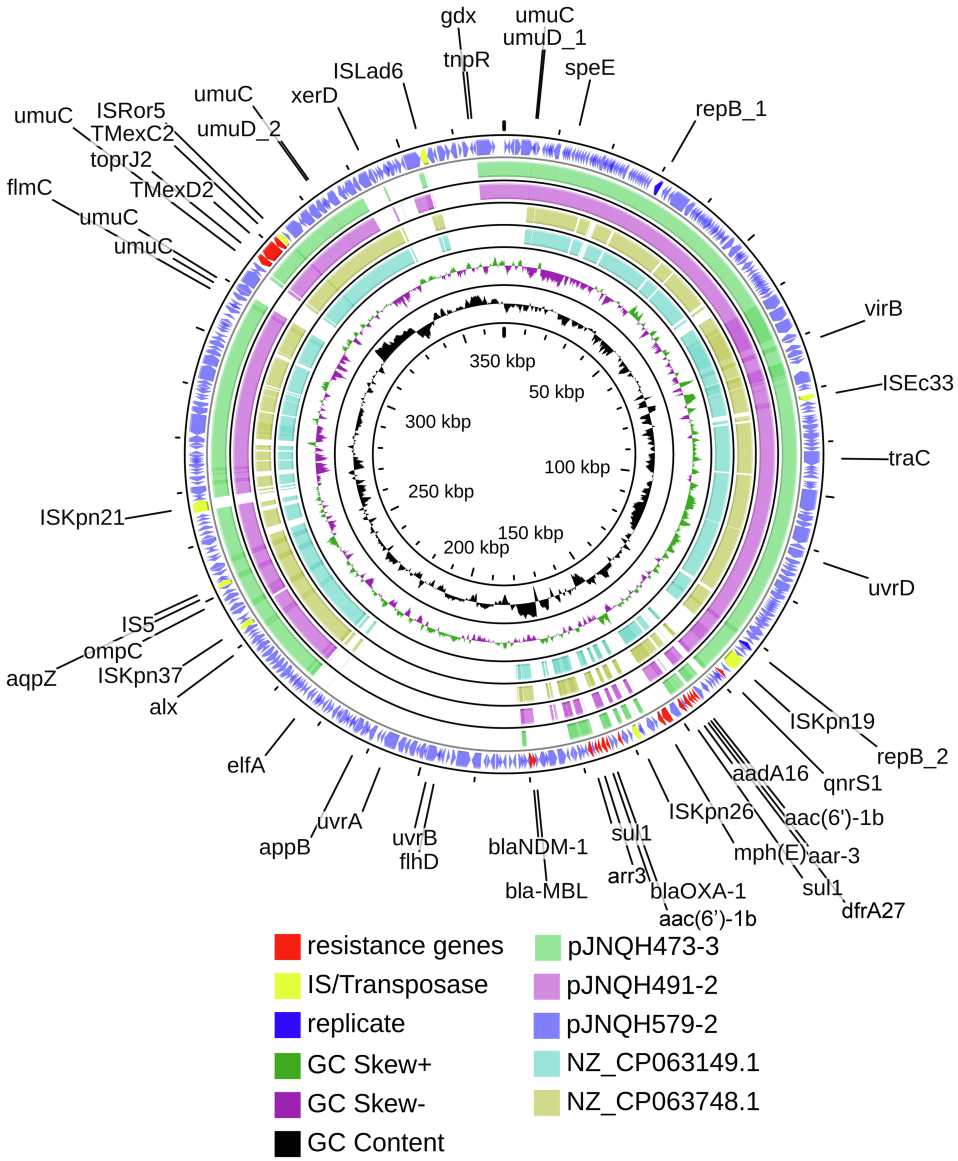

FIGURE 1 | Comparative structural analysis of pJNQH473-3, pJNQH491-2, pJNQH579-2, and two *TmexCD2-ToprJ2* harboring plasmids NZ_CP063149.1 and NZ_CP063748.1. Open reading frames (ORFs) of pJNQH579-2 are shown as the outermost ring, with plasmid replicons, insertion sequences (IS), and antimicrobial resistance genes highlighted.

J53 conjugants conferred resistance to tigecycline and all tested β-lactams except aztreonam. In addition, analysis of plasmids from the database from NCBI revealed frequent co-occurrence of *TmexCD2-ToprJ2* and carbapenem-resistant genes in the same plasmid. Our finding is of particular public health concern as the convergence of "mosaic" plasmids can confer both tigecycline and carbapenem resistance, thus leading to a serious challenge to the treatment of bacterial infections.

It has been demonstrated in a previous study that *TmexCD2-ToprJ2* functions as an efflux pump system by the efflux inhibition experiments (Wang et al., 2021a). *TmexCD2-ToprJ2* exhibits a broad substrate spectrum toward tetracyclines, eravacycline, tigecycline (8-fold MIC increase), ciprofloxacin (4-fold MIC increase), and slightly decreased susceptibility (2-fold MIC increase) to cefotaxime and cefepime (Wang et al., 2021a). Our finding is consistent with previous study that *TmexCD2-ToprJ2* gene cluster caused 8-fold increase in the tigecycline MICs in the *E. coli* transconjugants (Wang et al., 2021a). However, strain *K. michiganensis* JNQH491 was susceptible to tigecycline with a MIC value of 1 μg/ml irrespective of the presence of *TmexCD2-ToprJ2* gene. We speculated that the differences in plasmid copy numbers or transcription of promoter sequence in this *K. michiganensis* strain might contribute to the different susceptibility profiles observed in strains from this study (Shaheen et al., 2011). Further studies are needed to evaluate how much *TmexCD2-ToprJ2* will affect the therapeutic

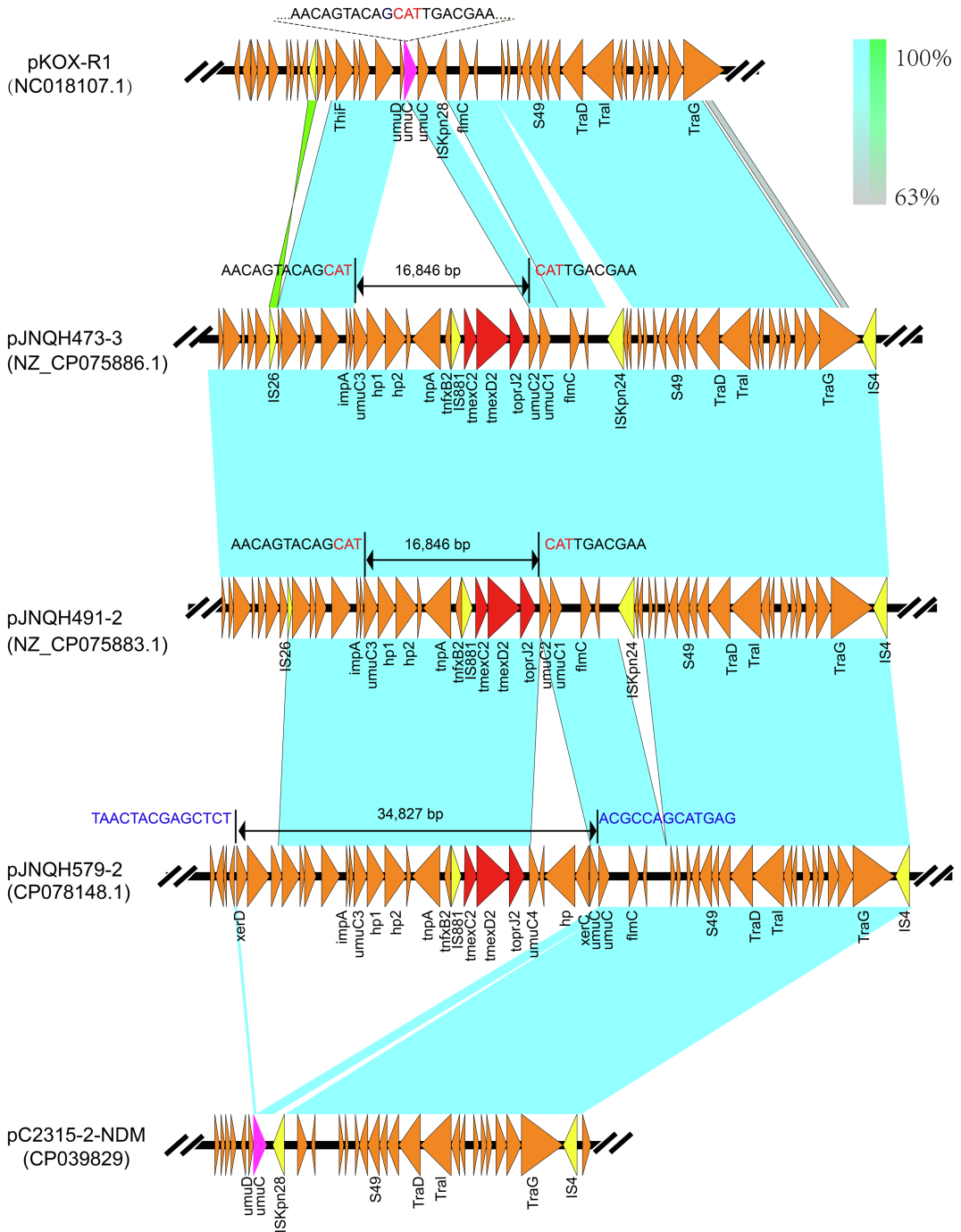

FIGURE 2 | Linear comparisons of *TmexCD2-ToprJ2*-bearing genetic contexts in pJNQH473-3 and that in pJNQH579-2, pC2315-2-NDM, and plasmid pKOX_R1(NC018107.1). Light blue shading indicates shared regions of homology, while green shading indicates inversely displayed regions of homology. Colored arrows indicate ORFs. The red arrows indicate the antibiotic resistance genes. The yellow arrows indicate IS. The nucleotide sequence of the *umuC* gene (green arrow) representing the insertion site is shown above the gene. The 16,846 bp putative "*hp1-hp2-tnpA-tnfxB2-IS881-TmexCD2-ToprJ2*" transposon located on pJNQH473-3 and 34,827 bp larger putative transposon on pJNQH579-2 are marked with bilateral black arrows.

effects of tigecycline *in vivo*, including clinical isolates with low MIC values.

An increasing number of studies have supported that the *TmexCD-ToprJ*-like efflux pump system may originate from the chromosome of *Pseudomonas* species, as their structures are closely related to the chromosomal *MexCD-OprJ* system in *P. aeruginosa* (Lv et al., 2020; Sun et al., 2020; Wang et al., 2021a,b). These findings suggested *TmexCD-ToprJ*-like clusters

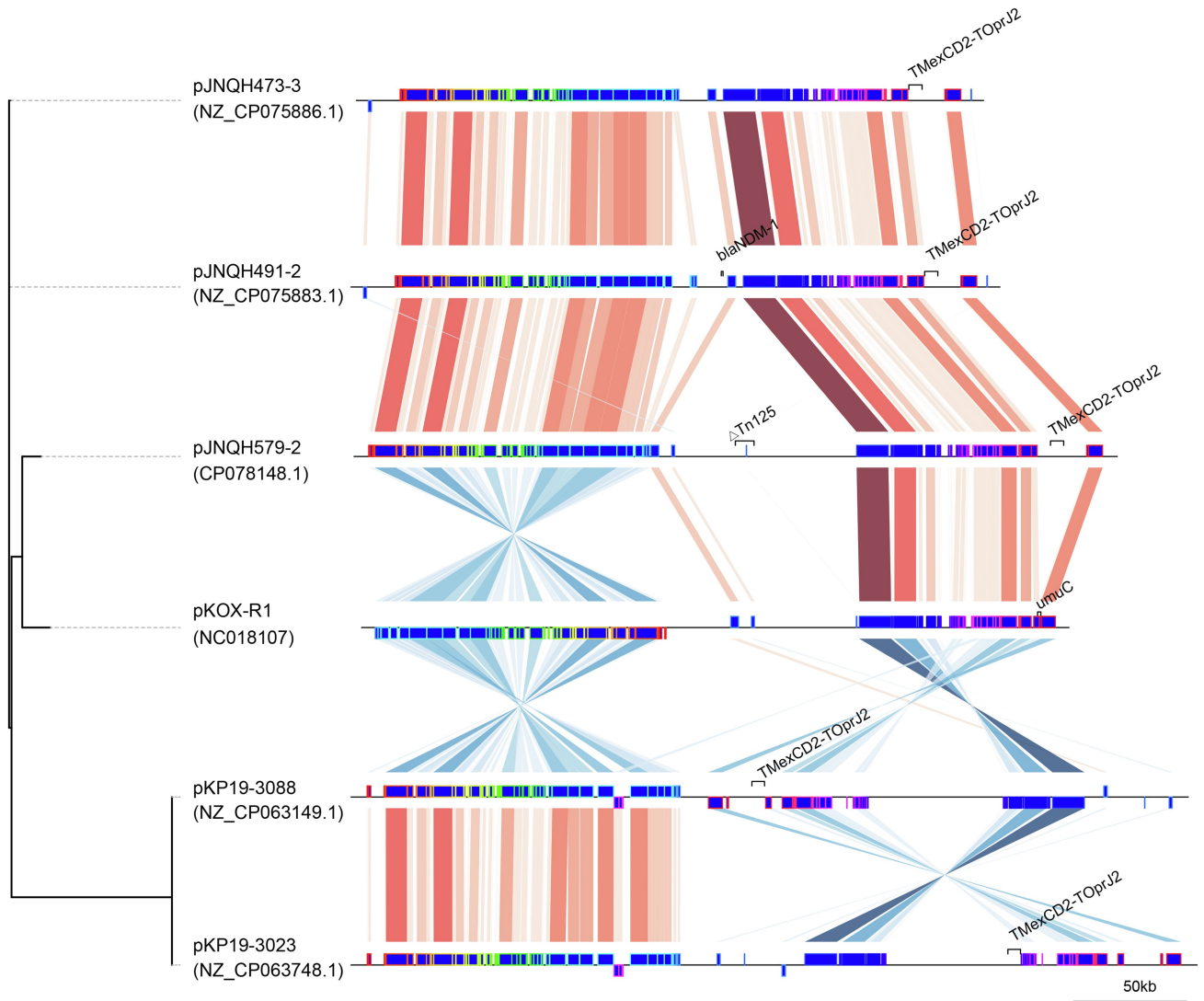

FIGURE 3 | Comparison of linear plasmid maps of four *TmexCD2-ToprJ2*-bearing plasmids and the related plasmid pKOX-R1. The genomes were compared with Mauve and the elements were designated as Mauve blocks. Red shaded regions between plasmids indicates shared regions of homology, while blue shading indicates inversely displayed regions of homology. The tree was created using Mashtree.

might be originated from chromosomal genes in *Pseudomonas* species, through horizontal transfer into *Enterobacteriaceae* species. The *MexCD-OprJ* family proteins act as efflux pumps, conferring intrinsic resistance to tetracycline, chloramphenicol, and norfloxacin in *P. aeruginosa* (Poole et al., 1993). The rapid expansion of the *TmexCD-ToprJ* cluster has been attributed to various mobile genetic elements, such as ICEs, transposons (e.g., Tn5393), or IS element (e.g., IS*26*; Sun et al., 2020; Wan et al., 2020; Wang et al., 2021b; Yang et al., 2021). In our study, a genetic structure (*hp1-hp2-tnpA-tnfxB2-IS881-TmexCD2-ToprJ2*) constitutes a putative transposon system. Further, a larger putative transposon comprised of 34,827 bp harboring *TmexCD2-ToprJ2* was also inserted into the *umuC*-like gene of pJNQH579-2. As such, the *umuC* gene appears to be a "hotspot" for *TmexCD2-ToprJ2* integration in IncHIB plasmids, while the molecular mechanism underlying the site-specific integration deserves further studies.

CONCLUSION

Overall, we report the first time of three IncHI1B type plasmids encoding efflux pump *TmexCD2-ToprJ2* in carbapenem-resistant *K. variicola*, *K. michiganensis*, and *K. quasipneumoniae* species. The sequence analysis identified a putative transposon element for *TmexCD2-ToprJ2* transmission, with the genetic structure of "*hp1-hp2-tnpA-tnfxB2-IS881-TmexCD2-ToprJ2*." Of note, the co-existence of bla_{NDM-1} and *TmexCD2-ToprJ2* is of particular public health concern. The emergence of such *Klebsiella* strains underscores

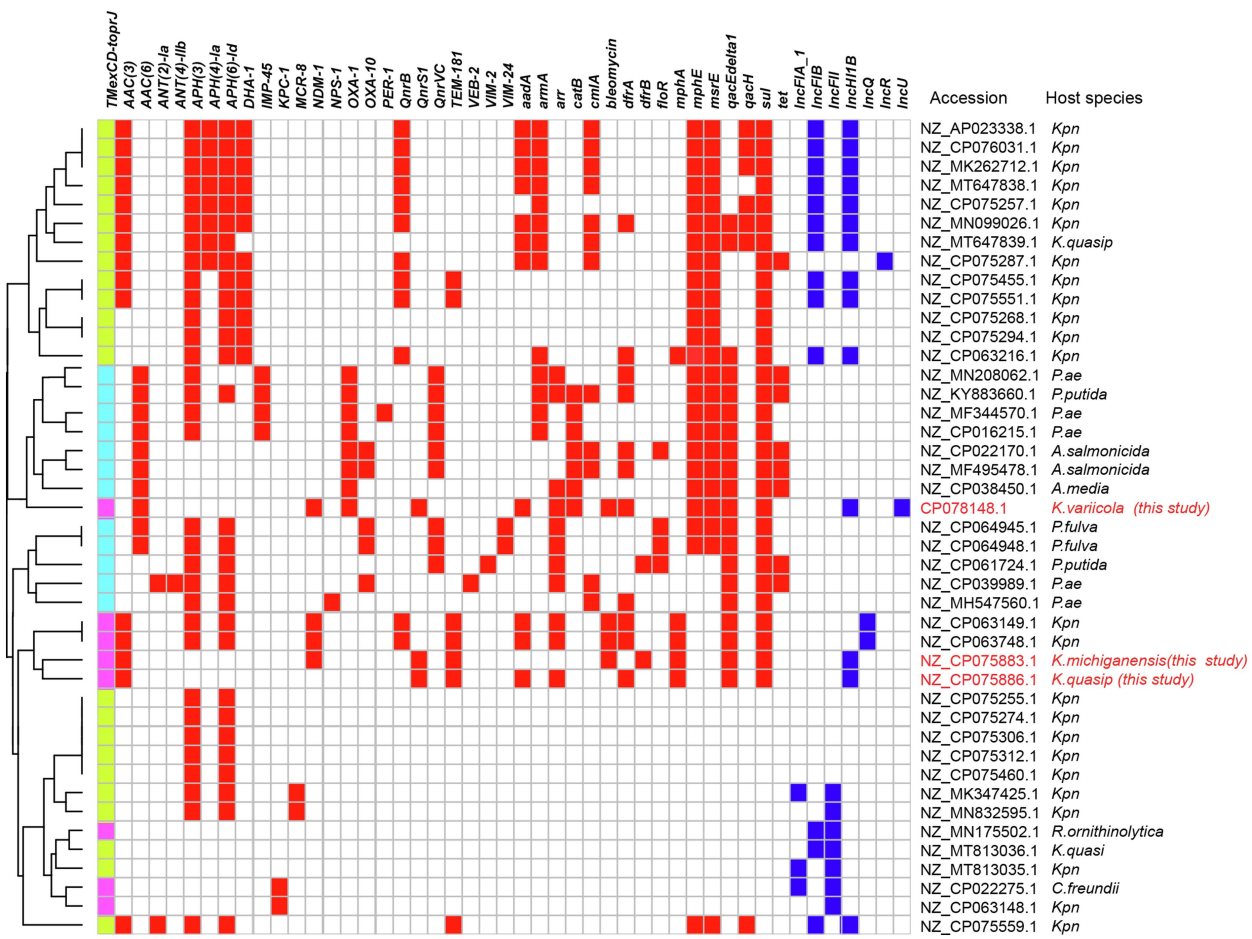

FIGURE 4 | *TMexCD-toprJ*-harboring plasmids. The heatmap shows the distribution of plasmid replicons (dark blue boxes) and antibiotic resistance genes (red boxes) detected within 51 *TMexCD-toprJ*-harboring plasmids. The variants of *TMexCD-toprJ* resistance genes are indicated in green (*TMexCD1-toprJ1*), pink (*TMexCD2-toprJ2*), and light blue (*TMexCD3-toprJ3*) boxes. GenBank accession numbers and species are listed on the right-hand side. *Kpn*, *Klebsiella pneumoniae*; *K. quasip*, *Klebsiella quasipneumoniae*; *Pae*, *Pseudomonas aeruginosa*; *P. putida*, *Pseudomonas putida*; *A. salmonicida*, *Aeromonas salmonicida*; *A. media*, *Aeromonas media*; *K. variicola*, *Klebsiella variicola*; *P. fulva*, *Pseudomonas fulva*; *P.* sp., *Pseudomonas* species; *R. ornithinolytica*, *Raoultella ornithinolytica*; *C. freundii*, *Citrobacter freundii*.

the importance of clinical awareness of this pathotype and the need for continued monitoring of *TmexCD-ToprJ* family resistance genes in China and around the world.

DATA AVAILABILITY STATEMENT

Complete sequences of the chromosomes and plasmids of strain JNQH473, JNQH491, and JNQH579 have been deposited in the GenBank databases under accession numbers NZ_CP075884.1-NZ_CP075888.1, NZ_CP075881.1-NZ_CP075883.1, and NZ_CP078146.1-NZ_CP078148.1, respectively.

ETHICS STATEMENT

The studies involving human participants were reviewed and approved by the First Affiliated Hospital of Shandong First Medical University. Written informed consent to participate in this study was provided by the participants' legal guardian/next of kin. Written informed consent was obtained from the individual(s), and minor(s)' legal guardian/next of kin, for the publication of any potentially identifiable images or data included in this article.

AUTHOR CONTRIBUTIONS

MH and WM conceived the study and designed the experimental procedures. BZ and XD collected the strains. YW, BZ, ML, JM, XL, and FC performed the experiments. MH, JG, and SL analyzed the data. WM, YH, and YW contributed to reagents and materials. MH and LC wrote the manuscript. All authors contributed to the article and approved the submitted version.

SUPPLEMENTARY MATERIAL

The Supplementary Material for this article can be found online at: https://www.frontiersin.org/articles/10.3389/fmicb.2021.759208/full#supplementary-material

Supplementary Figure S1 | Multiple sequence alignment of amino acids of *TmexCD1-ToprJ1*, *TmexCD2-ToprJ2*, and *TmexCD3-ToprJ3*. Conserved residues were displayed in dark blue background and mutants were highlighted in white background.

Supplementary Figure S2 | PCR amplification of plasmid replicons and resistance genes of JNQH473, 491, 579, and their *E. coli* J53 transconjugants.

REFERENCES

Bolger, A. M., Lohse, M., and Usadel, B. (2014). Trimmomatic: a flexible trimmer for Illumina sequence data. *Bioinformatics* 30, 2114–2120. doi: 10.1093/bioinformatics/btu170

Brettin, T., Davis, J. J., Disz, T., Edwards, R. A., Gerdes, S., Olsen, G. J., et al. (2015). RASTtk: a modular and extensible implementation of the RAST algorithm for building custom annotation pipelines and annotating batches of genomes. *Sci. Rep.* 5:8365. doi: 10.1038/srep08365

Carattoli, A., Zankari, E., Garcia-Fernandez, A., Voldby Larsen, M., Lund, O., Villa, L., et al. (2014). In silico detection and typing of plasmids using PlasmidFinder and plasmid multilocus sequence typing. *Antimicrob. Agents Chemother.* 58, 3895–3903. doi: 10.1128/AAC.02412-14

Cheng, Y., Chen, Y., Liu, Y., Guo, Y., Zhou, Y., Xiao, T., et al. (2020). Identification of novel tetracycline resistance gene tet(X14) and its co-occurrence with tet(X2) in a tigecycline-resistant and colistin-resistant *Empedobacter stercoris*. *Emerg. Microbes Infect.* 9, 1843–1852. doi: 10.1080/22221751.2020.1803769

Chiu, S. K., Chan, M. C., Huang, L. Y., Lin, Y. T., Lin, J. C., Lu, P. L., et al. (2017). Tigecycline resistance among carbapenem-resistant *Klebsiella pneumoniae*: clinical characteristics and expression levels of efflux pump genes. *PLoS One* 12:e0175140. doi: 10.1371/journal.pone.0175140

Darling, A. E., Mau, B., and Perna, N. T. (2010). progressiveMauve: multiple genome alignment with gene gain, loss and rearrangement. *PLoS One* 5:e11147. doi: 10.1371/journal.pone.0011147

Grant, J. R., and Stothard, P. (2008). The CGView server: a comparative genomics tool for circular genomes. *Nucleic Acids Res.* 36, W181–W184. doi: 10.1093/nar/gkn179

Grossman, T. H. (2016). Tetracycline antibiotics and resistance. *Cold Spring Harb. Perspect. Med.* 6:a025387. doi: 10.1101/cshperspect.a025387

Guy, L., Kultima, J. R., and Andersson, S. G. (2010). genoPlotR: comparative gene and genome visualization in R. *Bioinformatics* 26, 2334–2335. doi: 10.1093/bioinformatics/btq413

Hao, M., Schuyler, J., Zhang, H., Shashkina, E., Du, H., Fouts, D. E., et al. (2021). Apramycin resistance in epidemic carbapenem-resistant *Klebsiella pneumoniae* ST258 strains. *J. Antimicrob. Chemother.* 76, 2017–2023. doi: 10.1093/jac/dkab131

He, T., Wang, R., Liu, D., Walsh, T. R., Zhang, R., Lv, Y., et al. (2019). Emergence of plasmid-mediated high-level tigecycline resistance genes in animals and humans. *Nat. Microbiol.* 4, 1450–1456. doi: 10.1038/s41564-019-0445-2

Henderson, T. A., Young, K. D., Denome, S. A., and Elf, P. K. (1997). AmpC and AmpH, proteins related to the class C beta-lactamases, bind penicillin and contribute to the normal morphology of *Escherichia coli*. *J. Bacteriol.* 179, 6112–6121. doi: 10.1128/jb.179.19.6112-6121.1997

Hirabayashi, A., Ha, V. T. T., Nguyen, A. V., Nguyen, S. T., Shibayama, K., and Suzuki, M. (2021). Emergence of a plasmid-borne tigecycline resistance in *Klebsiella pneumoniae* in Vietnam. *J. Med. Microbiol.* 70:001320. doi: 10.1099/jmm.0.001320

Jia, B., Raphenya, A. R., Alcock, B., Waglechner, N., Guo, P., Tsang, K. K., et al. (2017). CARD 2017: expansion and model-centric curation of the comprehensive antibiotic resistance database. *Nucleic Acids Res.* 45, D566–D573. doi: 10.1093/nar/gkw1004

Jiang, X., Yin, Z., Yin, X., Fang, H., Sun, Q., Tong, Y., et al. (2017). Sequencing of blaIMP-carrying IncN2 plasmids, and comparative genomics of IncN2 plasmids harboring class 1 integrons. *Front. Cell. Infect. Microbiol.* 7:102. doi: 10.3389/fcimb.2017.00102

Kolmogorov, M., Yuan, J., Lin, Y., and Pevzner, P. A. (2019). Assembly of long, error-prone reads using repeat graphs. *Nat. Biotechnol.* 37, 540–546. doi: 10.1038/s41587-019-0072-8

Lam, M. M. C., Wick, R. R., Watts, S. C., Cerdeira, L. T., Wyres, K. L., and Holt, K. E. (2021). A genomic surveillance framework and genotyping tool for *Klebsiella pneumoniae* and its related species complex. *Nat. Commun.* 12:4188. doi: 10.1038/s41467-021-24448-3

Linkevicius, M., Sandegren, L., and Andersson, D. I. (2016). Potential of tetracycline resistance proteins to evolve tigecycline resistance. *Antimicrob. Agents Chemother.* 60, 789–796. doi: 10.1128/AAC.02465-15

Katz, L. S., Griswold, T., Morrison, S. S., Caravas, J. A., Zhang, S., Den Bakker, H. C., et al. (2019). Mashtree: a rapid comparison of whole genome sequence files. *J. Open Source Softw.* 4:1762. doi: 10.21105/joss.01762

Lv, L., Wan, M., Wang, C., Gao, X., Yang, Q., Partridge, S. R., et al. (2020). Emergence of a plasmid-encoded resistance-nodulation-division efflux pump conferring resistance to multiple drugs, including tigecycline, in *Klebsiella pneumoniae*. *MBio* 11:e02930-19. doi: 10.1128/mBio.02930-19

Madeira, F., Park, Y. M., Lee, J., Buso, N., Gur, T., Madhusoodanan, N., et al. (2019). The EMBL-EBI search and sequence analysis tools APIs in 2019. *Nucleic Acids Res.* 47, W636–W641. doi: 10.1093/nar/gkz268

Poirel, L., Bonnin, R. A., Boulanger, A., Schrenzel, J., Kaase, M., and Nordmann, P. (2012). Tn125-related acquisition of blaNDM-like genes in *Acinetobacter baumannii*. *Antimicrob. Agents Chemother.* 56, 1087–1089. doi: 10.1128/AAC.05620-11

Poole, K., Krebes, K., Mcnally, C., and Neshat, S. (1993). Multiple antibiotic resistance in *Pseudomonas aeruginosa*: evidence for involvement of an efflux operon. *J. Bacteriol.* 175, 7363–7372. doi: 10.1128/jb.175.22.7363-7372.1993

Roberts, A. P., Chandler, M., Courvalin, P., Guedon, G., Mullany, P., Pembroke, T., et al. (2008). Revised nomenclature for transposable genetic elements. *Plasmid* 60, 167–173. doi: 10.1016/j.plasmid.2008.08.001

Ruzin, A., Immermann, F. W., and Bradford, P. A. (2008). Real-time PCR and statistical analyses of acrAB and ramA expression in clinical isolates of *Klebsiella pneumoniae*. *Antimicrob. Agents Chemother.* 52, 3430–3432. doi: 10.1128/AAC.00591-08

Ruzin, A., Visalli, M. A., Keeney, D., and Bradford, P. A. (2005). Influence of transcriptional activator RamA on expression of multidrug efflux pump AcrAB and tigecycline susceptibility in *Klebsiella pneumoniae*. *Antimicrob. Agents Chemother.* 49, 1017–1022. doi: 10.1128/AAC.49.3.1017-1022.2005

Seemann, T. (2014). Prokka: rapid prokaryotic genome annotation. *Bioinformatics* 30, 2068–2069. doi: 10.1093/bioinformatics/btu153

Shaheen, B. W., Nayak, R., Foley, S. L., Kweon, O., Deck, J., Park, M., et al. (2011). Molecular characterization of resistance to extended-spectrum cephalosporins in clinical *Escherichia coli* isolates from companion animals in the United States. *Antimicrob. Agents Chemother.* 55, 5666–5675. doi: 10.1128/AAC.00656-11

Sullivan, M. J., Petty, N. K., and Beatson, S. A. (2011). Easyfig: a genome comparison visualizer. *Bioinformatics* 27, 1009–1010. doi: 10.1093/bioinformatics/btr039

Sun, J., Chen, C., Cui, C. Y., Zhang, Y., Liu, X., Cui, Z. H., et al. (2019). Plasmid-encoded tet(X) genes that confer high-level tigecycline resistance in *Escherichia coli*. *Nat. Microbiol.* 4, 1457–1464. doi: 10.1038/s41564-019-0496-4

Sun, S., Gao, H., Liu, Y., Jin, L., Wang, R., Wang, X., et al. (2020). Co-existence of a novel plasmid-mediated efflux pump with colistin resistance gene mcr in one plasmid confers transferable multidrug resistance in *Klebsiella pneumoniae*. *Emerg. Microbes Infect.* 9, 1102–1113. doi: 10.1080/22221751.2020.1768805

Vaser, R., Sovic, I., Nagarajan, N., and Sikic, M. (2017). Fast and accurate de novo genome assembly from long uncorrected reads. *Genome Res.* 27, 737–746. doi: 10.1101/gr.214270.116

Walker, B. J., Abeel, T., Shea, T., Priest, M., Abouelliel, A., Sakthikumar, S., et al. (2014). Pilon: an integrated tool for comprehensive microbial variant detection and genome assembly improvement. *PLoS One* 9:e112963. doi: 10.1371/journal.pone.0112963

Wan, M., Gao, X., Lv, L., Cai, Z., and Liu, J. H. (2020). IS26 mediate the acquisition of tigecycline resistance gene cluster tmexCD1-toprJ1 by IncHI1B-

FIB plasmids in *Klebsiella pneumoniae* and *Klebsie lla quasipneumoniae* from food market sewage. *Antimicrob. Agents Chemother.* 65:e02178-20. doi: 10.1128/AAC.02178-20

Wang, C. Z., Gao, X., Yang, Q. W., Lv, L. C., Wan, M., Yang, J., et al. (2021a). Novel transferable resistance-nodulation-division pump gene cluster tmexCD2-toprJ2 that confers tigecycline resistance in *Raoultella ornithinolytica*. *Antimicrob. Agents Chemother.* 65:e02229-20. doi: 10.1128/AAC.02229-20

Wang, Q., Peng, K., Liu, Y., Xiao, X., Wang, Z., and Li, R. (2021b). Characterization of TMexCD3-TOprJ3, an RND-type efflux system conferring resistance to tigecycline in *Proteus mirabilis*, and its associated integrative conjugative element. *Antimicrob. Agents Chemother.* 65:e0271220. doi: 10.1128/AAC.02712-20

Wyres, K. L., Lam, M. M. C., and Holt, K. E. (2020). Population genomics of *Klebsiella pneumoniae*. *Nat. Rev. Microbiol.* 18, 344–359. doi: 10.1038/s41579-019-0315-1

Yang, X., Ye, L., Chan, E. W., Zhang, R., and Chen, S. (2021). Characterization of an IncFIB/IncHI1B plasmid encoding efflux pump TMexCD1-TOprJ1 in a clinical tigecycline and carbapenem-resistant *Klebsiella pneumoniae* strain. *Antimicrob. Agents Chemother.* 65:e02340-20. doi: 10.1128/AAC.02340-20

Conflict of Interest: The authors declare that the research was conducted in the absence of any commercial or financial relationships that could be construed as a potential conflict of interest.

frontiers in Microbiology

ORIGINAL RESEARCH
published: 11 November 2021
doi: 10.3389/fmicb.2021.763288

Histone-Like Nucleoid Structuring Protein Modulates the Fitness of *tet*(X4)-Bearing IncX1 Plasmids in Gram-Negative Bacteria

Wenhui Cai[1], Feifei Tang[1], Lijie Jiang[1], Ruichao Li[1,2,3,4], Zhiqiang Wang[1,2,3] and Yuan Liu[1,2,3,4]**

[1] College of Veterinary Medicine, Yangzhou University, Yangzhou, China, [2] Jiangsu Co-innovation Center for Prevention and Control of Important Animal Infectious Diseases and Zoonoses, Yangzhou University, Yangzhou, China, [3] Joint International Research Laboratory of Agriculture and Agri-Product Safety, The Ministry of Education of China, Yangzhou University, Yangzhou, China, [4] Institute of Comparative Medicine, Yangzhou University, Yangzhou, China

OPEN ACCESS

Edited by:
Steven Lee Foley,
National Center for Toxicological Research (FDA), United States

Reviewed by:
Miguel A. Ares,
Mexican Social Security Institute (IMSS), Mexico
Nesreen H. Aljahdali,
King Abdulaziz University, Saudi Arabia

***Correspondence:**
Zhiqiang Wang
zqwang@yzu.edu.cn
Yuan Liu
liuyuan2018@yzu.edu.cn

Specialty section:
This article was submitted to Antimicrobials, Resistance and Chemotherapy, a section of the journal Frontiers in Microbiology

Received: 23 August 2021
Accepted: 14 October 2021
Published: 11 November 2021

Citation:
Cai W, Tang F, Jiang L, Li R, Wang Z and Liu Y (2021) Histone-Like Nucleoid Structuring Protein Modulates the Fitness of tet(X4)-Bearing IncX1 Plasmids in Gram-Negative Bacteria. Front. Microbiol. 12:763288. doi: 10.3389/fmicb.2021.763288

The emergence of plasmid-mediated tigecycline resistance gene *tet*(X4) poses a challenging threat to public health. Based on the analysis of *tet*(X4)-positive plasmids in the NCBI database, we found that the IncX1-type plasmid is one of the most common vectors for spreading *tet*(X4) gene, but the mechanisms by which these plasmids adapt to host bacteria and maintain the persistence of antibiotic resistance genes (ARGs) remain unclear. Herein, we investigated the underlying mechanisms of how host bacteria modulate the fitness cost of IncX1 plasmids carrying *tet*(X4) gene. Interestingly, we found that the *tet*(X4)-bearing IncX1 plasmids encoding H-NS protein imposed low or no fitness cost in *Escherichia coli* and *Klebsiella pneumoniae*; instead, they partially promoted the virulence and biofilm formation in host bacteria. Regression analysis revealed that the expression of *hns* gene in plasmids was positively linked to the relative fitness of host bacteria. Furthermore, when pCE2::*hns* was introduced, the fitness of *tet*(X4)-positive IncX1 plasmid pRF55-1 without *hns* gene was significantly improved, indicating that *hns* mediates the improvement of fitness. Finally, we showed that the expression of *hns* gene is negatively correlated with the expression of *tet*(X4) gene, suggesting that the regulatory effect of H-NS on adaptability may be attributed to its inhibitory effect on the expression of ARGs. Together, our findings suggest the important role of plasmid-encoded H-NS protein in modulating the fitness of *tet*(X4)-bearing IncX1 plasmids, which shed new insight into the dissemination of *tet*(X4) gene in a biological environment.

Keywords: H-NS protein, fitness, *tet*(X4), IncX1 plasmids, Gram-negative bacteria (GNB)

INTRODUCTION

Antibiotic resistance has constituted a growing threat to global public health. According to the data released by WHO, it is estimated that by 2050, the number of human deaths caused by multiple-drug resistance will increase to 10 million, surpassing the number of cancer deaths and becoming one of the leading causes of human death worldwide (Kuehn, 2011). Because of the widespread distribution of carbapenem resistance gene, bla_{NDM} (Nordmann et al., 2011), and

polymyxin resistance gene, *mcr-1* (Liu et al., 2016), worldwide, the clinical efficacy of carbapenems and polymyxin, two high-priority agents for treatment of multidrug-resistant (MDR) Gram-negative bacterial infections (Kumarasamy et al., 2010; Rodríguez-Baño et al., 2018), was severely diminished. Therefore, tigecycline is recognized as the last option for treating serious infections (Tasina et al., 2011). However, with the emergence of high-level tigecycline resistance gene *tet*(X3/X4) (He et al., 2019; Sun et al., 2019), few choices were left for clinicians from the traditional antibiotic pipeline. Conjugable plasmid-mediated horizontal gene transfer is the dominant pathway accounting for the spread of antibiotic resistance genes (ARGs) (San Millan, 2018; Lerminiaux and Cameron, 2019). Plasmids, as mobile genetic elements, mediate the transmission of genetic information between bacteria and promote the adaptation of bacteria to various environments and the development of bacterial resistance (Lopatkin et al., 2017). Nevertheless, the high expression of plasmid-related genes would impose additional energy and metabolic burden to host bacteria, thereby resulting in fitness cost (San Millan and MacLean, 2017). Accordingly, the fitness cost elicited by resistance plasmids is closely associated with the dissemination of ARGs (Alonso-Del Valle et al., 2021). Since its first description in China in 2019, *tet*(X4)-bearing plasmids have been found worldwide (Ding et al., 2020; Zhang et al., 2020; Mohsin et al., 2021). For example, it is reported that *tet*(X4)-positive plasmids were widely distributed in the gut microbiota of Singaporeans (Ding et al., 2020). Besides, *tet*(X4)-bearing plasmids were identified from poultry, food, and environmental samples in South Asia (Mohsin et al., 2021). The prevalence of *tet*(X4) gene has posed a great challenge to human safety (Fu et al., 2021). IncX1 plasmid is one of the important vectors of *tet*(X4) gene (Li et al., 2020b), but the physiological mechanisms of widespread of *tet*(X4)-harboring IncX1 plasmids in different host strains are still unclear.

Histone-like nucleoid structuring (H-NS) protein is a kind of DNA-binding protein, which exists widely in Gram-negative bacteria (Navarre et al., 2006). H-NS protein not only participates in the regulation of cell metabolism and cellular stress response, but also responds to various environmental changes, such as pH, metal ion concentration, osmotic pressure, temperature, and stringent response (Gao et al., 2018). Notably, H-NS protein can act as a transcriptional inhibitor, silencing the expression of many genes (Dorman, 2007), including pathogenicity islands (SPIs) and fimbriae gene *pef* in *Salmonella* (Ali et al., 2014; Hurtado-Escobar et al., 2019), virulence genes *virF*, *virB*, and *icsA/B/P* in *Shigella* (Picker and Wing, 2016) and some costly conjugation genes (Doyle et al., 2007). The basis of H-NS silencing gene is its ability to target an AT-rich sequence, thus hindering its transcription (Dorman, 2014). As a global regulator, it is indicated that H-NS can regulate bacteria fitness by inhibiting the expression of certain genes. For example, the overexpression of the *Salmonella* pathogenicity island SPI2 generally acquired by horizontal gene transfer can lead to the growth defect of *Salmonella*, and H-NS inhibited the expression of SPI2 to improve the fitness of *Salmonella* (Lucchini et al., 2006). It was found that some plasmids also have genes encoding H-NS family proteins, and the deletion of *hns* decreases the fitness of host bacteria (Doyle et al., 2007), indicating that H-NS is likely to mediate the fitness cost of plasmids. A recent study showed that H-NS plays an important role in the dissemination of bla_{NDM-1}-bearing IncX3 Plasmid in *Escherichia coli* by regulating the expression of plasmid-related genes (Liu et al., 2020).

In this study, we explored the role of H-NS protein in the prevalence of *tet*(X4)-bearing IncX1 plasmids by a series of assays, including bacterial growth curve, relative fitness evaluation, and virulence assay. Most importantly, we investigated the correlation between the expression of hns and fitness cost of *tet*(X4)-positive IncX1 plasmids in various host bacteria. Our data show that H-NS plays a crucial role in alleviating the fitness cost of plasmids, which may explain the successful epidemic of *tet*(X4)-positive IncX1 plasmids in the clinical setting and provide new insights for addressing the global bacterial resistance crisis.

MATERIALS AND METHODS

Bacterial Strains and Plasmids

The accession numbers of 51 *tet*(X4)-positive plasmids from NCBI databases are listed in **Supplementary Table 1**. Three *tet*(X4)-positive plasmids carrying *hns* gene used in this experiment are shown in **Supplementary Table 2** and **Supplementary Figure 1**, in which pRF14-1 plasmid was isolated from the slaughterhouse of Jiangsu Province, China (Li et al., 2020b), and the other two plasmids pSC4R and pHS14-2 were isolated from Chinese pork samples. Standard strains involving *E. coli* TOP10, *Klebsiella pneumoniae* ATCC700603, and *Salmonella* Enteritidis ATCC13076 were used in this experiment.

Plasmid Extraction, Whole Genome Sequencing, and Bioinformatics Analysis

Plasmids were extracted using the Plasmid Mini Kit I (Omega, China). Combined with the highly accurate short-read Illumina and long-read Oxford Nanopore Technologies (ONT) MinION platforms, WGS and *de novo* assembly using the hybrid strategy was performed. Plasmid sequences were annotated using the RAST[1] automatically and modified manually. BRIG (Alikhan et al., 2011) and Easyfig (Sullivan et al., 2011) tools were used to visualize the genetic comparisons.

Preparation of Competent Cells and Electroporation Experiment

As described in a previous study (Choi et al., 2006), the *E. coli* TOP10, *K. pneumonia*e ATCC700603, and *S.* Enteritidis ATCC13076 were cultured in LB broth to the logarithmic growth phase at 37°C and 200 rpm. The strains were precooled for 30 min and centrifuged at 4°C and 5,000 rpm for 5 min. Then, the clumps of bacteria are washed with water once and with 10% glycerin three times. Bacterial liquid (50 ml) was condensed into three tubes of 100 μl of competent cells.

A tube of competent cells was taken and then mixed with the plasmids including pRF14-1, pSC4R, and pHS14-2 separately

[1]http://rast.nmpdr.org/

(the volume is not greater than 10% of the competent cells volume). Immediately after electroporation, 1 ml of LB was added to the competent cells and recovered in 37°C and 200 rpm for 1 h. Then, the positive strains were screened by agar plate with tigecycline (2 μg/ml) and polymerase chain reaction (PCR) was used to verify whether the plasmid was successfully transferred into the cell. Nine transformants were obtained.

Bacterial Growth Curve Assay

According to a previous method (Liu et al., 2020), overnight cultures of strains carrying pRF14-1, pSC4R, pHS14-2, and its recipient bacteria were diluted 1:1,000 into fresh LB broth and were incubated at 37°C with 200 rpm for 12 h. Growth curves were obtained by measuring the optical density of cultures at 620 nm every hour by Multiskan FC (Thermo Fisher Scientific). All experiments were conducted in triplicate and repeated three times independently, and the average values were used to estimate growth parameters.

Plasmid Stability Experiment

Plasmid stability testing was performed by the serial passage method for 25 consecutive days at 1:1,000 dilutions without antibiotic pressure (two generations of growth per day) (Gao et al., 2020). Strains with different plasmids were propagated in antibiotic-free LB medium at 37°C with 200 rpm and shaken for 25 days (50 generations) to determine their stability in a different strain background. PCR was conducted every 10 generations to detect the plasmid and *tet*(X4).

In vitro Competition Experiment

Overnight cultures of plasmid-carrying clone and corresponding recipient bacteria were diluted 1:1,000 in LB broth and mixed at 1:1 ratio. Then, this mixture was incubated for 3 days at 37°C with 200 rpm, and diluted 1:100 into fresh LB broth every 24 h. The competition mixture at 0, 24, 48, and 72 h was plated on LB agar without drug and LB agar containing tigecycline with proper dilution to count the colony numbers. The formula $Wt = \ln(N_{f,\ R}/N_{i,R})/\ln\ (N_{f,S}/N_{i,S})$ was used to calculate the Wt, namely, relative fitness of plasmid-carrying strain (R) compared to the recipient strain (S). $N_{i,R}$ and $N_{f,R}$ are the numbers of cells of R at the beginning and end of the competition, and $N_{i,S}$ and $N_{f,S}$ are the densities of cells of S at the start and end of the competition, respectively (DelaFuente et al., 2020). Each experiment was set in three parallel and repeated three times.

Biofilm Formation Assay

Biofilm formation assay was performed using crystal violet staining (Rossi Gonçalves et al., 2017). Specifically, 200 μl of bacteria suspension containing 1×10^6 CFU/ml prepared in LB broth was added to 96-well polystyrene plates (flat bottom with cover, aseptic) and incubated at 37°C for 36 h, at which time the biofilm had been attached to the bottom and wall of the well, and the culture medium was carefully removed. The wells were washed with PBS twice and fixed 15 min with methanol of 50 μl. The methanol was removed and the 0.1% crystal purple solution of 100 μl was added to stain 30 min. After cleaning the wells with PBS, 33% glacial acetic acid solution of 100 μl was added, and 30 min was incubated at 37°C. The OD value at 570 nm of each well was determined. The same operation was carried out with the LB broth without bacteria as a negative control. Experiments were performed with three biological replicates.

Galleria mellonella Infection Model

In order to evaluate the effects of three plasmids on the virulence of different receptor bacteria, *G. mellonella* larvae were used as an *in vivo* infection model (Tsai et al., 2016). Eight healthy and uniform larvae were used for each strain. The bacterial particles were washed with aseptic saline and then they were diluted with aseptic saline to an appropriate concentration. Using the Hamilton syringe of 25 μl, the bacterial liquid of 10 μl was inoculated into the left forefoot of the last pair of larvae. There were two control groups; one was inoculated with 10 μl of sterile saline, and the other received simulated injection to ensure no physical trauma. All the larvae were incubated in a constant temperature incubator at 37°C for 5 days. During this period, the larvae were observed. If the larvae no longer move when they are touched or blacken, they are considered dead. Results were analyzed by Kaplan–Meier survival curves (GraphPad Prism version 8.3.0 statistics software).

Motility Test

The method of semisolid medium was used to determine the movement ability of bacteria (Liu et al., 2020). Several single colonies were picked and were cultured in LB broth. Then, the bacteria liquid was centrifuged and resuspended with sterile saline. Meanwhile, sterile saline was used to uniformly adjust the concentration of bacteria to 0.6 McFarland. Then, 0.3% semisolid medium (3 g/L) agar plate was prepared, and the 2 μl of bacterial solution was added to the center of the semisolid medium. After the plates were incubated at 37°C for 48 h, the size of bacterial colonies was measured.

Quantitative Real-Time PCR

The absolute expression of *hns* and *tet*(X4) was detected by RT-qPCR. Firstly, *hns* and *tet*(X4) genes were, respectively, cloned into pBAD and pCE2 to generate pBAD-*hns* and pCE2-*tet*(X4). Plasmid pBAD-*hns* and pCE2-*tet*(X4) were used as template DNA with primers *hns*-RNA-F, *hns*-RNA-R, *tet*(X4)-RNA-F, and *tet*(X4)-RNA-R, respectively, to set up the corresponding standard curve. The total RNA of bacteria was extracted by Bacteria RNA Extraction Kit (Vazyme Biotech Co., Ltd) and then reverse transcribed into cDNA by 1 μg of RNA using the HiScript^R III RT SuperMix for qPCR (+gDNA wiper) Kits (Vazyme Biotech Co., Ltd), and the cDNA of 1 μl was used as template for RT-qPCR with primers *hns*-RNA-F, *hns*-RNA-R, *tet*(X4)-RNA-F, and *tet*(X4)-RNA-R using the ChamQTM Universal SYBR^R Color qPCR Master Mix Kits (Vazyme Biotech Co., Ltd). According to the standard curve, the absolute expression of *hns* and *tet*(X4) genes was calculated. The specific sequence of the primers is shown in **Supplementary Table 3**.

Determination of Uronic Acid Content

The strains in the exponential growth phase 400 μl were harvested by centrifugation at 8,000 × *g* for 10 min at 4°C and washed with 500 μl of 1 × PBS three times. Next, the

bacteria were resuspended in 500 μl of Tris-HCl buffer (pH = 7.0) and centrifuged at 8,000 × *g* for 5 min at 4°C to remove the supernatant and then resuspended with 500 μl of Tris-HCl buffer again. Subsequently, 2.4 ml of 12.5 mM tetraborate solution was mixed and heated at 100°C for 5 min. All of the samples were placed in ice, and 40 μl of 15% *m*-hydroxybiphenyl solution was added to each sample. Thorough mixing was needed. Finally, the concentration of each sample was detected in UV-visible spectroscopy reader at 520 nm (Zheng et al., 2020).

Statistical Analysis

Data are expressed as mean ± standard deviations (SD), and analyzed by either a non-parametric one-way ANOVA, unpaired *t*-test, or two-way ANOVA. Statistical analysis was conducted using GraphPad Prism version 8.3.0 statistics software. Results were considered significant with $p < 0.05$.

RESULTS

The Distribution of *hns* in IncX1-Type *tet*(X4)-Positive Plasmids

To understand the epidemic characteristics of *tet*(X4)-positive plasmids, the replicon types of a total of 51 *tet*(X4)-positive plasmids from different bacteria in NCBI database were analyzed. We found that the plasmids with multiple replicon types were the most common in *tet*(X4)-positive plasmids, while IncX1 plasmids were dominant in single replicon plasmid types, accounting for 72.2% (**Figure 1A**). Then, the genome sequences of these IncX1 plasmids were analyzed, and it was found that nearly half of the plasmids carry *hns* gene (46.16%) (**Figure 1B**). Combining these results, we hypothesized that H-NS protein may play an unappreciated role in the widespread prevalence of *tet*(X4)-harboring IncX1 plasmids.

Analysis of Fitness of *tet*(X4)-Positive Plasmids Encoding Histone-Like Nucleoid Structuring Protein

Three *hns* and *tet*(X4)-positive IncX1 plasmids, including pRF14-1, pSC4R, and pRF14-1, were applied as models to explore the role of H-NS protein in the prevalence of *tet*(X4) gene. Considering that fitness cost elicited by resistance plasmids directly affects the dissemination of resistance genes, we hypothesize that H-NS protein may modulate the fitness of host bacteria, which is critical for the transmission of plasmids. To test this hypothesis, these three plasmids were transferred into three recipient bacteria involving *E. coli* TOP10 (abbreviated as ECTOP10), *K. pneumoniae* ATCC700603 (abbreviated as KP700603), and *S.* Enteritidis ATCC13076 (abbreviated as SE13076) separately, and a total of nine transformants were obtained and designated as ECTOP10/pRF14-1, ECTOP10/pSC4R, ECTOP10/pHS14-2, KP700603/pRF14-1, KP700603/pSC4R, KP700603/pHS14-1, SE13076/pRF14-1, SE13076/pSC4R, and SE13076/pHS14-2, respectively. We analyzed the fitness of these nine transformants and their corresponding recipient bacteria, and determined their growth curve, relative fitness, and plasmid stability. Except for the slight slow growth of SE13076/pRF14-1, there was no significant difference in the growth curve in other transformants compared with recipient bacteria (**Figures 2A–C**). These results showed that the three *tet*(X4)-positive IncX1 plasmids encoding H-NS protein did not affect the growth rate of host bacteria, implying that the acquisition of these plasmids has no antagonistic effect on the growth of host cells.

Next, the *in vitro* competitive test, the most direct method for fitness evaluation (DelaFuente et al., 2020), was used to assess the fitness cost of three plasmids in different hosts. In ECTOP10 and KP700603, these three plasmids did not show obvious fitness cost at both three time points (**Figures 2D,E**), which were in agreement with the results of growth kinetics. It is demonstrated that the fitness cost is the key factor affecting the replacement rate of drug-resistant bacteria by sensitive bacteria (De Gelder et al., 2004). These results implied that the prevalence of *tet*(X4)-positive IncX1 plasmids may be due to their small fitness cost on host bacteria. Moreover, we found that even without antibiotic pressure, these three plasmids still conferred a fitness advantage in ECTOP10 during 40 passages (**Supplementary Figure 2**). In contrast, in SE13076 host bacteria, plasmids pRF14-1 and pHS14-2 showed a high fitness cost, especially after 24 h, whereas plasmid pSC4R did not show obvious fitness cost (**Figure 2F**).

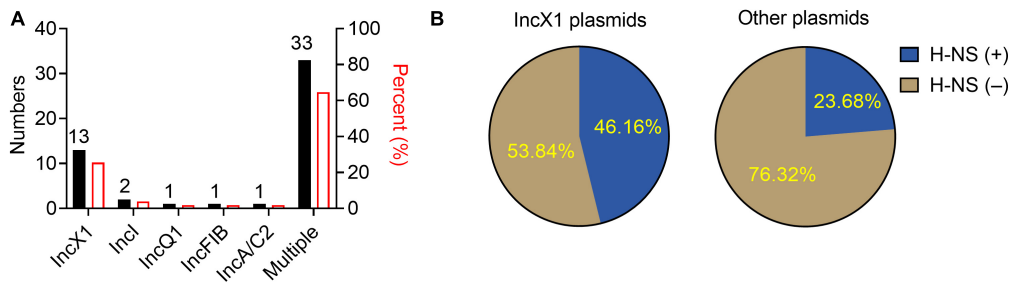

FIGURE 1 | IncX1 type is dominant in *tet*(X4)-bearing plasmids encoding H-NS from NCBI database. **(A)** The histogram shows plasmid typing and proportion of *tet*(X4)-positive plasmids from NCBI database. The black columns represent the numbers of *tet*(X4)-positive plasmids in different types. The red columns represent the corresponding percentage. **(B)** The left side of the pie graph shows the carrying rate of *hns* in *tet*(X4)-positive IncX1 plasmids. On the right is the carrying rate of *hns* gene in other types of plasmids.

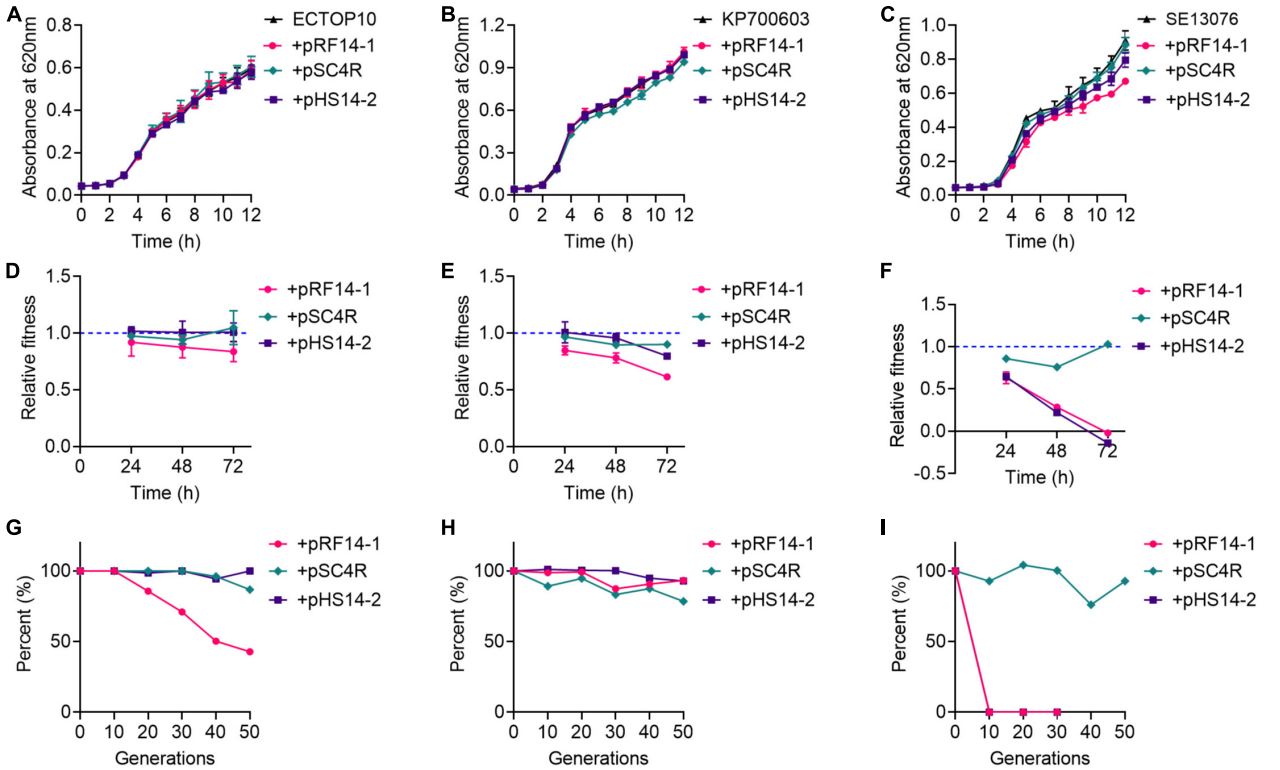

FIGURE 2 | *tet*(X4)-positive IncX1 plasmids encoding H-NS protein displays low fitness cost in host bacteria. **(A–C)** Growth curves of transformants with *E. coli* TOP10 **(A)**, *K. pneumoniae* ATCC700603 **(B)**, or *S.* Enteritidis ATCC13076 **(C)** as recipient strains. **(D–F)** Relative fitness of transformants with *E. coli* TOP10 **(D)**, *K. pneumoniae* ATCC 700603 **(E)**, or *S.* Enteritidis ATCC13076 **(F)** as recipient strains at 24, 48, and 72 h. **(G–I)** Plasmid stability in three recipient strains, including *E. coli* TOP10 **(G)**, *K. pneumoniae* ATCC700603 **(H)**, or *S.* Enteritidis ATCC13076 **(I)**. Data are representative of three biological replicates and shown as mean ± SD.

The high cost of resistance plasmids may also be manifested by the instability of plasmids in host bacteria (Wu et al., 2021). To fully understand the dissemination of *tet*(X4)-positive IncX1 plasmids, we investigated the stability of these plasmids in three host bacteria. The strains carrying plasmids were passaged for 25 days (a total of 50 generations) in the absence of drugs, and then the loss rate of plasmids at every 10 generations was detected. We found that plasmids pSC4R and pHS14-2 showed good stability in both ECTOP10 and KP7000603. The plasmid pRF14-1 had good stability in KP700603, but in ECTOP10, it began to be lost at the 10th generation, and the plasmid loss rate reached about 60% by the 50th generation (**Figures 2G,H**). For SE13076, the plasmid pSC4R showed good stability, while the other two plasmids were unstable and completely lost in the 10th generation (**Figure 2I**). The instability of these two plasmids in SE13076 may due to the low compatibility between plasmids and host bacteria. Thus, the high fitness cost of pRF14-1 and pHS14-2 in SE13076 may be attributed to their poor stability. Further conjugation experiments indicated that plasmid pRF14-1 had the highest conjugation frequency (**Supplementary Figure 3**), which may partly affect its stability in the recipient. Consistently, a previous study has shown that conjugation can easily offset the fitness cost of plasmids (Lopatkin et al., 2017), especially the high conjugation frequency. Combining with *in vitro* competition experiments and growth kinetics, these results indicate that *tet*(X4)-positive IncX1 plasmids carrying *hns* gene display great fitness advantages in various host bacteria.

Effect of *tet*(X4)-Positive Plasmids on Virulence of Host Bacteria

It is suggested that the fitness cost of antibiotic resistance plasmids may result in virulence reduction of host bacteria (Yang et al., 2017). To analyze the impact of *tet*(X4)-positive plasmids on the virulence of host cells, we first used the *Galleria mellonella* infection model to evaluate the pathogenicity changes of host bacteria after obtaining resistance plasmids. Interestingly, results showed that the carriage of plasmid pSC4R remarkably enhanced the virulence of host bacteria, while plasmid pRF14-1 reduced bacterial pathogenicity to larvae. However, the adoption of plasmid pHS14-2 showed different effect in three host bacteria (**Figures 3A–C**).

The formation of dormant or biofilm-grown cells has been one of the important ways for bacteria to adapt to the environmental pressure such as antibiotic killing (Flemming et al., 2016). Thus, we next investigated the effect of *tet*(X4)-positive IncX1 plasmids on the biofilm formation in host bacteria using crystal violet staining. These results showed that the introduction of plasmid pSC4R and pHS142 is able to significantly enhance the biofilm formation ability of ECTOP10 and SE13076, while plasmid

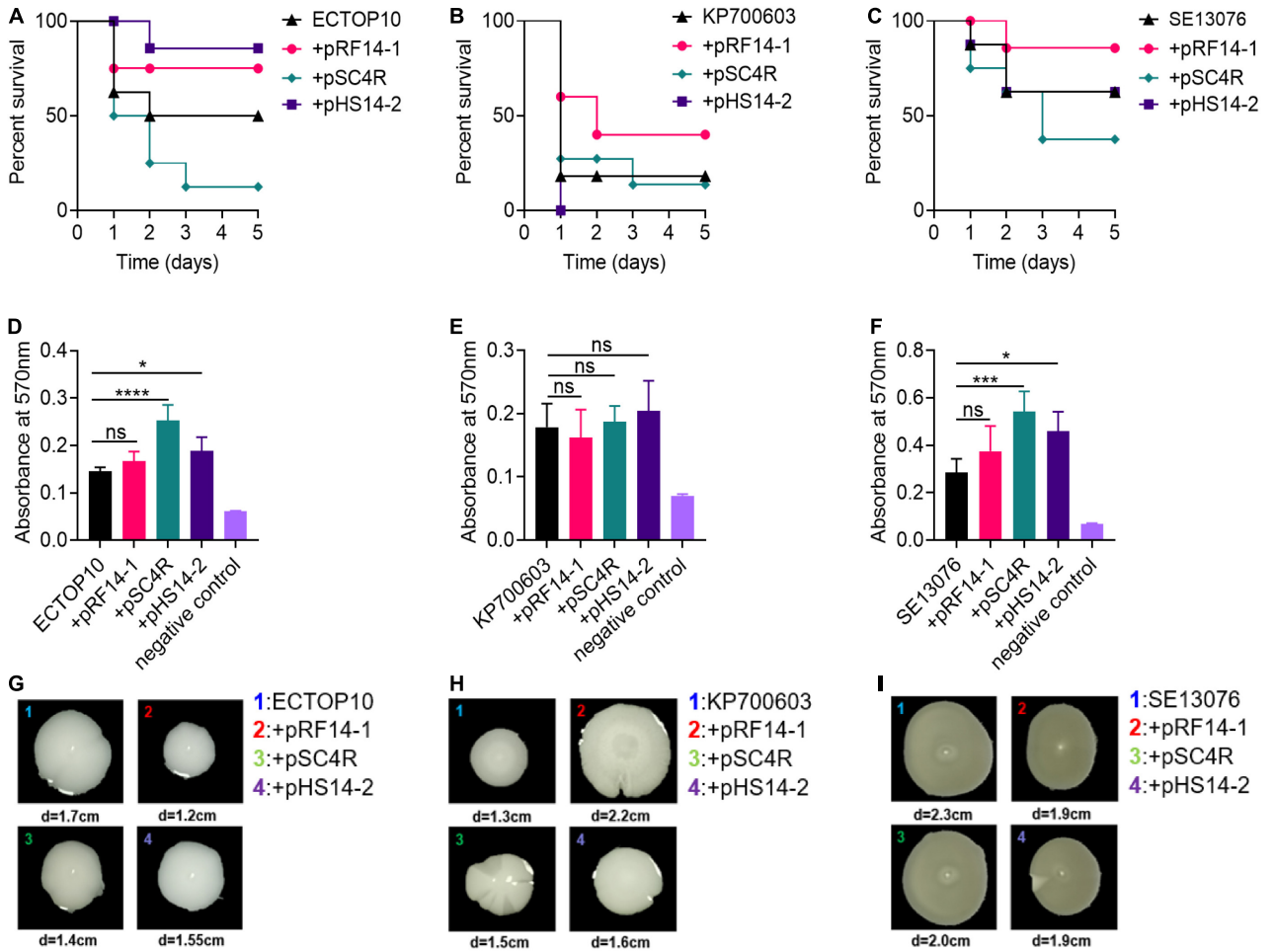

FIGURE 3 | Effect of *tet*(X4)-bearing IncX1 plasmids encoding H-NS on the virulence phenotype of different recipient strains. **(A–C)** Survival of *G. mellonella* larvae infected by recipient strains and corresponding transformants, including *E. coli* TOP10 **(A)**, *K. pneumoniae* ATCC700603 **(B)**, or *S.* Enteritidis ATCC13076 **(C)**. **(D–F)** Biofilm formation ability of three recipient strains and corresponding transformants, including *E. coli* TOP10 **(D)**, *K. pneumoniae* ATCC700603 **(E)**, or *S.* Enteritidis ATCC13076 **(F)**. Biofilm mass was monitored using crystal violet staining. Data are representative of three biological replicates and shown as mean ± SD. *p*-values were determined using a non-parametric one-way ANOVA (*$p < 0.05$; ***$p < 0.001$; ****$p < 0.0001$; ns, not significant). **(G–I)** Swimming motility of three recipient strains and corresponding transformants. The mean diameters from three biological replicates were shown.

pRF14-1 had no obvious effect on the biofilm generation in three host bacteria. In addition, the presence of three *tet*(X4)-positive plasmids did not influence the biofilm production in KP700603 (**Figures 3D–F**).

The swimming motility of bacteria is associated with the invasiveness and adhesion of pathogenic bacteria and thereby serves as an important indicator of bacterial virulence (Brunelle et al., 2017). Although the genes encoding bacterial flagella are usually on chromosomes (Samatey et al., 2001), the intake of plasmids will change the bacterial regulatory network (Li et al., 2020a), and the expression of plasmid genes will be strictly regulated accordingly. We compared the movement ability of bacteria with or without *tet*(X4)-positive IncX1 plasmids on 0.3% (w/v) agar media. In ECTOP10, plasmid pRF14-1 mildly reduced the movement ability of recipient bacteria, but markedly enhanced the swimming motility of KP700603 (**Figures 3G,H**). Considering that *K. pneumoniae* lack flagella, we supposed that the motility phenotype may be attributed to the capsule overproduction. Thus, we determined the capsule production of KP700603 and its transformants. Consistently, the results showed that plasmids pRF14-1 and pHS14-2 significantly increased the production of capsule in *K. pneumoniae* (**Supplementary Figure 4**). With regard to SE13076, these three plasmids had no remarkable effect on bacterial motility (**Figure 3I**). Collectively, our data suggest that the host bacteria commonly maintain their virulence, biofilm production, and motility after obtaining *tet*(X4)-positive plasmids carrying *hns* gene.

Histone-Like Nucleoid Structuring Protein Reduces the Fitness Cost Elicited by *tet*(X4)-Positive Plasmids

To understand whether H-NS really plays a direct role in plasmid fitness, we conducted a regression analysis of the relationship

between the relative fitness of plasmid-bearing host bacteria and the expression of *hns* gene by RT-qPCR analysis. Ct values were used to represent the expression of *hns*; the smaller the Ct, the higher the expression of *hns* gene. Interestingly, we found that the Ct value of *hns* was negatively correlated with the relative fitness of *tet*(X4)-positive plasmids in host bacteria (**Figure 4A**), indicating that plasmid-encoded H-NS protein was positively linked with the relative fitness. To further verify this finding, we tried to construct the *hns*-deletion plasmid using both CRISPR-Cas9 or λRed homologous recombination. However, we failed to obtain the *hns*-deficient plasmid without changes in the plasmid backbone. We speculated that the presence of *hns* gene is critical for the stability of clinical *tet*(X4)-positive plasmids. To address this issue, we cloned *hns* gene into pCE2 vector and successfully constructed pCE2::*hns*. A *tet*(X4)-positive IncX1 plasmid pRF55-1 without *hns* gene was introduced into ECTOP10. Subsequently, we compared the fitness of ECTOP10/pRF55-1 transformant before and after the introduction of plasmid pCE2::*hns*. Consistent with the regression analysis, we found that the fitness of TOP10/pRF55-1 was markedly improved after the acquisition of plasmid pCE2::*hns* (**Figure 4B**). These data support our hypothesis that H-NS protein can regulate the fitness cost induced by *tet*(X4)-positive plasmids in bacteria.

Fitness and *hns* Expression of Bacteria Carrying *tet*(X4)-Positive Plasmids Under Different Nutritional Conditions

Previous studies have reported that the expression of *hns* gene is negatively correlated with the concentration of intracellular (p)ppGpp (Brandi et al., 2020). Thus, it is plausible that the accumulation of (p)ppGpp under the condition of nutrient deficiency would lead to the inhibition of *hns* expression. To further strengthen our findings on the relationship between *hns* expression and fitness of *tet*(X4)-positive plasmids, we determined the relative fitness of host bacteria carrying *tet*(X4)-positive plasmids under different nutritional conditions, including brain heart infusion (BHI) high nutrition broth, LB broth, and M9CA(M9) broth low nutrition medium. Consistently, host bacteria showed the highest fitness in BHI broth, but relatively low fitness in M9 medium (**Figures 5A–C**). In addition, we measured the expression of *hns* gene in BHI high nutrition broth and LB common broth using SE13076 carrying *tet*(X4)-positive plasmids as a representative strain. Due to the lack of nutrition in M9 medium, the bacteria could not be expanded in enough numbers for following RNA extraction. As expected, we found that the expression of *hns* gene in BHI broth was higher than that in LB broth (**Figure 5D**). Taken together, our findings reveal that the altered *hns* expression in host bacteria carrying *tet*(X4)-positive plasmids under different nutritional conditions is related to their fitness changes.

Negative Correlation Between the Expression of *hns* and *tet*(X4) Gene

Having shown that plasmid-encoded H-NS protein plays an important role in the fitness of *tet*(X4)-bearing IncX1 plasmids, we next explored how H-NS regulates the adaptive cost of resistance plasmids in bacteria. To this end, we determined the correlation between the expression of *tet*(X4) and *hns* genes in SE13076 transformant. Interestingly, we found that the expression of *hns* in SE13076 carrying plasmids pRF14-1 or pHS14-2 was negatively correlated with that of *tet*(X4), while there was no significant relationship between *hns* and *tet*(X4) expresssion in plasmid pSC4R (**Figure 6**). In line with the previous relative fitness and stability results, the low relative fitness and instability of plasmids pRF14-1 or pHS14-2 in SE13076 may be attributed by the low expression of *hns* and the high expression of *tet*(X4) gene. By contrast, the better fitness advantage and stability of plasmid pSC4R may be caused by high expression of *hns* gene. Together, these results suggest that H-NS modulates fitness of *tet*(X4)-bearing IncX1 plasmids in Gram-negative bacteria by altering the expression of tigecycline resistance gene *tet*(X4).

DISCUSSION

The dissemination of *tet*(X4)-positive IncX1 plasmids have attracted much attention because it confers high level resistance to tigecycline, a clinically relevant antibiotic for Gram-negative bacterial infections (Ding et al., 2020; Li et al., 2020c). However, it remains unclear how *tet*(X4)-bearing IncX1 plasmids adapt to new hosts and further spread in various Gram-negative

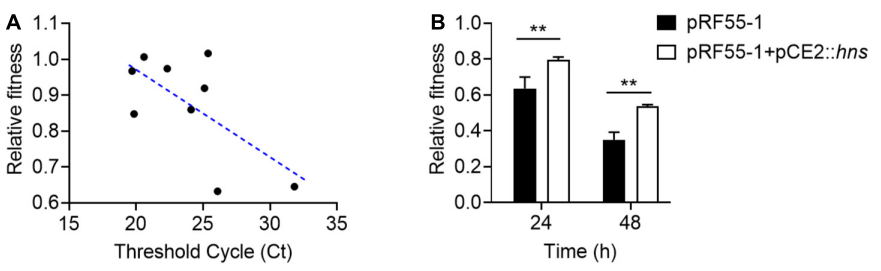

FIGURE 4 | H-NS has a critical role in the fitness of *tet*(X4)-positive IncX1 plasmids. **(A)** Negative correlation between relative fitness and *hns* Ct value by quantitative real-time PCR. **(B)** The presence of H-NS protein improves the relative fitness of *E. coli* TOP10 carrying plasmid pRF55-1. Plasmid pRF55-1 is *tet*(X4)-bearing IncX1 plasmid without *hns* gene. Data are representative of three biological replicates and shown as mean ± SD. *p*-values were determined by unpaired *t*-test (**$p < 0.01$).

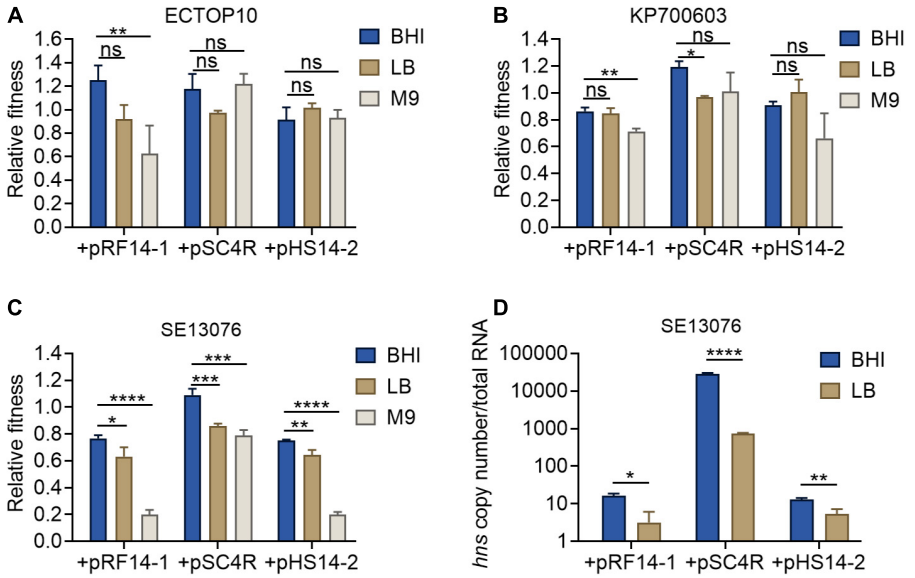

FIGURE 5 | Fitness and *hns* expression of host bacteria under different nutritional conditions. **(A–C)** Relative fitness of transformants of *E. coli* TOP10 **(A)**, *K. pneumoniae* ATCC700603 **(B)**, or *S.* Enteritidis ATCC 13076 **(C)** carrying three *tet*(X4)-bearing IncX1 plasmids in high nutritional BHI culture, medium nutrition LB broth, and low nutrition M9 culture. *p*-values were determined using a non-parametric one-way ANOVA (**p* < 0.05, ***p* < 0.01; ns, not significant). **(D)** Absolute expression of *hns* gene in transformants of *S.* Enteritidis ATCC13076 as recipient. Data are representative of three biological replicates and shown as mean ± SD. *p*-values were determined by unpaired *t*-test (**p* < 0.05, ***p* < 0.01, ****p* < 0.001, *****p* < 0.0001; ns, not significant).

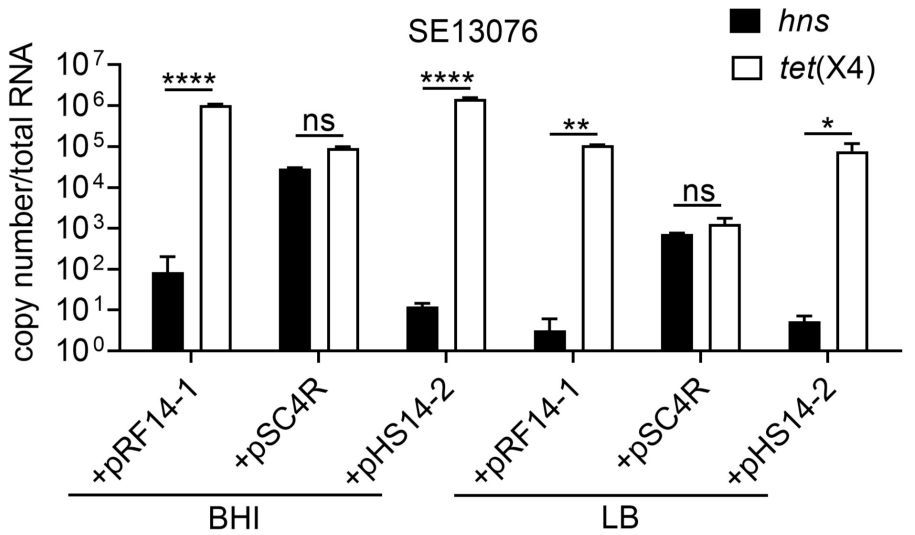

FIGURE 6 | Negative correlation between absolute expression of *hns* and *tet*(X4) gene in *S.* Enteritidis ATCC 13076 transformants under different nutritional cultures. The copy number of *hns* and *tet*(X4) in transformants using *S.* Enteritidis ATCC13076 as a recipient strain in BHI, LB, and M9 media. Data are representative of three biological replicates and shown as mean ± SD. *p*-values were determined by two-way ANOVA (**p* < 0.05; ***p* < 0.01; *****p* < 0.0001; ns, not significant).

microorganisms. In this study, we investigated the potential role of plasmid-encoded H-NS protein in the dissemination of *tet*(X4)-bearing IncX1 plasmid by monitoring bacterial growth, fitness, stability, and virulence. Interestingly, we found that the carriage of *tet*(X4)-positive plasmids encoding H-NS had low fitness cost in *E. coli* TOP10 and *K. pneumoniae* ATCC700603, rather than in *S.* Enteritidis ATCC13076. These findings support the fact that *tet*(X4) was reported in *E. coli* and *K. pneumoniae*, but not in *S.* Enteritidis (He et al., 2019; Yu et al., 2021), suggesting that the *tet*(X4)-carrying plasmids impose a high cost in *Salmonella*. It would be interesting to investigate the underlying mechanisms behind this phenomenon. Furthermore, we found that the expression of *hns* gene was positively associated with the fitness advantages of *tet*(X4)-bearing IncX1 plasmids,

indicating that H-NS plays a key role in the prevalence of *tet*(X4) genes in Gram-negative pathogens.

Accordingly, high-cost resistance plasmids will produce a burden in the host such as a reduced bacterial growth (San Millan and MacLean, 2017). For example, previous studies have reported that the high cost caused by overexpression of *mcr-1* can lead to bacterial growth defects (Yang et al., 2021) and the low-cost bla_{NDM-5}-carrying IncX3 plasmid has no significant effect on the growth of bacteria (Ma et al., 2020). Consistently, our results showed that three *tet*(X4)-positive plasmids carrying *hns* gene did not bring obvious growth defects to the host bacteria, suggesting that these plasmids impose a low fitness cost. There were positive and negative effects between the acquisition of antibiotic resistance and bacterial virulence (Beceiro et al., 2013). The most worrying thing is that while antibiotic resistance is acquired, the virulence of bacteria is also increasing, which will greatly increase the difficulty of clinical treatment. In this study, plasmid pSC4R significantly enhanced the virulence of three recipient bacteria to larvae, which was consistent with the results of biofilm assay. Biofilms can adhere to cells and have an anti-phagocytic effect, thus enhancing the virulence of bacteria to the body (Koo et al., 2017). In fact, the phenotype of bacterial virulence is affected by many factors; in addition to the expression of virulence genes, it may also be affected by two-component regulatory systems, antibiotic resistance, and so on (Beceiro et al., 2013). For example, the expression of homogeneous methicillin resistance in *S. aureus* affects the biofilm phenotype and reduces virulence (Rudkin et al., 2012). Therefore, we supposed that plasmid pSC4R is likely to encode virulence regulators that enhance host virulence. The virulence difference of the same plasmid in various hosts implied that the virulence of bacteria may be regulated by both the host and plasmid, which requires further exploration.

It is suggested that the epidemic plasmids were stable in host bacteria, even in the absence of antibiotic pressure, and endow the host bacteria the advantage of fitness (Cottell et al., 2012; Fischer et al., 2014). Heretofore, some mechanisms have been shown to mitigate the fitness cost to host bacteria, such as compensatory mutations in host chromosomal genomes or plasmids. For example, the mutation of chromosome gene *gac*A/*gac*S, which is involved in the regulation of secondary metabolism, can alleviate the fitness cost of the pQBR103 plasmid in *Pseudomonas fluorescens* by reducing the expression of plasmid and chromosomal genes (Harrison et al., 2015). Another study showed that the *trf* A mutation in the plasmid pMS0506 leads to a significant increase in the copy number of plasmid, which greatly improved the plasmid stability and enhanced its adaptability to the host (Sota et al., 2010). In addition to compensatory mutations, there are also some regulatory factors that can directly or indirectly modulate the fitness of the plasmid-bearing host bacteria. For instance, it has been found that the plasmid pHNSHP45 carrying *mcr-1* resistance gene encodes a hypothetical ProQ/FinO family protein PcnR, which can control the appropriate expression of *mcr-1* by inhibiting the replication of plasmids, thereby reducing the fitness cost caused by high expression of *mcr-1* (Yang et al., 2021). The toxin–antitoxin (TA) system, which was originally found on plasmids, can also maintain the stable existence of plasmids (Hayes, 2003). Besides, several studies showed that H-NS protein can inhibit the expression of high-cost genes and improve the fitness advantages of bacteria (Ali et al., 2014; Jian et al., 2016). H-NS protein can bind to the gene promoter and further inhibit the transcriptional expression of genes (Navarre et al., 2006). Reducing the cost of plasmids by inhibiting the expression of high cost genes such as ARGs on *tet*(X4)-bearing IncX1 plasmids may be a key factor for the persistence of *tet*(X4)-plasmids in bacterial populations. This view was supported by our observation that plasmids pRF14-1 and pHS14-2 with low-level of *hns* gene expression had a lower fitness in SE13076. In addition, our study also proved that when the plasmid pCE2:*hns* was introduced, the fitness of plasmid pRF55-1 without *hns* in ECTOP10 was significantly improved, which clearly indicated that H-NS could improve the fitness of *tet*(X4)-bearing IncX1 plasmids. Consistent with our findings, it is shown that H-NS family proteins can regulate the expression of genes on the plasmid and further reduce the fitness cost of plasmids (Doyle et al., 2007). Nevertheless, the detailed mechanisms underlying how H-NS protein regulate the transcription and translation of *tet*(X4) gene warrant further studies.

CONCLUSION

In conclusion, our study indicates that *tet*(X4)-bearing IncX1 plasmids carrying *hns* gene result in low fitness costs in various Gram-negative pathogens, but instead confer fitness advantages to the host such as enhanced virulence and biofilm formation. Importantly, we find that plasmid-encoded H-NS protein inhibits the expression of *tet*(X4) gene, thereby reducing the fitness cost of IncX1 plasmids. Together, these data highlight the important role of H-NS protein in the dissemination of *tet*(X4)-positive plasmids.

DATA AVAILABILITY STATEMENT

The original contributions presented in the study are included in the article/**Supplementary Material**, further inquiries can be directed to the corresponding author/s.

AUTHOR CONTRIBUTIONS

YL and ZW designed this study. WC and FT performed all experiments and wrote the draft manuscript. YL, WC, LJ, and RL analyzed the data. All authors have read and agreed to the published version of the manuscript.

FUNDING

This work was supported by the National Natural Science Foundation of China (32172907, 32002331, and 31872526), the Agricultural Science and Technology Independent Innovation Fund of Jiangsu Province [CX(20)3091 and CX(21)2010],

the China Postdoctoral Science Foundation funded project (2019M651984 and 2021T140579), a project funded by the Priority Academic Program Development of Jiangsu Higher Education Institutions (PAPD), and the Young Elite Scientists Sponsorship Program by CAST (2020QNRC001).

SUPPLEMENTARY MATERIAL

The Supplementary Material for this article can be found online at: https://www.frontiersin.org/articles/10.3389/fmicb.2021.763288/full#supplementary-material

REFERENCES

Ali, S. S., Soo, J., Rao, C., Leung, A. S., Ngai, D. H., Ensminger, A. W., et al. (2014). Silencing by H-NS potentiated the evolution of *Salmonella*. *PLoS Pathog.* 10:e1004500. doi: 10.1371/journal.ppat.1004500

Alikhan, N.-F., Petty, N. K., Ben Zakour, N. L., and Beatson, S. A. (2011). BLAST ring image generator (BRIG): simple prokaryote genome comparisons. *BMC Genomics* 12:402. doi: 10.1186/1471-2164-12-402

Alonso-Del Valle, A., León-Sampedro, R., Rodríguez-Beltrán, J., Delafuente, J., Hernández-García, M., Ruiz-Garbajosa, P., et al. (2021). Variability of plasmid fitness effects contributes to plasmid persistence in bacterial communities. *Nat. Commun.* 12:2653. doi: 10.1038/s41467-021-22849-y

Beceiro, A., Tomás, M., and Bou, G. (2013). Antimicrobial resistance and virulence: a successful or deleterious association in the bacterial world? *Clin. Microbiol. Rev.* 26, 185–230. doi: 10.1128/cmr.00059-12

Brandi, A., Giangrossi, M., Fabbretti, A., and Falconi, M. (2020). The gene of is transcriptionally down-regulated by (p)ppGpp. *Microorganisms* 8:1558. doi: 10.3390/microorganisms8101558

Brunelle, B. W., Bearson, B. L., Bearson, S. M. D., and Casey, T. A. (2017). Multidrug-resistant *Salmonella enterica* serovar *Typhimurium* isolates are resistant to antibiotics that influence their swimming and swarming motility. *mSphere* 2:e00306. doi: 10.1128/mSphere.00306-17

Choi, K.-H., Kumar, A., and Schweizer, H. P. (2006). A 10-min method for preparation of highly electrocompetent *Pseudomonas aeruginosa* cells: application for DNA fragment transfer between chromosomes and plasmid transformation. *J. Microbiol. Methods* 64, 391–397. doi: 10.1016/j.mimet.2005.06.001

Cottell, J. L., Webber, M. A., and Piddock, L. J. V. (2012). Persistence of transferable extended-spectrum-β-lactamase resistance in the absence of antibiotic pressure. *Antimicrob. Agents Chemother.* 56, 4703–4706. doi: 10.1371/journal.pone.0123039

De Gelder, L., Ponciano, J. M., Abdo, Z., Joyce, P., Forney, L. J., and Top, E. M. (2004). Combining mathematical models and statistical methods to understand and predict the dynamics of antibiotic-sensitive mutants in a population of resistant bacteria during experimental evolution. *Genetics* 168, 1131–1144. doi: 10.1534/genetics.104.033431

DelaFuente, J., Rodriguez-Beltran, J., and San Millan, A. (2020). Methods to study fitness and compensatory adaptation in plasmid-carrying bacteria. *Methods Mol. Biol.* 2075, 371–382. doi: 10.1007/978-1-4939-9877-7_26

Ding, Y., Saw, W.-Y., Tan, L. W. L., Moong, D. K. N., Nagarajan, N., Teo, Y. Y., et al. (2020). Emergence of tigecycline- and eravacycline-resistant Tet(X4)-producing *Enterobacteriaceae* in the gut microbiota of healthy Singaporeans. *J. Antimicrob. Chemother.* 75, 3480–3484. doi: 10.1093/jac/dkaa372

Dorman, C. J. (2007). H-NS, the genome sentinel. *Nat. Rev. Microbiol.* 5, 157–161. doi: 10.1038/nrmicro1598

Dorman, C. J. (2014). H-NS-like nucleoid-associated proteins, mobile genetic elements and horizontal gene transfer in bacteria. *Plasmid* 75, 1–11. doi: 10.1016/j.plasmid.2014.06.004

Doyle, M., Fookes, M., Ivens, A., Mangan, M. W., Wain, J., and Dorman, C. J. (2007). An H-NS-like stealth protein aids horizontal DNA transmission in bacteria. *Science* 315, 251–252. doi: 10.1126/science.1137550

Fischer, E. A. J., Dierikx, C. M., Van Essen-Zandbergen, A., Van Roermund, H. J. W., Mevius, D. J., Stegeman, A., et al. (2014). The IncI1 plasmid carrying the blaCTX-M-1 gene persists in in vitro culture of a *Escherichia coli* strain from broilers. *BMC Microbiol.* 14:77. doi: 10.1186/1471-2180-14-77

Flemming, H.-C., Wingender, J., Szewzyk, U., Steinberg, P., Rice, S. A., and Kjelleberg, S. (2016). Biofilms: an emergent form of bacterial life. *Nat. Rev. Microbiol.* 14, 563–575. doi: 10.1038/nrmicro.2016.94

Fu, Y., Chen, Y., Liu, D., Yang, D., Liu, Z., Wang, Y., et al. (2021). Abundance of tigecycline resistance genes and association with antibiotic residues in Chinese livestock farms. *J. Hazard. Mater.* 409:124921. doi: 10.1016/j.jhazmat.2020.124921

Gao, H., Liu, Y., Wang, R., Wang, Q., Jin, L., and Wang, H. (2020). The transferability and evolution of NDM-1 and KPC-2 co-producing *Klebsiella pneumoniae* from clinical settings. *Ebiomedicine* 51:102599. doi: 10.1016/j.ebiom.2019.102599

Gao, X., Yang, X., Li, J., Zhang, Y., Chen, P., and Lin, Z. (2018). Engineered global regulator H-NS improves the acid tolerance of E. coli. *Microb. Cell Fact.* 17:118. doi: 10.1186/s12934-018-0966-z

Harrison, E., Guymer, D., Spiers, A. J., Paterson, S., and Brockhurst, M. A. (2015). Parallel compensatory evolution stabilizes plasmids across the parasitism-mutualism continuum. *Curr. Biol.* 25, 2034–2039. doi: 10.1016/j.cub.2015.06.024

Hayes, F. (2003). Toxins-antitoxins: plasmid maintenance, programmed cell death, and cell cycle arrest. *Science* 301, 1496–1499. doi: 10.1126/science.1088157

He, T., Wang, R., Liu, D., Walsh, T. R., Zhang, R., Lv, Y., et al. (2019). Emergence of plasmid-mediated high-level tigecycline resistance genes in animals and humans. *Nat. Microbiol.* 4, 1450–1456. doi: 10.1038/s41564-019-0445-2

Hurtado-Escobar, G. A., Grépinet, O., Raymond, P., Abed, N., Velge, P., and Virlogeux-Payant, I. (2019). H-NS is the major repressor of *Salmonella Typhimurium* Pef fimbriae expression. *Virulence* 10, 849–867. doi: 10.1080/21505594.2019.1682752

Jian, H., Xu, G., Gai, Y., Xu, J., and Xiao, X. (2016). The histone-like nucleoid structuring protein (H-NS) is a negative regulator of the lateral flagellar system in the deep-sea bacterium *Shewanella piezotolerans* WP3. *Appl. Environ. Microbiol.* 82, 2388–2398. doi: 10.1128/AEM.00297-16

Koo, H., Allan, R. N., Howlin, R. P., Stoodley, P., and Hall-Stoodley, L. (2017). Targeting microbial biofilms: current and prospective therapeutic strategies. *Nat. Rev. Microbiol.* 15, 740–755.

Kuehn, B. M. (2011). Proposals seek to reduce resistance, boost development of new antibiotics. *JAMA* 305, 1845–1846. doi: 10.1001/jama.2011.598

Kumarasamy, K. K., Toleman, M. A., Walsh, T. R., Bagaria, J., Butt, F., Balakrishnan, R., et al. (2010). Emergence of a new antibiotic resistance mechanism in India, Pakistan, and the UK: a molecular, biological, and epidemiological study. *Lancet Infect. Dis.* 10, 597–602. doi: 10.1016/S1473-3099(10)70143-2

Lerminiaux, N. A., and Cameron, A. D. S. (2019). Horizontal transfer of antibiotic resistance genes in clinical environments. *Can. J. Microbiol.* 65, 34–44. doi: 10.1139/cjm-2018-0275

Li, L., Dechesne, A., Madsen, J. S., Nesme, J., Sørensen, S. J., and Smets, B. F. (2020a). Plasmids persist in a microbial community by providing fitness benefit to multiple phylotypes. *ISME J.* 14, 1170–1181. doi: 10.1038/s41396-020-0596-4

Li, R., Lu, X., Peng, K., Liu, Z., Li, Y., Liu, Y., et al. (2020b). Deciphering the structural diversity and classification of the mobile tigecycline resistance gene tet(X)-bearing plasmidome among bacteria. *mSystems* 5:e00134. doi: 10.1128/mSystems.00134-20

Li, R., Peng, K., Li, Y., Liu, Y., and Wang, Z. (2020c). Exploring tet(X)-bearing tigecycline-resistant bacteria of swine farming environments. *Sci. Total Environ.* 733:139306. doi: 10.1016/j.scitotenv.2020.139306

Liu, B., Shui, L., Zhou, K., Jiang, Y., Li, X., Guan, J., et al. (2020). Impact of plasmid-encoded H-NS-like protein on blaNDM-1-bearing IncX3 plasmid in *Escherichia coli*. *J. Infect. Dis.* 221, S229–S236. doi: 10.1093/infdis/jiz567

Liu, Y.-Y., Wang, Y., Walsh, T. R., Yi, L.-X., Zhang, R., Spencer, J., et al. (2016). Emergence of plasmid-mediated colistin resistance mechanism MCR-1 in animals and human beings in China: a microbiological and molecular biological study. *Lancet Infect. Dis.* 16, 161–168. doi: 10.1016/S1473-3099(15)00424-7

Lopatkin, A. J., Meredith, H. R., Srimani, J. K., Pfeiffer, C., Durrett, R., and You, L. (2017). Persistence and reversal of plasmid-mediated antibiotic resistance. *Nat. Commun.* 8:1689.

Lucchini, S., Rowley, G., Goldberg, M. D., Hurd, D., Harrison, M., and Hinton, J. C. D. (2006). H-NS mediates the silencing of laterally acquired genes in bacteria. *PLoS Pathog.* 2:e81. doi: 10.1371/journal.ppat.0020081

Ma, T., Fu, J., Xie, N., Ma, S., Lei, L., Zhai, W., et al. (2020). Fitness Cost of blaNDM-5-carrying p3R-IncX3 plasmids in wild-type NDM-Free *Enterobacteriaceae*. *Microorganisms* 8:377. doi: 10.3390/microorganisms8030377

Mohsin, M., Hassan, B., Martins, W. M. B. S., Li, R., Abdullah, S., Sands, K., et al. (2021). Emergence of plasmid-mediated tigecycline resistance tet(X4) gene in *Escherichia coli* isolated from poultry, food and the environment in south Asia. *Sci. Total Environ.* 787:147613. doi: 10.1016/j.scitotenv.2021.147613

Navarre, W. W., Porwollik, S., Wang, Y., Mcclelland, M., Rosen, H., Libby, S. J., et al. (2006). Selective silencing of foreign DNA with low GC content by the H-NS protein in *Salmonella*. *Science* 313, 236–238. doi: 10.1126/science.1128794

Nordmann, P., Poirel, L., Walsh, T. R., and Livermore, D. M. (2011). The emerging NDM carbapenemases. *Trends Microbiol.* 19, 588–595. doi: 10.1016/j.tim.2011.09.005

Picker, M. A., and Wing, H. J. (2016). H-NS, its family members and their regulation of virulence genes in *Shigella* species. *Genes* 7:112. doi: 10.3390/genes7120112

Rodríguez-Baño, J., Gutiérrez-Gutiérrez, B., Machuca, I., and Pascual, A. (2018). Treatment of infections caused by extended-spectrum-beta- lactamase-, ampc-, and carbapenemase-producing *Enterobacteriaceae*. *Clin. Microbiol. Rev.* 31:e79.

Rossi Gonçalves, I., Dantas, R. C. C., Ferreira, M. L., Batistão, D. W. D. F., Gontijo-Filho, P. P., and Ribas, R. M. (2017). Carbapenem-resistant *Pseudomonas aeruginosa*: association with virulence genes and biofilm formation. *Braz. J. Microbiol.* 48, 211–217. doi: 10.1016/j.bjm.2016.11.004

Rudkin, J. K., Edwards, A. M., Bowden, M. G., Brown, E. L., Pozzi, C., Waters, E. M., et al. (2012). Methicillin resistance reduces the virulence of healthcare-associated methicillin-resistant Staphylococcus aureus by interfering with the agr quorum sensing system. *J. Infect. Dis.* 205, 798–806. doi: 10.1093/infdis/jir845

Samatey, F. A., Imada, K., Nagashima, S., Vonderviszt, F., Kumasaka, T., Yamamoto, M., et al. (2001). Structure of the bacterial flagellar protofilament and implications for a switch for supercoiling. *Nature* 410, 331–337. doi: 10.1038/35066504

San Millan, A. (2018). Evolution of plasmid-mediated antibiotic resistance in the clinical context. *Trends Microbiol.* 26, 978–985.

San Millan, A., and MacLean, R. C. (2017). Fitness costs of plasmids: a limit to plasmid transmission. *Microbiol. Spectr.* 5:16.

Sota, M., Yano, H., Hughes, J. M., Daughdrill, G. W., Abdo, Z., Forney, L. J., et al. (2010). Shifts in the host range of a promiscuous plasmid through parallel evolution of its replication initiation protein. *ISME J.* 4, 1568–1580. doi: 10.1038/ismej.2010.72

Sullivan, M. J., Petty, N. K., and Beatson, S. A. (2011). Easyfig: a genome comparison visualizer. *Bioinformatics* 27, 1009–1010. doi: 10.1093/bioinformatics/btr039

Sun, J., Chen, C., Cui, C.-Y., Zhang, Y., Liu, X., Cui, Z.-H., et al. (2019). Plasmid-encoded tet(X) genes that confer high-level tigecycline resistance in *Escherichia coli*. *Nat. Microbiol.* 4, 1457–1464. doi: 10.1038/s41564-019-0496-4

Tasina, E., Haidich, A.-B., Kokkali, S., and Arvanitidou, M. (2011). Efficacy and safety of tigecycline for the treatment of infectious diseases: a meta-analysis. *Lancet Infect. Dis.* 11, 834–844. doi: 10.1016/s1473-3099(11)70177-3

Tsai, C. J.-Y., Loh, J. M. S., and Proft, T. (2016). Galleria mellonella infection models for the study of bacterial diseases and for antimicrobial drug testing. *Virulence* 7, 214–229. doi: 10.1080/21505594.2015.1135289

Wu, J., Dong, X., Zhang, L., Lin, Y., and Yang, K. (2021). Reversing antibiotic resistance caused by mobile resistance genes of high fitness cost. *mSphere* 6:e0035621. doi: 10.1128/mSphere.00356-21

Yang, J., Wang, H.-H., Lu, Y., Yi, L.-X., Deng, Y., Lv, L., et al. (2021). A ProQ/FinO family protein involved in plasmid copy number control favours fitness of bacteria carrying mcr-1-bearing IncI2 plasmids. *Nucleic Acids Res.* 49, 3981–3996. doi: 10.1093/nar/gkab149

Yang, Q., Li, M., Spiller, O. B., Andrey, D. O., Hinchliffe, P., Li, H., et al. (2017). Balancing mcr-1 expression and bacterial survival is a delicate equilibrium between essential cellular defence mechanisms. *Nat. Commun.* 8:2054. doi: 10.1038/s41467-017-02149-0

Yu, Y., Cui, C. Y., Kuang, X., Chen, C., Wang, M. G., Liao, X. P., et al. (2021). Prevalence of tet(X4) in *Escherichia coli* from duck farms in southeast China. *Front. Microbiol.* 12:716393. doi: 10.3389/fmicb.2021.716393

Zhang, R., Dong, N., Zeng, Y., Shen, Z., Lu, J., Liu, C., et al. (2020). Chromosomal and plasmid-borne tigecycline resistance genes tet(X3) and tet(X4) in dairy cows on a Chinese farm. *Antimicrob. Agents Chemother.* 64:e674–e620. doi: 10.1128/AAC.00674-20

Zheng, Y.-D., Pan, Y., He, K., Li, N., Yang, D., Du, G.-F., et al. (2020). SPD_1495 contributes to capsular polysaccharide synthesis and virulence in *Streptococcus pneumoniae*. *mSystems* 5:e25–e20. doi: 10.1128/mSystems.00025-20

Conflict of Interest: The authors declare that the research was conducted in the absence of any commercial or financial relationships that could be construed as a potential conflict of interest.

Publisher's Note: All claims expressed in this article are solely those of the authors and do not necessarily represent those of their affiliated organizations, or those of the publisher, the editors and the reviewers. Any product that may be evaluated in this article, or claim that may be made by its manufacturer, is not guaranteed or endorsed by the publisher.

frontiers in Microbiology

ORIGINAL RESEARCH
published: 20 December 2021
doi: 10.3389/fmicb.2021.751006

Occurrence and Molecular Characterization of Abundant *tet*(X) Variants Among Diverse Bacterial Species of Chicken Origin in Jiangsu, China

Yingshan Li[1,2†], Kai Peng[1,2†], Yi Yin[1,2], Xinran Sun[1,2], Wenhui Zhang[1,2], Ruichao Li[1,2,3] and Zhiqiang Wang[1,2*]*

[1] College of Veterinary Medicine, Yangzhou University, Yangzhou, China, [2] Jiangsu Co-innovation Center for Prevention and Control of Important Animal Infectious Diseases and Zoonoses, Yangzhou, China, [3] Institute of Comparative Medicine, Yangzhou University, Yangzhou, China

OPEN ACCESS

Edited by:
Eun-Jeong Yoon,
Korea National Institute of Health,
South Korea

Reviewed by:
Lin Liu,
Zhejiang University, China
Zhi Ruan,
Zhejiang University, China

***Correspondence:**
Ruichao Li
rchl88@yzu.edu.cn
Zhiqiang Wang
zqwang@yzu.edu.cn

[†] These authors have contributed equally to this work

Specialty section:
This article was submitted to Antimicrobials, Resistance and Chemotherapy, a section of the journal Frontiers in Microbiology

Received: 31 July 2021
Accepted: 17 November 2021
Published: 20 December 2021

Citation:
Li Y, Peng K, Yin Y, Sun X, Zhang W, Li R and Wang Z (2021) Occurrence and Molecular Characterization of Abundant tet(X) Variants Among Diverse Bacterial Species of Chicken Origin in Jiangsu, China. Front. Microbiol. 12:751006. doi: 10.3389/fmicb.2021.751006

Many novel tigecycline-inactivating enzymes encoded by *tet*(X) variants from different bacteria were discovered since the plasmid-mediated *tet*(X3) and *tet*(X4) genes conferring high-level resistance to tigecycline in Enterobacterales and *Acinetobacter* were reported. However, there have been no comprehensive studies of the prevalence of different *tet*(X) variants in poultry farms. In this study, we collected 45 chicken fecal samples, isolated *tet*(X)-positive strains, and performed antimicrobial susceptibility testing, conjugation assay, whole-genome sequencing, and bioinformatics analysis. A total of 15 *tet*(X)-bearing strains were isolated from 13 samples. Species identification and *tet*(X) subtyping analysis found that the 15 strains belonged to eight different species and harbored four different *tet*(X) variants. Genomic investigation showed that transmission of *tet*(X) variants was associated with various mobile genetic elements, and *tet*(X4) was the most prevalent variant transferred by conjugative plasmids. Meanwhile, we characterized a plasmid co-harboring *tet*(X6) and bla_{OXA-58} in *Acinetobacter baumannii*. In summary, we demonstrated that different *tet*(X) variants were widely disseminated in the chicken farming environment and dominated by *tet*(X4). This finding expands the understanding of the prevalence of *tet*(X) among different animal sources, and it was advocated to reduce the usage of antibiotics to limit the emergence and transmission of novel *tet*(X) variants in the poultry industry.

Keywords: tigecycline resistance, *tet*(X), plasmids, chickens, whole-genome sequencing

INTRODUCTION

Tigecycline is a broad-spectrum antibiotic of glycylcyclines and is one of the last-resort antibiotics to treat serious infections caused by multidrug-resistant (MDR) Gram-negative bacteria (Sun et al., 2013). The mechanisms of tigecycline resistance were mainly the overexpression of non-specific active efflux pumps or mutations within the drug-binding sites in the ribosome, which were limited

by less capability of horizontal transfer among bacteria (Pournaras et al., 2016). However, the emergence and dissemination of plasmid-mediated high-level tigecycline resistance genes *tet*(X3) and *tet*(X4) are bringing formidable threats to public health (He et al., 2019; Sun J. et al., 2019). A variety of *tet*(X) variants containing *tet*(X3.2) (Li et al., 2019), *tet*(X5) (Wang et al., 2019), *tet*(X6) (He et al., 2020; Liu et al., 2020; Peng et al., 2020), and *tet*(X14) (Cheng et al., 2020) have been detected in *Empedobacter*, Enterobacterales, and *Acinetobacter* so far. These widespread *tet*(X) variants will limit treatment options for MDR bacteria infections.

The livestock industry has been a critical reservoir of resistance genes due to the abuse and misuse of antibiotics in animal agriculture. Many clinically significant resistance genes, such as *mcr-1* (Liu et al., 2016), *tet*(X3), and *tet*(X4) (He et al., 2019), were first detected in bacteria of animal origin. According to a retrospective screening project, the prevalence of *tet*(X)-positive isolates of animal source (6.9%) was much higher than that of human source (0.07%) (He et al., 2019). Recent studies also showed that the detection rate of *tet*(X) genes in isolates from animals (Cui et al., 2020; Li et al., 2020b,c) was higher than that from humans (Wang et al., 2019). Hence, it is critical to enrich more information about the animal source associated with *tet*(X)-bearing pathogens. The prevalence of *tet*(X) genes in swine farms and slaughterhouses has been systematically investigated (Li et al., 2020b,c), but the comprehensive molecular characterization of *tet*(X)-bearing bacteria of chicken was unexplored. In this study, we focused on the prevalence of *tet*(X) variants in cultivable bacteria among chicken fecal microbiota and demonstrated that *tet*(X) genes in diverse bacteria are worthy of continuous surveillance among different sources.

MATERIALS AND METHODS

Sample Collection and Bacterial Isolates

A total of 45 chicken fecal samples were collected from a chicken farm in Jiangsu Province, China, in May 2020. We incubated 0.5 g feces in 5 ml of Tryptic Soy Broth (TSB) for 6 h to perform bacteria enrichment. The *tet*(X)-positive isolates were screened by Tryptic Soy Agar (TSA) plates supplemented with tigecycline (4 mg/L) and further identified by PCR using primers previously described (He et al., 2019). The species of all *tet*(X)-positive isolates were determined by 16S rRNA gene sequencing.

Antimicrobial Susceptibility Testing

The minimum inhibitory concentrations (MICs) of all *tet*(X)-positive isolates were tested by broth microdilution according to Clinical and Laboratory Standards Institute (CLSI) guidelines (CLSI, 2018). *Escherichia coli* ATCC25922 was used for quality control. The resistance breakpoint for tigecycline was interpreted as >0.5 mg/L according to European Committee on Antimicrobial Susceptibility Testing (EUCAST)[1].

[1]http://www.eucast.org/clinical_breakpoints/

Conjugation Experiments

In order to verify the transferability of *tet*(X) genes, we conducted conjugation experiments using *E. coli* C600 and a clinical carbapenem-resistant *Acinetobacter baumannii* 5AB as recipients. Briefly, the donor and recipient strains were cultured to the logarithmic growth phase with an optical density at 600 nm (OD_{600}) of 0.4 in LB broth, mixed at a ratio of 1:1, and cultured overnight on TSB agar plates at 37°C. For the *tet*(X)-positive *Acinetobacter*, we also conducted the conjugation assay at 30°C. Then, the transconjugants were selected using TSA plates containing tigecycline (2 mg/L) and rifampin (300 mg/L) or meropenem (2 mg/L). And we further confirmed the recovered transconjugants by PCR for *tet*(X) and 16S rRNA genes. The frequencies of conjugation transfer were calculated by the number of transconjugants per recipient.

Genomic DNA Extraction and Whole-Genome Sequencing

Genomic DNA of *tet*(X)-positive isolates were extracted using FastPure Bacteria DNA Isolation Mini Kit (Vazyme^{TM}, Nanjing, China) following the manufacturer's instruction. The quality and purity of genomic DNA were evaluated by Qubit 4 Fluorometer (Thermo Fisher Scientific^{TM}, Hennigsdorf, Germany) and Titertek-Berthold Colibri (Berthold^{TM}, Bad Wildbad, Germany). The genomic DNA of all *tet*(X)-positive isolates was subjected to the short-read sequencing (2 × 150 bp) by Illumina Hiseq 2500 platform. According to the assembly result of short-read sequencing, the genomic DNA of isolates with different *tet*(X) genetic contexts was further sequenced by long-read sequencing platform Oxford Nanopore Technologies MinION with a rapid barcoding library preparation strategy.

Bioinformatics Analysis

De novo short-read assembly was performed using SPAdes (Bankevich et al., 2012). The complete bacterial genomes were obtained using a hybrid assembly strategy combining long-read Nanopore and short-read Illumina sequencing data (Wick et al., 2017; Li R. et al., 2018). Antibiotic resistance genes, insertion sequence (IS) elements, and plasmid replicon types were identified by CGE services.[2] The draft genomes were annotated by Prokka (Seemann, 2014). Functional annotation of the complete genome sequences was annotated automatically using the RAST[3] and modified manually. Multilocus sequence typing (MLST) of assembled bacterial genomes was performed using the mlst tool[4] and Pubmlst.[5] The complete genomes of *tet*(X4)-bearing *E. coli* were downloaded from nr database in the National Center for Biotechnology Information (NCBI). The phylogenetic tree of strains was constructed using Roary and FastTree based on single-nucleotide polymorphisms (SNPs) of core genomes with default parameters (Price et al., 2009; Page et al., 2015). BRIG and Easyfig tools were used to visualize

[2]https://cge.cbs.dtu.dk/services/

[3]http://rast.nmpdr.org/

[4]https://github.com/tseemann/mlst

[5]https://pubmlst.org/

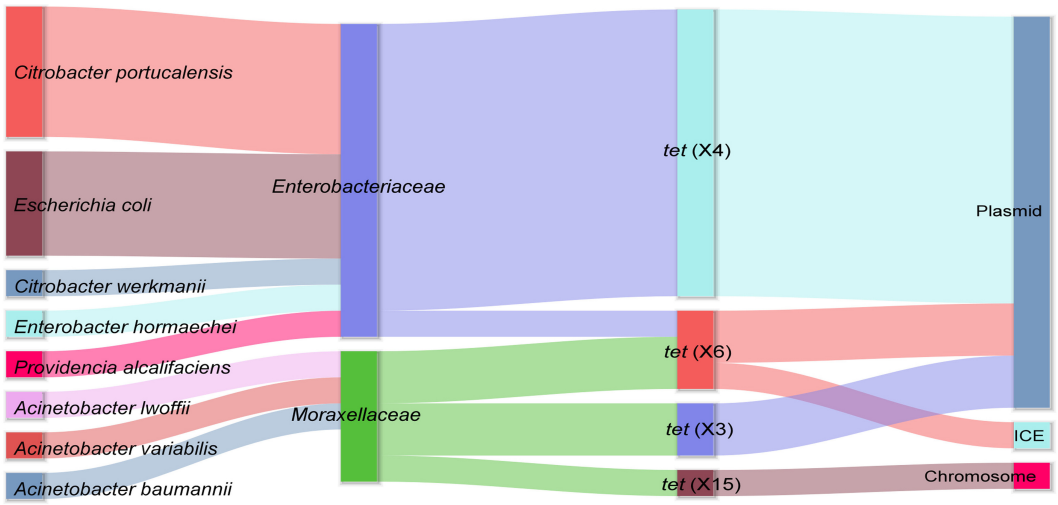

FIGURE 1 | The distribution of *tet*(X)-positive strains and the location of different *tet*(X) variants. The sankey diagram shows the host range diversity and genetic structure features of *tet*(X) variants investigated in this study.

TABLE 1 | Antimicrobial susceptibility testing (MICs, mg/L) of 15 *tet*(X)-positive strains and their transconjugants.

Strain	Source	Conjugation frequency to C600	ST type	Species	Antimicrobials							
					AMX	ENR	CFF	MEM	CL	KAN	TIG	FFC
SC2-6	Feces	/	284	*Citrobacter portucalensis*	>256	16	1	≤0.25	≤0.25	>128	32	>128
cSC2-6	Transconjugant	2.8×10^{-9}	/	*Escherichia coli*	>256	16	1	≤0.25	≤0.25	4	16	>128
LHC3	Feces	/	284	*C. portucalensis*	>256	16	1	≤0.25	≤0.25	>128	64	>128
cLHC3	Transconjugant	1.9×10^{-9}	/	*E. coli*	>256	16	1	≤0.25	≤0.25	8	32	>128
LHC31-1	Feces	/	284	*C. portucalensis*	>256	32	1	≤0.25	≤0.25	>128	32	>128
cLHC31-1	Transconjugant	3.9×10^{-11}	/	*E. coli*	>256	4	1	≤0.25	≤0.25	4	8	>128
XMY1F802-7	Feces	/	284	*C. portucalensis*	>256	16	0.5	≤0.25	≤0.25	4	64	128
cXMY1F802-7	Transconjugant	3.9×10^{-11}	/	*E. coli*	>256	4	0.5	≤0.25	≤0.25	4	64	>128
XM10F302-7	Feces	/	284	*C. portucalensis*	>256	32	1	≤0.25	≤0.25	>128	128	>128
cXM10F302-7	Transconjugant	1.4×10^{-10}	/	*E. coli*	>256	32	1	≤0.25	≤0.25	≤0.25	64	>128
LHC5-1	Feces	/	novel	*Citrobacter werkmanii*	>256	16	16	≤0.25	≤0.25	32	64	>128
cLHC5-1	Transconjugant	1.3×10^{-9}	/	*E. coli*	>256	0.5	≤0.25	≤0.25	≤0.25	≤0.25	32	>128
XM3F402-1	Feces	/	93	*E. coli*	>256	4	≤0.25	≤0.25	≤0.25	8	32	>128
cXM3F402-1	Transconjugant	4×10^{-11}	/	*E. coli*	>256	0.5	≤0.25	≤0.25	≤0.25	4	16	>128
XMC1F102-2	Feces	/	93	*E. coli*	>256	4	≤0.25	≤0.25	≤0.25	4	32	>128
cXMC1F102-2	Transconjugant	NA	/	*E. coli*	>256	4	≤0.25	≤0.25	≤0.25	4	16	>128
XM3F402-7	Feces	/	1,286	*E. coli*	>256	4	≤0.25	≤0.25	≤0.25	>128	64	>128
cXM3F402-7	Transconjugant	4×10^{-11}	/	*E. coli*	>256	4	≤0.25	≤0.25	≤0.25	≤0.25	16	>128
XM7F102	Feces	/	155	*E. coli*	>256	32	>64	≤0.25	≤0.25	8	32	>128
cXM7F102	Transconjugant	NA	/	*E. coli*	>256	2	≤0.25	≤0.25	≤0.25	4	16	>128
LHC3-2	Feces	/	327	*Enterobacter hormaechei*	>256	4	32	≤0.25	≤0.25	8	32	>128
cLHC3-2	Transconjugant	NA	/	*E. coli*	>256	4	≤0.25	≤0.25	≤0.25	4	16	128
LHC2-1	Feces	/	/	*Providencia alcalifaciens*	>256	8	32	≤0.25	>128	>128	>128	>128
XM9F202-2	Feces	/	/	*Acinetobacter variabilis*	2	4	4	≤0.25	≤0.25	>128	32	>128
XMC5X702	Feces	/	/	*Acinetobacter lwoffii*	128	0.5	1	≤0.25	≤0.25	8	32	>128
LHC22-2	Feces	/	1,459	*Acinetobacter baumannii*	>256	32	32	1	≤0.25	16	64	128

NA, not available. The transfer frequencies of these samples were too low to be calculated accurately.
MICs, minimum inhibitory concentrations; ST, sequence typing; AMX, amoxicillin; ENR, enrofloxacin; CFF, ceftiofur; MEM, meropenem; CL, colistin; KAN, kanamycin; TIG, tigecycline; FFC, florfenicol.

plasmid comparisons (Alikhan et al., 2011) and genetic context comparisons (Sullivan et al., 2011).

RESULTS

Characterization of Tigecycline-Resistant Strains

Out of 45 chicken fecal samples, a total of 15 *tet*(X)-positive strains were isolated from 13 samples (13/45, 28.89%). These *tet*(X)-positive strains consisted of eight different species including five *Citrobacter portucalensis*, four *E. coli*, one *Enterobacter hormaechei*, one *Citrobacter werkmanii*, one *Acinetobacter variabilis*, one *Acinetobacter lwoffii*, one *A. baumannii*, and one *Providencia alcalifaciens*. Meanwhile, four different *tet*(X) variants were detected in these strains, containing *tet*(X3), *tet*(X4), and *tet*(X6) reported previously and a novel *tet*(X) variant, designated as *tet*(X15) in another study (Li et al., 2021; **Figure 1**). Among them, *tet*(X4) carried by Enterobacteriaceae was the most pervasive. Although three different *tet*(X) variants, *tet*(X3), *tet*(X6), and the novel *tet*(X15), were found in *Acinetobacter*, all of them showed low prevalence. Notably, the phenomenon that such a number of *tet*(X) variants were distributed in bacteria with different species within a farm was not observed in other studies. The extensive prevalence of *tet*(X) genes in this chicken farm

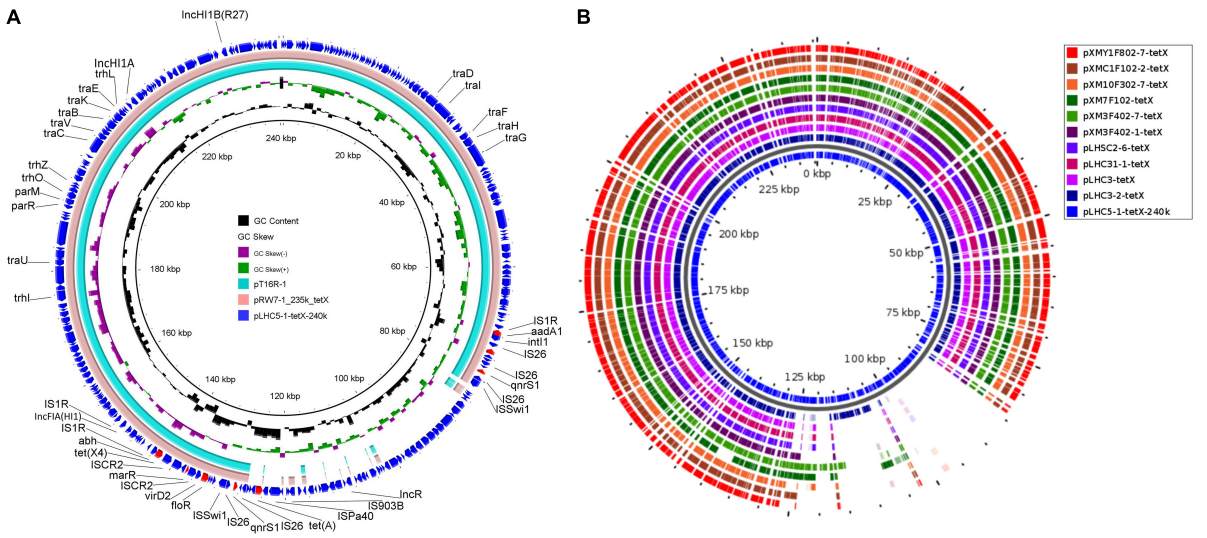

FIGURE 2 | Structure analysis of *tet*(X4)-bearing plasmids. **(A)** Comparison analysis of the plasmid pLHC5-1-tetX-240k with other similar plasmids including pRW7-1_235k_tetX (GenBank accession_number: MT219825) and pT16R-1 (CP046717). **(B)** Structure features of *tet*(X4)-bearing plasmids carried by Enterobacteriaceae in this study. The structural diversity of these plasmids existed within a multidrug-resistant (MDR) region. Resistance genes in plasmid pLHC5-1-tetX-240k were highlighted in red arrows. The reference sequence in panel **(B)** is pLHC5-1-tetX-240k, and colored circles indicate the sequences in draft genomes, which are mapped to the reference sequence.

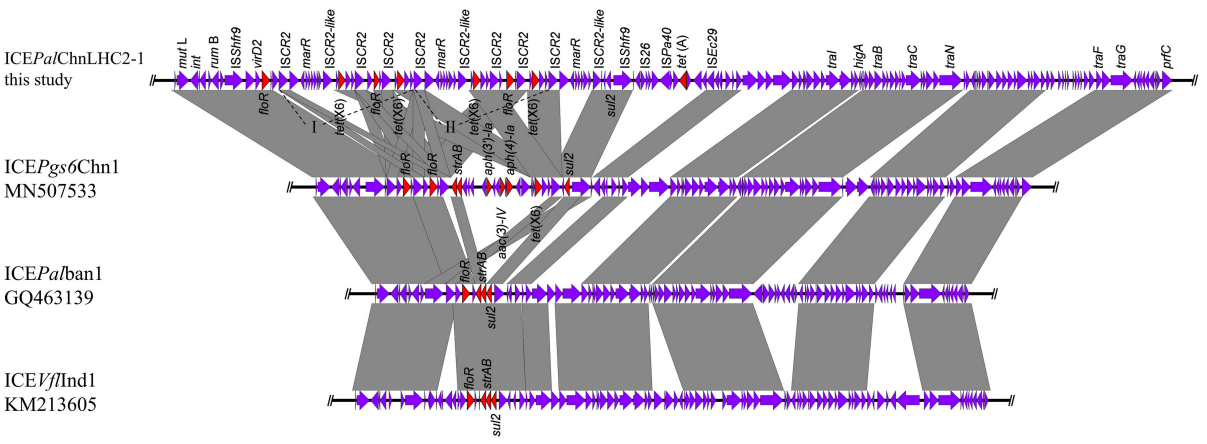

FIGURE 3 | Linear comparison of the *tet*(X6)-bearing integrative and conjugative element (ICE) ICE*Pal*ChnLHC2-1 with other similar ICEs. The multidrug-resistant (MDR) region encoding *tet*(X6) was inserted into variable region III conserved in ICEs.

suggested that poultry may be an important reservoir of *tet*(X), and the *tet*(X) genes are likely to be transmitted to humans through environmental interactions and chicken consumption (Sun et al., 2020).

Although *tet*(X4)-harboring *E. coli* was the most dominant in other research (He et al., 2019; Sun C. et al., 2019; Li et al., 2020a,b; Mohsin et al., 2021), *tet*(X4)-harboring *E. coli* of chicken source was rarely reported previously (Mohsin et al., 2021). To

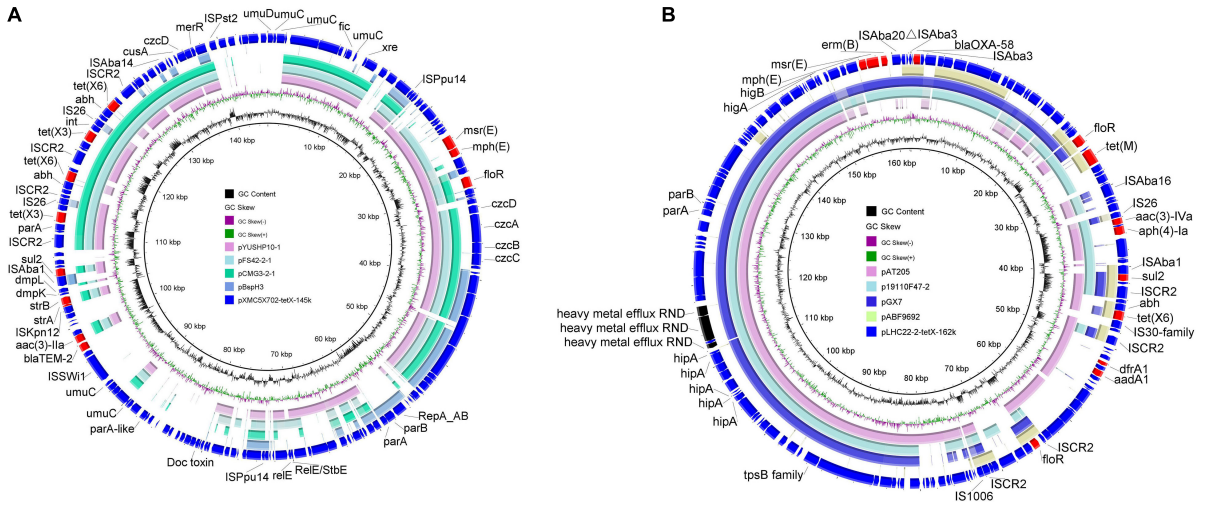

FIGURE 4 | Circular comparisons between *tet*(X)-positive plasmids of *Acinetobacter* origin in this study and similar plasmids in the National Center for Biotechnology Information (NCBI) database. **(A)** Comparative analysis of pXMC5X702-tetX-145k with four closely related plasmids including pBspH3 (GenBank accession_number: CP055285), pCMG3-2-1 (CP044446), pFS42-2-1 (CP046596), and pYUSHP10-1 (MT107270). pXMC5 × 102-tetX-145k was used as the reference plasmid. **(B)** Comparative analysis of pLHC22-2-tetX-162k with four closely related plasmids including pABF9692 (CP048828), pGX7 (CP071772), p19110F47-2 (CP046044), and pAT205 (CP048015). Plasmid pBspH3 in panel **(A)** shared the same replicon gene with plasmid pXMC5X702-tetX-145k. Plasmid pABF9692 co-harbored *tet*(X6) and bla_{OXA-58} but shared limited homologous regions with plasmid pLHC22-2-tetX-162k.

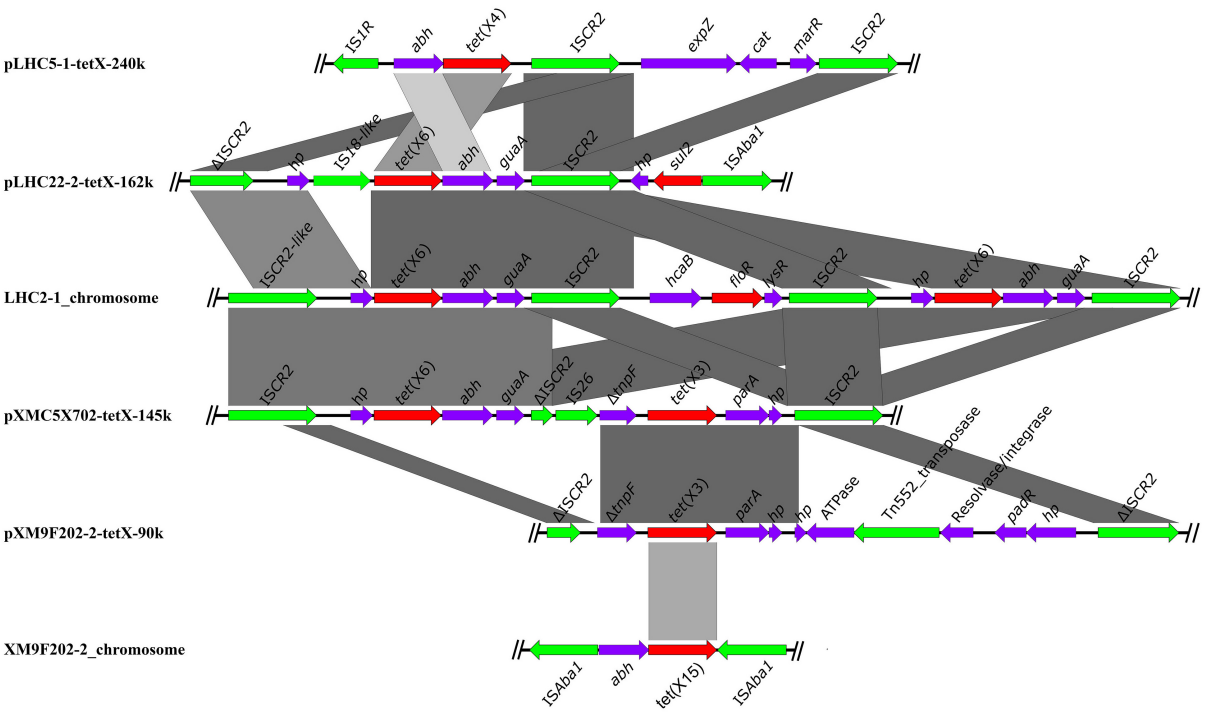

FIGURE 5 | The core genetic structures of *tet*(X) investigated in this study. The resistance genes are shown as red arrows, and the mobile elements are shown as green arrows.

investigate the clonal relationship of *tet*(X4)-harboring *E. coli* between chicken and other sources, the genomes of 26 *tet*(X4)-positive *E. coli* with different hosts including pig, dog, chicken, cow, and human were downloaded from NCBI database and analyzed. Phylogenetic analysis based on the core genome indicated that the prevalence feature of *tet*(X4)-harboring *E. coli* has no clear clonal relationship with their sources (**Supplementary Figure 1**). It is worth noting that a *tet*(X4)-harboring *E. coli* we detected showed a close relationship with a *tet*(X4)-positive *E. coli* detected in human gut microbiota (Ding et al., 2020; **Supplementary Figure 1**). Hence, the serious prevalence of *tet*(X) of animal source has a potential threat to human health.

Antimicrobial Susceptibility Testing and Transfer of Different *tet*(X) Variants

Resistance phenotype analysis found that 15 *tet*(X)-positive strains showed resistance to multiple antibiotics and were all resistant to tigecycline and florfenicol (**Table 1**). In addition, most of them also conferred resistance to amoxicillin and enrofloxacin, but all strains were still susceptible to meropenem. Subsequently, we analyzed the distribution of resistance genes in *tet*(X)-positive strains according to draft genome sequences constructed by Illumina sequencing data. These strains contained multiple antibiotic resistance genes ranging from 8 to 19 (**Supplementary Table 1**). Besides, an extended-spectrum beta-lactamase (ESBL) gene $bla_{\mathrm{CTX-M-55}}$ and a carbapenemase gene $bla_{\mathrm{OXA-58}}$ were detected in some *tet*(X)-positive strains.

To investigate the transmissibility of different *tet*(X) variants, all strains were performed by conjugation assay. All *tet*(X4) genes in this study were successfully transferred into the recipient *E. coli* C600 with low frequencies, resulting in resistance to tigecycline in transconjugants. The remaining *tet*(X)-positive strains failed in conjugation assay. The higher horizontal transfer percentage of *tet*(X4) might explain its high prevalence.

The Genetic Contexts of *tet*(X) Variants

In order to investigate the genetic contexts of different *tet*(X) variants, five strains (one *C. werkmanii* LHC5-1, one *P. alcalifaciens*, and three *Acinetobacter*) were performed with Nanopore long-read sequencing to obtain complete genomes together with short-read data (**Supplementary Table 1**). Genetic analysis of strain LHC5-1 found that *tet*(X4) gene was located in a 240-kb IncFIA(HI1)/IncHI1A/IncHI1B(R27)/IncR hybrid plasmid, named pLHC5-1-tetX-240k. Many plasmids with a similar structure to pLHC5-1-tetX-240k were found in the NCBI nr database (**Figure 2A**), and most of these plasmids were positive for *tet*(X4) and harbored by *E. coli*. The emergence of *tet*(X4)-bearing IncFIA(HI1)/IncHI1A/IncHI1B(R27)/IncR plasmid in *Citrobacter* spp. exacerbated the transmission of *tet*(X4) among different species of bacteria. Comparative analysis of plasmid pLHC5-1-tetX-240k and other similar hybrid plasmids found that a ca. 190-kb backbone region with replicons IncFIA(HI1)/IncHI1A/IncHI1B(R27) in these hybrid plasmids was conserved (**Figure 2A**). Some small plasmids with replicons IncX1, IncX4, and IncR could integrate into a hybrid plasmid with replicons IncFIA(HI1)/IncHI1A/IncHI1B(R27) and form larger and more complex plasmids, such as pRW7-1_235k_tetX (Li et al., 2020b). Subsequently, we investigated the genetic feature of *tet*(X4) in other strains in this study. The result showed that all *tet*(X4) genes in this study were carried by plasmids with a similar backbone to pLHC5-1-tetX-240k and located in a conserved ca. 190-kb region harboring IncFIA(HI1)/IncHI1A/IncHI1B(R27) plasmid replicons (**Figure 2B**). In addition, we found that these hybrid plasmids were widely distributed in different species of bacteria. Therefore, the diffusion of *tet*(X4) was strongly associated with the IncFIA(HI1)/IncHI1A/IncHI1B(R27) hybrid plasmids and their evolved complex plasmids. Apart from these *tet*(X4)-bearing plasmids in Enterobacteriaceae, one *tet*(X6) gene was detected in a *P. alcalifaciens* of Enterobacteriaceae for the first time. *tet*(X6) gene was located in variable region III (VRIII) of a chromosomal integrative and conjugative element (ICE), designated as ICE*Pal*ChnLHC2-1. A total of four *tet*(X6) genes were detected in VRIII within two tandem repeat units (**Figure 3**). Although tandem repeats of different *tet*(X) variants were frequently observed, two *tet*(X6) in one repeat unit have not been reported. The molecular mechanism of *tet*(X) tandem repeat deserved further investigations. Then, we searched for homologous ICEs with ICE*Pal*ChnLHC2-1 in the NCBI database, and three *tet*(X)-negative ICEs from *Proteus genomosp*, *P. alcalifaciens*, and *Vibrio fluvialis* were downloaded and compared. The four ICEs showed high similarity with each other, which implied that they originated from one ancestor and were popular because of horizontal transfer between different bacterial chromosomes. Meanwhile, we observed an evolution of genetic context in VRIII of the four ICEs, which was a manifestation of the adaptation of bacteria to changes in the external environment.

Although only three *tet*(X)-positive strains belonging to Moraxellaceae were identified, complex genetic contexts of *tet*(X) variants were found in the three strains. Co-occurrence of two different *tet*(X) variants in one strain was detected in strains XM9F202-2 and XMC5X702. A plasmid-mediated *tet*(X3) and a chromosomal novel *tet*(X) variant, designated as *tet*(X15), were found in *A. variabilis* XM9F202-2, which has been investigated in detail in our previous study (Li et al., 2021). In *A. lwoffii* XMC5X702, two different *tet*(X) variants corresponded to *tet*(X3) and *tet*(X6). Genetic analysis found that *tet*(X3) and *tet*(X6) were located on a 145-kb plasmid pXMC5X702-tetX-145k with unknown replicon types. Multiple plasmids co-harboring *tet*(X3) and *tet*(X6) carried by *Acinetobacter* were found in the nr database, and they share more than 50% coverage and more than 95% identify to pXMC5X702-tetX-145k (**Figure 4A**). However, the replicon gene in pXMC5X702-tetX-145k differed from those plasmids co-harboring *tet*(X3) and *tet*(X6). The plasmids that harbor the same replicon as pXMC5X702-tetX-145k showed low identity to pXMC5X702-tetX-145k. Hence, the structure of pXMC5X702-tetX-145k was novel, and it enriched the profile of *tet*(X)-bearing plasmids in *Acinetobacter*. *tet*(X6) gene in *A. baumannii* LHC22-2 was carried by a 162-kb plasmid pLHC22-2-tetX-162k. What is noteworthy is that a carbapenemase gene $bla_{\mathrm{OXA-58}}$ was found in the *tet*(X6)-bearing

plasmid. Although many plasmids co-harboring *tet*(X3) and bla_{OXA-58} have been reported in other species of *Acinetobacter* (Cui et al., 2020; Ma et al., 2020), *tet*(X6)- and bla_{OXA-58}-bearing plasmid was rarely reported (Zheng et al., 2020). As a clinically critical opportunistic pathogen, the emergence of carbapenem- and tigecycline-resistant *A. baumannii* poses a great threat to public health. Phenotype analysis of antimicrobial resistance showed that LHC22-2 was resistant to imipenem but susceptible to meropenem. The expression of bla_{OXA-58} could be enhanced by an intact upstream IS*Aba3* and result in resistance to meropenem (Hamidian and Nigro, 2019), but IS*Aba3* in plasmid pLHC22-2-tetX-162k was truncated. Subsequently, one plasmid pABF9692 co-harboring *tet*(X6)- and bla_{OXA-58} from *A. baumannii* and three plasmids with different sizes from *Acinetobacter towneri* showing similar backbone with pLHC22-2-tetX-162k were retrieved from the nr database and analyzed (**Figure 4B**). Notably, the backbone of pABF9692 was different with pLHC22-2-tetX-162k. In contrast, the three plasmids co-harboring *tet*(X3) and bla_{OXA-58} showed similar backbone with pLHC22-2-tetX-162k (**Figure 4B**). Two different *tet*(X) variants, *tet*(X3) and *tet*(X6), were detected in these plasmids, which indicated that such plasmids played a vital role in capturing and propagating the *tet*(X) genes.

The Core Genetic Structures of *tet*(X) Variants in This Study

The different *tet*(X) variants were harbored by various genetic structures and distributed in different bacteria in the chicken farm. However, IS*CR2* was always associated with different *tet*(X) variants except for the novel *tet*(X15) (**Figure 5**). This phenomenon was consistent with previous studies (He et al., 2019; Li et al., 2020b,c), implying that IS*CR2* was a major driving factor for the dissemination of *tet*(X) variants. We also found many other IS elements in the surroundings of different *tet*(X) variants, such as IS*Aba1* in the downstream of *tet*(X6) in plasmid pLHC22-2-tetX-162k and IS*26* in the upstream of *tet*(X3) in plasmid pXMC5X702-tetX-145k. These IS elements will probably be involved in the transfer of *tet*(X) variants and hereby have evolved novel genetic context of *tet*(X) variants. Apart from IS*CR2*-associated *tet*(X)-bearing genetic contexts, we identified a novel *tet*(X15) located in an IS*Aba1*-bound composite transposon Tn*6866* (Li et al., 2021). The IS*Aba1* in the composite transposon Tn*6866* is directly responsible for the movement of *tet*(X15), which differs from that of *tet*(X6). Therefore, monitoring the genetic context of *tet*(X) variants is important for understanding their transmission and evolution destiny.

DISCUSSION

The emergence of high-level tigecycline resistance genes *tet*(X3) and *tet*(X4) has caused great concern throughout the world. A large number of *tet*(X) variants, from *tet*(X3) to *tet*(X44), were identified from different bacteria in humans and animals within 2 years (Wang et al., 2019; Cheng et al., 2020; Gasparrini et al., 2020; Peng et al., 2020; Zheng et al., 2020; Umar et al., 2021). The current outbreak and widespread situation of *tet*(X) is rapidly diminishing the effectiveness of tetracycline antibiotics, including tigecycline and the US Food and Drug Administration (FDA) newly approved eravacycline and omadacycline. Tetracyclines have been used in livestock farms for many years in China. However, few studies investigated the epidemiological and genetic features of *tet*(X) in livestock farms, with limited research focusing on the *tet*(X)-bearing Enterobacterales or *Acinetobacter* (Cui et al., 2020; Li et al., 2020c). Meanwhile, the prevalence of *tet*(X) in bacteria of chicken origin has not been investigated fully to date. In this work, we systematically explored the distribution and genetic characteristics of different *tet*(X) variants and their host bacteria in a chicken farm. We found that the prevalence of mobilizable *tet*(X4) was the highest and more worrisome than that of other variants. Apart from *E. coli*, *Citrobacter* spp. was also an emerging host for *tet*(X4). The high prevalence of *tet*(X4) might be associated with their host plasmids. Although only three *tet*(X)-positive strains belonging to *Acinetobacter* spp. were identified, three different *tet*(X) variants were identified in them. The epidemic pattern of *tet*(X) in *Acinetobacter* differed from that in Enterobacterales, and the relationship between them warrants further investigations.

Genetic analysis found that plasmids are an important vector for the dissemination of *tet*(X). However, some chromosomal mobile elements, such as ICEs and transposons, also contribute to the transfer of *tet*(X). According to transfer experiments, all *tet*(X4)-positive plasmids in Enterobacterales could transfer to *E. coli* C600, and the other *tet*(X)-bearing genetic structures in Enterobacterales and *Acinetobacter* failed to transfer in conjugation assay. The phenomenon explained the high prevalence of *tet*(X4) in the chicken farm and demonstrated that the prevalence of *tet*(X) genes was positively related to the horizontal transferability of their vectors within specific bacterial hosts. Notably, the transmission of *tet*(X4) was associated with various plasmids reported in our previous study (Li et al., 2020b). In this study, we first noticed that serious prevalence of *tet*(X4) in different bacteria mediated by IncFIA(HI1)/IncHI1A/IncHI1B(R27) plasmids occurred in the chicken farm. Currently, the worldwide dissemination of critical resistance genes was possible with the help of some common types of plasmids, such as bla_{NDM-5}-positive IncX3 plasmid (Li X. et al., 2018; Liu et al., 2019; Zhao et al., 2021) and *mcr*-1-positive IncI2 plasmid (Elbediwi et al., 2019; Gelbicova et al., 2019; Lu et al., 2020). Hence, the emergence of *tet*(X4)-positive common plasmids with high mobility might cause an increasing prevalence of *tet*(X4). In addition, we found that all *tet*(X)-positive plasmids in *Acinetobacter* in the chicken farm had no ability of horizontal transfer, which is consistent with the previous reports (Cui et al., 2020; Ma et al., 2020; Wang et al., 2020). Genetic structure analysis found that those *tet*(X) genes in plasmids harbored by *Acinetobacter* were adjacent to IS*CR2*, indicating that IS*CR2*-mediated mobilization of *tet*(X) also deserved concerns among bacteria of different genus.

In conclusion, we comprehensively investigated the prevalence of *tet*(X) in a chicken farm first and identified multiple *tet*(X) variants from diversified bacteria. The prevalence of *tet*(X4) in the chicken farm was mainly determined by

their host plasmids. The *Acinetobacter* spp. is an important reservoir for other *tet*(X) variants. Apart from IS*CR2*, IS*Aba1* might also be an important element for the mobilization of *tet*(X). Therefore, we propose that effective measures should be formulated to decelerate the dissemination of *tet*(X) in animal- and human-associated environments.

DATA AVAILABILITY STATEMENT

The sequences obtained in this article have been deposited in the GenBank database under BioProject number: PRJNA750704.

AUTHOR CONTRIBUTIONS

RL and ZW conceived and designed the experiments, and manuscript reviewing and editing. YL and KP conducted the experiments, analyze the data, and wrote the draft. YY, XS, and WZ conducted long-read sequencing and bioinformatics analysis. All authors read and approved the final manuscript.

FUNDING

This work was supported in part by the National Natural Science Foundation of China (31872526 and 31872523) and the Priority Academic Program Development of Jiangsu Higher Education Institutions (PAPD).

SUPPLEMENTARY MATERIAL

The Supplementary Material for this article can be found online at: https://www.frontiersin.org/articles/10.3389/fmicb.2021.751006/full#supplementary-material

REFERENCES

Alikhan, N. F., Petty, N. K., Ben Zakour, N. L., and Beatson, S. A. (2011). BLAST ring image generator (BRIG): simple prokaryote genome comparisons. *BMC Genomics* 12:402. doi: 10.1186/1471-2164-12-402

Bankevich, A., Nurk, S., Antipov, D., Gurevich, A. A., Dvorkin, M., Kulikov, A. S., et al. (2012). SPAdes: a new genome assembly algorithm and its applications to single-cell sequencing. *J. Comput. Biol.* 19, 455–477. doi: 10.1089/cmb.2012.0021

Cheng, Y., Chen, Y., Liu, Y., Guo, Y., Zhou, Y., Xiao, T., et al. (2020). Identification of novel tetracycline resistance gene *tet*(X14) and its co-occurrence with *tet*(X2) in a tigecycline-resistant and colistin-resistant *Empedobacter stercoris*. *Emerg. Microbes Infect.* 9, 1843–1852. doi: 10.1080/22221751.2020.1803769

CLSI (2018). *Performance Standards for Antimicrobial Susceptibility Testing*, 28th Edn. Wayne, PA: Clinical and Laboratory Standards Institute. CLSI supplement M100.

Cui, C. Y., Chen, C., Liu, B. T., He, Q., Wu, X. T., Sun, R. Y., et al. (2020). Co-occurrence of plasmid-mediated tigecycline and carbapenem resistance in *Acinetobacter* spp. from waterfowls and their neighboring environment. *Antimicrob. Agents Chemother.* 64:e02502-19. doi: 10.1128/AAC.02502-19

Ding, Y., Saw, W. Y., Tan, L. W. L., Moong, D. K. N., Nagarajan, N., Teo, Y. Y., et al. (2020). Emergence of tigecycline- and eravacycline-resistant *tet*(X4)-producing *Enterobacteriaceae* in the gut microbiota of healthy Singaporeans. *J. Antimicrob. Chemother.* 75, 3480–3484. doi: 10.1093/jac/dkaa372

Elbediwi, M., Li, Y., Paudyal, N., Pan, H., Li, X., Xie, S., et al. (2019). Global burden of colistin-resistant bacteria: mobilized colistin resistance genes study (1980-2018). *Microorganisms* 7:461. doi: 10.3390/microorganisms7100461

Gasparrini, A. J., Markley, J. L., Kumar, H., Wang, B., Fang, L., Irum, S., et al. (2020). Tetracycline-inactivating enzymes from environmental, human commensal, and pathogenic bacteria cause broad-spectrum tetracycline resistance. *Commun. Biol.* 3:241. doi: 10.1038/s42003-020-0966-5

Gelbicova, T., Barakova, A., Florianova, M., Jamborova, I., Zelendova, M., Pospisilova, L., et al. (2019). Dissemination and comparison of genetic determinants of *mcr*-mediated colistin resistance in *Enterobacteriaceae* via retailed raw meat products. *Front. Microbiol.* 10:2824. doi: 10.3389/fmicb.2019.02824

Hamidian, M., and Nigro, S. J. (2019). Emergence, molecular mechanisms and global spread of carbapenem-resistant. *Acinetobacter baumannii*. *Microb. Genom.* 5:e000306. doi: 10.1099/mgen.0.000306

He, D., Wang, L., Zhao, S., Liu, L., Liu, J., Hu, G., et al. (2020). A novel tigecycline resistance gene, *tet*(X6), on an SXT/R391 integrative and conjugative element in a *Proteus genomospecies 6* isolate of retail meat origin. *J. Antimicrob. Chemother.* 75, 1159–1164. doi: 10.1093/jac/dkaa012

He, T., Wang, R., Liu, D., Walsh, T. R., Zhang, R., Lv, Y., et al. (2019). Emergence of plasmid-mediated high-level tigecycline resistance genes in animals and humans. *Nat. Microbiol.* 4, 1450–1456. doi: 10.1038/s41564-019-0445-2

Li, R., Lu, X., Peng, K., Liu, Z., Li, Y., Liu, Y., et al. (2020b). Deciphering the structural diversity and classification of the mobile tigecycline resistance gene *tet*(X)-Bearing plasmidome among bacteria. *mSystems* 5:e00134-20. doi: 10.1128/mSystems.00134-20

Li, R., Peng, K., Li, Y., Liu, Y., and Wang, Z. (2020c). Exploring *tet*(X)-bearing tigecycline-resistant bacteria of swine farming environments. *Sci. Total Environ.* 733:139306. doi: 10.1016/j.scitotenv.2020.139306

Li, R., Lu, X., Liu, Z., Liu, Y., Xiao, X., and Wang, Z. (2020a). Rapid detection and characterization of *tet*(X4)-positive *Escherichia coli* strains with nanopore sequencing. *J. Antimicrob. Chemother.* 75, 1068–1070. doi: 10.1093/jac/dkz528

Li, R., Peng, K., Xiao, X., Wang, Y., and Wang, Z. (2021). Characterization of novel IS*Aba1*-bounded *tet*(X15)-bearing composite transposon Tn*6866* in *Acinetobacter variabilis*. *J. Antimicrob. Chemother.* 76, 2481–2483.

Li, R., Xie, M., Dong, N., Lin, D., Yang, X., Wong, M. H. Y., et al. (2018). Efficient generation of complete sequences of MDR-encoding plasmids by rapid assembly of MinION barcoding sequencing data. *Gigascience* 7, 1–9.

Li, X., Fu, Y., Shen, M., Huang, D., Du, X., Hu, Q., et al. (2018). Dissemination of *bla*NDM-5 gene via an IncX3-type plasmid among non-clonal *Escherichia coli* in China. *Antimicrob. Resist. Infect. Control* 7:59. doi: 10.1186/s13756-018-0349-6

Li, R., Liu, Z., Peng, K., Liu, Y., Xiao, X., and Wang, Z. (2019). Co-occurrence of two *tet*(X) variants in an *Empedobacter brevis* of shrimp origin. *Antimicrob. Agents Chemother.* 63:e01636-19. doi: 10.1128/AAC.01636-19

Liu, D., Zhai, W., Song, H., Fu, Y., Schwarz, S., He, T., et al. (2020). Identification of the novel tigecycline resistance gene *tet*(X6) and its variants in *Myroides*, *Acinetobacter* and *Proteus* of food animal origin. *J. Antimicrob. Chemother.* 75, 1428–1431. doi: 10.1093/jac/dkaa037

Liu, Y. Y., Wang, Y., Walsh, T. R., Yi, L. X., Zhang, R., Spencer, J., et al. (2016). Emergence of plasmid-mediated colistin resistance mechanism MCR-1 in animals and human beings in China: a microbiological and molecular biological study. *Lancet Infect. Dis.* 16, 161–168. doi: 10.1016/S1473-3099(15)00424-7

Liu, Z., Xiao, X., Li, Y., Liu, Y., Li, R., and Wang, Z. (2019). Emergence of IncX3 Plasmid-Harboring *bla* NDM-5 Dominated by *Escherichia coli* ST48 in a Goose Farm in Jiangsu. China. *Front. Microbiol.* 10:2002. doi: 10.3389/fmicb.2019.02002

Lu, X., Xiao, X., Liu, Y., Huang, S., Li, R., and Wang, Z. (2020). Widespread prevalence of plasmid-mediated colistin resistance gene *mcr*-1 in *Escherichia coli* from Pere David's Deer in China. *mSphere* 5:e01221-2. doi: 10.1128/mSphere.01221-2

Ma, J., Wang, J., Feng, J., Liu, Y., Yang, B., Li, R., et al. (2020). Characterization of three porcine *Acinetobacter towneri* strains co-harboring *tet*(X3) and *bla* OXA-58. *Front. Cell Infect. Microbiol.* 10:586507. doi: 10.3389/fcimb.2020.586507

Mohsin, M., Hassan, B., Martins, W., Li, R., Abdullah, S., Sands, K., et al. (2021). Emergence of plasmid-mediated tigecycline resistance *tet*(X4) gene in *Escherichia coli* isolated from poultry, food and the environment in South Asia. *Sci. Total Environ.* 787:147613. doi: 10.1016/j.scitotenv.2021.147613

Page, A. J., Cummins, C. A., Hunt, M., Wong, V. K., Reuter, S., Holden, M. T. G., et al. (2015). Roary: rapid large-scale prokaryote pan genome analysis. *Bioinformatics* 31, 3691–3693. doi: 10.1093/bioinformatics/btv421

Peng, K., Li, R., He, T., Liu, Y., and Wang, Z. (2020). Characterization of a porcine *Proteus cibarius* strain co-harbouring *tet*(X6) and *cfr*. *J. Antimicrob. Chemother.* 75, 1652–1654. doi: 10.1093/jac/dkaa047

Pournaras, S., Koumaki, V., Spanakis, N., Gennimata, V., and Tsakris, A. (2016). Current perspectives on tigecycline resistance in *Enterobacteriaceae*: susceptibility testing issues and mechanisms of resistance. *Int. J. Antimicrob. Agents* 48, 11–18. doi: 10.1016/j.ijantimicag.2016.04.017

Price, M. N., Dehal, P. S., and Arkin, A. P. (2009). FastTree: computing large minimum evolution trees with profiles instead of a distance matrix. *Mol. Biol. Evol.* 26, 1641–1650. doi: 10.1093/molbev/msp077

Seemann, T. (2014). Prokka: rapid prokaryotic genome annotation. *Bioinformatics* 30, 2068–2069. doi: 10.1093/bioinformatics/btu153

Sullivan, M. J., Petty, N. K., and Beatson, S. A. (2011). Easyfig: a genome comparison visualizer. *Bioinformatics* 27, 1009–1010. doi: 10.1093/bioinformatics/btr039

Sun, C., Cui, M., Zhang, S., Wang, H., Song, L., Zhang, C., et al. (2019). Plasmid-mediated tigecycline-resistant gene *tet*(X4) in *Escherichia coli* from food-producing animals, China, 2008-2018. *Emerg. Microbes Infect.* 8, 1524–1527. doi: 10.1080/22221751.2019.1678367

Sun, J., Chen, C., Cui, C. Y., Zhang, Y., Liu, X., Cui, Z. H., et al. (2019). Plasmid-encoded *tet*(X) genes that confer high-level tigecycline resistance in *Escherichia coli*. *Nat. Microbiol.* 4, 1457–1464. doi: 10.1038/s41564-019-0496-4

Sun, J., Liao, X. P., D'souza, A. W., Boolchandani, M., Li, S. H., Cheng, K., et al. (2020). Environmental remodeling of human gut microbiota and antibiotic resistome in livestock farms. *Nat. Commun.* 11:1427. doi: 10.1038/s41467-020-15222-y

Sun, Y., Cai, Y., Liu, X., Bai, N., Liang, B., and Wang, R. (2013). The emergence of clinical resistance to tigecycline. *Int. J. Antimicrob. Agents* 41, 110–116.

Umar, Z., Chen, Q., Tang, B., Xu, Y., Wang, J., Zhang, H., et al. (2021). The poultry pathogen *Riemerella anatipestifer* appears as a reservoir for Tet(X) tigecycline resistance. *Environ. Microbiol.* doi: 10.1111/1462-2920.15632

Wang, J., Wang, Y., Wu, H., Wang, Z. Y., Shen, P. C., Tian, Y. Q., et al. (2020). Coexistence of *bla*OXA-58 and *tet*(X) on a Novel Plasmid in *Acinetobacter* sp. from Pig in Shanghai, China. *Front. Microbiol.* 11:578020. doi: 10.3389/fmicb.2020.578020

Wang, L., Liu, D., Lv, Y., Cui, L., Li, Y., Li, T., et al. (2019). Novel plasmid-mediated *tet*(X5) gene conferring resistance to tigecycline, eravacycline, and omadacycline in a clinical *Acinetobacter baumannii* Isolate. *Antimicrob. Agents Chemother.* 64:e01326-19. doi: 10.1128/AAC.01326-19

Wick, R. R., Judd, L. M., Gorrie, C. L., and Holt, K. E. (2017). Unicycler: resolving bacterial genome assemblies from short and long sequencing reads. *PLoS Comput. Biol.* 13:e1005595. doi: 10.1371/journal.pcbi.1005595

Zhao, Q., Berglund, B., Zou, H., Zhou, Z., Xia, H., Zhao, L., et al. (2021). Dissemination of *bla*NDM-5 via IncX3 plasmids in carbapenem-resistant *Enterobacteriaceae* among humans and in the environment in an intensive vegetable cultivation area in eastern China. *Environ. Pollut.* 273:116370. doi: 10.1016/j.envpol.2020.116370

Zheng, X. R., Zhu, J. H., Zhang, J., Cai, P., Sun, Y. H., Chang, M. X., et al. (2020). A novel plasmid-borne *tet*(X6) variant co-existing with *bla*NDM-1 and *bla*OXA-58 in a chicken *Acinetobacter baumannii* isolate. *J. Antimicrob. Chemother.* 75, 3397–3399.

Conflict of Interest: The authors declare that the research was conducted in the absence of any commercial or financial relationships that could be construed as a potential conflict of interest.

Publisher's Note: All claims expressed in this article are solely those of the authors and do not necessarily represent those of their affiliated organizations, or those of the publisher, the editors and the reviewers. Any product that may be evaluated in this article, or claim that may be made by its manufacturer, is not guaranteed or endorsed by the publisher.

frontiers | Frontiers in Microbiology

ORIGINAL RESEARCH
published: 29 April 2022
doi: 10.3389/fmicb.2022.868705

Emergence of a Hypervirulent Tigecycline-Resistant *Klebsiella pneumoniae* Strain Co-producing bla_{NDM-1} and bla_{KPC-2} With an Uncommon Sequence Type ST464 in Southwestern China

Jingchen Hao[1†], Bangqin Zhang[1†], Jiamin Deng[2†], Yueshuai Wei[1], Xue Xiao[3] and Jinbo Liu[1]*

[1] Department of Laboratory Medicine, The Affiliated Hospital of Southwest Medical University, Luzhou, China, [2] Department of Respiratory and Critical Care Medicine, The Affiliated Hospital of Southwest Medical University, Luzhou, China, [3] Department of Laboratory Medicine, Southwest Medical University, Luzhou, China

OPEN ACCESS

Edited by:
Eun-Jeong Yoon, Korea National Institute of Health, South Korea

Reviewed by:
Shangshang Qin, Zhengzhou University, China
Vincenzo Di Pilato, University of Genoa, Italy

***Correspondence:**
Jinbo Liu
liulab2019@163.com

[†] These authors have contributed equally to this work

Specialty section:
This article was submitted to Antimicrobials, Resistance and Chemotherapy, a section of the journal Frontiers in Microbiology

Received: *03 February 2022*
Accepted: *21 March 2022*
Published: *29 April 2022*

Citation:
Hao J, Zhang B, Deng J, Wei Y, Xiao X and Liu J (2022) Emergence of a Hypervirulent Tigecycline-Resistant Klebsiella pneumoniae Strain Co-producing bla_{NDM-1} and bla_{KPC-2} With an Uncommon Sequence Type ST464 in Southwestern China. Front. Microbiol. 13:868705. doi: 10.3389/fmicb.2022.868705

Emergence of bla_{NDM-1} and bla_{KPC-2} co-producing *Klebsiella pneumoniae* strains is currently attracting widespread attention, but little information is available about their tigecycline resistance, virulence, and prevalence in Southwest China. In July 2021, an extensively drug-resistant *K. pneumoniae* strain AHSWKP25 whose genome contained both bla_{NDM-1} and bla_{KPC-2} genes was isolated from the blood of a patient with the malignant hematological disease in Luzhou, China. We investigated the resistance profiles of AHSWKP25 using microbroth dilution, agar dilution, modified carbapenemase inactivation (mCIM), and EDTA-modified carbapenemase inactivation methods (eCIM). The virulence of AHSWKP25 was assessed through string tests, serum killing assays, and a *Galleria mellonella* larval infection model. Conjugation and plasmid stability experiments were conducted to determine the horizontal transfer capacity of plasmids. And efflux pump phenotype test and real-time quantitative reverse transcription-PCR (RT-PCR) were used to determine its efflux pump activity. Sequencing of AHSWKP25 determined that AHSWKP25 belonged to ST464, which is resistant to antibiotics such as carbapenems, tetracycline, fluoroquinolones, tigecycline, and fosfomycin. The efflux pump phenotype tests and RT-PCR results demonstrated that efflux pumps were overexpressed in the AHSWKP25, which promoted the tigecycline resistance of the bacteria. AHSWKP25 also showed hypervirulence and serum resistance *in vitro* model. AHSWKP25 carried several different plasmids that contained bla_{NDM-1}, bla_{KPC-2}, and mutated *tet(A)* genes. Sequence alignment revealed that the plasmids carrying bla_{NDM-1} and bla_{KPC-2} underwent recombination and insertion events, respectively. We demonstrated that an X3 plasmid carrying bla_{NDM-1} was transferred from pSW25NDM1

to *E. coli* J53. We also identified missense mutations in the *ramR*, *rcsA*, *lon*, and *csrD* genes of AHSWKP25. Our results highlighted the potential of bla_{NDM-1} and bla_{KPC-2} co-producing *K. pneumoniae* strains to further develop antimicrobial resistance and hypervirulent phenotypes, but measures should be taken to closely monitor and control the spread of superbugs with multidrug-resistant phenotypes and hypervirulence.

Keywords: *Klebsiella pneumoniae*, NDM-1, KPC-2, tigecycline resistance, hypervirulent

INTRODUCTION

Klebsiella pneumoniae is a common Gram-negative bacteria without spores or flagella that belongs to the *Bacillus* genus. In clinical infections involving *K. pneumoniae*, the classical (cKp) and hypervirulent (hvKp) strains are the most common, and the hvkp strains are considerably more dangerous because they can infect multiple organs, leading to high mortality rates from multiorgan failure. The pathogenicity of hvKp is usually attributed to multiple virulence factors, one of the most representative of which is the capsular antigen, which not only enhances virulence but also allows the bacterium to evade the host's immune response (Podschun and Ullmann, 1998). There are six main types of the capsular antigen that enable the invasion of the species: K1, K2, K5, K54, K20, and K57. These antigens together with other virulence factors form the hypervirulence phenotype of *K. pneumoniae* (Turton et al., 2010; Shon et al., 2013). K1 and K2 are the most well-described capsular serotypes and are often detected in the *K. pneumoniae* multilocus sequence types ST23 and ST65 (Liao et al., 2014). Virulence plasmids are a significant marker of these hvkp strains (Shon et al., 2013). The *rmpA* gene product regulates the synthesis of capsular polysaccharides, conferring a hypermucoviscous phenotype on these pathogens (Cheng et al., 2010). A recent study revealed that, in addition to *rmpA*, the presence of *rmpC* and *rmpD* genes at the *rmp* locus also contributed to the formation of the hypermucoviscous *K. pneumoniae* phenotype (Walker et al., 2020). However, not all hypervirulent strains have a mucinous phenotype or carry the *rmpA*/*rmpA2* or *iucA* genes (Yan et al., 2021). One study indicated that mutations in the genes (wzi, wza, wzc, *rcsAB*, and *lon)* that encode the enzymes and regulators responsible for capsule production contributed to aberrant capsule production that promoted the pathogenicity and antiserum phagocytosis of *K. pneumoniae* strains. And these mutants producing hypercapsule are often associated with bloodstream infection (Ernst et al., 2020). Therefore, more studies are required to better understand the hvKp strains.

The resistance status of hvKp is not promising. Like cKp, hvKp can acquire resistance to antimicrobial agents with the acquisition of mobile elements carbapenem-resistant-hvKp is a typical example of a stain that can acquire resistance to various antimicrobial agents by obtaining exogenous plasmids carrying antimicrobial resistance genes (Yao et al., 2015). cKp can also develop into hypervirulent strains by acquiring virulence plasmids. The high pathogenicity and antimicrobial resistance of these pathogens translate to high treatment costs and poor prognoses (Shankar et al., 2018). Colistin and tigecycline represent the last line of defense against carbapenem-resistant Enterobacteriaceae bacteria, especially metallo-beta-lactamase-producing strains (Maltezou, 2009). The horizontal transfer of *mcr*, *tet(A)*, and *tet(X)* allowed *K. pneumoniae* to rapidly acquire resistance to colistin and tigecycline. Also, disruptions in chromosomal genes (*mgrB*, *pmrAB*, and *phoPQ*), as well as resistance nodulation cell division (RND)-type efflux transporters and their regulators (*marRA*, *ramRA*, and *rarA*), are prominently responsible for conferring resistance of these microorganisms to antimicrobial agents (Osei Sekyere et al., 2016; Poirel et al., 2017). Recently, one study reported the emergence of bla_{NDM-1} and bla_{KPC-2} co-producing *K. pneumoniae* strains that could have both high-level carbapenem resistance and hypervirulent phenotypes (Liu et al., 2019; Gao et al., 2020). However, little information is available on the virulence characteristics, or tigecycline resistance of the bla_{NDM-1} and bla_{KPC-2} co-producing *K. pneumoniae* strains. To monitor these bacteria and prevent the development of further antimicrobial resistance, more information on these strains is required. In this study, we isolated an extensively drug-resistant *K. pneumoniae* isolate (AHSWKP25) from the blood of a patient with a bloodstream infection. AHSWKP25 was found to be an isolate harboring bla_{NDM-1}, bla_{KPC-2}, and *tet(A)* with an uncommon sequence type and was resistant to tigecycline and fosfomycin. In this study, we examined the virulence, genetic characteristics, and resistance mechanisms of AHSWKP25.

MATERIALS AND METHODS

Source of the Isolate

In July 2021, AHSWKP25 was isolated from the blood of a patient diagnosed with acute myeloid leukemia with a bloodstream infection at the Affiliated Hospital of Southwest Medical University (Luzhou, China). The patient had previously been tread with ceftazidime, meropenem, moxifloxacin, tigecycline, and voriconazole for fungal infection and repeated fever. The clinical microbiology laboratory identified AHSWKP25 as *K. pneumonia* that was resistant to carbapenems, tigecycline, fluoroquinolones, and other common antimicrobial agents. The patient ultimately died of multiorgan failure. To better understand the antimicrobial resistance mechanisms and virulence characteristics of AHSWKP25, we undertook a series of experiments described below.

Antimicrobial Susceptibility Testing, Efflux Pump Phenotype Test, and DNA Amplification

The antimicrobial minimum inhibitory concentrations (MICs) of ceftazidime, cefepime, gentamicin, amikacin, chloramphenicol, ciprofloxacin, levofloxacin, tetracycline, polymyxin B, ceftazidime/avibactam, fosfomycin (agar dilution method), and tigecycline were determined according to the (Clinical and Laboratory Standards Institute (CLSI), 2020) standards. The MIC breakpoints of imipenem, ertapenem, aztreonam, levofloxacin, nitrofurantoin, and trimethoprim-sulfamethoxazole were determined using the MicroScan Walk Away System (Siemens, Germany). The breakpoint of tigecycline was interpreted according to the guidelines of the United States Food and Drug Administration (FDA[1]) on Antimicrobial Susceptibility Testing. The modified carbapenemase inactivation (mCIM) and EDTA-modified carbapenemase inactivation methods (eCIM) were also used following the CLSI 2020 standards.

To evaluate the efflux pump activity of AHSWKP25, we first measured the changes in the MICs of several antimicrobial agents in the presence of 1-(1-Naphthylmethyl)-piperazine (NMP, 100 mg/L). A fourfold or greater reduction in MIC was considered an indicator of overexpression in the efflux pumps (Schumacher et al., 2006). Polymerase chain reaction (PCR) was performed to detect whether the isolate carried the bla_{KPC} or bla_{NDM} genes, and the primers used are listed in **Supplementary Table 1**.

String Test, Serum Killing Assay, and *Galleria mellonella* Infection Model

The hypermucoviscous phenotype was determined using a string test. A single purified colony on a blood agar plate incubated at 37°C for 18-24 hours was picked with an inoculation loop for string, and the string test was considered positive if the length of the viscous string was longer than 5 mm (Yan et al., 2021). A serum killing assay was performed as described previously. In brief, 25 μL of the bacterial suspension (concentration of $\sim 1 \times 10^6$ CFU/mL) was added to 75 μL of healthy human serum for co-culture. After 0, 1, 2, and 3 h, the plates were inoculated with the mixture and the numbers of viable bacteria were calculated. The strains were classified as "highly sensitive," "moderately sensitive," or "resistant" to serum, depending on the results (Liu et al., 2017).

The pathogenicity of AHSWKP25 was assessed using a *G. mellonella* larvae infection model as previously described (Kim et al., 2021). A total of 15 healthy vigorous larvae were inoculated with the bacterial suspension of AHSWKP25 isolate at a dose equivalent to 10^6 CFU. When the larvae were inactive and black, they were considered dead. The numbers of larval deaths were recorded every 12 h. *K. pneumoniae* NTUH-K2044 and ATCC 700603 were used as the hypervirulent control and negative control, respectively. The bacterial suspension was serially diluted and injected into *G. mellonella* larvae for 3 days of incubation, and the lethal dose 50 (LD_{50}) was calculated using the probit model (Shi et al., 2018).

Whole Genome Sequencing, Identification of Mutant *rcsAB*, *lon*, *csrD*, and *pal*, Phylogenetic Reconstruction

Luria–Bertani (LB) broth was inoculated with the selected purified *Klebsiella* colonies, and the bacteria were cultured to log phase. Extraction of bacterial genomic DNA using a magnetic bead-based kit (Qiagen, Germany). The extracted bacterial DNA was purified and sequenced using the Illumina NovaSeq PE150 and Oxford nanopore platforms. The bacterial genome was assembled *de novo* using Canu (v 1.7). Prokka (v 1.10) was used to predict and annotate the coding genes, tRNAs, and rRNAs in the assembled genome. The plasmid replicon types, acquired resistance genes, sequence types, and virulence genes were determined using the online services of the Center for Genomic Epidemiology[2] and VFDB (virulence factor database[3]). IS finder[4] was used to identify the insertion sequences. The genomes were compared using the Basic Local Alignment Search Tool (BLAST[5]), BRIG v0.95, Mauve[6], and the OAT software (Lee I. et al., 2016).

We used *K. pneumoniae* UCI 38 (accession number: JCMB01) as a reference strain to identify point mutations in the *rcsAB* and *lon* (Lon protease) genes of AHSWKP25 to evaluate whether AHSWKP25 was associated with hypercapsule production (Ernst et al., 2020). The *rscD* and *pal* mutants were identified using *K. pneumoniae* ATCC13883 (accession number: JOOW01) as the reference genome.

A goeBURST full MST analysis based on multilocus sequence typing data was performed by the Phyloviz 1.1a software to infer the phylogeny of the sequence types[7]. The Orthologous average nucleotide identity (OrthoANI) was calculated by comparing homologous genes between the genomes to construct a phylogenetic tree (Lee I. et al., 2016), which was visualized by iTOL[8]. The accession numbers of the genomes/sequences obtained from the NCBI database were listed in **Supplementary Table 2**.

Measurement of Efflux Pump Transcription Levels Using Quantitative Reverse Transcription-PCR

To evaluate the role of chromosomal point mutations in the antimicrobial resistance of AHSWKP25, we used RT-PCR to measure the transcriptional levels of efflux pump-encoding genes (*acrA*, *acrB*, *marA*, *marR*, *rarA*, and *ramA*) involved in conferring tigecycline resistance. In brief, single purified colonies of AHSWKP25 were inoculated into 5 mL

[1]https://www.fda.gov

[2]http://www.genomicepidemiology.org/

[3]http://www.mgc.ac.cn/VFs/

[4]https://www-is.biotoul.fr/blast.php

[5]https://blast.ncbi.nlm.nih.gov/Blast.cgi

[6]https://sourceforge.net/projects/mauve/

[7]http://www.phyloviz.net/

[8]https://itol.embl.de/

of LB broth and the bacteria were grown to log phase. Their RNA was extracted according to the recommendations of the reagent's manufacturer (Magen, China). The RT-PCR primers used in the present study are listed in **Supplementary Table 1**. The *rpoB gene* was used as the internal reference, and the tigecycline-susceptible *K. pneumoniae* strain NTUH-K2044 was used as the control strain. All experiments were performed in triplicate independently, with three biological replicates per experiment. The gene expression results were compared to the expression levels of *rpoB* to calculate the relative expression of the target genes ($2^{-\Delta\Delta Ct}$ method).

Conjugation Experiments and Plasmid Stability

Sodium azide-resistant *Escherichia coli* J53 was used as the recipient and AHSWKP25 as the donor in the conjugation experiments. The McFarland (McF) standard turbidity of the bacterial suspension was adjusted to 0.5 McF. The recipient bacteria (200 μL) and donor bacteria (400 μL) were inoculated into LB broth (800 μL) (Xiang et al., 2020). After 16–18 h of culturing at 35°C, MH plates containing 180 μg/mL sodium azide and antimicrobial agents [4 μg/mL meropenem; 4 μg/mL meropenem + 5 mM EDTA (final concentration); 0.25 μg/mL ciprofloxacin] were inoculated with 100 μL of the culture solution to screen for transconjugants. The transferred genes in the transconjugants were confirmed by PCR using the primers listed in **Supplementary Table 1**.

The stability of the self-transferred plasmids in the positive transconjugants was calculated using the plate count method, as described previously with some modifications (Nang et al., 2018). Briefly, antibiotic-free LB broth was inoculated with the positive transconjugants at a ratio of 1,000:1, and the bacteria were passaged continuously for 10 days. The mixed culture was sampled every day by inoculating aliquots (100 μL) of the mixed culture into meropenem-containing (4 μg/mL), antibiotic-free LB agar plates. The plates were incubated for 24 h to calculate the plasmid retention rate.

RESULTS

Antimicrobial Susceptibility and General Characteristics of AHSWKP25

The antimicrobial susceptibility tests indicated that AHSWKP25 was resistant to common antibacterial agents, such as meropenem, tetracycline, ciprofloxacin, levofloxacin, and gentamicin. Notably, AHSWKP25 was also resistant to fosfomycin, tigecycline (16 μg/mL), and ceftazidime-avibactam, as shown in **Table 1**. The mCIM and eCIM results suggested that AHSWKP25 carries serine carbapenems. Subsequently, PCR and Sanger sequencing confirmed that AHSWKP25 was a bla_{NDM-1} and bla_{KPC-2} co-producing *K. pneumonia* isolate.

The string test of AHSWKP25 was negative, as the mucoid string length was < 5 mm. AHSWKP25 was highly pathogenic in the *G. mellonella* infection model. Of the 15 *G. mellonella* larvae that were inoculated with 10^6 CFU of AHSWKP25, 15 died within 24 h, corresponding to a mortality rate of 100%, which was similar to the rate for the hypervirulent control strain NTUH-K2044 ($P > 0.05$) but different from that of *K. quasipneumoniae* ATCC700603 (negative control, $P < 0.0001$) (**Figure 1B**). The LD_{50} of AHSWKP25 was 4.44 ± 0.23 (log10 CFU), and the LD_{50} of the NTUH-K2044 was 4.21 ± 0.17 (log10 CFU) ($P > 0.05$, **Supplementary Figure 1**). Both NTUH-K2044 and AHSWKP25 showed resistance to the serum, whereas ATCC 700603 was highly sensitive to the serum (**Figure 1A** and **Supplementary Table 3**). To further investigate the virulence characteristics and resistance mechanisms of AHSWKP25, we sequenced its whole genome to identify mutations in the genes that regulate the resistance mechanisms.

Sequence Characteristics of the AHSWKP25 Genome

The full length of the AHSWKP25 genome was 5,874,657 bp, and it consisted of a chromosomal backbone carrying bla_{SHV-5} and seven circular plasmids. Of these, the plasmid incompatibility (Inc) groups for pSW25NDM1, pSW25HRG, and pSW25tet(A) were X3, FIB, and FII/FIA, respectively. The bla_{KPC-2} and bla_{NDM-1} genes were located on plasmids pSW25KPC2 and pSW25NDM1, respectively. The AHSWKP25 genome was longer than *K. pneumoniae* MGH78578 (5,694,894 bp, GenBank accession number: CP000647-652) and ATCC13883 (5,545,784 bp, accession number: JOOW01). The capsular serotype of AHSWKP25 was identified as K53 based on the wzc locus, which was consistent with the serotype of *K. quasipneumoniae* ATCC700603 (GenBank accession number: CP014696.2). The wzi allele (wzi outer membrane protein of cluster) of AHSWKP25 was most similar to allele 534 but it differed by one base pair. Therefore, we uploaded the wzi allele of AHSWKP25 into a public database[9] and assigned a novel profile to it defined as wzi 725. The *mrkABCDFHIJ*, *fimABCDEFGHIK*, *rcsAB*, *entABCDEFS,* and *iroE* genes were all identified on the chromosomal backbone of AHSWKP25, whereas the *iucA* and *rmpA*/*rmpA2* genes were not detected (**Supplementary Table 4**). AHSWKP25 shared an average nucleotide identity (ANI) of 98.97 and 98.96% with *K. pneumonia* MGH78578 and ATCC 13883 (**Supplementary Figure 2**), respectively. The multilocus sequence type of AHSWKP25 was ST464, which differed from ST4292 and ST2439 by only one allele, whereas ST464 differed from ST11 by five alleles (**Supplementary Figure 3**). The amino acid substitutions in *ramR*, *acrR,* and *ompK36*/*ompK37* genes of AHSWKP25, as shown in **Table 2**. Furthermore, we also identified Ser35Asn, Glu259Ala, and Gln110His missense mutations in the *rcsA*, *lon,* and *csrD* genes of AHSWKP25, respectively. However, no missense mutations were found in the *pal* gene. A phylogenetic tree generated from orthoANI data revealed that AHSWKP25 and the *K. pneumoniae* strains co-producing NDM-1 and KPC-2 previously isolated from other regions of China (Liu et al., 2019; Gao et al., 2020; Xu et al., 2020) had obvious regional and temporal differences and were significantly separated phylogenetically (**Figure 2**).

[9]http://bigsdb.pasteur.fr

TABLE 1 | Antibiotic susceptibility tests of AHSWKP25 and its conjugants, and efflux pump phenotype test of AHSWKP25.

	Antibiotics		MIC(μg/ml)	
	AHSWKP25	**AHSWKP25 + NMP (100 μg/mL)**	**J53**	**J53 + pSW25NDM1**
Ceftazidime	>128 (R)	>128 (R)	/	/
Meropenem	64 (R)	64 (R)	0.5 (S)	8 (R)
Tetracycline	>128 (R)	128 (R)	1	1
Ciprofloxacin	8 (R)	1 (R)	0.0625 (S)	0.0625 (S)
Gentamicin	32 (R)	16 (R)	0.5 (S)	0.5 (S)
Chloramphenicol	>128 (R)	64(R)	/	/
Polymyxin B	2 (I)	2 (I)	1(I)	1(I)
Tigecycline	16 (R)	1 (S)	0.125 (S)	0.125 (S)
Cefepime	>128 (R)	/	1	128 (R)
Aztreonam	>16 (R)	/	/	/
Imipenem	>8 (R)	/	/	/
Levofloxacin	>4 (R)	/	/	/
Ceftazidime/Avibactam	>32/4 (R)	/	/	/
Trimethoprim/Sulfamethoxazole	>4/76 (R)	/	/	/
Fosfomycin	>256 (R)	/	/	/

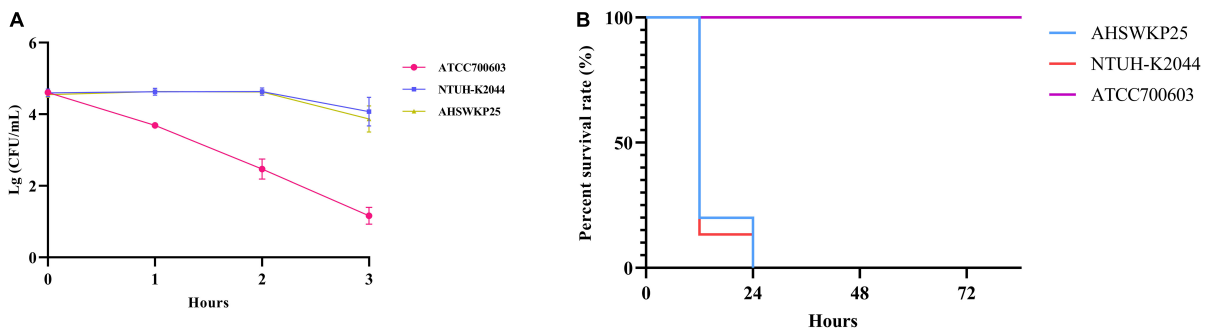

FIGURE 1 | Serum resistance and pathogenicity of AHSWKP25.**(A)** The survival rate of AHSWKP25, ATCC700603, and NTUH-K2044 in healthy human serum over 3 h. The data are expressed as the mean ± SEM (standard error of the mean). **(B)** The survival rate of *G. mellonella* larvae (15 biological replicates) inoculated with AHSWKP25, NTUH-K2044, and ATCC700603, respectively. The experiments were repeated in triplicate independently.

Sequence Analysis of Plasmids Carried by AHSWKP25

Among the seven circular plasmids carried by AHSWKP25, we focused on four of them, namely pSW25KPC2, pSW25HRG, pSW25tet_A, and pSW25NDM1. pSW25KPC2 was a circular plasmid with a length of 248,847 bp, but we failed to identify its incompatibility group with Plasmid Finder 2.1. This plasmid carried multiple resistance determinants, including bla_{KPC-2} (beta-lactam resistance), *aadA16* (aminoglycosides resistance), *aac(3)-IId* (aminoglycosides resistance), *sul1* (sulfamethoxazole resistance), *dfrA27* (trimethoprim resistance), *qnrB4* (quinolones resistance), *ARR-3* (rifampicin resistance), *merR* [Hg(II)-responsive transcriptional regulator] and *qacEΔ1* (quaternary ammonium compound resistance) (**Figure 3A**). We searched the National Center for Biotechnology Information (NCBI) database and found that pSW25KPC2 shared a 99.97% identity (with an 92% query coverage) compared to the plasmid pYNKP001-dfrA isolated from *R. ornithinolytica* (GenBank accession number: KY270853.1). Sequence alignment indicated that the backbone of pSW25KPC2 was highly similar to the plasmids pKP04VIM (*K. pneumoniae*), pYNKP001-dfrA (*R. ornithinolytica*), and pRJA166a (*K. pneumoniae*), but there were multiple Local Colinear Blocks (LCBs) that were inverted (**Figures 3A**, **4A**). Notably, pKP04VIM, pYNKP001-dfrA (*K. pneumoniae*), and pRJA166a (*K. pneumoniae*) did not carry the bla_{KPC-2} gene. Further analysis revealed that the bla_{KPC-2} gene of pSW25KPC2 was located in an LCB of about 6 kb that was highly homologous with pK55602_2 (GenBank accession number: CP042976.1) and pKPC2_095132 (GenBank accession number: CP028389.3) and was highly collinear with no inversions or rearrangements. The mapping of this LCB to **Figure 4B** revealed that pSW25KPC2, pK55602_2, and pKPC2_095132 all contained a conserved region carrying *korC* (encoding transcriptional repressor protein), IS*Kpn6*, bla_{KPC-2}, IS*Kpn27*, Tn*3*, and a truncated bla_{TEM}. Transposase Tn*As1* (Tn*3*-like element) and IS*4321* were also present on the pSW25KPC2 plasmid flanking a region encoding bla_{KPC-2}. Additionally, a region encoding *aac(3)-IId* was inverted in pSW25KPC2 compared

TABLE 2 | Genomic characterization of AHSWKP25.

ID	Size (bp)	GC Ratio	Resistance genes[a]	Point mutations[a]	Incompatibility group[a]
Chromosome	5,244,699	0.5759	bla_{SHV-5}, *fosA*	*ramR* (D152Y, K194*); *ompK36* (N49S, L59V, L191S, F207W, A217S, N218H, D224E, L228V, E232R, N304E); *ompK37* (I70M, I128M); *acrR* (P161R, G164A, F172S, R173G, L195V, F197I, K201M); *rcsA* (S35N)[b]; *lon* (E259A)[b]; *csrD* (Q110H)[c]	NA
pSW25KPC2	248,847	0.4661	*aadA16*, *qnrB4*, *aac(3)-IId*, *sul1*, *ARR-3*, Δbla_{TEM}, *dfrA27*, bla_{KPC-2}, *qacE*Δ*1*, *merR*	NA	Unknown
pSW25HRG	140,379	0.4968	*pcoABCDERS*, *silBCEFGPRS*, *terABCDEWXYZ*	NA	FIB
pSW25tet_A	120,990	0.5334	*tet(A)*, *qnrS1*, *dfrA14*, *sul2*, bla_{LAP-2}, *floR*	*tet(A)*[d] (I5R, V55M, I75V, T84A, S201A, F202S, V203F)	FII/FIA
pSW25NDM1	59,349	0.4906	bla_{SHV-12}, bla_{NDM-1}	NA	X3
pSW25H01	54,244	0.5176	NA	NA	Unknown
pSW25H02	3,482	0.5017	NA	NA	Unknown
pSW25H03	2,667	0.4578	NA	NA	Unknown

NA, not applicable; [a]*Data was obtained from the online website (https://cge.cbs.dtu.dk/, https://bigsdb.pasteur.fr/),* [b]*Reference sequence: K. pneumoniae UCI 38 (accession number: JCMB01),* [c]*Reference sequence: K. pneumoniae ATCC 13883 (accession number: JOOW01), d: Reference sequence: tet (A) (GenBank accession number: X00006).*

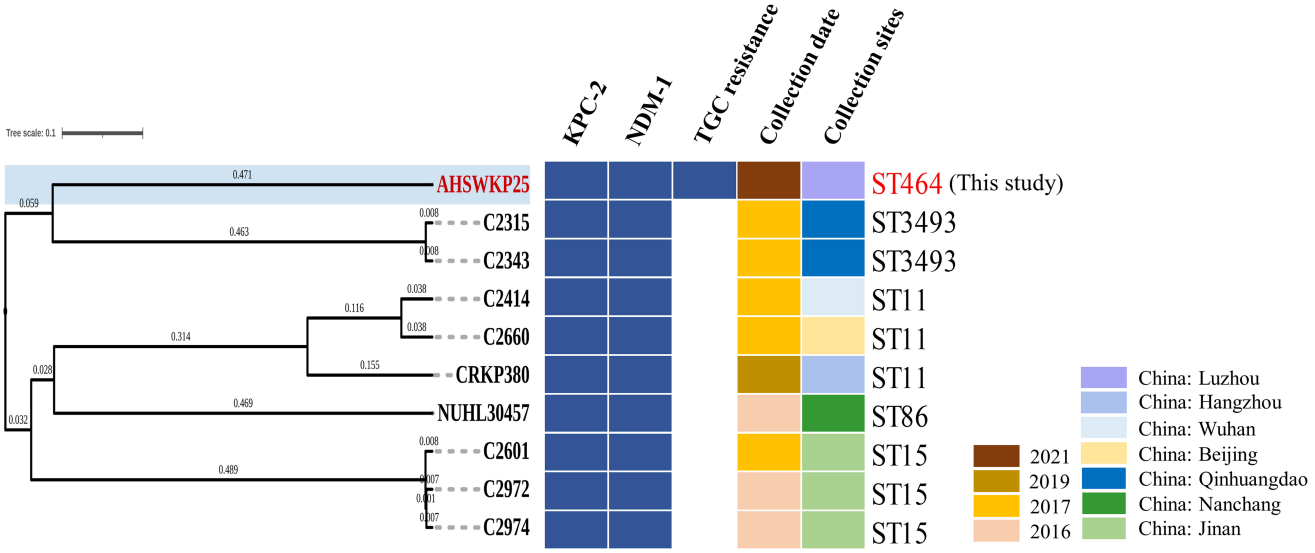

FIGURE 2 | OrthoANI-based phylogenetic tree of AHSWKP25 and other 9 NDM-1 and KPC-2 co-producing *K. pneumoniae* strains previously isolated from other parts of China. The different colors, respectively represented the resistance genes, collection date, and sites, blanks represent strains that are susceptible to tigecycline.

to pKPC2_095132 (**Figure 4A**). The Tn*4401* transposon and its variants were not identified in pSW25KPC2. Lastly, pSW25KPC2 also contained a region connecting *ISCR1* and *intI1*, that contained *ARR-3-dfrA27-aadA16- qacE*Δ*1-sul1* genes (**Figure 3A**).

pSW25HRG was a FIB plasmid that did not carry any acquired antimicrobial resistance genes. There were several heavy metal resistance genes in the backbone of pSW25HRG: *pcoABCDERS* (copper resistance), *silBCEFGPRS* (silver resistance), and *terABCDEWXYZ* (tellurium resistance). Sequence alignments constructed with BLAST (see text footnote 5) revealed that most plasmid sequences similar to pSW25HRG have been isolated from *K. pneumoniae* strains. pSW25HRG shared a 99.93% identity (with an 80% query coverage) with a plasmid isolated from the *K. pneumoniae* strain FDAARGOS_1322 (GenBank accession number: CP070038.1) and a 99.90% identity (with an 83% query coverage) with a plasmid isolated from *K. pneumoniae* strain NICU_2_P7 (GenBank accession

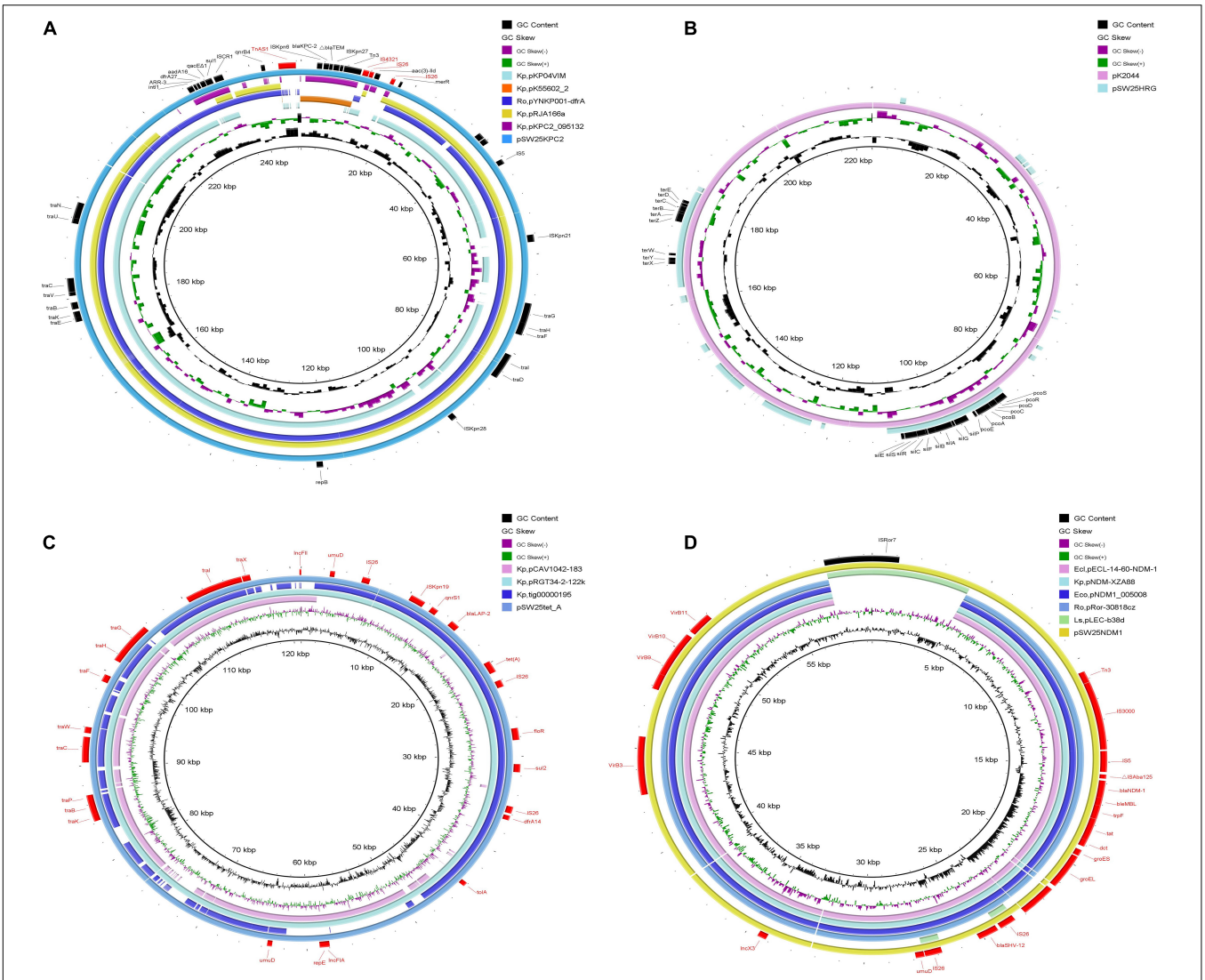

FIGURE 3 | Comparative genomic circle of plasmids. **(A)** Circular comparison of pSW25KPC2 with other similar plasmids, pSW25KPC2 was used as a reference. **(B)** Circular comparison between pSW25HRG and virulence plasmid pK2044, pK2044 was used as a reference. **(C)** Circular comparison of pSW25tet_A with other similar plasmids, pSW25tet_A was used as a reference. **(D)** Circular comparison of pSW25NDM1 with other similar plasmids, pSW25NDM1 was used as a reference. The outermost circle annotates the genetic information, and different plasmids are assigned different colors. Blanks represent deleted regions compared to the reference plasmids. Kp: *K. pneumoniae*, Ro: *R. ornithinolytica*, Ecl: *E. cloacae*, Eco: *E. coli*, Ls: *Leclercia* sp.

number: CP060050.1). Notably, pSW25HRG had a 23-kb homologous region compared to the well-known virulence plasmid pK2044 (GenBank accession number: NC_006625.1), wherein the above mentioned heavy-metal-resistance genes mainly occurred (**Figure 3B**).

The pSW25tet_A carried two replicon types, FII and FIA, and was 120,990 bp in length. Similar to pSW25KPC2, pSW25tet_A carried many genes encoding type IV conjugative transfer systems and multiple antimicrobial resistance determinants, including *tet(A)* (tetracycline resistance), *dfrA14* (trimethoprim resistance), *sul2* (sulfamethoxazole resistance), *qnrS1* (quinolones resistance), and $bla_{\mathrm{LAP-2}}$ (penicillins resistance). We identified that *tet(A)* in the pSW25tet_A was a type I mutant with a mutation profile of I5R, V55M, I75V, T84A, S201A, F202S, and V203F. This *tet(A)* mutant was previously demonstrated to be associated with reduced tigecycline susceptibility (Chiu et al., 2017). By searching the NCBI database, we found that pSW25tet_A was also similar to several other plasmids isolated from *K. pneumoniae* strains. Of these, pSW25tet_A shared a 99.97% identify (with a 100% query coverage) with a plasmid pRGT34-2-122k (GenBank accession number: CP075310.1) that was also isolated from *K. pneumoniae*. The homology between pSW25tet_A and pRGT34-2-122k was confirmed by comparing genomic circles (**Figure 3C**). pSW25tet_A shared only 28 and 29% coverage compared with pYUSHP2-2 (GenBank accession number: CP073773.1), a plasmid isolated from *E. hormaechei*, and pWP8-W19-CRE-01_3 (GenBank

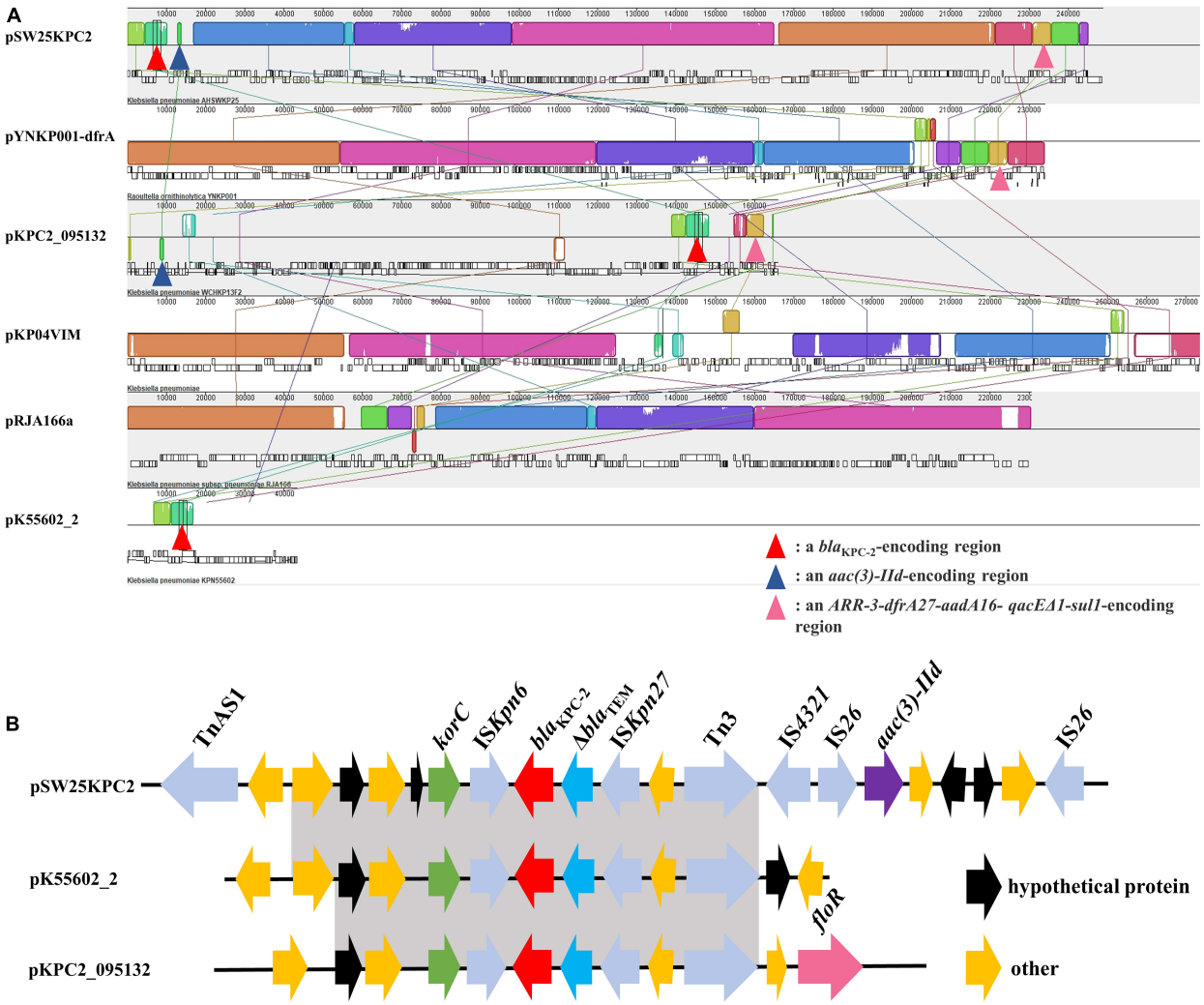

FIGURE 4 | (A) Mauve alignment between pSW25KPC2 and other five plasmids. The grids of the same color represent collinear areas and are connected by lines. The blank area in the grid indicates that the sequences are incompletely aligned. **(B)** Comparison of genetic elements surrounding bla_{KPC-2} between pSW25KPC2 and plasmids carrying bla_{KPC-2}. Gray areas represent homologous portions between sequences.

accession number: AP022271.1), a plasmid isolated from *R. ornithinolytica*, respectively.

Lastly, pSW25NDM1 was identified as an X3 plasmid carrying bla_{NDM-1} and bla_{SHV-12} genes. It was 59,349 bp in length and had a GC ratio of 49.06%. The genetic structure surrounding bla_{NDM-1} included IS*3000*, IS*5*, ble_{MBL}, *trpF*, *tat*, *dct*, *groES* and *groEL*. pSW25NDM1 shared a 100% identity (with an 89% query coverage) with pECL-14-60-NDM-1 (GenBank accession number: MN061454.1), a plasmid isolated from *E. cloacae*. Sequence alignment revealed that pSW25NDM1 was very similar to plasmids isolated from *K. pneumoniae*, *E. coli*, *E. cloacae*, and *R. ornithinolytica* (**Figure 3D**). pSW25NDM1 contained an additional region of about 6 kb, which was not present in other plasmids carrying NDM-1, and it was highly homologous to a plasmid isolated from *Leclercia* sp. (GenBank accession number: CP026168.1) (**Figure 3D**). Further analysis showed that this region could be inserted by IS*Ro7* (marked black in **Figure 3D**). The bla_{SHV-12} was located in a 4-kb inserted region that could be inserted by IS*26* at both ends.

Stable Dissemination and Expression of pSW25NDM1 Carrying bla_{NDM-1} Among Species

Among the three plasmids carrying the acquired antimicrobial resistance genes mentioned above, we only demonstrated the horizontal transferability of pSW25NDM1 in conjugation experiments. The pSW25NDM1 can be transferred to *E. coli* J53 at a transfer frequency of about 2.03×10^{-3}. Recipient strain *E. coli* J53 showed significantly reduced susceptibility to meropenem and cefepime after the acquisition of plasmid pSW25NDM1 (**Table 1**). *E. coli* J53 carrying pSW25NDM1 displayed high plasmid stability during its continuous passage in an antibiotic-free environment for 10 days, and more than 95%

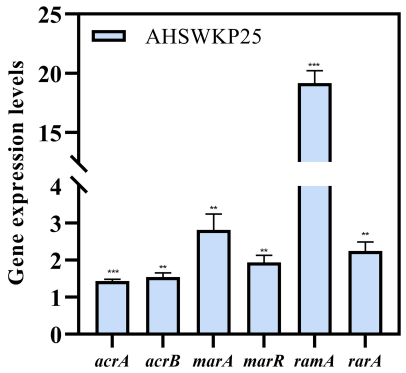

FIGURE 5 | Relative expression levels of *acrA*, *acrB*, *marA*, *marR*, *ramA,* and *rarA* genes in AHSWKP25. Gene expression levels were normalized using the *rpoB* (RNA polymerase) gene. The experiment was repeated in triplicate independently, and data are expressed as the mean ± SD (standard deviation). $^{**}P < 0.01$; $^{***}P < 0.001$ by Student's *t*-test.

of the recipient strains cells still retained pSW25NDM1 on day 10 (**Supplementary Figure 4**).

Efflux Pump Phenotype Test and RT-PCR

The MICs of ceftazidime and meropenem for AHSWKP25 did not change significantly after the addition of NMP (100 μg/mL). However, there were ≥ 4-fold reductions in the MICs of ciprofloxacin and chloramphenicol in the presence of NMP (100 μg/mL). And NMP restored the susceptibility of AHSWKP25 to tigecycline (**Table 1**). Furthermore, the RT-PCR results indicated that the expressions of *acrA* and *acrB* genes were up-regulated by 1.4-fold (1.43 ± 0.05) and 1.5-fold (1.54 ± 0.12), respectively, in AHSWKP25 compared to that in NTUH-K2044. The expressions of *rarA*, *marA,* and *marR* were up-regulated approximately twofold in AHSWKP25 (2.25 ± 0.24, 2.82 ± 0.43, 1.94 ± 0.19, respectively), while *ramA* was up-regulated 19-fold (19.18 ± 1.04) (**Figure 5**).

DISCUSSION

In this study, we reported on a bla_{NDM-1} and bla_{KPC-2} co-producing *K. pneumoniae* isolate (AHSWKP25) that was isolated in Southwestern China. To the best of our knowledge, this is the first report of a tigecycline resistant *K. pneumoniae* wzi 725 strain co-producing bla_{NDM-1} and bla_{KPC-2} in China, and its resistance profiles meet the definition of extensively drug-resistant (Magiorakos et al., 2012). In particular, AHSWKP25 belonged to an uncommon sequence type ST464, that was previously identified in neonatal patients in a few countries and for which little formation is available (Rakovitsky et al., 2020; Sands et al., 2021). We searched the database and found here was a one-allele difference between ST464 and ST2439 and two-allele differences between ST464 and ST5620, respectively. ST464 is markedly different from the sequence types of other bla_{NDM-1} and bla_{KPC-2} co-producing *K. pneumoniae* strains that have been reported in previous studies, suggesting that the combination of bla_{KPC-2} and bla_{NDM-1} not only appeared in several common sequence types (**Figure 2** and **Supplementary Figure 3**). Therefore, continuous monitoring of such bacteria is still necessary. To date, we have not isolated any other *K. pneumoniae* strains with the same resistance pattern and sequence type as AHSWKP25 from other patients and settings in the local hospital. However, the patient was dead, and we were unable to obtain further information regarding colonization. The AHSWKP25 genome contained seven circular plasmids carrying multiple mobile elements and acquired antimicrobial resistance genes, reflecting the high plasticity of the *K. pneumoniae* genome. In marked contrast to bla_{NDM-1} and bla_{KPC-2} co-producing *K. pneumoniae* strains previously isolated from other parts of China, AHSWKP25 was also resistant to fosfomycin and tigecycline (**Figure 2**). As a common tetracycline-resistance determinant of Gram-negative bacteria, *tet(A)* can increase the efflux of tetracyclines by activating the expression of the major facilitator superfamily (MFS) efflux pumps (Nguyen et al., 2014). Tigecycline belongs to the glycylcycline family of antibiotics and has a much stronger antimicrobial activity than both tetracycline and minocycline. *tet(A)* mutants are associated with reduced bacterial susceptibility to tigecycline (Linkevicius et al., 2016). Mutated *tet(A)* can act synergistically with defective *ramR* to significantly increase the level of tigecycline resistance in *K. pneumoniae* strains (Chiu et al., 2017). Because the patient in this study had previously received tigecycline therapy, we speculated that the selection pressure exerted by tigecycline might have promoted the formation of *tet(A)* mutants (Xu et al., 2021). Furthermore, overexpression of *acrAB* and *ramA* is another common mechanism of tigecycline resistance in Enterobacteriaceae (Zhong et al., 2014; Osei Sekyere et al., 2016). In this study, we determined the role of efflux pumps in the tigecycline resistance of AHSWKP25 using the efflux pump inhibition test and RT-PCR (**Figure 4**). the transcriptional regulation of *acrAB* and *ramA* was closely related to the mutation in *ramR* (Abouzeed et al., 2008). Previous studies showed that the A19V substitution mutation in the *ramR* gene was more common in tigecycline and carbapenem-resistant *K. pneumoniae* (Sheng et al., 2014; Chiu et al., 2017). However, we did not find the A19V mutation in the *ramR* of AHSWKP25, rather, we did identify a D152Y substitution mutation that was previously identified in a tigecycline-non-susceptible *K. pneumoniae* strain that did not carry *tet(A)* mutant (MIC: 4 μg/ml) (Cheng et al., 2020). Thus, we considered that the tigecycline resistance of AHSWKP25 could be manifested by the combination of the *tet(A)* variant and the *ramR* mutation. *rarA* encodes an AraC-type regulator that can also independently activate the AcrAB and OqxAB efflux pumps, endowing *K. pneumoniae* with a multidrug resistance phenotype and tigecycline resistance (Veleba et al., 2012; De Majumdar et al., 2013).

Of the three antibiotic resistance plasmids carried by AHSWKP25, only the X3 plasmid pSW25NDM1 containing the bla_{NDM-1} gene was shown to be horizontally transferred in the present conjugation experiments. The horizontal transfer of plasmids is often more restricted in stains carrying multiple plasmids compared to strains with only single plasmid. Distorting

interactions, which can affect the horizontal transfer efficiency, have previously been observed between three plasmids carried by the same host, (Gama et al., 2017a). In addition to being inhibited by fertility inhibition systems (FIN), the co-transfer of multiple plasmids is also limited in plasmids with low conjugation rates (Gama et al., 2017b). Additionally, the horizontal transfer of these resistant plasmids may result in huge fitness costs to the recipient, thereby disturbing conjugation (San Millan and MacLean, 2017). Furthermore, the host ranges of plasmids pSW25KPC2, pSW25HRG, and pSW25tet_A could be relatively narrow (**Figure 3**). Therefore, when assessing the horizontal transfer capacity of multiple plasmids carried by the same host, the influence of several factors must be considered. Sequence alignment showed that although the backbones of pSW25KPC2 and pSW25NDM1 were homologous to those of other plasmids isolated from Enterobacteriaceae, the plasmids acquired other genes by mobile elements, demonstrating the evolutionary potential of these antibiotic resistance plasmids (**Figure 3**). Because IS*CR1* can mobilize its adjacent sequences through rolling circle transposition, we speculated that the *ISCR1* element was involved in the capture of multiple antimicrobial resistance genes, including *ARR-3-dfrA27-aadA16-qacEΔ1-sul1* on pSW25KPC2 (**Figure 3A**; Cheng et al., 2016). Transposition events mediated by transposon Tn*4401* were the predominant reason for the rapid spread of the bla_{KPC} genes to different plasmids (Naas et al., 2008). While we did not identify the Tn*4401* transposon and its variants in pSW25KPC2, the region on pSW25KPC2 encoding bla_{KPC-2} was homologous with other plasmids carrying bla_{KPC-2}. In addition, the backbone of pSW25KPC2 was highly similar to other plasmids without bla_{KPC-2}, suggesting that the acquisition of bla_{KPC-2} by pSW25KPC2 can be enabled by homologous recombination between plasmids (**Figures 3A**, **4**). Tn*As1*, Tn*3*, and IS*4321* may play a significant role in this process. Notably, our results revealed that pSW25NDM1 carrying bla_{NDM-1} was capable of horizontal transfer to the recipient strain *E. coli* J53 and a variety of other wide hosts (**Figure 3D**), highlighting the flexibility of plasmids carrying bla_{NDM-1} in the formation of bla_{NDM-1} and bla_{KPC-2} co-producing strains (Gao et al., 2020).

The virulence phenotype of AHSWKP25 was also a cause for concern (**Figure 1**). Our results also supported the observation that *K. pneumoniae* strains did not carry *rmpA*/*rmpA2*, *iucA*, and capsular serotype other than K1, K2, K5, K20, K54, and K57 could be had a hypervirulent phenotype (**Supplementary Table 4**). However, the accuracy of distinguishing cKp and hvKp strains based on the *G. mellonella* infection model was insufficient compared to the murine model (Russo and MacDonald, 2020). Therefore, the lack of a mammalian infection model for evaluating the pathogenicity of AHSWKP25 was a limitation of this study. In hvkp strains, the emergence of tigecycline resistance mediated predominantly by *ramR* mutations was accompanied by decreased mucoviscosity and serum resistance (Park et al., 2020; Di Pilato et al., 2022). This phenomenon can be explained by the fitness cost, meaning, in the absence of antibiotic selection, resistance mutations could disturb the physiological function of bacteria, resulting in reduced pathogenicity, growth rate, and competitiveness compared to susceptive strains accordingly (Andersson and Hughes, 2010). However, several recent studies have revealed that genes and their regulators responsible for capsule biosynthesis play a dominant role in the adaptive evolution of *K. pneumoniae*. Disruption to these genes (*rsAB*, *lon*, and *csrD*) can ultimately affect capsule production, especially if these disruptions promote capsule hyperproduction, which would lead to enhancements in the pathogenicity and serum resistance of *K. pneumoniae* (Ernst et al., 2020; Mike et al., 2021). And mutations in the *pal* are mainly associated with reduced virulence (Hsieh et al., 2013). As mentioned above, missense mutations were identified in the *rcsA*, *lon,* and *csrD* genes that regulate capsule production in AHSWKP25. In particular, the S35N missense mutation in the *rcsA* gene of the AHSWKP25 genome was previously identified in a hypervirulent and hypermucoviscous *K. pneumoniae* isolate with hypercapsule production (Morales-León et al., 2021). The hypercapsule production is not necessarily associated with hypermucoviscosity (Mike et al., 2021). Therefore, the hypervirulent phenotype of AHSWKP25 was more likely to be associated with hypercapsule production through the regulators of capsule production mutations, but the exact mechanism remains to be further studied. The Type 3 fimbriae-encoding genes *mrkABCDFHIJ* and the Type I fimbriae-encoding gene *fimABCEFGHIK* are common in ckp and hvkp strains and can promote bacterial adhesion during pathogenic infection and biofilm formation (Di Martino et al., 2003). Among the siderophores carried by AHSWKP25, enterobactin is produced in both cKp and hvKp, whereas salmonellin is found more commonly in hvKp (El Fertas-Aissani et al., 2013; Lee I. R. et al., 2016). Furthermore, the heavy metal resistance genes carried by pSW25HRG were highly homologous to the gene carried by the virulence plasmid pK2044 and might be associated with the homologous recombination in these variable regions carrying heavy metal resistance genes of virulence plasmids. Although previous studies of *S. aureus* and *A. baumannii* demonstrated a relationship between these heavy metal resistance genes and pathogenicity, their contribution to the virulence of *K. pneumoniae* strains is still unclear (Alquethamy et al., 2019; Lawal et al., 2021). Overall, we determined that virulence of AHSWKP25 differ from those of common hypervirulent strains, and our results suggested that the emergence of hvkp strains might not depend exclusively on the genetic backgrounds and that point mutations in chromosomal loci also contributed to the development of the hypervirulent phenotype (Ernst et al., 2020).

There were several other limitations of this study that must be addressed in subsequent studies. First, although we reported NDM-1 and KPC-2 co-producing *K. pneumoniae* in Southwest China for the first time, the local prevalence of such microorganisms requires further clarification. Second, as mentioned above, mammalian models are still necessary to further elucidate the virulence behavior of AHSWKP25 in the future. Third, we used only *E. coli* J53 as the recipient in the conjugation experiments, in subsequent studies, we will use *K. pneumoniae* stains as recipients to assess the horizontal transferability of these plasmids.

CONCLUSION

In conclusion, this study was the first to describe and sequence a hypervirulent tigecycline-resistant and serum-resistant *K. pneumoniae* strain containing both bla_{NDM-1} and bla_{KPC-2} in Southwestern China. The resistance phenotypes displayed by AHSWKP25 suggested that bla_{NDM-1} and bla_{KPC-2} co-producing *K. pneumoniae* strains can potentially develop further antimicrobial resistance. Notably, we identified missense mutations in the genes associated with hypercapsule production in AHSWKP25, which will provide valuable information for illustrating the formation mechanism of hypervirulent *K. pneumoniae*. Importantly, strict monitoring measures must be taken to prevent the spread of these superbugs.

DATA AVAILABILITY STATEMENT

The datasets presented in this study can be found in online repositories. The names of the repository/repositories and accession number(s) can be found below: NCBI GenBank, CP091048-CP091055 (*K. pneumoniae* AHSWKP25).

ETHICS STATEMENT

The study protocol was approved by the Institutional Review Board of the Affiliated Hospital of Southwest Medical University (Project No. KY2020043).

AUTHOR CONTRIBUTIONS

JH, BZ, JD, and JL isolated AHSWKP25 and designed the study and experiments. JH, JD, and YW performed the assays. JH, BZ, and XX analyzed the data. JH and BZ drafted and revised the manuscript. All authors contributed to manuscript revision, read, and approved the submitted version.

FUNDING

This study was supported by the grants from Sichuan Science and Technology Department Program (20QYCX0056 and 2021YFH001), and Sichuan Education Department Training Program of Innovation and Entrepreneurship for College Students (S202010632250).

ACKNOWLEDGMENTS

We thank the team of the curators of the Institut Pasteur MLST system (Paris, France) for importing novel alleles, profiles, and/or isolates at http://bigsdb.pasteur.fr.

SUPPLEMENTARY MATERIAL

The Supplementary Material for this article can be found online at: https://www.frontiersin.org/articles/10.3389/fmicb.2022.868705/full#supplementary-material

REFERENCES

Abouzeed, Y. M., Baucheron, S., and Cloeckaert, A. (2008). ramR mutations involved in efflux-mediated multidrug resistance in *Salmonella enterica* serovar Typhimurium. *Antimicrob. Agents Chemother.* 52, 2428–2434. doi: 10.1128/aac.00084-08

Alquethamy, S. F., Khorvash, M., Pederick, V. G., Whittall, J. J., Paton, J. C., Paulsen, I. T., et al. (2019). The Role of the CopA Copper Efflux System in *Acinetobacter baumannii* Virulence. *Int. J. Mol. Sci.* 20:13. doi: 10.3390/ijms20030575

Andersson, D. I., and Hughes, D. (2010). Antibiotic resistance and its cost: is it possible to reverse resistance? *Nat. Rev. Microbiol.* 8, 260–271. doi: 10.1038/nrmicro2319

Cheng, C., Sun, J., Zheng, F., Lu, W., Yang, Q., and Rui, Y. (2016). New structures simultaneously harboring class 1 integron and ISCR1-linked resistance genes in multidrug-resistant Gram-negative bacteria. *BMC Microbiol.* 16:71. doi: 10.1186/s12866-016-0683-x

Cheng, H. Y., Chen, Y. S., Wu, C. Y., Chang, H. Y., Lai, Y. C., and Peng, H. L. (2010). RmpA Regulation of Capsular Polysaccharide Biosynthesis in *Klebsiella pneumoniae* CG43. *J. Bacteriol.* 192, 3144–3158. doi: 10.1128/jb.00031-10

Cheng, Y. H., Huang, T. W., Juan, C. H., Chou, S. H., Tseng, Y. Y., Chen, T. W., et al. (2020). Tigecycline-non-susceptible hypervirulent *Klebsiella pneumoniae* strains in Taiwan. *J. Antimicrob. Chemother.* 75, 309–317. doi: 10.1093/jac/dkz450

Chiu, S. K., Huang, L. Y., Chen, H., Tsai, Y. K., Liou, C. H., Lin, J. C., et al. (2017). Roles of ramR and tet(A) Mutations in Conferring Tigecycline Resistance in Carbapenem-Resistant *Klebsiella pneumoniae* Clinical Isolates. *Antimicrob. Agents Chemother.* 61, e391–e317. doi: 10.1128/aac.00391-17

Clinical and Laboratory Standards Institute. (2020). *Performance Standards for Antimicrobial Susceptibility Testing*, 30th Edn. Wayne: Clinical and Laboratory Standards Institute.

De Majumdar, S., Veleba, M., Finn, S., Fanning, S., and Schneiders, T. (2013). Elucidating the Regulon of Multidrug Resistance Regulator RarA in *Klebsiella pneumoniae*. *Antimicrob. Agents Chemother.* 57, 1603–1609. doi: 10.1128/aac.01998-12

Di Martino, P., Cafferini, N., Joly, B., and Darfeuille-Michaud, A. (2003). *Klebsiella pneumoniae* type 3 pili facilitate adherence and biofilm formation on abiotic surfaces. *Res. Microbiol.* 154, 9–16. doi: 10.1016/s0923-2508(02)00004-9

Di Pilato, V., Henrici De Angelis, L., Aiezza, N., Baccani, I., Niccolai, C., Parisio, E. M., et al. (2022). Resistome and virulome accretion in an NDM-1-producing ST147 sublineage of *Klebsiella pneumoniae* associated with an outbreak in Tuscany, Italy: a genotypic and phenotypic characterisation. *Lancet Microb.* 3, e224–e234. doi: 10.1016/S2666-5247(21)00268-8

El Fertas-Aissani, R., Messai, Y., Alouache, S., and Bakour, R. (2013). Virulence profiles and antibiotic susceptibility patterns of *Klebsiella pneumoniae* strains isolated from different clinical specimens. *Pathol. Biol.* 61, 209–216. doi: 10.1016/j.patbio.2012.10.004

Ernst, C. M., Braxton, J. R., Rodriguez-Osorio, C. A., Zagieboylo, A. P., Li, L., Pironti, A., et al. (2020). Adaptive evolution of virulence and persistence in carbapenem-resistant *Klebsiella pneumoniae*. *Nat. Med.* 26, 705–711. doi: 10.1038/s41591-020-0825-4

Gama, J. A., Zilhao, R., and Dionisio, F. (2017a). Multiple plasmid interference - Pledging allegiance to my enemy's enemy. *Plasmid* 93, 17–23. doi: 10.1016/j.plasmid.2017.08.002

Gama, J. A., Zilhao, R., and Dionisio, F. (2017b). Co-resident plasmids travel together. *Plasmid* 93, 24–29. doi: 10.1016/j.plasmid.2017.08.004

Gao, H., Liu, Y. D., Wang, R. B., Wang, Q., Jin, L. Y., and Wang, H. (2020). The transferability and evolution of NDM-1 and KPC-2 co-producing *Klebsiella pneumoniae* from clinical settings. *Ebiomedicine* 51:11. doi: 10.1016/j.ebiom.2019.102599

Hsieh, P. F., Liu, J. Y., Pan, Y. J., Wu, M. C., Lin, T. L., Huang, Y. T., et al. (2013). *Klebsiella pneumoniae* peptidoglycan-associated lipoprotein and murein lipoprotein contribute to serum resistance, antiphagocytosis, and proinflammatory cytokine stimulation. *J. Infect. Dis.* 208, 1580–1589. doi: 10.1093/infdis/jit384

Kim, M., Park, J., and Park, W. (2021). Genomic and phenotypic analyses of multidrug-resistant *Acinetobacter baumannii* NCCP 16007 isolated from a patient with a urinary tract infection. *Virulence* 12, 150–164. doi: 10.1080/21505594.2020.1867421

Lawal, O. U., Fraqueza, M. J., Worning, P., Bouchami, O., Bartels, M. D., Goncalves, L., et al. (2021). Staphylococcus saprophyticus Causing Infections in Humans Is Associated with High Resistance to Heavy Metals. *Antimicrob. Agents Chemother.* 65:17. doi: 10.1128/aac.02685-20

Lee, I., Ouk Kim, Y., Park, S. C., and Chun, J. (2016). OrthoANI: an improved algorithm and software for calculating average nucleotide identity. *Int. J. Syst. Evol. Microbiol.* 66, 1100–1103. doi: 10.1099/ijsem.0.000760

Lee, I. R., Molton, J. S., Wyres, K. L., Gorrie, C., Wong, J., Hoh, C. H., et al. (2016). Differential host susceptibility and bacterial virulence factors driving Klebsiella liver abscess in an ethnically diverse population. *Sci. Rep.* 6:12. doi: 10.1038/srep29316

Liao, C. H., Huang, Y. T., Chang, C. Y., Hsu, H. S., and Hsueh, P. R. (2014). Capsular serotypes and multilocus sequence types of bacteremic *Klebsiella pneumoniae* isolates associated with different types of infections. *Eur. J. Clin. Microbiol. Infect. Dis.* 33, 365–369. doi: 10.1007/s10096-013-1964-z

Linkevicius, M., Sandegren, L., and Andersson, D. I. (2016). Potential of Tetracycline Resistance Proteins To Evolve Tigecycline Resistance. *Antimicrob. Agents Chemother.* 60, 789–796. doi: 10.1128/aac.02465-15

Liu, Y., Liu, P. P., Wang, L. H., Wei, D. D., Wan, L. G., and Zhang, W. (2017). Capsular Polysaccharide Types and Virulence-Related Traits of Epidemic KPC-Producing *Klebsiella pneumoniae* Isolates in a Chinese University Hospital. *Microb. Drug Resist.* 23, 901–907. doi: 10.1089/mdr.2016.0222

Liu, Y., Long, D., Xiang, T. X., Du, F. L., Wei, D. D., Wan, L. G., et al. (2019). Whole genome assembly and functional portrait of hypervirulent extensively drug-resistant NDM-1 and KPC-2 co-producing *Klebsiella pneumoniae* of capsular serotype K2 and ST86. *J. Antimicrob. Chemother.* 74, 1233–1240. doi: 10.1093/jac/dkz023

Magiorakos, A. P., Srinivasan, A., Carey, R. B., Carmeli, Y., Falagas, M. E., Giske, C. G., et al. (2012). Multidrug-resistant, extensively drug-resistant and pandrug-resistant bacteria: an international expert proposal for interim standard definitions for acquired resistance. *Clin. Microbiol. Infect.* 18, 268–281. doi: 10.1111/j.1469-0691.2011.03570.x

Maltezou, H. C. (2009). Metallo-beta-lactamases in Gram-negative bacteria: introducing the era of pan-resistance? *Int. J. Antimicrob. Agents* 33:7. doi: 10.1016/j.ijantimicag.2008.09.003

Mike, L. A., Stark, A. J., Forsyth, V. S., Vornhagen, J., Smith, S. N., Bachman, M. A., et al. (2021). A systematic analysis of hypermucoviscosity and capsule reveals distinct and overlapping genes that impact *Klebsiella pneumoniae* fitness. *PLoS Pathog.* 17:e1009376. doi: 10.1371/journal.ppat.1009376

Morales-León, F., Opazo-Capurro, A., Caro, C., Lincopan, N., Cardenas-Arias, A., Esposito, F., et al. (2021). Hypervirulent and hypermucoviscous extended-spectrum β-lactamase-producing *Klebsiella pneumoniae* and Klebsiella variicola in Chile. *Virulence* 12, 35–44. doi: 10.1080/21505594.2020.1859274

Naas, T., Cuzon, G., Villegas, M. V., Lartigue, M. F., Quinn, J. P., and Nordmann, P. (2008). Genetic structures at the origin of acquisition of the beta-lactamase bla KPC gene. *Antimicrob. Agents Chemother.* 52, 1257–1263. doi: 10.1128/aac.01451-07

Nang, S. C., Morris, F. C., McDonald, M. J., Han, M. L., Wang, J. P., Strugnell, R. A., et al. (2018). Fitness cost of mcr-1-mediated polymyxin resistance in *Klebsiella pneumoniae*. *J. Antimicrob. Chemother.* 73, 1604–1610. doi: 10.1093/jac/dky061

Nguyen, F., Starosta, A. L., Arenz, S., Sohmen, D., Donhofer, A., and Wilson, D. N. (2014). Tetracycline antibiotics and resistance mechanisms. *Biol. Chem.* 395, 559–575. doi: 10.1515/hsz-2013-0292

Osei Sekyere, J., Govinden, U., Bester, L. A., and Essack, S. Y. (2016). Colistin and tigecycline resistance in carbapenemase-producing Gram-negative bacteria: emerging resistance mechanisms and detection methods. *J. Appl. Microbiol.* 121, 601–617. doi: 10.1111/jam.13169

Park, S., Lee, H., Shin, D., and Ko, K. S. (2020). Change of Hypermucoviscosity in the Development of Tigecycline Resistance in Hypervirulent *Klebsiella pneumoniae* Sequence Type 23 Strains. *Microorganisms* 8:1562. doi: 10.3390/microorganisms8101562

Podschun, R., and Ullmann, U. (1998). Klebsiella spp. as nosocomial pathogens: epidemiology, taxonomy, typing methods, and pathogenicity factors. *Clin. Microbiol. Rev.* 11, 589–603. doi: 10.1128/cmr.11.4.589

Poirel, L., Jayol, A., and Nordmann, P. (2017). Polymyxins: antibacterial Activity, Susceptibility Testing, and Resistance Mechanisms Encoded by Plasmids or Chromosomes. *Clin. Microbiol. Rev.* 30, 557–596. doi: 10.1128/cmr.00064-16

Rakovitsky, N., Frenk, S., Kon, H., Schwartz, D., Temkin, E., Solter, E., et al. (2020). Fourier Transform Infrared Spectroscopy Is a New Option for Outbreak Investigation: a Retrospective Analysis of an Extended-Spectrum-Beta-Lactamase-Producing *Klebsiella pneumoniae* Outbreak in a Neonatal Intensive Care Unit. *J. Clin. Microbiol.* 58:8. doi: 10.1128/jcm.00098-20

Russo, T. A., and MacDonald, U. (2020). The Galleria mellonella Infection Model Does Not Accurately Differentiate between Hypervirulent and Classical *Klebsiella pneumoniae*. *Msphere* 5:7. doi: 10.1128/mSphere.00850-19

San Millan, A., and MacLean, R. C. (2017). Fitness costs of plasmids: a limit to plasmid transmission. *Microbiol. Spectr.* 5. doi: 10.1128/microbiolspec.MTBP-0016-2017

Sands, K., Carvalho, M. J., Portal, E., Thomson, K., Dyer, C., Akpulu, C., et al. (2021). Characterization of antimicrobial-resistant Gram-negative bacteria that cause neonatal sepsis in seven low- and middle-income countries. *Nat. Microbiol.* 6, 512–523. doi: 10.1038/s41564-021-00870-7

Schumacher, A., Steinke, P., Bohnert, J. A., Akova, M., Jonas, D., and Kern, W. V. (2006). Effect of 1-(1-naphthylmethyl)-piperazine, a novel putative efflux pump inhibitor, on antimicrobial drug susceptibility in clinical isolates of *Enterobacteriaceae* other than *Escherichia coli*. *J. Antimicrob. Chemother.* 57, 344–348. doi: 10.1093/jac/dki446

Shankar, C., Nabarro, L. E., Anandan, S., Ravi, R., Babu, P., Munusamy, E., et al. (2018). Extremely High Mortality Rates in Patients with Carbapenem-resistant, Hypermucoviscous *Klebsiella pneumoniae* Blood Stream Infections. *J. Assoc. Physicians India* 66, 13–16.

Sheng, Z. K., Hu, F. P., Wang, W. X., Guo, Q. L., Chen, Z. J., Xu, X. G., et al. (2014). Mechanisms of Tigecycline Resistance among *Klebsiella pneumoniae* Clinical Isolates. *Antimicrob. Agents Chemother.* 58, 6982–6985. doi: 10.1128/aac.03808-14

Shi, Q., Lan, P., Huang, D., Hua, X., Jiang, Y., Zhou, J., et al. (2018). Diversity of virulence level phenotype of hypervirulent *Klebsiella pneumoniae* from different sequence type lineage. *BMC Microbiol.* 18:94. doi: 10.1186/s12866-018-1236-2

Shon, A. S., Bajwa, R. P. S., and Russo, T. A. (2013). Hypervirulent (hypermucoviscous) *Klebsiella pneumoniae* A new and dangerous breed. *Virulence* 4, 107–118. doi: 10.4161/viru.22718

Turton, J. F., Perry, C., Elgohari, S., and Hampton, C. V. (2010). PCR characterization and typing of *Klebsiella pneumoniae* using capsular type-specific, variable number tandem repeat and virulence gene targets. *J. Med. Microbiol.* 59, 541–547. doi: 10.1099/jmm.0.015198-0

Veleba, M., Higgins, P. G., Gonzalez, G., Seifert, H., and Schneiders, T. (2012). Characterization of RarA, a Novel AraC Family Multidrug Resistance Regulator in *Klebsiella pneumoniae*. *Antimicrob. Agents Chemother.* 56, 4450–4458. doi: 10.1128/aac.00456-12

Walker, K. A., Treat, L. P., Sepúlveda, V. E., and Miller, V. L. (2020). The Small Protein RmpD Drives Hypermucoviscosity in *Klebsiella pneumoniae*. *mBio* 11, e1750–e1720. doi: 10.1128/mBio.01750-20

Xiang, T., Chen, C., Wen, J., Liu, Y., Zhang, Q., Cheng, N., et al. (2020). Resistance of *Klebsiella pneumoniae* strains carrying bla_{NDM-1} gene and the genetic environment of bla_{NDM-1}. *Front. Microbiol.* 11:700. doi: 10.3389/fmicb.2020.00700

Xu, J., Zhao, Z., Ge, Y., and He, F. (2020). Unravelling the genome sequence of NDM-1 and KPC-2 co-producing *Klebsiella pneumoniae* ST11 isolated from a bloodstream infection. *J. Glob. Antimicrob. Resist.* 20, 339–341. doi: 10.1016/j.jgar.2020.01.021

Xu, J., Zhu, Z. L., Chen, Y. M., Wang, W. Z., and He, F. (2021). The Plasmid-Borne tet(A) Gene Is an Important Factor Causing Tigecycline Resistance in ST11 Carbapenem-Resistant *Klebsiella pneumoniae* Under Selective Pressure. *Front. Microbiol.* 12:10. doi: 10.3389/fmicb.2021.644949

Yan, R., Lu, Y., Zhu, Y., Lan, P., Jiang, S., Lu, J., et al. (2021). A Sequence Type 23 Hypervirulent *Klebsiella pneumoniae* Strain Presenting Carbapenem Resistance by Acquiring an IncP1 bla (KPC-2) Plasmid. *Front. Cell Infect. Microbiol.* 11:641830. doi: 10.3389/fcimb.2021.641830

Yao, B., Xiao, X. M., Wang, F., Zhou, L., Zhang, X. W., and Zhang, J. (2015). Clinical and molecular characteristics of multi-clone carbapenem-resistant hypervirulent (hypermucoviscous) *Klebsiella pneumoniae* isolates in a tertiary hospital in Beijing, China. *Int. J. Infect. Dis.* 37, 107–112. doi: 10.1016/j.ijid.2015.06.023

Zhong, X., Xu, H. T., Chen, D. K., Zhou, H. J., Hu, X., and Cheng, G. (2014). First Emergence of acrAB and oqxAB Mediated Tigecycline Resistance in Clinical Isolates of *Klebsiella pneumoniae* Pre-Dating the Use of Tigecycline in a Chinese Hospital. *PLoS One* 9:11. doi: 10.1371/journal.pone.0115185

Conflict of Interest: The authors declare that the research was conducted in the absence of any commercial or financial relationships that could be construed as a potential conflict of interest.

Publisher's Note: All claims expressed in this article are solely those of the authors and do not necessarily represent those of their affiliated organizations, or those of the publisher, the editors and the reviewers. Any product that may be evaluated in this article, or claim that may be made by its manufacturer, is not guaranteed or endorsed by the publisher.

frontiers | Frontiers in Microbiology

ORIGINAL RESEARCH
published: 04 May 2022
doi: 10.3389/fmicb.2022.868152

Phenotypic and Genotypic Characteristics of a Tigecycline-Resistant *Acinetobacter pittii* Isolate Carrying bla_{NDM-1} and the Novel bla_{OXA} Allelic Variant $bla_{OXA-1045}$

*Zixuan Ding†, Zhaoyinqian Li†, Yuanqing Zhao†, Jingchen Hao, Tingting Li, Yao Liu, Zhangrui Zeng and Jinbo Liu**

Department of Laboratory Medicine, The Affiliated Hospital of Southwest Medical University, Luzhou, China

OPEN ACCESS

Edited by:
Eun-Jeong Yoon, Korea National Institute of Health, South Korea

Reviewed by:
Siqiang Niu, The First Affiliated Hospital of Chongqing Medical University, China
Somdatta Chatterjee, IGeneX Inc., United States

***Correspondence:**
Jinbo Liu
Liulab2019@163.com

†These authors have contributed equally to this work and share first authorship

Specialty section:
This article was submitted to Antimicrobials, Resistance and Chemotherapy, a section of the journal Frontiers in Microbiology

Received: *02 February 2022*
Accepted: *30 March 2022*
Published: *04 May 2022*

Citation:
Ding Z, Li Z, Zhao Y, Hao J, Li T, Liu Y, Zeng Z and Liu J (2022) Phenotypic and Genotypic Characteristics of a Tigecycline-Resistant Acinetobacter pittii Isolate Carrying bla_{NDM-1} and the Novel bla_{OXA} Allelic Variant $bla_{OXA-1045}$. Front. Microbiol. 13:868152. doi: 10.3389/fmicb.2022.868152

A tigecycline-resistant *Acinetobacter pittii* clinical strain from pleural fluid carrying a bla_{NDM-1} gene and a novel bla_{OXA} gene, $bla_{OXA-1045}$, was isolated and characterized. The AP2044 strain acquired two copies of the bla_{NDM-1} gene and six antibiotic resistance genes (ARGs) from other pathogens. According to the whole-genome investigation, the GC ratios of ARGs (50–60%) were greater than those of the chromosomal backbone (39.46%), indicating that ARGs were horizontally transferred. OXA-1045 belonged to the OXA-213 subfamily and the amino acid sequence of OXA-1045 showed 89% similarity to the amino acid sequences of OXA-213. Then, $bla_{OXA-1045}$ and $bla_{OXA-213}$ were cloned and the minimum inhibitory concentrations (MICs) of β-lactams in the transformants were determined using the broth microdilution method. OXA-1045 was able to confer a reduced susceptibility to piperacillin and piperacillin-tazobactam compared to OXA-213. AP2044 strain exhibited low pathogenicity in *Galleria mellonella* infection models. The observation of condensed biofilm using the crystal violet staining method and scanning electron microscopy (SEM) suggested that the AP2044 strain was a weak biofilm producer. Quantitative reverse transcription-PCR (qRT-PCR) was used to detect the expression of resistance-nodulation-cell division (RND) efflux pump-related genes. The transcription level of *adeB* and *adeJ* genes increased significantly and was correlated with tigecycline resistance. Therefore, our genomic and phenotypic investigations revealed that the AP2044 strain had significant genome plasticity and natural transformation potential, and the emergence of antibiotic resistance in these unusual bacteria should be a concern for future investigations.

Keywords: ***Acinetobacter pittii*, tigecycline resistance, carbapenem resistance, OXA-1045, whole genome sequencing**

INTRODUCTION

Acinetobacter spp. has been a global threat in the healthcare setting since they rapidly develop resistance to antibiotics. Among these species, *Acinetobacter baumannii*, *Acinetobacter nosocomialis*, and *Acinetobacter pittii* are the most common isolates in hospitals and are associated with nosocomial infections (Weber et al., 2015; Almasaudi, 2018). *A. pittii*, previously known as

Acinetobacter genomic species three, is the most frequently isolated from nosocomial infections among inpatients in general wards and intensive care units (ICU) in Germany and is increasingly found in France, South Asia, and even China (Yang et al., 2012; Schleicher et al., 2013; Ji et al., 2014; Jones et al., 2015; Al Atrouni et al., 2016; Singkham-In and Chatsuwan, 2018).

The emergence of carbapenem-resistant bacteria has been a significant challenge to clinicians worldwide with limited therapeutic options. Tigecycline is a member of the glycylcyclines and serves as a last resort to treat multidrug-resistant (including carbapenem-resistant) *Acinetobacter* infections (Yang et al., 2017). The resistance mechanism of *Acinetobacter* spp. to carbapenem antibiotics is based on the production of the carbapenem-hydrolyzing class D β-lactamases (CHDLs), such as $bla_{\mathrm{OXA-23-}like}$ (Singkham-In and Chatsuwan, 2018), $bla_{\mathrm{OXA-24-}like}$ (Ji et al., 2014), $bla_{\mathrm{OXA-58-}like}$ (Ji et al., 2014), $bla_{\mathrm{OXA-72-}like}$ (Montealegre et al., 2012), and other variants. They can be intrinsic and have a limited ability to hydrolyze carbapenems, but can also result in a resistant phenotype, particularly when overproduced (Tietgen et al., 2021). There are three characterized resistance-nodulation-cell division (RND) efflux pumps: AdeABC, AdeFGH, and AdeIJK. They have been linked to antibiotic resistance, especially tigecycline resistance. Among them, the AdeABC and AdeIJK efflux pumps have been shown to play a major role in tigecycline resistance (Ruzin et al., 2007; Leus et al., 2018). In contrast to intrinsic determinants, acquired antibiotic resistance, such as New Delhi metallo-β-lactamase (NDM), has recently gained importance and contributed to reduced susceptibility of the *Acinetobacter* species. Specifically, the emergence of NDM-1-producing *A. pittii* was first reported in China, (Yang et al., 2012), followed by other regions, such as Korea (Sung et al., 2015), France (Pailhoriès et al., 2017), and Denmark (Hammerum et al., 2015) before spreading around the world.

The objectives of the present study were to systematically analyze the tigecycline-resistant *A. pittii* isolated from an ICU patient, which co-produces $bla_{\mathrm{NDM-1}}$ and $bla_{\mathrm{OXA-1045}}$. As a result, a novel OXA enzyme was found and its active spectrum was identified. The strain was also described using an antimicrobial susceptibility profile, biofilm-forming ability, *Galleria mellonella* infection model, expression of efflux pump-related genes, conjunction experiment, and whole-sequence analysis.

MATERIALS AND METHODS

Data Collection, Bacterial Isolate, and Susceptibility Testing

A total of 104 non-duplicate *Acinetobacter* spp. isolates were obtained between January 2020 and April 2021 in the Affiliated Hospital of Southwest Medical University. Bacterial identification was confirmed by matrix-assist laser desorption ionization time-of-flight mass spectrometry (MALDI-TOF MS) (Bruker, Bremen, Germany) and 16s rRNA sequencing (**Supplementary Datasheet 1**). The antimicrobial susceptibility profiles were tested by MicroScan Walk-Away 96 Plus system (Siemens, Germany). The minimum inhibitory concentrations (MICs) of meropenem, imipenem, tigecycline, and colistin were determined using the broth microdilution method, and results were interpreted following the Clinical and Laboratory Standards Institute 2020 standards (CLSI, 2020). *Escherichia coli* ATCC25922 and *Pseudomonas aeruginosa* ATCC27853 were used as a quality control. ATCC19606 (lab-WT) was used as the reference strain in this study.

Whole-Genome Sequencing and Sequence Analysis

Genomic DNA of *Acinetobacter pittii* AP2044 strain was extracted using a DNA extraction kit (Qiagen, Hilden, Germany) and then sequenced using the Illumina NovaSeq 6000 PE150 (Illumina Inc, San Diego, CA, United States) and nanopore platforms (Sangon Biotech, Shanghai, China). Read sequences were *de novo* assembled using Canu workflow (v1.7) (Koren et al., 2017). Prokka (v1.10) was utilized to predict coding genes, tRNA, and rRNA in the assembled genome Seemann, 2014. All genomic data were uploaded in the National Center for Biotechnology Information (NCBI) database under the accession number CP087716-CP087718. A novel OXA variant was then identified and termed OXA-1045 (accession no. OL790815). The ResFinder[1] and NCBI BLAST[2] were used to determine the acquired resistance genes. The GC Content Calculator web tool[3] was used to measure the GC ratio. Additionally, the IS finder[4] and VFDB[5] databases were used to determine the insertion sequence (IS) elements and virulence genes. The genomic island (GI) sequences were predicted based on GI prediction software packages (IslandPATH-DIMOB) (Hsiao et al., 2003). Chromosome comparison was performed using BLAST Ring Image Generator (BRIG) in the default settings (Alikhan et al., 2011).

Conjugation

As previously mentioned, mating experiments were conducted in broth and on filters using *Escherichia coli* J53 AizR (an azide resistant strain of J53) as the recipient at 37°C (Fu et al., 2012). Potential transconjugants were selected on Luria-Bertani (LB) broth agar plates containing 0.5 mg/L of imipenem and 180 mg/L of sodium azide (Xiang et al., 2020). Transconjugants were verified by MALDI-TOF MS and polymerase chain reaction (PCR), respectively.

Characterization of the New β-Lactamase OXA-1045

Sequence alignment of OXA-1045 with OXA-213 was investigated using Clustal Omega (Sievers et al., 2011) and ESPript 3.0[6]. The secondary structure of OXA-1045 β-lactamase

[1]https://cge.cbs.dtu.dk/services/ResFinder-3.2/

[2]https://blast.ncbi.nlm.nih.gov/Blast.cgi

[3]https://www.biologicscorp.com/tools/GCContent/#. XnIhjqgzZPY

[4]https://isfinder.biotoul.fr/blast.php

[5]http://www.mgc.ac.cn/VFs/main.htm

[6]https://espript.ibcp.fr/ESPript/ESPript/

was predicted using the JPred4 online tool[7], which is based on neural networks. To investigate the phylogenetic relationship of OXA-213-like proteins, we collected a total of 78 OXA amino acid sequences from Beta-Lactamase DataBase (BLDB)[8] (accessed 11 March 2022). Protein sequence alignment of these aa sequences and of OXA-1045 was computed using Clustal Omega. This alignment was used to reconstruct the maximum-likelihood phylogeny by MEGA 7.0 (Kumar et al., 2016).

Cloning of β-Lactamase Genes and Expression

To evaluate the impact of resistance-determinant genes on MICs, $bla_{OXA-1045}$ and $bla_{OXA-213}$ were cloned into the vector pET28b (MiaoLingBio, Wuhan, China). To make pET28b-OXA1045 and pET28b-OXA213, PCR amplification and vector pET-28b were digested with *Bam*HI and *Xho*I and then ligated to the pET-28b vector (Invitrogen, Carlsbad, California, United States). As previously described, the generated plasmid was chemically converted into *E. coli* strain BL21 (Sigma-Aldrich, St. Louis, MO, United States) (Liu et al., 2021). Potential transformants containing pET28b-OXA1045 were identified on LB agar plates (Sigma-Aldrich, St. Louis, MO, United States) containing 20 mg/L of kanamycin (TransGen, Beijing, China). PCR primers PET28AVF2/PET-VF were used to screen colonies on plates, followed by Sanger sequencing (**Supplementary Datasheet 1**). The empty vector pET-28b was turned into BL21 for use as a control.

MICs of ampicillin, ampicillin-sulbactam, piperacillin, piperacillin-tazobactam, oxacillin, cefazolin, cefoxitin, cefuroxime, ceftazidime, cefotaxime, imipenem, and meropenem for the transformants containing pET28b-OXA1045 (BL21:pET28b-OXA1045) and pET28b-OXA213 (BL21:pET28b-OXA213) were determined by the broth microdilution method. MICs for ampicillin in the presence of 4 mg/L of sulbactam were also determined based on the methods used to establish MICs for piperacillin-tazobactam.

Biofilm Formation Assay

The biofilm formation ability of AP2044 strain and lab-WT was determined by the crystal violet staining method and field-emission scanning electron microscope (FE-SEM) as described previously with minor adjustment. Briefly, the strains were cultured overnight and adjusted to a final OD_{600} of 0.1. A total of 20 μL of each bacterial suspension and 180 μL of LB broth (Haibo, Qingdao, China) were inoculated into a 96-well polystyrene microtiter plate (Costar#3524, Corning, United States) in triplicate. After incubation at 37°C overnight, the plate was washed with phosphate-buffered saline (PBS, Solarbio, Beijing, China) to remove planktonic cells, and the plate was stained with crystal violet (Solarbio, Beijing, China) and solubilized with 95% ethanol (v/v), after which its absorbance was measured at 570 nm.

In addition, the biofilm formation capacity of each strain was used for SEM analysis. Biofilms were cultured for 24 h on coverslips as described above and planktonic cells were removed using PBS. First, the cells were fixed with 2.5% glutaraldehyde in PBS for 4 h. Second, the cells were gently washed with PBS twice. The samples were then gradually treated with ethanol (30, 50, 70, 80, 90, and 100%) for 20 min at each concentration. The dried samples were coated with platinum and visualized using FE-SEM (Thermo Fisher Scientific, Waltham, Massachusetts, United States).

Galleria mellonella Infection Model

Prior to all injections, *Galleria mellonella* larvae were stored at 20°C for 4 h to increase susceptibility to infection. A total of 10 μL of bacterial suspension of AP2044 strain and lab-WT were injected into the last left proleg of *G. mellonella* larvae and incubated at 37°C. Larvae were scored for survival every 24 h for 7 days of incubation. Then, 15 larvae were injected at a concentration of 10^6 CFU/mL of each strain, which was repeated three times. A negative control group (10 μL of PBS buffer were injected) was set for each batch of experiments. Larvae were identified as dead when failure to move in response to external touch was noted (Kim et al., 2021).

RNA Isolation and qPCR

Total RNA extraction and reverse transcription were conducted according to a previously described protocol (Tang et al., 2020). The quantitative reverse transcription-PCR (qRT-PCR) was used to detect the expression level of efflux pump-related genes (**Supplementary Datasheet 1**). The $2^{-\Delta\Delta Ct}$ method was used to calculate the fold change of mRNA expression. The relative gene expression level was compared to the control sample (tigecycline-susceptible *A. pittii,* TSAP) (Salehi et al., 2021), which was assigned a value of 1 arbitrary unit. All assays were performed in triplicate in three independent cultures.

RESULTS AND DISCUSSION

Bacterial Isolate

A total of 69 carbapenem-resistant *Acinetobacter* spp. samples were obtained from sputum (40, 58%), urine (13, 18.8%), secreta (6, 8.7%), pleural fluid (6, 8.7%), and blood (4, 5.8%). The majority of them (35, 50.7%) was collected from the ICU. Among these clinical isolates, 36 (52.2%) were considered as extensively drug-resistant (XDR, the isolates are resistant to all antimicrobial classes, except colistin and/or tigecycline). Surprisingly, only the AP2044 strain was resistant to tigecycline. The MICs of the AP2044 strain increased drastically compared to the MICs of ATCC19606 among all tested antibiotics (**Table 1**). The increases were eightfold for gentamicin, 16-fold for piperacillin, more than 32-fold for ciprofloxacin, 64-fold for tigecycline more than 256-fold for carbapenems, more than 64-fold for tetracycline, and in the range more than 32–256-fold for cephalosporins. However, MICs of colistin were almost the same between the two strains, which meant that they are all susceptible to colistin. The AP2044 strain was recovered from a patient with a lung tumor who underwent multiple surgical and invasive procedures at the ICU. With previous treatments of ceftazidime,

[7]https://www.compbio.dundee.ac.uk/jpred/

[8]http://bldb.eu/BLDB.php?class=D#OXA

TABLE 1 | MICs (mg/L) of common antibiotics in AP2044 and ATCC19606.

	AP2044	ATCC19606
Gentamicin	256	32
Meropenem	256	<1
Imipenem	256	<1
Ciprofloxacin	32	<1
Ceftazidime	>1,024	4
Ceftriaxone	>1,024	32
Cefotaxime	>1,024	16
Cefepime	>1,024	16
Tetracycline	>128	2
Tigecycline	64	1
Piperacillin	512	32
Colistin	<0.5	<0.5

TABLE 2 | Genome characteristics of *Acinetobacter pittii* strain AP2044.

Context	Size (bp)	G + C (%)	No. of predicted ORFs
Chromosome	3,921,810	39.0	3,795
Plasmid pAP2044-1	283,349	39.4	290
Plasmid pAP2044-2	43,577	39.1	47

sulperazon, and moxifloxacin, the patient was polymicrobial-positive, which included *Pseudomonas aeruginosa, A. pittii*, and *Stenotrophomonas maltophilia.*

Conjugation and Whole-Genome Analysis of AP2044

The genome of AP2044 was assembled into three contigs of 4,248,736 bp, consisting of one chromosomal backbone and two plasmids. The chromosome, pAP2044-1, and pAP2044-2 had 3,921,810, 283,349, and 43,577 bp and 39, 39.4, and 39.14% G + C content, respectively (**Table 2**). The genome had 18 rRNA operons, 74 tRNAs, and 4,128 predicted protein coding sequences. Indeed, conjugation experiments of the AP2044 strain failed to transfer the plasmid into an *E. coli* recipient. Antimicrobial resistance can be acquired through horizontal gene transfer (HGT) of antibiotic resistance genes (ARGs) and plasmids are critical for HGT and serve as a support for other mobile genetic elements (MGEs) (Vrancianu et al., 2020). The plasmid carrying $bla_{\mathrm{NDM-1}}$, pAP2044-1, is similar to plasmid pXBB1-9 (accession no. CP010351.1) from *Acinetobacter johnsonii* and pALWED1.1 (accession no. KX426227.1) from *Acinetobacter lwoffii*. pAP2044-2 plasmid shows similarity among the sequenced plasmids to p1_010059 from *Acinetobacter junii* (accession no. CP028798.2) and pACI-235c from *Acinetobacter* sp. (accession no. CP026414.1). We speculated that pAP2044-1 and pAP2044-2 plasmids have narrow bacterial host spectrums, which may have a dominant transmission in *Acinetobacter* spp. The genome analyses demonstrated that the AP2044 strain possessed a total of 12 ARGs linked to five different classes of antibiotics, including carbapenem, β-lactam, aminoglycoside, macrolide, and sulfonamide (**Figure 1A**) (**Table 3**). The GC content of a gene can be compared to the whole genome of an organism to determine if that gene comes from that organism. If this is the case, the two GC content profiles are likely to be the same (Evans and Amyes, 2014). Furthermore, the GC ratios (50–60%) of several ARGs, including $bla_{\mathrm{NDM-1}}$, *aac(3″)-IIb, aph(3″)-Ib, aph(6)-Id,* and *sul2*, were much greater than those of the chromosomal backbone (39.46%), implying that the ARGs were acquired from other bacterial species. Therefore, we used the Center for Genomic Epidemiology database[9] to examine the homology of the ARGs to see if they originated from other bacterial species. Eight of the 12 ARGs appeared to be originating from other pathogens, with gene homologies exceeding 99% identities (**Table 3**).

Bacterial survival tactics against aminoglycoside antibiotics include altering enzymes to inactivate aminoglycosides, increasing efflux pump production, lowering membrane permeability, and interfering with aminoglycoside binding *via* modification of 16S ribosomal RNA (Su et al., 2018). Interestingly, the AP2044 genome has four distinct aminoglycoside resistance genes, conferring remarkable cell resistance to a wide variety of aminoglycoside antibiotics (eightfold greater than ATCC19606, **Table 1**, and **Supplementary Datasheet 2**). Two genes [*aac(3″)-IIb* and *aph(6)-Id*] were most likely transmitted from *E. coli*, whereas one *aph(3″)-Ib* gene was likely transferred from *Shigella flexneri*. This might add phosphate, acetyl, adenyl, or methyl groups to aminoglycosides to alter them. Macrolide antibiotics inhibit protein synthesis by targeting the bacterial ribosome (Vázquez-Laslop and Mankin, 2018). Furthermore, the *msr(E)* gene in the AP2044 strain's genome, which comes from *Pasteurella multocida via* HGT, may protect ribosomes from macrolides. Under antibiotic selection pressure, random mutations, ARG acquisition *via* HGT, and activation of mobile DNA elements are viable mechanisms (Salehi et al., 2021). Surprisingly, the XDR *A. pittii* AP2044 strain most likely acquired many ARGs *via* HGT, resulting in high levels of resistance to the majority of the antibiotics tested (**Table 1**). Additionally, a total of four different IS elements next to the ARGs are found in AP2044 plasmids. Several different IS elements were identical (100%) to IS*Alw125*, IS*17*, and IS*Aba2* of *Acinetobacter* spp., which are adjacent to the *aph(3′)-VIa,aph(3″)-Ib*, and *sul2* genes. The *aac(3″)-IIb* gene was located between two IS*30* family elements. As a result, the AP2044 strain's remarkable XDR capacity was related to the enormous amount of ARGs and IS elements in its genome.

Interestingly, the AP2044 strain had a high level of carbapenem resistance and carried the $bla_{\mathrm{NDM-1}}$ gene. The presence of NDM, a widespread metallo-β-lactamase (MBL) in *Acinetobacter* was noteworthy (Perez et al., 2007). The increased number and diversity of MBLs in *Acinetobacter* spp. indicated a concerning trend in the global emergence of resistance in this pathogen (Dortet et al., 2014). In *Acinetobacter*, the bla_{NDM}-type genes were located on either the plasmid or chromosome (Wong et al., 2017). Nevertheless, the AP2044 strain carried two copies of $bla_{\mathrm{NDM\text{-}1}}$ genes, which are located on both the plasmid and chromosome. The $bla_{\mathrm{NDM-1}}$ gene is typically located between two copies of the IS*Aba125* element in NDM-producing *A. baumannii*, forming a composite transposon termed Tn*125* (Bonnin et al., 2012, 2014; Krahn et al., 2016).

[9]https://cge.cbs.dtu.dk/services/

TABLE 3 | Resistance gene distribution in *Acinetobacter pittii* strain AP2044.

	Resistance gene	Identity%	Query/template length	Position in context	Predicted phenotype	Source	GC content of AR gene (%)	Accession number
Chromosome	bla_{NDM-1}	100	813/813	3178789.3179601	Beta-lactam resistance	*Klebsiella pneumoniae* plasmid pKpANDM-1	61	FN396876
	bla_{ADC-25}	91.93	1,152/1,152	1279039.1280190	Beta-lactam resistance	*Acinetobacter baumannii* strain	34	EF016355
	$bla_{OXA-1045}$	100	822/822	2227748.2228569	Beta-lactam resistance	*Acinetobacter pittii strain* AP2044	36	OL790815
pAP2044-1	*aac(3″)-IIb*	99.88	861/861	24804.25664	Aminoglycoside resistance	*Escherichia coli*	58	EU022314
	aph(3′)-Via	100	780/780	201505.202284	Aminoglycoside resistance	*Acinetobacter baumannii*	32	X07753
	bla_{NDM-1}	100	813/813	194810.195622	Beta-lactam resistance	*Klebsiella pneumoniae* plasmid pKpANDM-1	61	FN396876
pAP2044-2	*aph(3″)-Ib*	100	804/804	22734.23537	Aminoglycoside resistance	*Shigella flexneri* plasmid Pstr1	55	AF321551
	aph(6)-Id	100	837/837	23537.24373	Aminoglycoside resistance	*Escherichia coli* plasmid RSF1010	55	M28829
	mph(E)	100	885/885	6420.7304	Macrolide resistance	Uncultured bacterium plasmid pRSB105	36	DQ839391
	msr(E)	100	1,476/1,476	4889.6364	Macrolide, Lincosamide and Streptogramin B resistance	*Pasteurella multocida*	39	FR751518
	sul2	100	816/816	20562.21377	Sulfonamide resistance	*Vibrio cholerae*	60	AY034138
	tet(39)	99.91	1,122/1,122	8331.9452	Tetracycline resistance	*Acinetobacter baumannii* strain RCH52 plasmid pRCH52-1	40	KT346360

Except for the insertion of an IS*91* family transposon and deletion of *insE*, the genetic context of bla_{NDM-1} on the chromosome was similar to that of Tn*125*. Indeed, by the late 1970s, a worldwide lineage of *A. baumannii* had gained resistance to conventionally known antibiotic families. Further resistance was acquired in transposon lineages in the 1980s as new antibiotics became available (Blackwell et al., 2016). Transposon Tn*125* proved to be the primary vehicle for the spread of bla_{NDM-1} in *Acinetobacter* spp. (Poirel et al., 2012). Current observations suggested that the bla_{NDM-1} gene originated from an unknown environmental bacterial progenitor species and was integrated into the chromosome of *Acinetobacter* spp. The bla_{NDM-1}-bearing Tn*125* transposon was most likely derived from such *Acinetobacter* spp. and then transferred to broad-host-range plasmids before being horizontally transferred to *Enterobacteriaceae* and *P. aeruginos*a (Nordmann et al., 2012; Bonnin et al., 2014). Of greater interest was that this NDM-1 producer carried the structure (IS*30*-bla_{NDM-1}-ble_{MBL}-*trpF*-ORF-Y-family DNA polymerase-*umuD*-ORF-ORF-ORF-IS*Aha3*) surrounding the bla_{NDM-1} gene (**Figure 1B**), which was similar to that found in pAcsw19-2 (Sichuan, Luzhou) (accession no. CP043309.1). These two plasmids originate in the same area, and the personnel mobility is substantial. Moreover, sewage is the origin of pAcsw19-2. Several investigations have suggested that it could be a major source of resistance genes as well as a hotspot for transmitting resistance genes and MGEs to clinical microorganisms. Moreover, the possibility of gene cluster transfer should be considered due to the diversity of the bla_{NDM-1} gene environment. In addition, a massive resistance island in the *Acinetobacter*'s genome (Adams et al., 2008) could acquire additional genetic entities for resistance from other bacterial species. Genomic island GI_AP2044-4 (42,734 bp) carried the chromosome-borne bla_{NDM-1}. Sequence analysis showed that GI_AP2044-4 had 90% query cover and 98.8% sequence similarities with the DNA sequence of *A. pittii* strain ST220 chromosome (accession no. CP029610.1) genome (**Supplementary Datasheet 3**).

Identification of the Novel β-Lactamase OXA-1045 and Genetic Environment of $bla_{OXA-1045}$

Previously, two β-lactamase genes located on the chromosome were identified by WGS. One gene encoding an ADC-25-like cephalosporinase and another gene encoding a novel OXA

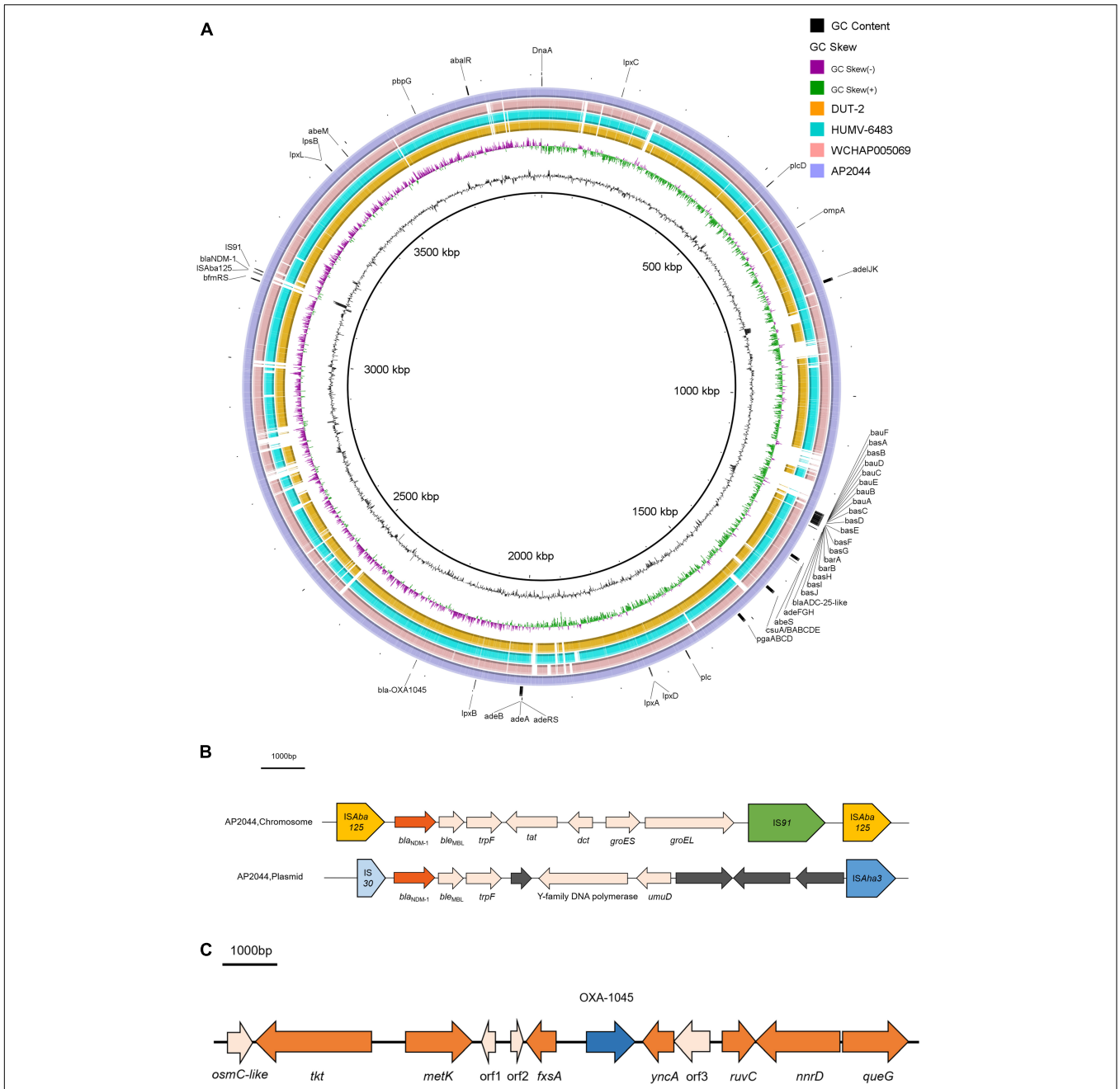

FIGURE 1 | (A) Chromosomal genomic sequence of *A. pittii* AP2044 strain. Alignment of AP2044 with DUT2, HUMV-6483, and WCHAP005069. AP2044 is the closest to DUT2 (accession no. CP014651.1) and HUMV-6483 (accession no. CP021428.1). HUMV-6483 was recovered in a hospital of a neighboring city (Chengdu, China) in 2018, with an 89% coverage and 96.47% identity. Annotations are provided by ResFinder[1], IS Finder[4], and VFDB[5] analysis. **(B)** Genetic environment of bla_{NDM-1} located on chromosome and pAP2044-1 from AP2044 strain. **(C)** Genetic environment of $bla_{OXA-1045}$ from AP2044 strain.

variant were determined to have an 89% aa identity (243/273 aa) and 100% coverage (273/273 aa) compared to OXA-213. The aa sequences of OXA enzymes are quite diverse, and a cutoff of 73.1% of aa identity has recently been proposed as a criterion for dividing OXA subfamilies (Yoon and Jeong, 2021). Therefore, the novel OXA variant belonged to the OXA-213-like subfamily. The Pathogen Detection group at GenBank's National Center for Biotechnology Information has awarded it the number OXA-1045 (accession no. OL790815) (Evans and Amyes, 2014; Yoon and Jeong, 2021). Sequence alignment of OXA-1045 with OXA-213 revealed 30 aa changes and the secondary structure of OXA-1045 contained nine α helixes and six β sheets (**Figure 2**). *Acinetobacter* isolates have shown complex interactions with multiple mechanisms

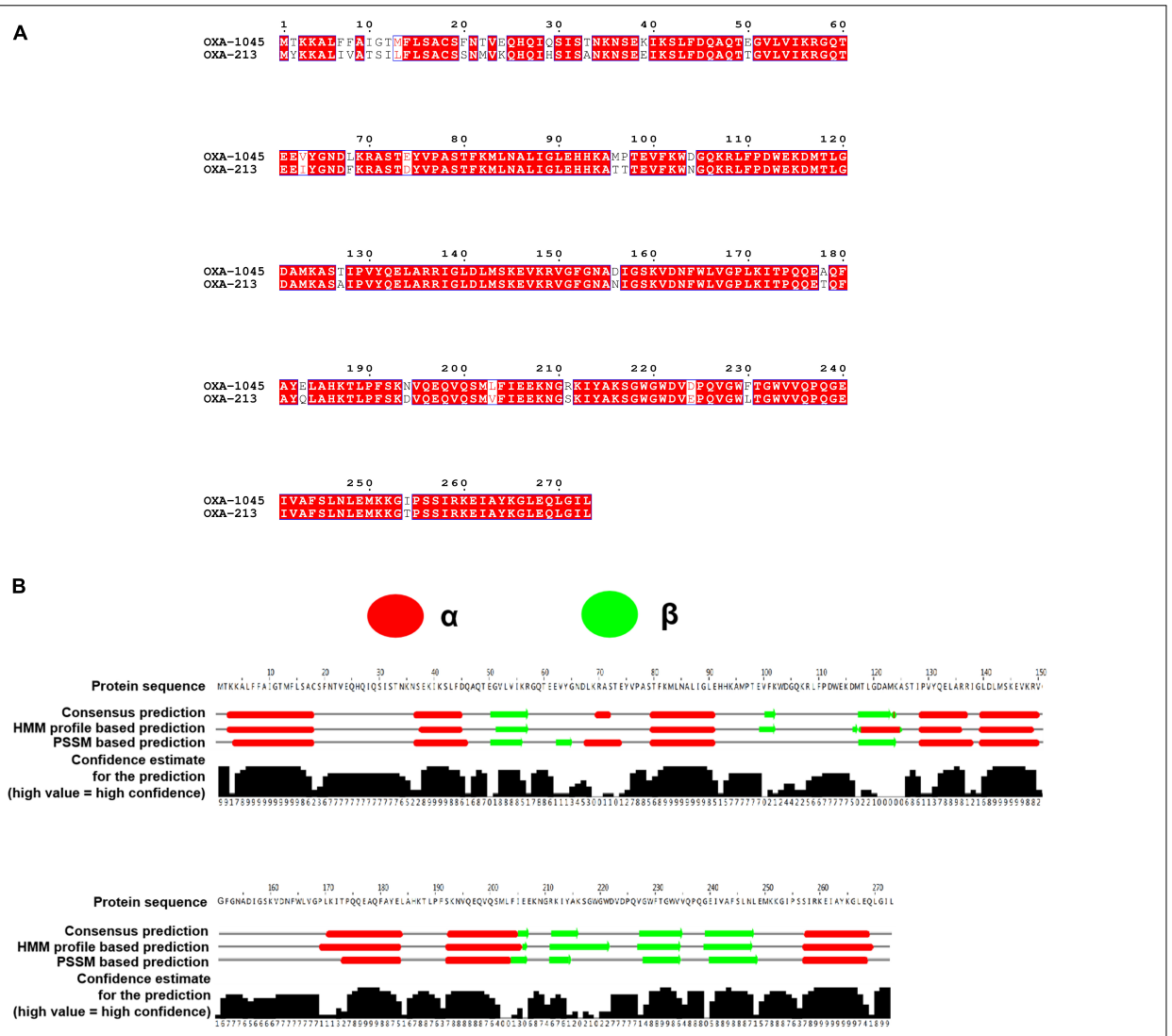

FIGURE 2 | (A) Clustal Omega and ESPript 3.0 were used to align the amino acid sequences of OXA-822 and OXA-213. Residues that have been conserved are highlighted in boxes. **(B)** Secondary structure of OXA-1045. The secondary structure was predicted using the neural network-based web service JPred4 with the default settings. Secondary structure elements, α helixes, β sheets.

of resistance to carbapenems, and the production of naturally occurring OXAs has been the most frequently observed. The predominance of OXAs (OXA-23, OXA-24 or –40, OXA-51, OXA-58, and OXA-143) is the major reason for phenotypic resistance to carbapenems, which have been detected in many parts of the world (Adams-Haduch et al., 2011; Principe et al., 2014; Kamolvit et al., 2015; Labarca et al., 2016). Among these carbapenem-hydrolyzing OXA-type lactamases, bla_{OXA-23} is regarded as an intrinsic gene of *Acinetobacter radioresistens*, OXA-51 is intrinsic to *A. baumannii* and the OXA-134 variant is intrinsic to *Acinetobacter schindleri* and *A. lwoffii* (Poirel et al., 2008; Turton et al., 2012; Périchon et al., 2014). OXA-213-like enzymes have been identified to be intrinsic to *A. calcoaceticus* and have been subsequently detected in *A. pittii* (Figueiredo et al., 2012; Tietgen et al., 2021). Phylogenetic analysis of OXA-213-like proteins identified two distinct subgroups within the OXA family. The first group was linked to *A. pittii* and the second group to *A. calcoaceticus* (**Supplementary Figure 1**).

The genetic environment of $bla_{OXA-1045}$ from the AP2044 strain is shown in **Figure 1C**. The *fxsA* gene, which is situated upstream of the $bla_{OXA-1045}$ gene, encoded the cytoplasmatic membrane protein. A potential redox protein-coding gene *osmC*-like, a transketolase protein-coding gene *tkt*, and an S adenosylmethionine synthase-coding gene *metK* were positioned upstream of *fxsA*. All $bla_{OXA-1045}$ downstream genes were *yncA, ruvC, nnrD,* and *queG*, which encoded the N-acetyltransferase family protein, crossover junction endodeoxyribonuclease, bifunctional NAD(P) H-hydrate repair enzyme, and epoxyqueuosine reductase, respectively. The genetic

context of $bla_{OXA-1045}$ showed the closest similarity with that of $bla_{OXA-417}$ in a BLAST search, which was naturally found on the chromosome of *A. pittii* and belonged to the $bla_{OXA-213-like}$ family. In addition, there was no mobile element found in the surrounding region of $bla_{OXA-1045}$. The above findings implied that the initial location of $bla_{OXA-1045}$ was in the chromosome. The presence of an IS upstream of the gene, which acted as a powerful promoter, can boost the production of OXAs (Turton et al., 2006). Hence, there was no evidence of OXA-1045 overproduction.

TABLE 4 | MICs (mg/L) of β-lactams.

	BL21:pET28b_ OXA1045	BL21:pET28b_ OXA213	BL21:pET28b
Ampicillin	4	4	2
Piperacillin	8	4	2
Oxacillin	256	256	256
Cefazolin	2	2	1
Cefoxitin	2	2	0.5
Cefuroxime	2	2	<0.025
Ceftazidime	<0.025	<0.025	<0.025
Cefotaxime	<0.025	<0.025	<0.025
Meropenem	<0.025	<0.025	<0.025
Imipenem	<0.025	<0.025	<0.025
Ampicillin-sulbactam	2/4	2/4	0.5/4
Piperacillin-tazobactam	4/4	2/4	1/4

Impact of OXA-1045 on Antibiotic Susceptibility to β-Lactams

Among the antibiotics tested, only the MICs of ampicillin, piperacillin, cefazolin, cefoxitin, cefuroxime, ampicillin-sulbactam, and piperacillin-tazobactam for the transformant containing pET28b-OXA1045 (BL21:pET28b-OXA1045) were increased by ≥ 2-fold, as compared to those for the transformant containing pET-28b (BL21:pET28b). In comparison with OXA-213, OXA-1045 elevated the MICs of piperacillin and piperacillin-tazobactam slightly, suggesting that OXA-1045 had a greater impact on piperacillin. Noteworthy, the MICs of ceftazidime, cefotaxime, meropenem, and imipenem for both transformants remained the same as the acceptor strain, demonstrating that the OXA-213 resistance profile to cephalosporins and carbapenem was similar to that of OXA-1045 (**Table 4**). A previous study has illustrated that the production of all OXAs

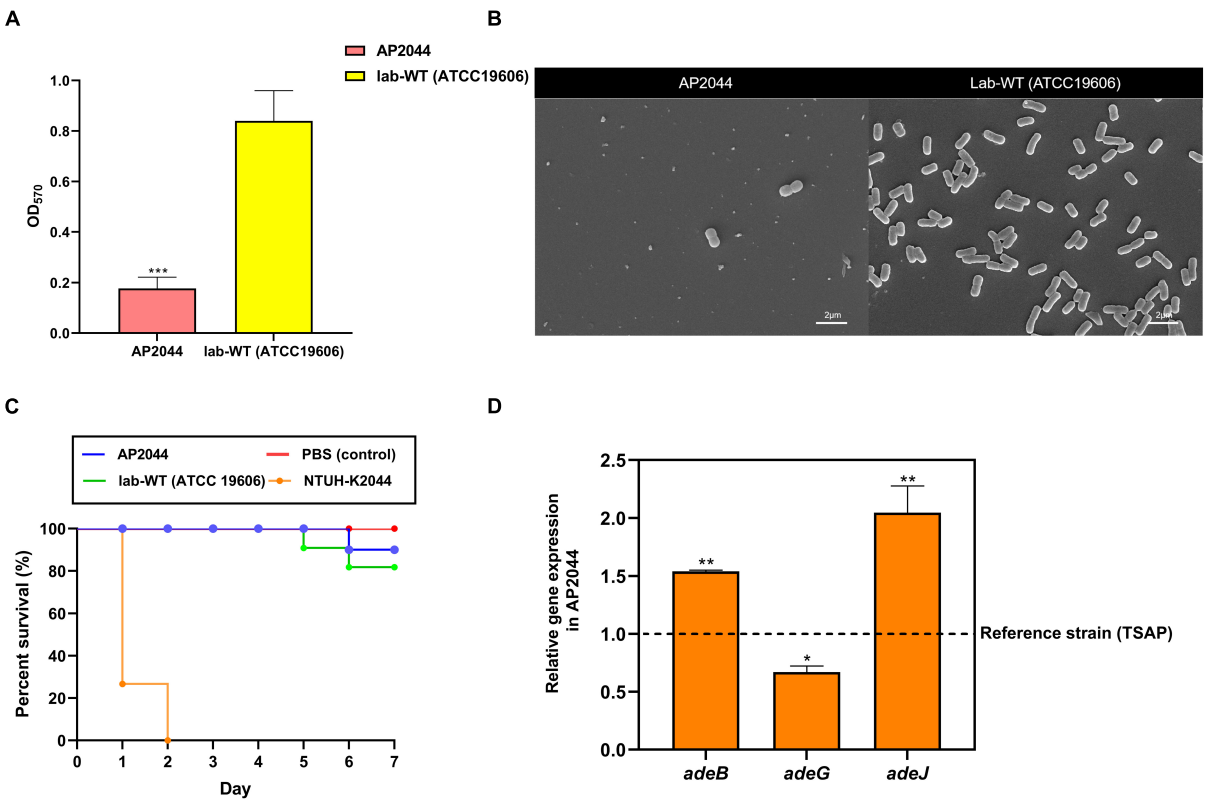

FIGURE 3 | (A) Crystal violet quantification of biofilm formation in the AP2044 and Lab-WT strains; Lab-WT was used as positive control and LB broth was used as negative control. **(B)** SEM images of the AP2044 and Lab-WT strains. **(C)** To compare pathogenicity *in vivo*, 15 *Galleria mellonella* larvae were infected with the common strain Lab-WT, typical hypervirulent strain NTUH-K2044, and strain AP2044 under each condition. Death was defined as a lack of reaction or melanization in infected *G. mellonella* at 37°C for 7 days. The mean (N = 15 biological replicates) is represented for the data. **(D)** The expression of *adeB*, *adeG*, and *adeJ* genes was quantified *via* qRT-PCR. Gene expression profiles of the strains were normalized to their respective 16S rRNA expression. Data represent the mean (± standard deviation, *SD*; N = 4–6 biological replicates). *P < 0.05; **P < 0.01; ***P < 0.001 by Student's t-test against theoretical value.

led to a significant increase in all carbapenem MICs in *A. baumannii,* while no elevation in MICs was observed in *E. coli* (Tietgen et al., 2021). Indeed, we could not rule out the possibility that the effect on MICs is a result of endogenous OXA cooperation with vector-expressed OXA-213-like variants in *Acinetobacter* spp. The results indicated that carbapenemase activity of tested OXAs may be related to the species-dependent effect.

Biofilm Production and Detection of Virulence Phenotype

The biofilm formation capacity was measured in the Lab-WT and AP2044 strains. The OD_{570} values for the Lab-WT and negative control were 0.84 ± 0.12 and 0.14 ± 0.008, respectively. The OD_{570} value for the AP2044 strain was 0.177 ± 0.045, which was a weak biofilm producer. Moreover, the SEM result was consistent with the OD_{570} values obtained by crystal violet staining (**Figures 3A,B**). The AP2044 strain presented mucoid phenotype, with moist colonies and an elevated surface (**Supplementary Figure 2**). Mucoid phenotype formation may influence the virulence of pathogenic microorganisms to varying degrees, which has allowed to make significant strides in characterizing the determinants of pathogenic mechanisms in *P. aeruginosa* and *Klebsiella pneumoniae* (Dennis et al., 2018; Ding et al., 2022). A previous study has demonstrated that mucoid *A. baumannii* strains were more virulent than non-mucoid isolates (Shan et al., 2021). Therefore, we analyzed the virulence of AP2044 strain by developing a *Galleria mellonella* infection model. As shown in **Figure 3C**, such virulence of AP2044 strain was comparable to that of the Lab-WT, which is well known for its lack of virulence (Khalil et al., 2021). The association between the virulence and mucoid phenotype in *Acinetobacter* spp. warrant further investigation. Indeed, the capacity of *A. baumannii* to form biofilm facilitated its survival and persistence in hospital environments (Donlan and Costerton, 2002; Gaddy et al., 2009). This, in turn, contributed to the extensive spread of this pathogen across the globe. Many virulence factors have been implicated in the initial adhesion process of biofilm (Zeighami et al., 2019). Likewise, biofilm development is one of the basic virulence traits of clinical isolates (Khalil et al., 2021). Mahmoud et al. reported biofilm formation as a potent virulence factor in *A. baumanni*, with the strong biofilm producers exhibiting a much greater ability to kill *G. mellonella* larvae than the moderate and weak biofilm producers (Khalil et al., 2021). Accordingly, AP2044 strain was a weak biofilm producer and a low virulence strain. Several previous studies have demonstrated that the majority of XDR and pandrug-resistant (PDR) clinical isolates were weak or non-biofilm producers, which is consistent with the present findings (Qi et al., 2016; Li et al., 2021). There may be a metabolic cost caused by high-level antibiotic resistance, which has been shown to cause a decrease in virulence (Roux et al., 2015). However, the emergence of carbapenem-resistant hypervirulent *A. baumannii* (CR-hvAB) strains presents significant challenges for public health and infection control (Li et al., 2020).

Relative Gene Expression

Compared to the reference strain, quantitative analysis demonstrated that AP2044 expressed 1. 54-, 0. 67-, and 2.05-fold more *adeB, adeJ*, and *adeG* genes, respectively (**Figure 3D**). In particular, the transcription level of *adeB* and *adeJ* in AP2044 was significantly overexpressed than that in TSAP (*t*-test, $P < 0.01$). The efflux pump plays a vital role in both biofilm formation and antibiotic resistance, particularly in tigecycline resistance (Lee et al., 2020). The tigecycline is one of the last resort options for XDR strain infection treatment (Wong et al., 2017). *Acinetobacter* has shown superior resistance to almost all available systemic antibiotics and demonstrates an XDR phenotype. Therefore, overcoming antibiotic resistance is the primary challenge of treating *Acinetobacter* infections (Wong et al., 2017). AdeABC in particular has been demonstrated to influence antibiotic sensitivity and to contribute to tigecycline resistance (Ruzin et al., 2007; Roca et al., 2011). The AdeRS two-component system, which consists of a sensor kinase and a response regulator, is in charge of expressing the transcription of the AdeABC efflux pumps. The aa changes or IS element insertion in the AdeRS two-component system can boost the transcription level of AdeABC efflux pumps (Yoon et al., 2013; Lucaßen et al., 2021). AdeIJK is regulated by the TetR-like repressor AdeN, whose overproduction results in antibiotic resistance and contributes to tigecycline resistance. The present findings indicated that AdeABC and AdeIJK overexpression was the cause of tigecycline resistance, which is consistent with previous studies. A previous study have demonstrated that the AdeABC and AdeIJK efflux systems contributed to tigecycline resistance in a synergistic manner (Damier-Piolle et al., 2008).

CONCLUSION

In summary, the present study found that XDR *A. pittii* carrying two copies of bla_{NDM-1}. The bla_{NDM-1} was located on the chromosome and plasmid in the *A. pittii* strain, which highlighted the fact that bla_{NDM-1}–bearing the Tn*125* transposon was most likely a vector of communication between such *Acinetobacter* spp. and uncommon *Enterobacteriaceae* strains. Then, transfer of the antibiotic-resistant plasmid in *Acinetobacter* spp. deserves special attention. The present work also identified a novel OXA variant in the OXA-213 family, OXA-1045, which was able to confer a reduced susceptibility to piperacillin and piperacillin-tazobactam compared to OXA-213. Phenotypic investigations have found that the AP2044 strain was comparable to the wild-type in terms of pathogenicity but with a weaker biofilm structure. In addition, the tigecycline resistance of the AP2044 strain may be due to the overproduction of AdeABC and AdeIJK.

DATA AVAILABILITY STATEMENT

The datasets presented in this study can be found in online repositories. The names of the repository/repositories and

accession number(s) can be found below: NCBI GenBank; CP087716-CP087718; OL790815.

AUTHOR CONTRIBUTIONS

JL designed this study. ZD, ZL, and YZ performed the experiments and analyzed the data. ZD and YZ wrote the manuscript. JH and TL uploaded the data and performed analysis of qRT-PCR. YL and ZZ revised the manuscript. All authors contributed to the article and approved the submitted version.

FUNDING

This work was supported by the grants from the Sichuan Science and Technology Program (2021YFH001 and 20QYCX0056).

SUPPLEMENTARY MATERIAL

The Supplementary Material for this article can be found online at: https://www.frontiersin.org/articles/10.3389/fmicb.2022.868152/full#supplementary-material

REFERENCES

Adams, M. D., Goglin, K., Molyneaux, N., Hujer, K. M., Lavender, H., Jamison, J. J., et al. (2008). Comparative genome sequence analysis of multidrug-resistant *Acinetobacter baumannii*. *J. Bacteriol.* 190, 8053–8064. doi: 10.1128/jb.00834-08

Adams-Haduch, J. M., Onuoha, E. O., Bogdanovich, T., Tian, G. B., Marschall, J., Urban, C. M., et al. (2011). Molecular epidemiology of carbapenem-nonsusceptible *Acinetobacter baumannii* in the United States. *J. Clin. Microbiol.* 49, 3849–3854. doi: 10.1128/jcm.00619-11

Al Atrouni, A., Joly-Guillou, M. L., Hamze, M., and Kempf, M. (2016). Reservoirs of non-baumannii *Acinetobacter* species. *Front. Microbiol.* 7:49. doi: 10.3389/fmicb.2016.00049

Almasaudi, S. B. (2018). *Acinetobacter* spp. as nosocomial pathogens: epidemiology and resistance features. *Saudi J. Biol. Sci.* 25, 586–596. doi: 10.1016/j.sjbs.2016.02.009

Alikhan, N. F., Petty, N. K., Ben Zakour, N. L., and Beatson, S. A. (2011). BLAST Ring Image Generator (BRIG): simple prokaryote genome comparisons. *BMC Genomics* 12:402. doi: 10.1186/1471-2164-12-402

Blackwell, G. A., Hamidian, M., and Hall, R. M. (2016). IncM Plasmid R1215 Is the source of chromosomally located regions containing multiple antibiotic resistance genes in the globally disseminated *Acinetobacter baumannii* GC1 and GC2 Clones. *mSphere* 1:e00117–16. doi: 10.1128/mSphere.00117-16

Bonnin, R. A., Poirel, L., Naas, T., Pirs, M., Seme, K., Schrenzel, J., et al. (2012). Dissemination of New Delhi metallo-β-lactamase-1-producing *Acinetobacter baumannii* in Europe. *Clin. Microbiol. Infect.* 18, E362–E365. doi: 10.1111/j.1469-0691.2012.03928.x

Bonnin, R. A., Poirel, L., and Nordmann, P. (2014). New Delhi metallo-β-lactamase-producing *Acinetobacter baumannii*: a novel paradigm for spreading antibiotic resistance genes. *Future Microbiol.* 9, 33–41. doi: 10.2217/fmb.13.69

CLSI (2020). *Performance Standards for Antimicrobial Susceptibility Testing; Thirtieth Informational Supplement. M100-S30*. Wayne, PA: Clinical and Laboratory Standards Institute.

Damier-Piolle, L., Magnet, S., Brémont, S., Lambert, T., and Courvalin, P. (2008). AdeIJK, a resistance-nodulation-cell division pump effluxing multiple antibiotics in *Acinetobacter baumannii*. *Antimicrob. Agents Chemother.* 52, 557–562. doi: 10.1128/aac.00732-07

Dennis, E. A., Coats, M. T., Griffin, S., Pang, B., Briles, D. E., Crain, M. J., et al. (2018). Hyperencapsulated mucoid pneumococcal isolates from patients with cystic fibrosis have increased biofilm density and persistence in vivo. *Pathog. Dis.* 76:fty073. doi: 10.1093/femspd/fty073

Ding, Z., Li, Z., Tang, M., Zeng, Z., Song, M., Yang, K., et al. (2022). The molecular characteristics, clinical manifestations, and risk factors of hypervirulent *Klebsiella pneumoniae* infections in a large teaching hospital in southwest China. *Microb. Pathog.* 162:05152. doi: 10.1016/j.micpath.2021.105152

Donlan, R. M., and Costerton, J. W. (2002). Biofilms: survival mechanisms of clinically relevant microorganisms. *Clin. Microbiol. Rev.* 15, 167–193. doi: 10.1128/cmr.15.2.167-193.2002

Dortet, L., Poirel, L., Errera, C., and Nordmann, P. (2014). CarbAcineto NP test for rapid detection of carbapenemase-producing *Acinetobacter* spp. *J. Clin. Microbiol.* 52, 2359–2364. doi: 10.1128/jcm.00594-14

Evans, B. A., and Amyes, S. G. (2014). OXA β-lactamases. *Clin. Microbiol. Rev.* 27, 241–263. doi: 10.1128/cmr.00117-13

Figueiredo, S., Bonnin, R. A., Poirel, L., Duranteau, J., and Nordmann, P. (2012). Identification of the naturally occurring genes encoding carbapenem-hydrolysing oxacillinases from *Acinetobacter* haemolyticus. *Acinetobacter johnsonii, and Acinetobacter calcoaceticus*. *Clin. Microbiol. Infect.* 18, 907–913. doi: 10.1111/j.1469-0691.2011.03708.x

Fu, Y., Du, X., Ji, J., Chen, Y., Jiang, Y., and Yu, Y. (2012). Epidemiological characteristics and genetic structure of blaNDM-1 in non-baumannii *Acinetobacter* spp. in China. *J. Antimicrob. Chemother* .67, 2114–2122. doi: 10.1093/jac/dks192

Gaddy, J. A., Tomaras, A. P., and Actis, L. A. (2009). The *Acinetobacter baumannii* 19606 OmpA protein plays a role in biofilm formation on abiotic surfaces and in the interaction of this pathogen with eukaryotic cells. *Infect. Immun.* 77, 3150–3160. doi: 10.1128/iai.00096-09

Hammerum, A. M., Hansen, F., and Littauer, P. (2015). Use of whole-genome sequencing for characterisation of a ST119 NDM-1-producing *Acinetobacter* pittii from a patient in Denmark with no history of recent travel. *Int. J. Antimicrob. Agents* 46, 351–352. doi: 10.1016/j.ijantimicag.2015.05.005

Hsiao, W., Wan, I., Jones, S. J., and Brinkman, F. S. (2003). IslandPath: aiding detection of genomic islands in prokaryotes. *Bioinformatics* 19, 418–420. doi: 10.1093/bioinformatics/btg004

Ji, S., Chen, Y., Ruan, Z., Fu, Y., Ji, J., Fu, Y., et al. (2014). Prevalence of carbapenem-hydrolyzing class D β-lactamase genes in *Acinetobacter* spp. isolates in China. *Eur. J. Clin. Microbiol. Infect. Dis.* 33, 989–997. doi: 10.1007/s10096-013-2037-z

Jones, L. S., Carvalho, M. J., Toleman, M. A., White, P. L., Connor, T. R., Mushtaq, A., et al. (2015). Characterization of plasmids in extensively drug-resistant *Acinetobacter* strains isolated in India and Pakistan. *Antimicrob. Agents Chemother.* 59, 923–929. doi: 10.1128/aac.03242-14

Kamolvit, W., Sidjabat, H. E., and Paterson, D. L. (2015). Molecular epidemiology and mechanisms of carbapenem resistance of *Acinetobacter* spp. in Asia and Oceania. *Microb. Drug Resist.* 21, 424–434. doi: 10.1089/mdr.2014.0234

Khalil, M. A. F., Ahmed, F. A., Elkhateeb, A. F., Mahmoud, E. E., Ahmed, M. I., Ahmed, R. I., et al. (2021). Virulence characteristics of biofilm-forming *acinetobacter baumannii* in clinical isolates using a *Galleria Mellonella* Model. *Microorganisms* 9:2365. doi: 10.3390/microorganisms9112365

Kim, M., Park, J., and Park, W. (2021). Genomic and phenotypic analyses of multidrug-resistant *Acinetobacter baumannii* NCCP 16007 isolated from a patient with a urinary tract infection. *Virulence* 12, 150–164. doi: 10.1080/21505594.2020.1867421

Krahn, T., Wibberg, D., Maus, I., Winkler, A., Bontron, S., Sczyrba, A., et al. (2016). Intraspecies transfer of the chromosomal *Acinetobacter baumannii* blaNDM-1 Carbapenemase Gene. *Antimicrob. Agents Chemother.* 60, 3032–3040. doi: 10.1128/aac.00124-16

Koren, S., Walenz, B. P., Berlin, K., Miller, J. R., Bergman, N. H., and Phillippy, A. M. (2017). Canu: scalable and accurate long-read assembly via adaptive k-mer weighting and repeat separation. Genome Res. 27, 722–736. doi: 10.1101/gr.215087.116

Kumar, S., Stecher, G., and Tamura, K. (2016). MEGA7: molecular evolutionary genetics analysis version 7.0 for bigger datasets. *Mol. Biol. Evol.* 33, 1870–1874. doi: 10.1093/molbev/msw054

Labarca, J. A., Salles, M. J., Seas, C., and Guzmán-Blanco, M. (2016). Carbapenem resistance in *Pseudomonas aeruginosa* and *Acinetobacter baumannii* in the

nosocomial setting in Latin America. *Crit. Rev. Microbiol.* 42, 276–292. doi: 10.3109/1040841x.2014.940494

Lee, Y. T., Chen, H. Y., Yang, Y. S., Chou, Y. C., Chang, T. Y., Hsu, W. J., et al. (2020). AdeABC efflux pump controlled by AdeRS two component system conferring resistance to tigecycline, omadacycline and eravacycline in clinical carbapenem resistant *Acinetobacter* nosocomialis. *Front. Microbiol.* 11:584789. doi: 10.3389/fmicb.2020.584789

Leus, I. V., Weeks, J. W., Bonifay, V., Smith, L., Richardson, S., and Zgurskaya, H. I. (2018). Substrate specificities and efflux efficiencies of RND efflux pumps of *Acinetobacter baumannii*. *J. Bacteriol.* 200, e49–e18. doi: 10.1128/jb.00049-18

Li, J., Yu, T., Luo, Y., Peng, J. Y., Li, Y. J., Tao, X. Y., et al. (2020). Characterization of carbapenem-resistant hypervirulent *Acinetobacter baumannii* strains isolated from hospitalized patients in the mid-south region of China. *BMC Microbiol.* 20:281. doi: 10.1186/s12866-020-01957-7

Li, Z., Ding, Z., Liu, Y., Jin, X., Xie, J., Li, T., et al. (2021). Phenotypic and genotypic characteristics of biofilm formation in clinical isolates of *Acinetobacter baumannii*. *Infect. Drug Resist.* 14, 2613–2624. doi: 10.2147/idr.S310081

Liu, L., Feng, Y., Wei, L., Xiao, Y., and Zong, Z. (2021). KPC-2-producing carbapenem-resistant *Klebsiella pneumoniae* of the uncommon ST29 type carrying OXA-926, a novel narrow-spectrum OXA β-lactamase. *Front. Microbiol.* 12:701513. doi: 10.3389/fmicb.2021.701513

Lucaßen, K., Müller, C., Wille, J., Xanthopoulou, K., Hackel, M., Seifert, H., et al. (2021). Prevalence of RND efflux pump regulator variants associated with tigecycline resistance in carbapenem-resistant *Acinetobacter baumannii* from a worldwide survey. *J. Antimicrob. Chemother.* 76, 1724–1730. doi: 10.1093/jac/dkab079

Montealegre, M. C., Maya, J. J., Correa, A., Espinal, P., Mojica, M. F., Ruiz, S. J., et al. (2012). First identification of OXA-72 carbapenemase from *Acinetobacter* pittii in Colombia. *Antimicrob. Agents Chemother.* 56, 3996–3998. doi: 10.1128/aac.05628-11

Nordmann, P., Dortet, L., and Poirel, L. (2012). Carbapenem resistance in *Enterobacteriaceae*: here is the storm! *Trends Mol. Med.* 18, 263–272. doi: 10.1016/j.molmed.2012.03.003

Pailhoriès, H., Hadjadj, L., Mahieu, R., Crochette, N., Rolain, J. M., and Kempf, M. (2017). Fortuitous diagnosis of NDM-1-producing *Acinetobacter* pittii carriage in a patient from France with no recent history of travel. *J. Antimicrob. Chemother.* 72, 942–944. doi: 10.1093/jac/dkw505

Perez, F., Hujer, A. M., Hujer, K. M., Decker, B. K., Rather, P. N., and Bonomo, R. A. (2007). Global challenge of multidrug-resistant *Acinetobacter baumannii*. *Antimicrob. Agents Chemother.* 51, 3471–3484. doi: 10.1128/aac.01464-06

Périchon, B., Goussard, S., Walewski, V., Krizova, L., Cerqueira, G., Murphy, C., et al. (2014). Identification of 50 class D β-lactamases and 65 *Acinetobacter*-derived cephalosporinases in *Acinetobacter* spp. *Antimicrob. Agents Chemother.* 58, 936–949. doi: 10.1128/aac.01261-13

Poirel, L., Bonnin, R. A., Boulanger, A., Schrenzel, J., Kaase, M., and Nordmann, P. (2012). Tn125-related acquisition of blaNDM-like genes in *Acinetobacter baumannii*. *Antimicrob. Agents Chemother.* 56, 1087–1089. doi: 10.1128/aac.05620-11

Poirel, L., Figueiredo, S., Cattoir, V., Carattoli, A., and Nordmann, P. (2008). *Acinetobacter* radioresistens as a silent source of carbapenem resistance for *Acinetobacter* spp. *Antimicrob. Agents Chemother.* 52, 1252–1256. doi: 10.1128/aac.01304-07

Principe, L., Piazza, A., Giani, T., Bracco, S., Caltagirone, M. S., Arena, F., et al. (2014). Epidemic diffusion of OXA-23-producing *Acinetobacter baumannii* isolates in Italy: results of the first cross-sectional countrywide survey. *J. Clin. Microbiol.* 52, 3004–3010. doi: 10.1128/jcm.00291-14

Qi, L., Li, H., Zhang, C., Liang, B., Li, J., Wang, L., et al. (2016). Relationship between antibiotic resistance, biofilm formation, and biofilm-specific resistance in *Acinetobacter baumannii*. *Front. Microbiol.* 7:483. doi: 10.3389/fmicb.2016.00483

Roca, I., Espinal, P., Martí, S., and Vila, J. (2011). First identification and characterization of an AdeABC-like efflux pump in *Acinetobacter* genomospecies 13TU. *Antimicrob. Agents Chemother.* 55, 1285–1286. doi: 10.1128/aac.01142-10

Roux, D., Danilchanka, O., Guillard, T., Cattoir, V., Aschard, H., Fu, Y., et al. (2015). Fitness cost of antibiotic susceptibility during bacterial infection. *Sci. Transl. Med.* 7:297ra114. doi: 10.1126/scitranslmed.aab1621

Ruzin, A., Keeney, D., and Bradford, P. A. (2007). AdeABC multidrug efflux pump is associated with decreased susceptibility to tigecycline in *Acinetobacter* calcoaceticus-*Acinetobacter baumannii* complex. *J. Antimicrob. Chemother.* 59, 1001–1004. doi: 10.1093/jac/dkm058

Salehi, B., Ghalavand, Z., Yadegar, A., and Eslami, G. (2021). Characteristics and diversity of mutations in regulatory genes of resistance-nodulation-cell division efflux pumps in association with drug-resistant clinical isolates of *Acinetobacter baumannii*. *Antimicrob. Resist. Infect. Control* 10:53. doi: 10.1186/s13756-021-00924-9

Seemann, T. (2014). Prokka: rapid prokaryotic genome annotation. *Bioinformatics* 30, 2068–2069. doi: 10.1093/bioinformatics/btu153

Schleicher, X., Higgins, P. G., Wisplinghoff, H., Körber-Irrgang, B., Kresken, M., and Seifert, H. (2013). Molecular epidemiology of *Acinetobacter baumannii* and *Acinetobacter* nosocomialis in Germany over a 5-year period (2005-2009). *Clin. Microbiol. Infect.* 19, 737–742. doi: 10.1111/1469-0691.12026

Shan, W., Zhang, H., Kan, J., Yin, M., Zhang, J., Wan, L., et al. (2021). Acquired mucoid phenotype of *Acinetobacter baumannii*: impact for the molecular characteristics and virulence. *Microbiol. Res.* 246:126702. doi: 10.1016/j.micres.2021.126702

Sievers, F., Wilm, A., Dineen, D., Gibson, T. J., Karplus, K., Li, W., et al. (2011). Fast, scalable generation of high-quality protein multiple sequence alignments using clustal Omega. *Mol. Syst. Biol.* 7:539. doi: 10.1038/msb.2011.75

Singkham-In, U., and Chatsuwan, T. (2018). Mechanisms of carbapenem resistance in *Acinetobacter* pittii and *Acinetobacter* nosocomialis isolates from Thailand. *J. Med. Microbiol.* 67, 1667–1672. doi: 10.1099/jmm.0.000845

Su, W., Kumar, V., Ding, Y., Ero, R., Serra, A., Lee, B. S. T., et al. (2018). Ribosome protection by antibiotic resistance ATP-binding cassette protein. *Proc. Natl. Acad. Sci. U.S.A* 115, 5157–5162. doi: 10.1073/pnas.1803313115

Sung, J. Y., Koo, S. H., Kim, S., and Kwon, G. C. (2015). Emergence of *Acinetobacter* pittii harboring New Delhi metallo-beta-lactamase genes in Daejeon. Korea. *Ann. Lab. Med.* 35, 531–534. doi: 10.3343/alm.2015.35.5.531

Tang, M., Wei, X., Wan, X., Ding, Z., Ding, Y., and Liu, J. (2020). The role and relationship with efflux pump of biofilm formation in *Klebsiella pneumoniae*. *Microb. Pathog.* 147:104244. doi: 10.1016/j.micpath.2020.104244

Tietgen, M., Leukert, L., Sommer, J., Kramer, J. S., Brunst, S., Wittig, I., et al. (2021). Characterization of the novel OXA-213-like β-lactamase OXA-822 from *Acinetobacter* calcoaceticus. *J. Antimicrob. Chemother.* 76, 626–634. doi: 10.1093/jac/dkaa488

Turton, J. F., Hyde, R., Martin, K., and Shah, J. (2012). Genes encoding OXA-134-like enzymes are found in *Acinetobacter* lwoffii and A. schindleri and can be used for identification. *J. Clin. Microbiol.* 50, 1019–1022. doi: 10.1128/jcm.06173-11

Turton, J. F., Ward, M. E., Woodford, N., Kaufmann, M. E., Pike, R., Livermore, D. M., et al. (2006). The role of ISAba1 in expression of OXA carbapenemase genes in *Acinetobacter baumannii*. *FEMS Microbiol. Lett.* 258, 72–77. doi: 10.1111/j.1574-6968.2006.00195.x

Vázquez-Laslop, N., and Mankin, A. S. (2018). How macrolide antibiotics work. *Trends Biochem. Sci.* 43, 668–684. doi: 10.1016/j.tibs.2018.06.011

Vrancianu, C. O., Popa, L. I., Bleotu, C., and Chifiriuc, M. C. (2020). Targeting plasmids to limit acquisition and transmission of antimicrobial resistance. *Front. Microbiol.* 11:761. doi: 10.3389/fmicb.2020.00761

Weber, B. S., Harding, C. M., and Feldman, M. F. (2015). Pathogenic *Acinetobacter*: from the cell surface to infinity and beyond. *J. Bacteriol.* 198, 880–887. doi: 10.1128/jb.00906-15

Wong, D., Nielsen, T. B., Bonomo, R. A., Pantapalangkoor, P., Luna, B., and Spellberg, B. (2017). Clinical and pathophysiological overview of *Acinetobacter* infections: a century of challenges. *Clin. Microbiol. Rev.* 30, 409–447. doi: 10.1128/cmr.00058-16

Xiang, T., Chen, C., Wen, J., Liu, Y., Zhang, Q., Cheng, N., et al. (2020). Resistance of *Klebsiella pneumoniae* strains carrying bla (NDM-1) gene and the genetic environment of bla (NDM-1). *Front. Microbiol.* 11:700. doi: 10.3389/fmicb.2020.00700

Yang, J., Chen, Y., Jia, X., Luo, Y., Song, Q., Zhao, W., et al. (2012). Dissemination and characterization of NDM-1-producing *Acinetobacter* pittii in an intensive care unit in China. *Clin. Microbiol. Infect.* 18, E506–E513. doi: 10.1111/1469-0691.12035

Yang, Q., Xu, Y. C., Kiratisin, P., and Dowzicky, M. J. (2017). Antimicrobial activity among gram-positive and gram-negative organisms collected from the Asia-Pacific region as part of the tigecycline evaluation and surveillance trial: comparison of 2015 results with previous years. *Diagn. Microbiol. Infect. Dis.* 89, 314–323. doi: 10.1016/j.diagmicrobio.2017.08.014

Yoon, E. J., Courvalin, P., and Grillot-Courvalin, C. (2013). RND-type efflux pumps in multidrug-resistant clinical isolates of *Acinetobacter baumannii*: major role for AdeABC overexpression and AdeRS mutations. *Antimicrob. Agents Chemother.* 57, 2989–2995. doi: 10.1128/aac.02556-12

Yoon, E. J., and Jeong, S. H. (2021). Class D β-lactamases. *J. Antimicrob. Chemother.* 76, 836–864. doi: 10.1093/jac/dkaa513

Zeighami, H., Valadkhani, F., Shapouri, R., Samadi, E., and Haghi, F. (2019). Virulence characteristics of multidrug resistant biofilm forming *Acinetobacter baumannii* isolated from intensive care unit patients. *BMC Infect. Dis.* 19:629. doi: 10.1186/s12879-019-4272-0

Conflict of Interest: The authors declare that the research was conducted in the absence of any commercial or financial relationships that could be construed as a potential conflict of interest.

Publisher's Note: All claims expressed in this article are solely those of the authors and do not necessarily represent those of their affiliated organizations, or those of the publisher, the editors and the reviewers. Any product that may be evaluated in this article, or claim that may be made by its manufacturer, is not guaranteed or endorsed by the publisher.

frontiers | Frontiers in Microbiology

TYPE Original Research
PUBLISHED 09 August 2022
DOI 10.3389/fmicb.2022.967313

OPEN ACCESS

EDITED BY
Kristina Kadlec,
Independent Researcher, Wunstorf, Germany

REVIEWED BY
Jianmin Zhang,
South China Agricultural University, China
Po-Xing Zheng,
Academia Sinica, Taiwan

*CORRESPONDENCE
Xinan Jiao
jiao@yzu.edu.cn

SPECIALTY SECTION
This article was submitted to Antimicrobials, Resistance and Chemotherapy, a section of the journal Frontiers in Microbiology

RECEIVED 12 June 2022
ACCEPTED 19 July 2022
PUBLISHED 09 August 2022

CITATION
Wang J, Lu M-J, Wang Z-Y, Jiang Y, Wu H, Pan Z-M and Jiao X (2022) Tigecycline-resistant *Escherichia coli* ST761 carrying *tet*(X4) in a pig farm, China.
Front. Microbiol. 13:967313.
doi: 10.3389/fmicb.2022.967313

Tigecycline-resistant *Escherichia coli* ST761 carrying *tet*(X4) in a pig farm, China

Jing Wang[1,2], Meng-Jun Lu[1,2], Zhen-Yu Wang[1,2], Yue Jiang[1,2], Han Wu[1,2], Zhi-Ming Pan[1,2] and Xinan Jiao[1,2]*

[1]Jiangsu Key Laboratory of Zoonosis, Jiangsu Co-Innovation Center for Prevention and Control of Important Animal Infectious Diseases and Zoonoses, Yangzhou University, Yangzhou, China, [2]Key Laboratory of Prevention and Control of Biological Hazard Factors (Animal Origin) for Agrifood Safety and Quality, Ministry of Agriculture of China, Yangzhou University, Yangzhou, China

This study aimed to investigate the prevalence and characterization of *tet*(X4) in *Escherichia coli* isolates from a pig farm in Shanghai, China, and to elucidate *tet*(X4) dissemination mechanism in this swine farm. Forty-nine (80.33%) *E. coli* strains were isolated from 61 samples from a pig farm and were screened for the presence of *tet*(X). Among them, six (12.24%) strains were positive for *tet*(X4) and exhibited resistance to tigecycline (MIC $\geq$ 16 mg/L). They were further sequenced by Illumina Hiseq. Six *tet*(X4)-positive strains belonged to ST761 with identical resistance genes, resistance profiles, plasmid replicons, and cgMLST type except that additional ColE10 plasmid was present in isolate SH21PTE35. Isolate SH21PTE31, as a representative ST761 *E. coli* strain, was further sequenced using Nanopore MinION. The *tet*(X4) in SH21PTE31 was located on IncFIA18/IncFIB(K)/IncX1 hybrid plasmid pYUSHP31-1, highly similar to other *tet*(X4)-carrying IncFIA18/IncFIB(K)/IncX1 plasmids from ST761 *E. coli* and other *E. coli* lineages in China. These IncFIA18/IncFIB(K)/IncX1 plasmids shared closely related multidrug resistance regions, and could reorganize, acquire or lose resistance modules mediated by mobile elements such as IS*CR2* and IS*26*. Phylogenetic analysis were performed including all *tet*(X4)-positive isolates obtained in this pig farm combined with 43 *tet*(X4)-positive *E. coli* from pigs, cow, pork, wastewater, and patients with the same ST from NCBI. The 50 *tet*(X4)-carrying *E. coli* ST761 isolates from different areas in China shared a close phylogenetic relationship (0-49 SNPs). In conclusion, clonal transmission of *tet*(X4)-positive *E. coli* ST761 has occurred in this swine farm. *E. coli* ST761 has the potential to become a high-risk clone for *tet*(X4) dissemination in China.

KEYWORDS

plasmids, ST761, tigecycline resistance, *tet*(X4), *Escherichia coli*

Introduction

Tigecycline is considered as a last-resort antimicrobial agent to treat serious infections caused by multidrug-resistant bacteria, particularly carbapenem-resistant *Enterobacteriaceae* (Yaghoubi et al., 2021). However, the recent identification of novel plasmid-borne tigecycline resistance genes *tet*(X3) in *Acinetobacter baumannii* and *tet*(X4) in *Escherichia coli* from animals in China significantly impairs the clinical efficacy of tigecycline (He et al., 2019). Thus far, *tet*(X) and its variants [*tet*(X1)∼*tet*(X47)] have been identified in Gram-negative pathogens and encode flavin-dependent monooxygenase that modify tigecycline (Aminov, 2021; Li R. et al., 2021; Umar et al., 2021; Zhang et al., 2021). Among them, the mobile *tet*(X4) gene has been increasingly identified in *E. coli* from various sources including food-producing animals, wild birds, food products, humans, and the environment, mainly in China (He et al., 2019; Fang et al., 2020; Li et al., 2020; Li Y. et al., 2021; Dong et al., 2022; Liu et al., 2022). It has sporadically reported in countries outside of China, e.g., Singapore, Pakistan, Vietnam, United Kingdom, and Norway (Ding et al., 2020; Marathe et al., 2021; Mohsin et al., 2021; Dao et al., 2022; Martelli et al., 2022). The *tet*(X4) has subsequently detected in various *Enterobacteriaceae* species, such as *Proteus*, *A. baumannii*, *Aeromonas caviae*, *Citrobacter freundii*, *Enterobacter cloacae*, *E. hormaechei*, *Klebsiella pneumoniae*, and *Shewanella xiamenensis* (Chen et al., 2019; He et al., 2019; Zeng et al., 2021; Dao et al., 2022; Li et al., 2022; Wu et al., 2022; Zhai et al., 2022).

Although tigecycline is not applied in livestock, the *tet*(X4) gene and tigecycline resistance are frequently described in *E. coli* from food-producing animals (mainly pigs) in China (He et al., 2019; Fang et al., 2020; Li Y. et al., 2021; Liu et al., 2022). The heavy use of tetracyclines in animal production might facilitate the emergence and spread of *tet*(X) in livestock (He et al., 2019). In addition, conjugative/mobilizable plasmids and mobile elements play an essential role in the dissemination of *tet*(X4) in Enterobacteriaceae (Aminov, 2021). In this study, we aimed to investigate the prevalence and characterization of *tet*(X4) in *E. coli* isolates from one pig farm in Shanghai, China, to provide insights into the spread of *tet*(X4) in this swine farm.

Materials and methods

Sample collection and *tet*(X) detection

On 15 July 2021, 61 non-duplicate samples from pig feces (n = 41) and pig feed (n = 20) were collected from a pig farm in Shanghai, China. Samples were incubated in LB broth for 18∼24 h and then cultured on the MacConkey agar with and without 2 mg/L tigecycline. One *E. coli* isolate per plate was selected and identified by 16S rRNA gene sequencing (Kim et al., 2010). The presence of *tet*(X) were detected by PCR and sequencing (Wang et al., 2019).

Antimicrobial susceptibility testing

The MICs of tigecycline were determined in all *E. coli* strains using the broth microdilution method and interpreted according to EUCAST clinical breakpoint (MIC ≥ 1 mg/L)[1]. The *tet*(X4)-positive isolates were further tested susceptibility to other 13 antimicrobial agents including ampicillin, cefotaxime, meropenem, gentamicin, amikacin, streptomycin, tetracycline, chloramphenicol, florfenicol, nalidixic acid, ciprofloxacin, colistin, and sulfamethoazole/trimethoprim by using the broth microdilution method. The results were interpreted according to Clinical Laboratory Standards Institute (CLSI) M100, 30th edition. Florfenicol (> 16 mg/L) and streptomycin (> 16 mg/L) were interpreted according to the epidemiological cut-off values for *E. coli* set by EUCAST (see Text Footnote 1). The *E. coli* strain ATCC 25922 was used for quality control.

Conjugation experiments

Conjugation experiments were conducted according to a previously described protocol (Chen et al., 2007) using *E. coli* C600 (streptomycin-resistant) as the recipient strain. Transconjugants were selected on MacConkey agar plates supplemented with 2 mg/L tigecycline and 3,000 mg/L streptomycin.

Whole genome sequencing and analysis

The *tet*(X4)-positive *E. coli* strains were sequenced on the Illumina Hiseq platform, and the quality-trimmed raw sequence data were assembled into contigs using SPAdes v.3.8.2 with -careful and -cov cut-off auto options. One representative *E. coli* isolate SH21PTE31 was sequenced using Nanopore MinION, assembling with Unicycler version 0.4.9. The genome sequences of them were analyzed multilocus sequence typing (MLST), resistance genes, and plasmid replicons by using the Center for Genomic Epidemiology (CGE) pipeline[2]. The *tet*(X4)-carrying plasmid pYUSHP31-1 in strain SH21PTE31 was analyzed by ISfinder[3], BLAST[4] and the Gene Construction Kit 4.5 (Textco BioSoftware, Inc., Raleigh, NC, United States).

1 www.eucast.org
2 http://www.genomicepidemiology.org/
3 https://www-is.biotoul.fr/
4 https://blast.ncbi.nlm.nih.gov/Blast.cgi

pYUSHP31-1 was compared with other similar plasmids using BLASTn and BRIG.

Phylogenetic analysis of *tet*(X4)-Positive ST761 *Escherichia coli* strains

The genome sequences of 43 *tet*(X4)-positive ST761 *E. coli* strains in the NCBI database were downloaded (data collected on July 7th, 2022) (**Supplementary Table 1**). The phylogenetic tree of all the *tet*(X4)-carrying ST761 *E. coli* strains obtained from this pig farm and NCBI was constructed using Parsnp[5] and visualized by iTOL[6]. Core genome MLST (cgMLST) profiles based on 2,513 alleles were analyzed using cgMLSTFinder 1.2[7].

Nucleotide sequence accession number

The whole genome sequences of *tet*(X4)-positive *E. coli* isolates have been deposited in the GenBank under accession number PRJNA836295.

Results and discussion

Characterization of *tet*(X4)-positive *Escherichia coli* isolates

A total of 49 *E. coli* strains were obtained from 61 samples. Among them, six strains (12.24%) from different fecal samples were positive for *tet*(X4), including five strains isolated under selection with tigecycline and one strain isolate without selection. The *tet*(X4)-positive isolates exhibited resistance to tigecycline (MIC $\geq$ 16 mg/L), and the remaining isolates showed susceptibility to tigecycline with MICs of 0.125 to 0.5 mg/L. These *tet*(X4)-positive isolates were also resistant to ampicillin, tetracycline, chloramphenicol, florfenicol, and sulfamethoazole/trimethoprim, but susceptible to cefotaxime, meropenem, gentamicin, amikacin, streptomycin, colistin, nalidixic acid, and ciprofloxacin (**Supplementary Table 2**). However, all tigecycline-resistant isolates failed to transfer *tet*(X4) to *E. coli* C600 *via* conjugation.

The draft genome sequences of six *tet*(X4)-positive *E. coli* strains were obtained by Illumina (**Supplementary Table 3**). All six *tet*(X4)-positive *E. coli* strains belonged to ST761 with identical resistance genes [bla_{TEM-1}, *tet*(A), *tet*(M), *floR*, *qnrS1*, *sul3*, *dfrA5* and *mef*(B)] and plasmid replicons [IncFIA, IncFIB(K), IncX1, IncR], except that additional ColE10 plasmid was present in isolate SH21PTE35 (**Figure 1**).

tet(X4)-Carrying plasmid pYUSHP31-1

The complete sequences of isolate SH21PTE31, as a representative ST761 *E. coli* strain, was obtained. A total of 43,674 reads were obtained, and the sequencing data volume was approximately 1,000 Mbp. The minimal, maximum and average read lengths were 8,260 bp, 150,801 bp and 22,897.3 bp, respectively. The read length N50 of the total sequencing data were 28,637 bp. The isolate SH21PTE31 consisted of one chromosome (4,706,168 bp) and four plasmids (**Supplementary Table 3**). Among them, *tet*(X4) and another eight resistance genes were co-located on the largest plasmid, designated as pYUSHP31-1. This plasmid had a size of 104,163 bp, and belonged to the hybrid IncFIA18/IncFIB(K)/IncX1 plasmid. It was highly similar to our previously reported plasmid pYUSHP6-tetX (GenBank accession no. MW423609) from ST761 *E. coli* isolate SH19PTE6 collected from the same pig farm in 2019 (Wang et al., 2021), and also showed high identity (> 99.7%) to multiple *tet*(X4)-carrying IncFIA18/IncFIB(K)/IncX1 plasmids from ST761 *E. coli* strains in China, such as pNT1W22-tetX4 (pig, CP075470), pRF108-2_97k_tetX (pig, MT219820), pSTB20-1T (pig, CP050174), p54-tetX (cow, CP041286), pYPE12-101k-tetX4 (pork, CP041443), and pYPE3-92k-tetX4 (pork, CP041453) (**Figure 2**). Similar IncFIA18/IncFIB(K)/IncX1 plasmids harboring *tet*(X4) were also present among other *E. coli* lineages obtained from a pig farm in Jiangsu province, China (Li Y. et al., 2021), e.g., pNT1N31-tetX4 (ST716, CP075481), pNT1F25-tetX4 (ST1421, CP075471), pNT1F31-tetX4 (ST206, CP045188), pNT1N25-tetX4 (ST641, CP075485), and pNT1F34-tetX (ST10115, CP075486) (**Figure 2**), highlighting the importance role of horizontal transfer of plasmids in the *tet*(X4) dissemination between different bacteria.

As shown in **Figure 3**, these IncFIA18/IncFIB(K)/IncX1 plasmids shared closely related multidrug resistance regions (MRRs). The MRRs in all were bounded by one copy of IS*26* and IS*1*, respectively. The pYUSHP31-1 MRR (53,134 bp) contained nine resistance genes and consisted of five regions bounded by IS*26* or IS*CR2* (**Figure 3A**). The first of these (2,813 bp) comprised one copy of IS*26* and a putative open reading frame encoding recombinase family protein, which was absent in other similar plasmids.

The second part (~14.8 kb) contained three resistance genes *mefB*, *sul3*, and *dfrA5*; four copies of IS*26* and incomplete transposon Tn*2* and Tn*21*. This fragment was also present in other IncFIA18/IncFIB(K)/IncX1 plasmids, but differed by 46-bp shorter (limited to pNT1N25-tetX4) or 126-bp longer Tn*2* except pYUSHP6-tetX (identical to pYUSHP31-1, obtained

5 https://harvest.readthedocs.io/en/latest/content/parsnp.html

6 https://itol.embl.de/

7 https://cge.food.dtu.dk/services/cgMLSTFinder/

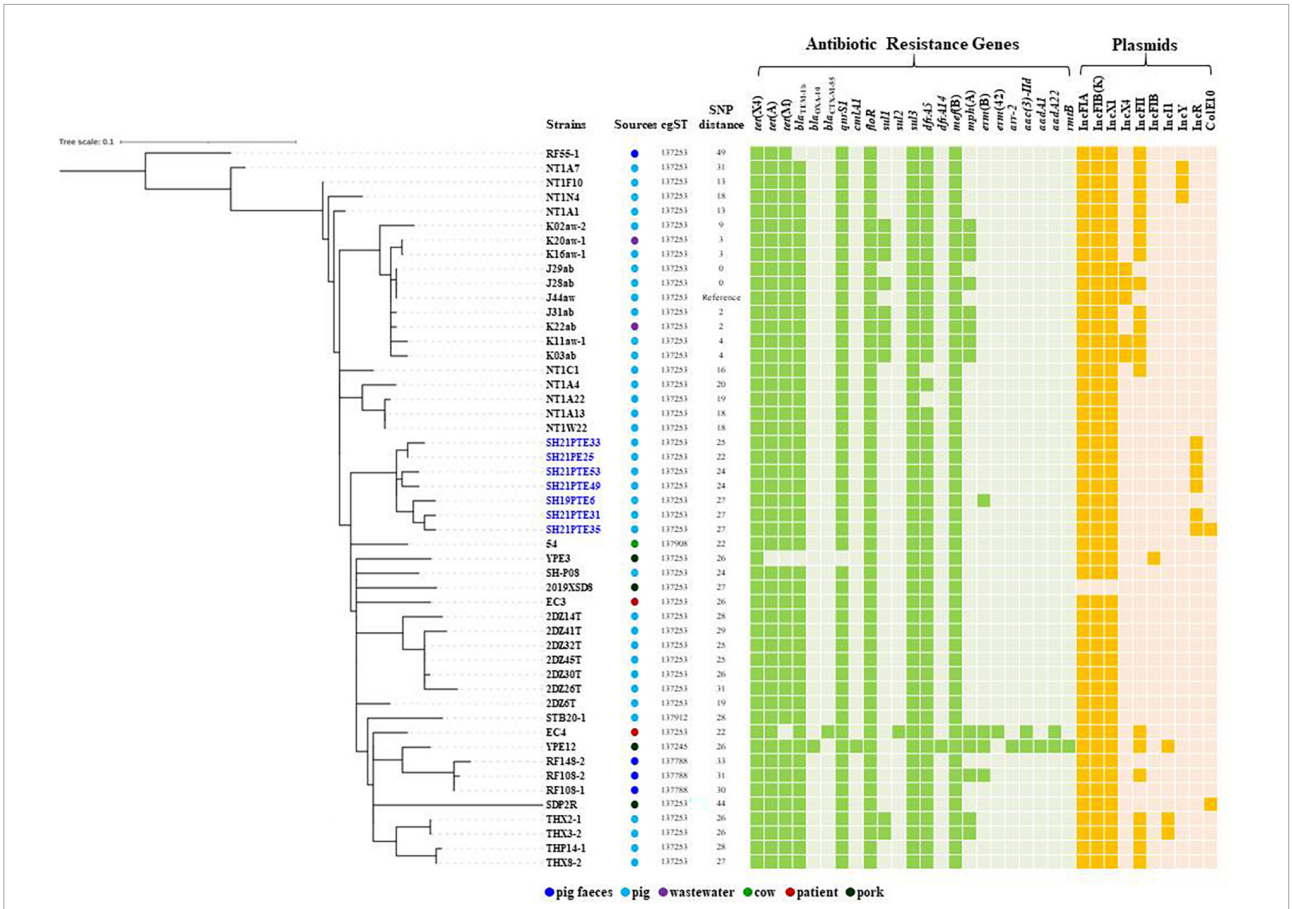

FIGURE 1
The maximum likelihood tree of *tet*(X4)-positive *E. coli* ST761 isolates in this study compared with *tet*(X4)-positive *E. coli* ST761 isolates from NCBI based on cgSNP analysis. Antibiotic resistance genes and plasmid replicons with >95% sequence homology and >60% coverage are shown. The isolates obtained in this study and in the same pig farm were indicated in blue.

from the same pig farm); deletion of a 5,198-bp structure (IS*26*-ΔTn*2*-ΔTn*21*) in pNT1F31-tetX4 (Figure 3G).

The third region corresponded to the core *tet*(X4) structure [ΔIS*CR2*-*orf1*-*abh*-*tet*(X4)-IS*CR2*-*orf2*-*orf3*-*orf4*-ΔIS*CR2*] and downstream *floR*-ΔIS*CR2* module, as observed in other IncFIA18/IncFIB(K)/IncX1 plasmids with one to four copies of *tet*(X4) structure (Figures 3A–J). Compared with that of pYUSHP31-1, partial *tet*(X4) structure [ΔIS*CR2*-*orf1*-*abh*-*tet*(X4)-IS*CR2*] with varied copies was identified in plasmids pNT1F10-tetX4, pRF108-2_97k_tetX, pSTB20-1T, pRF148-2_101k_tetX, and NT1N25-tetX4 (Figures 3K–N); one copy of IS*1* was inserted into *orf1* within the *tet*(X4) structure with 9-bp direct repeats in plasmids pNT1F10-tetX4 and pNT1N31-tetX4, and the latter plasmid carried the *tet*(X4) fragment in the opposite orientation and additional two copies of IS*26* upstream of *floR*-ΔIS*CR2* module (Figure 3J). As previously described (Liu et al., 2022), IS*CR2* is associated with *tet*(X4) transmission by forming an rolling-cycle transposable unit, thus generating tandem copies of *tet*(X4)-harboring structures in different IncFIA18/IncFIB(K)/IncX1 plasmids.

The fourth segment (~18.4 kb) included one copy of IS*26*, an incomplete Tn*1721* carrying tetracycline resistance gene *tet*(A) and an intact Tn*2* (*tnpA*-*tnpR*-bla_{TEM-1b}), followed by 5,391-bp module [Δ*intI4*-IS*440 tnpA*-*tet*(M)-ΔIS*26*] and *qnrS1* structure (IS*26*-*qnrS1*-ΔIS*Kpn19*). This region was also found in other IncFIA18/IncFIB(K)/IncX1 plasmids with the same ΔIS*Kpn19*/IS*26* boundary except pYPE3-92k-tetX4 (Figure 3F). IS*26*-mediated homologous recombination could explain the loss or acquisition of this region.

The last segment comprising a 3,507-bp structure (IS*26*-ΔIS*1294*-*gshB*-IS*1*) was identical to segments in other plasmids except p54-tetX (Figure 3D). Insertion of an extra copy of IS*26* downstream of *gshB*, followed by homologous recombination between it and the first IS*26* of MRR, may explain the opposite location of an approximately 50.2-kb fragment within MRR in p54-tetX compared to pYUSHP31-1. Similar recombination between two IS*26* elements located in inverse orientations may also occur in pYPE12-101k-tetX4, leading to the presence of ~47.8 kb fragment with the opposite orientation within MRR (Figure 3C).

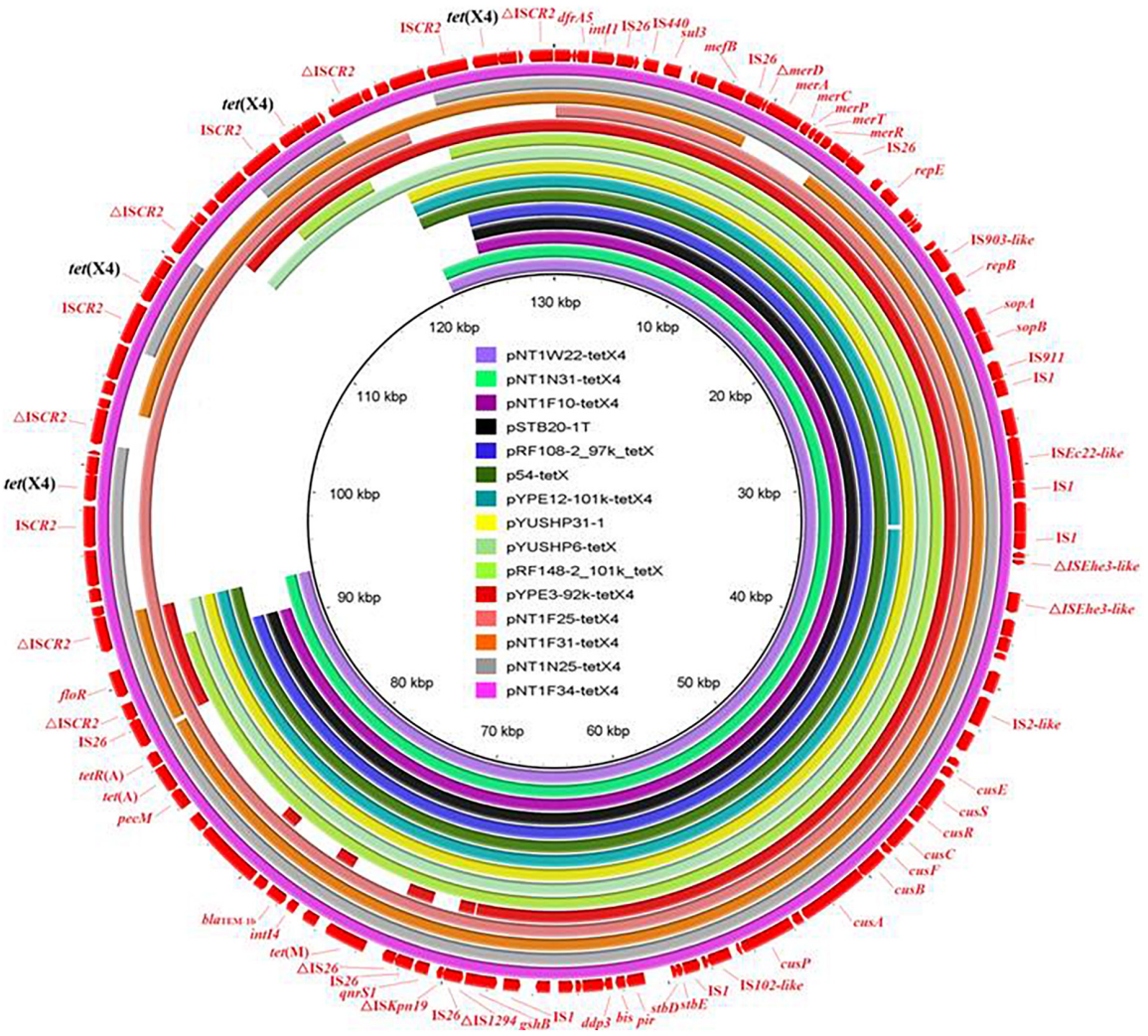

FIGURE 2
Sequence comparison of *tet*(X4)-carrying plasmid pYUSHP31-1 from *E. coli* isolate SH21PTE31 in this study with other similar IncFIA18/IncFIB(K)/IncX1 plasmids using BRIG. The reference sequence pNT1F34-tetX (CP075486) is indicated in red in the outer circle.

These *tet*(X4)-carrying IncFIA18/IncFIB(K)/IncX1 plasmids may evolve from the same ancestor, and form variable but related MRRs by insertions, deletions, or rearrangements of different resistance modules mediated by mobile elements such as IS*26* and IS*CR2*.

Phylogenomic analysis of *tet*(X4)-Positive ST761 *Escherichia coli* strains

Escherichia coli ST761 has been increasingly reported in different sources associated with *tet*(X4) in China, particularly from pigs (**Supplementary Table 1**). To further compare the genetic differences between *tet*(X4)-positive *E. coli* isolates of the same ST, we performed a phylogenomic analysis based on cgSNP. The results revealed a relatively close genetic relationship (0-49 SNPs) among 50 *tet*(X4)-positive ST761 *E. coli* isolates (**Figure 1**). Among them, cgST 137253 (n = 44) was the most prevalent type, and it contained two isolates from patients, two from wastewater, three from pork, and 37 from pigs including six strains obtained in this study and SH19PTE6 from the same pig farm (**Figure 1**). It indicates that clonal transmission has occurred in this swine farm. The plasmid replicons [IncFIA, IncFIB(K), IncX1] possibly associated with *tet*(X4) were present in all isolates, and the core resistance genes [bla_{TEM-1}, *tet*(A), *tet*(M), *floR*, *qnrS1*, *sul3*, *dfrA5* and *mef*(B)] within *tet*(X4)-carrying IncFIA/IncFIB(K)/IncX1 plasmid pYUSHP31-1 were shared by 45 strains (**Figure 1**).

Although horizontal transfer mediated by plasmids (e.g., IncQ, and IncX1) and insertion sequences (e.g., IS*CR2*, IS*26*, and IS*1*) is the main mechanism for *tet*(X4) transmission

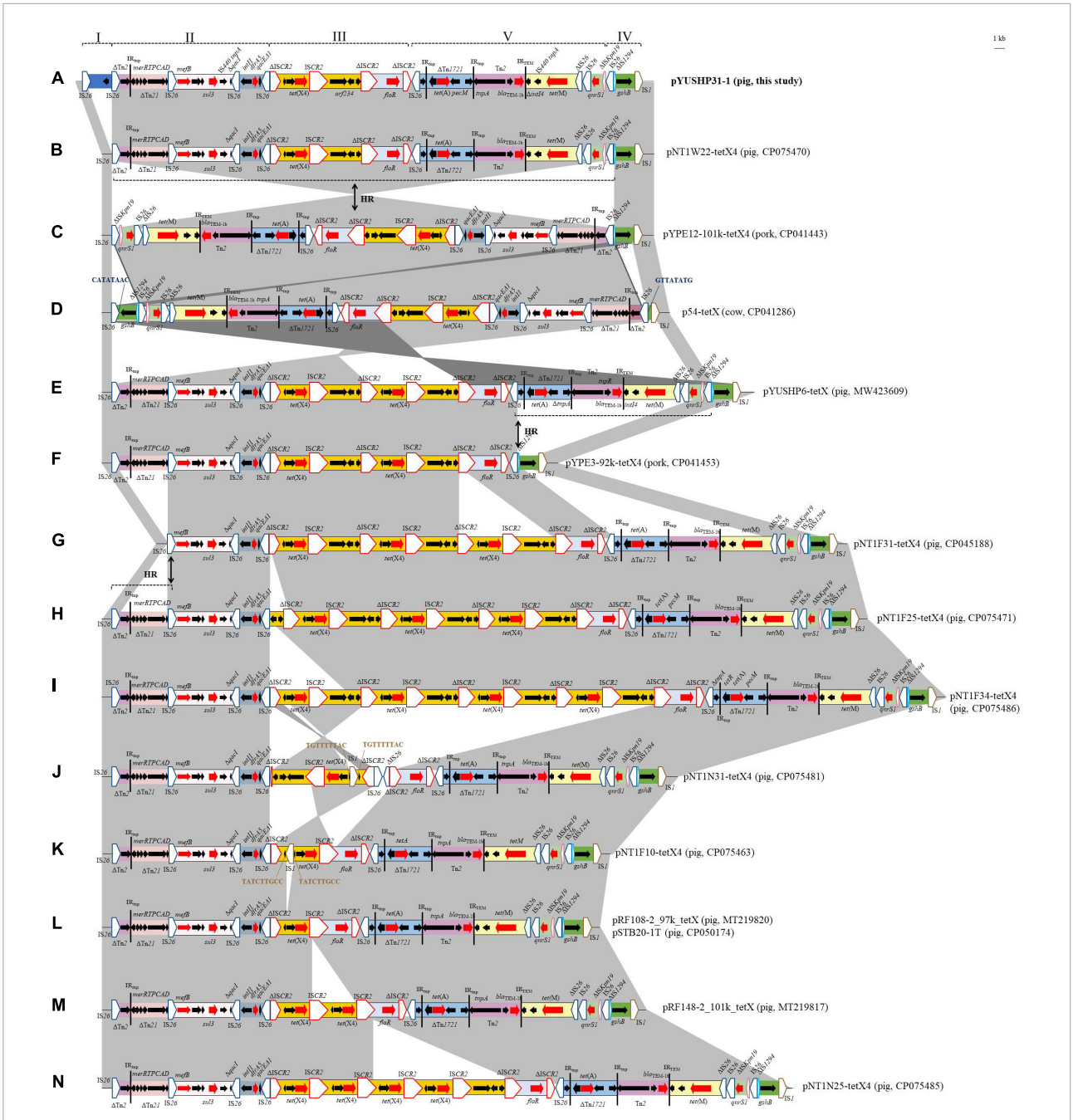

FIGURE 3
Genetic organization of the multidrug resistance region of plasmid pYUSHP31-1 and structural comparison with other IncFIA18/IncFIB(K)/IncX1 plasmids. I to IV indicate five regions bounded by IS26 or ISCR2 in pYUSHP31-1. The extents and directions of orientation of resistance genes (thick red arrow) and other genes are indicated by arrows. Regions with >99% identity are shaded in gray. 1 indicates a truncated gene or mobile element. Insertion sequences (ISs) are shown as boxes labeled with the IS name. Labeled vertical arrows with IS boxes denote the insertion position of IS elements. Direct repeats are indicated by arrows and sequences. Tall bars represent the 38-bp IR of transposons (Tn). Arrows labeled with "HR" and dotted lines indicate where homologous recombination could explain differences between structures.

(Aminov, 2021; Liu et al., 2022; Yu et al., 2022), clonal spread of *tet*(X4)-carrying strains, such as *E. coli* ST877, ST10, and ST48 clones is also responsible for *tet*(X4) dissemination between animals and humans (Cui et al., 2022). The *E. hormaechei* co-harboring *tet*(X4) and bla_{NDM} could also clonally spread from the slaughterhouse to the retail market (Li et al., 2022). *E. coli* ST761 isolates carrying *tet*(X4) has been detected in pigs, cow, pork, wastewater, and patients in different areas from China sharing a close phylogenetic relationship, suggesting that the ST761 lineage has the potential to be

a successful clone to transfer *tet*(X4) and other resistance genes as well in China.

Conclusion

Our findings suggest that *tet*(X4)-positive ST761 *E. coli* was the main reason for spread and persistence of *tet*(X4) in this pig farm. Importantly, *E. coli* ST761 has the potential to become a high-risk clone for *tet*(X4) dissemination in China. On the other hand, the *tet*(X4)-carrying IncFIA18/IncFIB(K)/IncX1 hybrid plasmids within ST761 *E. coli* lineage could reorganize, acquire or lose resistance modules mediated by mobile elements such as IS*CR2* and IS*26*. The horizontal transfer of similar IncFIA18/IncFIB(K)/IncX1 plasmids further facilitates the *tet*(X4) dissemination in distinct lineages.

Data availability statement

The datasets presented in this study can be found in online repositories. The names of the repository/repositories and accession number(s) can be found in the article/**Supplementary material**.

Author contributions

XJ and JW conceived the study. M-JL, HW, Z-YW, and YJ carried out the experiments. JW, Z-YW, and YJ analyzed the data. JW wrote the manuscript. Z-MP and XJ revised the manuscript. All authors read and approved the final manuscript.

Funding

This work was funded by the fifth phase of "333 Project" Scientific Research project in Jiangsu Province (BRA2020002) and Key Research and Development Program (Modern Agriculture) project of Jiangsu Province (grant no. BE2021331).

Conflict of interest

The authors declare that the research was conducted in the absence of any commercial or financial relationships that could be construed as a potential conflict of interest.

Publisher's note

All claims expressed in this article are solely those of the authors and do not necessarily represent those of their affiliated organizations, or those of the publisher, the editors and the reviewers. Any product that may be evaluated in this article, or claim that may be made by its manufacturer, is not guaranteed or endorsed by the publisher.

Supplementary material

The Supplementary Material for this article can be found online at: https://www.frontiersin.org/articles/10.3389/fmicb.2022.967313/full#supplementary-material

References

Aminov, R. (2021). Acquisition and spread of antimicrobial resistance: A tet(X) case study. *Int. J. Mol. Sci.* 22:3905. doi: 10.3390/ijms22083905

Chen, C., Chen, L., Zhang, Y., Cui, C. Y., Wu, X. T., He, Q., et al. (2019). Detection of chromosome-mediated tet(X4)-carrying Aeromonas caviae in a sewage sample from a chicken farm. *J. Antimicrob. Chemother.* 74, 3628–3630. doi: 10.1093/jac/dkz387

Chen, L., Chen, Z. L., Liu, J. H., Zeng, Z. L., Ma, J. Y., and Jiang, H. X. (2007). Emergence of RmtB methylase-producing *Escherichia coli* and *Enterobacter cloacae* isolates from pigs in China. *J. Antimicrob. Chemother.* 59, 880–885. doi: 10.1093/jac/dkm065

Cui, C. Y., Li, X. J., Chen, C., Wu, X. T., He, Q., Jia, Q. L., et al. (2022). Comprehensive analysis of plasmid-mediated tet(X4)-positive *Escherichia coli* isolates from clinical settings revealed a high correlation with animals and environments-derived strains. *Sci. Total Environ.* 806:150687. doi: 10.1016/j.scitotenv.2021.150687

Dao, T. D., Kasuga, I., Hirabayashi, A., Nguyen, D. T., Tran, H. T., Vu, H., et al. (2022). Emergence of mobile tigecycline resistance gene tet(X4)-harbouring Shewanella xiamenensis in a water environment. *J. Glob. Antimicrob. Resist.* 28, 140–142. doi: 10.1016/j.jgar.2021.12.022

Ding, Y., Saw, W. Y., Tan, L., Moong, D., Nagarajan, N., Teo, Y. Y., et al. (2020). Emergence of tigecycline- and eravacycline-resistant Tet(X4)-producing *Enterobacteriaceae* in the gut microbiota of healthy Singaporeans. *J. Antimicrob. Chemother.* 75, 3480–3484. doi: 10.1093/jac/dkaa372

Dong, N., Zeng, Y., Cai, C., Sun, C., Lu, J., Liu, C., et al. (2022). Prevalence, transmission, and molecular epidemiology of tet(X)-positive bacteria among humans, animals, and environmental niches in China: An epidemiological, and genomic-based study. *Sci. Total Environ.* 818:151767. doi: 10.1016/j.scitotenv.2021.151767

Fang, L. X., Chen, C., Cui, C. Y., Li, X. P., Zhang, Y., Liao, X. P., et al. (2020). Emerging high-level tigecycline resistance: Novel tetracycline destructases spread via the mobile Tet(X). *Bioessays* 42:e2000014. doi: 10.1002/bies.202000014

He, T., Wang, R., Liu, D., Walsh, T. R., Zhang, R., Lv, Y., et al. (2019). Emergence of plasmid-mediated high-level tigecycline resistance genes in animals and humans. *Nat. Microbiol.* 4, 1450–1456. doi: 10.1038/s41564-019-0445-2

Kim, T. W., Kim, Y. H., Kim, S. E., Lee, J. H., Park, C. S., and Kim, H. Y. (2010). Identification and distribution of Bacillus species in doenjang by whole-cell protein patterns and 16S rRNA gene sequence analysis. *J. Microbiol. Biotechnol.* 20, 1210–1214. doi: 10.4014/jmb.1002.02008

Li, R., Liu, Z., Li, Y., Xiao, X., and Wang, Z. (2022). Characterization of blaNDM-positive *Enterobacteriaceae* reveals the clonal dissemination of *Enterobacter* hormaechei coharboring blaNDM and tet(X4) along the pork

production chain. *Int. J. Food Microbiol.* 372:109692. doi: 10.1016/j.ijfoodmicro.2022.109692

Li, R., Lu, X., Peng, K., Liu, Z., Li, Y., Liu, Y., et al. (2020). Deciphering the structural diversity and classification of the mobile tigecycline resistance gene tet(X)-bearing plasmidome among bacteria. *mSystems* 5:e00134–20. doi: 10.1128/mSystems.00134-20

Li, R., Peng, K., Xiao, X., Wang, Y., and Wang, Z. (2021). Characterization of novel ISAba1-bounded tet(X15)-bearing composite transposon Tn6866 in Acinetobacter variabilis. *J. Antimicrob. Chemother.* 76, 2481–2483. doi: 10.1093/jac/dkab182

Li, Y., Wang, Q., Peng, K., Liu, Y., Xiao, X., Mohsin, M., et al. (2021). Distribution and genomic characterization of tigecycline-resistant tet(X4)-positive *Escherichia coli* of swine farm origin. *Microb. Genom.* 7:000667. doi: 10.1099/mgen.0.000667

Liu, D., Wang, T., Shao, D., Song, H., Zhai, W., Sun, C., et al. (2022). Structural diversity of the ISCR2-mediated rolling-cycle transferable unit carrying tet(X4). *Sci. Total Environ.* 826:154010. doi: 10.1016/j.scitotenv.2022.154010

Marathe, N. P., Svanevik, C. S., Ghavidel, F. Z., and Grevskott, D. H. (2021). First report of mobile tigecycline resistance gene tet(X4)-harbouring multidrug-resistant *Escherichia coli* from wastewater in Norway. *J. Glob. Antimicrob. Resist.* 27, 37–40. doi: 10.1016/j.jgar.2021.07.019

Martelli, F., AbuOun, M., Cawthraw, S., Storey, N., Turner, O., Ellington, M., et al. (2022). Detection of the transferable tigecycline resistance gene tet(X4) in *Escherichia coli* from pigs in the United Kingdom. *J. Antimicrob. Chemother.* 77, 846–848. doi: 10.1093/jac/dkab439

Mohsin, M., Hassan, B., Martins, W., Li, R., Abdullah, S., Sands, K., et al. (2021). Emergence of plasmid-mediated tigecycline resistance tet(X4) gene in *Escherichia coli* isolated from poultry, food and the environment in South Asia. *Sci. Total Environ.* 787:147613. doi: 10.1016/j.scitotenv.2021.147613

Umar, Z., Chen, Q., Tang, B., Xu, Y., Wang, J., Zhang, H., et al. (2021). The poultry pathogen Riemerella anatipestifer appears as a reservoir for Tet(X) tigecycline resistance. *Environ. Microbiol.* 23, 7465–7482. doi: 10.1111/1462-2920.15632

Wang, J., Wu, H., Mei, C. Y., Wang, Y., Wang, Z. Y., Lu, M. J., et al. (2021). Multiple mechanisms of tigecycline resistance in *Enterobacteriaceae* from a pig farm. China. *Microbiol. Spectr.* 9:e0041621. doi: 10.1128/Spectrum.00416-21

Wang, L., Liu, D., Lv, Y., Cui, L., Li, Y., Li, T., et al. (2019). Novel plasmid-mediated tet(X5) gene conferring resistance to tigecycline, eravacycline, and omadacycline in a clinical *Acinetobacter baumannii* isolate. *Antimicrob. Agents Chemother.* 64:e01326–19. doi: 10.1128/AAC.01326-19

Wu, Y., He, R., Qin, M., Yang, Y., Chen, J., Feng, Y., et al. (2022). Identification of plasmid-mediated tigecycline-resistant gene tet(X4) in *Enterobacter cloacae* from pigs in China. *Microbiol. Spectr.* 10:e0206421. doi: 10.1128/spectrum.02064-21

Yaghoubi, S., Zekiy, A. O., Krutova, M., Gholami, M., Kouhsari, E., Sholeh, M., et al. (2021). Tigecycline antibacterial activity, clinical effectiveness, and mechanisms and epidemiology of resistance: Narrative review. *Eur. J. Clin. Microbiol. Infect. Dis.* 5, 1–20. doi: 10.1007/s10096-020-04121-1

Yu, R., Chen, Z., Schwarz, S., Yao, H., and Du, X. D. (2022). Mobilization of tet(X4) by IS1 family elements in porcine *Escherichia coli* isolates. *Antimicrob. Agents Chemother.* 66:e0159721. doi: 10.1128/AAC.01597-21

Zeng, Y., Dong, N., Liu, C., Lu, J., and Zhang, R. (2021). Presence of tet(X4)-positive Citrobacter freundii in cancer patient with chemotherapy-induced persistent diarrhea. *J. Glob. Antimicrob. Resist.* 24, 88–89. doi: 10.1016/j.jgar.2020.11.007

Zhai, W., Tian, Y., Lu, M., Zhang, M., Song, H., Fu, Y., et al. (2022). Presence of mobile tigecycline resistance gene tet(X4) in clinical *Klebsiella pneumoniae*. *Microbiol. Spectr.* 10:e0108121. doi: 10.1128/spectrum.01081-21

Zhang, R. M., Sun, J., Sun, R. Y., Wang, M. G., Cui, C. Y., Fang, L. X., et al. (2021). Source tracking and global distribution of the tigecycline non-susceptible tet(X). *Microbiol. Spectr.* 9:e0116421. doi: 10.1128/Spectrum.01164-21

frontiers | Frontiers in Microbiology

TYPE Original Research
PUBLISHED 23 August 2022
DOI 10.3389/fmicb.2022.974432

OPEN ACCESS

EDITED BY
Ning Dong,
Soochow University, China

REVIEWED BY
Hua Zhou,
Zhejiang University, China
Shangshang Qin,
Zhengzhou University, China
Cong Shen,
Guangdong Provincial Hospital of Chinese Medicine, China

*CORRESPONDENCE
Jin-Lin Huang
jinlin@yzu.edu.cn

SPECIALTY SECTION
This article was submitted to Antimicrobials, Resistance and Chemotherapy, a section of the journal Frontiers in Microbiology

RECEIVED 21 June 2022
ACCEPTED 08 August 2022
PUBLISHED 23 August 2022

CITATION
Chen C, Huang P-Y, Cui C-Y, He Q, Sun J, Liu Y-H and Huang J-L (2022) Classification and molecular characteristics of *tet*(X)-carrying plasmids in *Acinetobacter* species. *Front. Microbiol.* 13:974432. doi: 10.3389/fmicb.2022.974432

Classification and molecular characteristics of *tet*(X)-carrying plasmids in *Acinetobacter* species

Chong Chen[1,2,3], Ping-Yu Huang[2,3], Chao-Yue Cui[4], Qian He[4], Jian Sun[4,5], Ya-Hong Liu[4,5] and Jin-Lin Huang[1,2,3]*

[1]Joint International Research Laboratory of Agriculture and Agri-Product Safety, Ministry of Education of China, Institutes of Agricultural Science and Technology Development, Yangzhou University, Yangzhou, China, [2]Jiangsu Key Laboratory of Zoonosis, Jiangsu Co-innovation Center for Prevention and Control of Important Animal Infectious Diseases and Zoonoses, Yangzhou University, Yangzhou, China, [3]Key Laboratory of Prevention and Control of Biological Hazard Factors (Animal Origin) for Agrifood Safety and Quality, Ministry of Agriculture of China, Yangzhou University, Yangzhou, China, [4]National Risk Assessment Laboratory for Antimicrobial Resistance of Animal Original Bacteria, South China Agricultural University, Guangzhou, China, [5]Guangdong Laboratory for Lingnan Modern Agriculture, South China Agricultural University, Guangzhou, China

The rapid dissemination of plasmid-mediated *tet*(X) genes in *Acinetobacter* species has compromised the clinical effectiveness of tigecycline, one of the last-resort antibiotics. However, the classification strategy and homology group of *tet*(X)-positive *Acinetobacter* spp. plasmids remain largely unknown. In this study, we classified them by genome-based replicon typing, followed by analyses of structural characteristics, transferability and *in vivo* effect. A total of 34 plasmids distributed in at least nine *Acinetobacter* species were collected, including three *tet*(X3)-positive plasmids and one *tet*(X6)-positive plasmid from our genome sequencing results. Among them, there were 28 plasmids carrying Rep_3 superfamily replicase genes and classified into six homology groups, consisting of GR31 (82.1%), GR26 (3.6%), GR41 (3.6%), GR59 (3.6%), and novel groups GR60 (3.6%) and GR61 (3.6%). Our *tet*(X3)-positive plasmids pYH16040-1, pYH16056-1, and pYH12068-1 belonged to the dominant GR31 group, whereas the *tet*(X6)-positive plasmid pYH12068-2 was unclassified. Structurally, all *tet*(X)-positive GR31 plasmids shared similar plasmid replication (*repB*), stability (*parA* and *parB*) and accessory modules [*tet*(X) and *sul2*], and 97.6% of plasmid-mediated *tet*(X) genes in *Acinetobacter* species were adjacent to IS*CR2*. Conjugation and susceptibility testing revealed pYH16040-1, pYH16056-1, and pYH12068-2, carrying plasmid transfer modules, were able to mediate the mobilization of multiple antibiotic resistance. Under the treatment of tigecycline, the mortality rate of *Galleria mellonella* infected by pYH16040-1-mediated *tet*(X3)-positive *Acinetobacter* spp. isolate significantly increased

when compared with its plasmid-cured strain ($p < 0.0001$). The spread of such plasmids is of great clinical concern, more effects are needed and will facilitate the future analysis of *tet*(X)-positive *Acinetobacter* spp. plasmids.

KEYWORDS

***Acinetobacter* species, mobile tigecycline resistance, *tet*(X), replicon typing, GR31 plasmid**

Introduction

Tigecycline, the first glycylcycline antibiotic, exhibits a broad spectrum of antibacterial activities against multidrug-resistant (MDR) Gram-negative and Gram-positive pathogens (Sader et al., 2019). However, the recent emergence and spread of novel tigecycline resistance mechanisms Tet(X3), Tet(X4), Tet(X5), Tet(X6), and other variants have compromised its clinical efficacy by enzymatic degradation (He et al., 2019; Sun et al., 2019; Wang et al., 2019; Chen et al., 2021). *Acinetobacter* species is a heterogeneous group of opportunistic pathogens and easily acquires antibiotic resistance genes (ARGs) (Wong et al., 2017). To date, the *tet*(X) genes have been reported in at least 10 different *Acinetobacter* species, including *Acinetobacter baumannii*, *Acinetobacter gandensis*, *Acinetobacter piscicola*, *Acinetobacter schindleri*, *Acinetobacter johnsonii*, *Acinetobacter indicus*, *Acinetobacter towneri*, *Acinetobacter lwoffii*, *Acinetobacter pseudolwoffii,* and *Acinetobacter variabilis* (Chen et al., 2020; Liu et al., 2020; Zheng et al., 2020; Cheng Y. et al., 2021; Li et al., 2021). Worrisomely, the plasmid-mediated *tet*(X3) and *tet*(X6) genes were detected with carbapenem resistance gene bla_{NDM-1} in *A. baumannii*, *A. indicus*, *A. schindleri,* and *A. lwoffii* isolates, posing a serious public health threat (Cui et al., 2020; He et al., 2020; Zheng et al., 2020).

The plasmid is a self-replicating component of *Acinetobacter* spp. genome and plays an important role in the horizontal transmission of ARGs, such as bla_{NDM-1} and bla_{OXA-23} (Wang and Sun, 2015; Silva et al., 2018). With the increasing number of complete *Acinetobacter* spp. plasmids deposited at the National Center for Biotechnology Information (NCBI), a series of plasmid classification schemes were developed based on replication initiator protein, mobilization protein and plasmid size (Bertini et al., 2010; Salto et al., 2018; Mindlin et al., 2020). As the latest research showed, there were a total of 59 homology groups identified by plasmid replicon typing (Li et al., 2022). However, there was a lack of systematic classification of *tet*(X)-positive *Acinetobacter* spp. plasmids since the first mobile plasmid-mediated *tet*(X3) gene in 2019, and their homology groups remained to be analyzed (He et al., 2019; Wang J. et al., 2020; Cheng Y. et al., 2021). Herein, we intend to explore the classification and homology group of complete *tet*(X)-carrying *Acinetobacter* spp. plasmids by genome-based replicon typing, followed by analyses of structural characteristics, transferability, and *in vivo* effect.

Materials and methods

Bacterial strains and plasmids

During an epidemiological surveillance between 2015 and 2018, we reported the prevalence of *tet*(X)-positive *Acinetobacter* spp. strains in China (Chen et al., 2020), of which seven isolates belonging to different sources were selected for next analyses in this study (**Table 1**). These included: *tet*(X3)-positive *Acinetobacter* spp. YH16040 and *tet*(X3)- and *tet*(X6)-positive *Acinetobacter* spp. YH12068 from pig; *tet*(X3)-positive *Acinetobacter* spp. YH16056 from soil; *tet*(X3)-positive *A. pseudolwoffii* YH18001 from human; *tet*(X4)-positive *A. indicus* Q22-2, Q85-2, and Q278-1 from migratory bird. In addition, a newly isolated *tet*(X6)-positive *A. baumannii* YC103 by CHROMagar^{TM} *Acinetobacter* plates (CHROMagar, Paris, France) containing tigecycline (2 μg/mL) from duck in 2019 was also analyzed (**Table 1**). With the amino acid sequence of Tet(X3) as a template, the complete *tet*(X)-harboring *Acinetobacter* spp. plasmids deposited at the NCBI database were collected by tblastn (**Supplementary Table 1**; accessed 23 Mar 2022).

Whole genome sequencing and assembly

Genomic DNA of eight *tet*(X)-positive *Acinetobacter* spp. isolates were sequenced by Oxford Nanopore (Nextomics, Wuhan, China), respectively. Combining the clean data with our previous Illumina HiSeq data (Chen et al., 2020) as well as that of *A. baumannii* YC103 (Novogene, Beijing, China), genome assembly was performed by Unicycler version 0.4.1 and corrected by Pilon version 1.12 (Walker et al., 2014; Wick et al., 2017).

TABLE 1 Bacterial information of *tet*(X)-positive *Acinetobacter* spp. isolates by WGS.

Strains	Years	Provinces	Sources	*tet*(X)-carrying structures	
				Size (bp)	GenBank
Acinetobacter spp. YH16040	2016	Jiangxi	Pig	87,435	CP094542
Acinetobacter spp. YH16056	2016	Hunan	Soil	98,709	CP094546
Acinetobacter spp. YH12068	2017	Fujian	Pig	100,866	CP094556
				61,481	CP094557
A. pseudolwoffii YH18001	2017	Guangdong	Human	5,117	JALHBG010000013
A. indicus Q22-2	2017	Qinghai	Migratory bird	15,225	JALHBD010000003
A. indicus Q85-2	2017	Qinghai	Migratory bird	7,406	JALHBE010000004
A. indicus Q278-1	2017	Qinghai	Migratory bird	22,321	JALHBF010000002
A. baumannii YC103	2019	Jiangsu	Duck	4,021,945	CP054560

Bioinformatics analyses

All *tet*(X)-harboring plasmids were annotated by Rapid Annotation using Subsystem Technology (RAST) version 2.0 (Aziz et al., 2008). Plasmid-mediated ARGs were analyzed by ResFinder version 4.0 and a heatmap was then constructed by ImageGP (Bortolaia et al., 2020; Chen et al., 2022). Plasmid replication and transfer proteins were detected by the Conserved Domain Database (CDD) (Lu et al., 2020). A maximum-likelihood phylogenetic tree of replication initiator proteins was constructed by MEGA-X version 10.1.8 and visualized by Evolview version 3.0 (Kumar et al., 2018; Subramanian et al., 2019). Plasmid classification was performed according to the *A. baumannii* replicon typing scheme, with at least 80% nucleotide coverage and at least 75% nucleotide identity of replicase genes in the same group (Bertini et al., 2010; Castro-Jaimes et al., 2022; Li et al., 2022). Similarly, the bacterial host ranges of different plasmid groups were also evaluated by querying the NCBI database with representative replicase genes (accessed 24 May 2022). Sequence comparison of *tet*(X)-positive structures was conducted by Easyfig version 2.2.5 (Sullivan et al., 2011).

Conjugation experiment

Transferability of plasmid-borne *tet*(X)-mediated tigecycline resistance was evaluated by filter mating with rifampin-resistant *Acinetobacter baylyi* ADP1 and *A. baumannii* ATCC 19606 (Chen et al., 2020). The putative transconjugants were selected on Luria-Bertani (LB) agar plates containing tigecycline (2 μg/mL) and rifampin (100 μg/mL), followed by *tet*(X) detection and PCR-based fingerprinting (Versalovic et al., 1991). In parallel, the recipient strains were selected with rifampin (100 μg/mL), and transfer efficiencies were calculated by colony counts of the transconjugant and recipient bacterial cells (Zhu et al., 2013).

Plasmid curing

The *tet*(X3)-harboring GR31 plasmid pYH16040-1 was cured of *Acinetobacter* spp. YH16040 using sodium dodecyl sulfate (SDS) with adjustment (Chen et al., 2017). An overnight culture was diluted 100-fold in LB broth supplemented with 0.02% SDS and serially passaged at 38°C by shaking per 24 h. One week later, 100 μL dilution was streaked onto LB agar plate and 50 colonies were subcultured with or without tigecycline (4 μg/mL). The colony that did not grow in tigecycline was probably the plasmid-cured isogeneic strain (namely YH16040C) and confirmed by detecting *tet*(X3) gene (Chen et al., 2020) and replicase gene *repB* (repB-F, 5′-GCCCAATCGAATTATCAGCCA-3′; repB-R, 5′-TGGCAACAGAATCTAGGGCA-3′).

Antimicrobial susceptibility testing

Minimum inhibitory concentrations (MICs) of all strains were determined by broth microdilution and interpreted according to the Clinical and Laboratory Standards Institute guideline M100-Ed28 (Clinical and Laboratory Standards Institute [CLSI], 2018). The tested antibiotics contained tetracycline, tigecycline, eravacycline, omadacycline, amikacin, gentamicin, ciprofloxacin, colistin, cefotaxime, meropenem, sulfamethoxazole-trimethoprim, and florfenicol. Particularly, the resistance breakpoints of tigecycline (≥8 μg/mL) and omadacycline (≥16 μg/mL) referred to the Food and Drug Administration (FDA) criteria for Enterobacteriaceae,[1] whereas

1 https://www.fda.gov/

eravacycline was uninterpreted with no breakpoint. *Escherichia coli* ATCC 25922 served as a quality control strain.

Galleria mellonella infection model

As previously described (Dong et al., 2017; Xu et al., 2021), the healthy larvae of *G. mellonella* (Huiyude, Tianjin, China) were randomly grouped (16 per group), and then infected with GR31 plasmid-mediated *tet*(X3)-positive *Acinetobacter* spp. YH16040 or its plasmid-cured strain YH16040C [*tet*(X3)-negative, 5×10^6 colony-forming units] via the last left proleg. After incubation at 35°C for 2 h, the infected larvae were treated with tigecycline (2 μg/g) or phosphate-buffered saline (PBS) by injection into the last right proleg. Finally, the larvae were observed for survival rates per 24 h in the next 4 days. All *in vivo* experiments were performed in triplicate.

Results and discussion

Distribution of *tet*(X)-carrying plasmids in *Acinetobacter* species

WGS analyses of eight *tet*(X)-positive *Acinetobacter* spp. isolates successfully revealed four *tet*(X)-carrying plasmids. These included *tet*(X3)-positive plasmids pYH16040-1 (GenBank accession number: CP094542) from *Acinetobacter* spp. YH16040, pYH16056-1 (CP094546) from *Acinetobacter* spp. YH16056, and pYH12068-1 (CP094556) as well as a *tet*(X6)-positive plasmid pYH12068-2 (CP094557) from *Acinetobacter* spp. YH12068 (**Table 1**). Meanwhile, a *tet*(X6)-positive chromosome cYC103 (CP054560) from *A. baumannii* YC103 was also obtained (**Table 1**). For the remaining four *tet*(X)-positive strains *A. pseudolwoffii* YH18001, *A. indicus* Q278-1, *A. indicus* Q85-2, and *A. indicus* Q22-2 (**Table 1**), we failed to acquire the complete *tet*(X)-harboring plasmids or chromosomes despite repeated attempts. By querying Nanopore raw data of *A. pseudolwoffii* YH18001 ($n \geq 18$, SRR18497244), *A. indicus* Q278-1 ($n \geq 4$, SRR18497245), *A. indicus* Q85-2 ($n \geq 13$, SRR18497246), and *A. indicus* Q22-2 ($n \geq 4$, SRR18497247), a repeated structure consisting of multiple copies of *tet*(X) genes was detected, respectively, which may lead to the failure of complete sequence assemblies.

Since the first report in 2019 (He et al., 2019), the number of complete *tet*(X)-positive *Acinetobacter* spp. plasmids deposited at the NCBI database has been growing ($n = 34$; **Supplementary Table 1**), including four plasmids mentioned above. There were three *tet*(X) subtypes located on plasmids (**Figure 1A**), namely *tet*(X3) (82.4%, 28/34), *tet*(X5) (5.9%, 2/34), and *tet*(X6) (35.3%, 12/34), of which *tet*(X3) usually coexisted with *tet*(X6) (23.5%, 8/34). Besides *tet*(X) genes, large amounts of plasmid-mediated genes conferring resistance to tetracyclines, aminoglycosides, β-lactams, phenicols, sulfonamides, macrolides, lincosamides, and rifamycins were present (**Figure 1A**). Worrisomely, the *tet*(X)-positive plasmids ranging from 42,489 to 332,451 bp were widely distributed in *A. indicus* (26.5%, 9/34), *A. baumannii* (14.7%, 5/34), *A. towneri* (11.8%, 4/34), *A. schindleri* (8.8%, 3/34), *A. variabilis* (2.9%, 1/34), *A. pseudolwoffii* (2.9%, 1/34), *A. piscicola* (2.9%, 1/34), *Acinetobacter junii* (2.9%, 1/34), *Acinetobacter pittii* (2.9%, 1/34), and unidentified *Acinetobacter* spp. strains (23.5%, 8/34; **Figures 1B,C**). Given the genetic and host diversity, more attention should be paid to the evolution of *tet*(X)-positive MDR *Acinetobacter* spp. plasmids.

Classification of *tet*(X)-positive *Acinetobacter* spp. plasmids

Replicon conserved domain analyses showed that 82.4% (28/34) of *tet*(X)-positive *Acinetobacter* spp. plasmids carried replicase genes and all of them belonged to a Rep_3 superfamily (pfam01051). Therefore, plasmid classification was conducted based on nucleotide sequence alignment with already classified replicase genes (Castro-Jaimes et al., 2022; Li et al., 2022). Among the *tet*(X)-positive Rep_3 superfamily plasmids, a total of six homology groups were successfully identified, such as the dominant GR31 (82.1%, 23/28), GR26 (3.6%, 1/28), GR41 (3.6%, 1/28), and GR59 (3.6%, 1/28; **Figure 2**). Especially, our *tet*(X3)-positive plasmids pYH16040-1 (CP094542), pYH16056-1 (CP094546), and pYH12068-1 (CP094556) fell within the same group GR31, which has been sporadically detected with *tet*(X) genes in *A. baumannii*, *A. indicus*, *A. schindleri*, *A. towneri*, and other *Acinetobacter* spp. strains (**Figure 2** and **Supplementary Table 1**). However, our *tet*(X6)-positive plasmid pYH12068-2 (CP094557) was unclassified due to the lack of replicase genes. In contrast, the replicase genes of *tet*(X3)- and *tet*(X6)-carrying plasmids pXMC5X702-tetX-145k (CP084302) and pYH12207-2 (CP048661) have < 75% nucleotide identities with existing homology groups GR1-GR59, and therefore were defined as novel groups GR60 (3.6%, 1/28) and GR61 (3.6%, 1/28), respectively (**Figure 2**). We provided the updated replicase gene and protein sequences in **Supplementary Files 1, 2**, and hoped they will facilitate the future analyses of the increasing number of *tet*(X)-positive *Acinetobacter* spp. plasmids.

In order to evaluate the host range of plasmids belonging to GR26, GR31, GR41, GR59, GR60, and GR61, we conducted a blastn search against the NCBI database and confirmed they were mainly distributed in *Acinetobacter* spp. isolates (99.0%, 201/203). In essence, the GR31 plasmids have been detected in 13 validly named *Acinetobacter* species, including *A. baumannii* (18.3%, 15/82), *A. lwoffii* (17.1%, 14/82), *A. indicus* (12.2%, 10/82), *A. towneri* (8.5%, 7/82), *A. schindleri* (7.3%, 6/82), and others (**Supplementary Figure 1**). The plasmids belonging

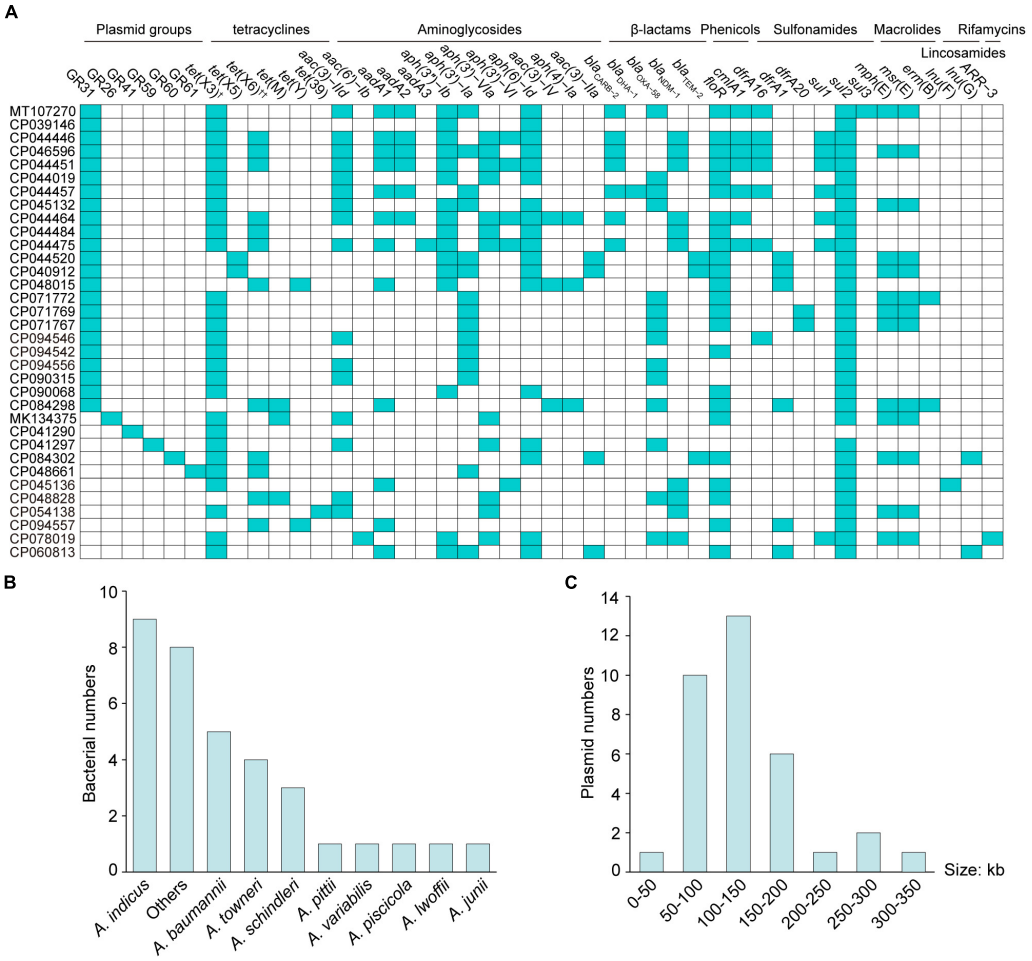

FIGURE 1
Collection of the complete *tet*(X)-positive plasmids from *Acinetobacter* spp. strains. The distribution of plasmid groups (cyan, **A**), plasmid-mediated ARGs (cyan, **A**), bacterial species **(B)** and plasmid sizes **(C)** is presented. †One *tet*(X3) variant with a 99.7% amino acid identity (CP045132) with *tet*(X3) is included. ††Two *tet*(X6) variants (CP048828 and CP048661) with a 97.4% amino acid identity with *tet*(X6) are included.

to GR26, GR41, GR59, GR60, and GR61 have also been identified in at least four *Acinetobacter* species, except two *E. coli* strains carrying GR41 plasmids (**Supplementary Figure 1**). Particularly, a few unassigned *Acinetobacter* species harbored GR26, GR31, GR59, GR60, and GR61 plasmids (**Supplementary Figure 1**), but the bacterial characteristics remained to be explored. All the results suggested a potential transmission risk of plasmid-mediated *tet*(X) genes especially in the genera *Acinetobacter*.

Structural characteristics of *tet*(X)-carrying *Acinetobacter* spp. plasmids

Predominantly, we compared the complete plasmid sequences of pYH16040-1, pYH16056-1, and pYH12068-1 with *tet*(X)-carrying GR31 plasmids available in the NCBI database. A total of 23 plasmids belonging to GR31 were analyzed and they exhibited GC contents ranging from 39.1 to 46.1%. According to our WGS results, pYH16040-1 was 87,435 bp and harbored 94 putative open reading frames (ORFs), whereas pYH16056-1 was 98,709 bp consisting of 107 ORFs and pYH12068-1 was 100,866 bp consisting of 115 ORFs. Although they originated from different sources, pYH16056-1 and pYH12068-1 showed an average 76.5% nucleotide coverage and 99.8% nucleotide identity to pYH16040-1, with the encoding sequence insertion, deletion and rearrangement (**Figure 3A**). Moreover, they shared high homologies (≥64.0% nucleotide coverage and ≥ 96.2% nucleotide identity) with MDR plasmids from the pig (MT107270), goose (CP044484), pigeon (CP044457), and soil (CP044451; **Figure 3A**). Archetypically, *Acinetobacter* spp. plasmids contained the backbone (namely plasmid replication, stability and transfer modules) and the

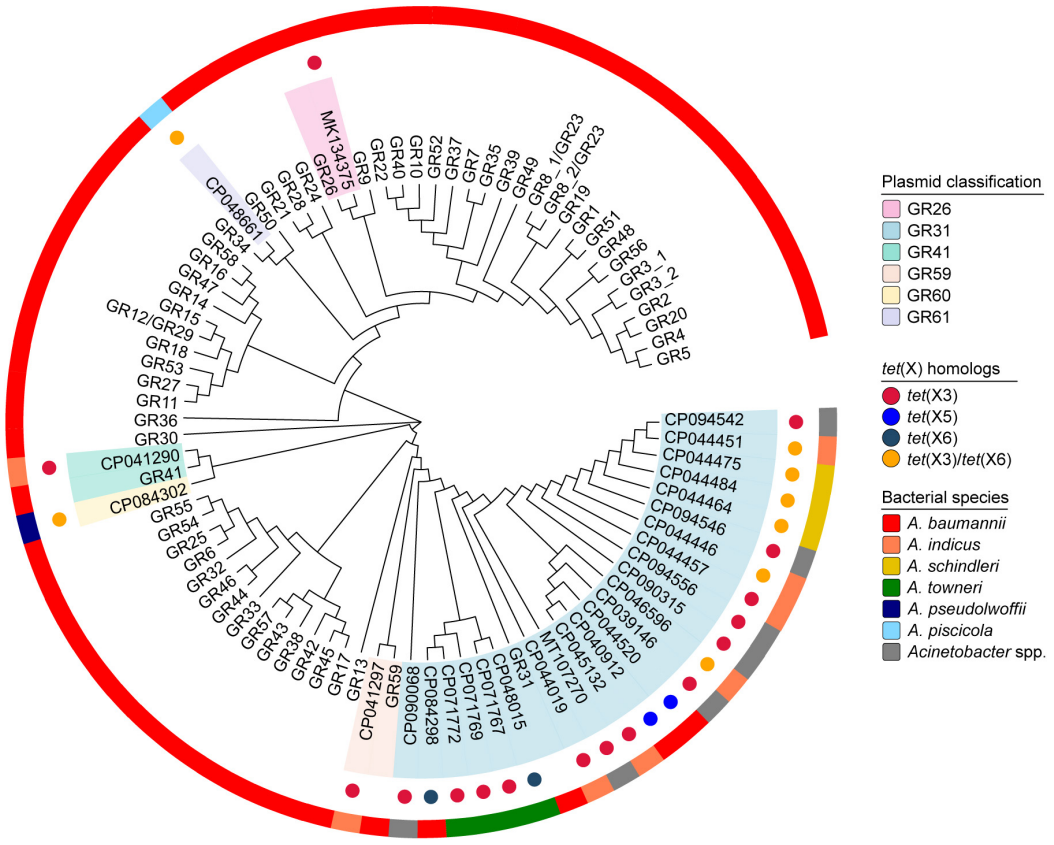

FIGURE 2
Maximum-likelihood phylogenetic analysis of *Acinetobacter* spp. plasmids based on replication initiator proteins. In parallel, the plasmid classification, *tet*(X) homologs and bacterial species are indicated from the inside out.

accessory modules (Brovedan et al., 2020). Our results revealed all *tet*(X)-positive GR31 plasmids owned a *repB* gene involved in plasmid replication, and *parA* and *parB* genes responsible for plasmid stability. However, only 21.7% (5/23) of them harbored plasmid transfer modules, including conjugal transfer (n = 3) and mobilization genes (n = 2). For accessory modules, they mainly consisted of ARGs [e.g., *tet*(X) and *sul2*, 100% (23/23)] and heavy-metal resistance gene clusters [e.g., *czcA-czcD*, 78.3% (18/23)].

Genetic environments of all plasmid-mediated *tet*(X) genes in *Acinetobacter* species, including *tet*(X3) (n = 28), *tet*(X6) (n = 12), and *tet*(X5) (n = 2), were further analyzed (**Figures 3B–D**). The result showed 97.6% (41/42) of them were adjacent to IS*CR2*, which is able to transpose ARGs through a rolling-circle transposition process (Liu et al., 2022). For GR31 plasmids, the IS*CR2*-mediated transposition units were constantly truncated by IS*26* (n = 22) and IS*Aba14* (n = 3). Similarly, the truncation by IS*26* was found on GR60 (n = 2) and GR61 (n = 2) plasmids, one of which was also upstream truncated by IS*Acsp12*. Except the GR26 plasmid carrying a complete IS*CR2*-mediated transposition unit (n = 1), GR41 and GR59 plasmids were detected with truncation by IS*3* (n = 1) and IS*1006* (n = 1), respectively. In addition, our WGS results of *A. pseudolwoffii* YH18001 (JALHBG010000013), *A. indicus* Q278-1 (JALHBF010000002), *A. indicus* Q85-2 (JALHBE010000004), and *A. indicus* Q22-2 (JALHBD010000003) revealed the incomplete *tet*(X)-carrying structures were also related to IS*CR2* (**Figures 3B,E**). The close association between *tet*(X) variants and IS*CR2* as well as truncation by other insertion sequences indicated the frequent recombination events.

Transferability of *Acinetobacter* spp. plasmid-mediated *tet*(X) genes

Conjugation experiments showed the GR31 plasmid-mediated *tet*(X3) genes were successfully transferred from *Acinetobacter* spp. YH16040 (pYH16040-1, CP094542) and YH16056 (pYH16056-1, CP094546) to the recipient *A. baylyi* ADP1 (transfer efficiency, approximately 10^{-8}), but failed to *A. baumannii* ATCC 19606. In *Acinetobacter* spp. YH12068, the *tet*(X3)-carrying GR31 plasmid pYH12068-1 (CP094556) couldn't be transferred, which may be explained by the lack of

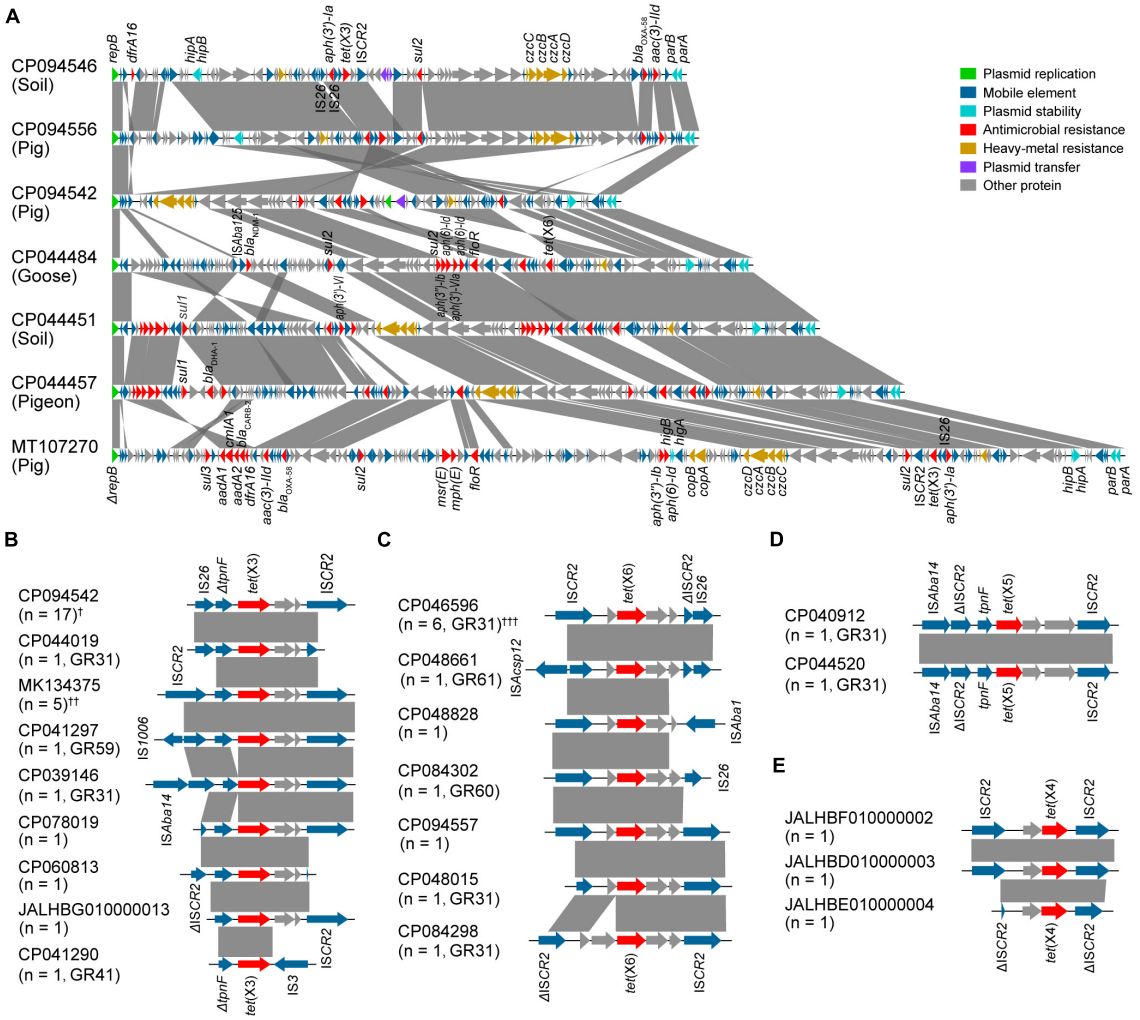

FIGURE 3

Characteristics of *tet*(X)-carrying structures in *Acinetobacter* species. The arrow represents the position and transcriptional direction of ORFs, while the Δ symbol indicates the gene is truncated. Regions of > 85% nucleotide sequence homology are marked by gray shading. **(A)** Linear sequence alignment of *tet*(X)-positive GR31 plasmids. The bacterial sources are listed in parenthesis. **(B–E)** Genetic environments of *tet*(X3) **(B)**, *tet*(X6) **(C)**, *tet*(X5) **(D)**, and *tet*(X4) **(E)** genes. The number of genetic environments and the plasmid homology groups are also given in parenthesis. †These include *tet*(X3)-carrying GR31 (*n* = 15, e.g., CP094542), GR60 (*n* = 1) and GR61 plasmids (*n* = 1). ††These include *tet*(X3)-carrying GR26 (*n* = 1, MK134375), GR31 (*n* = 2), and unclassified plasmids (*n* = 2). †††All of these belong to GR31 plasmids (*n* = 6, e.g., CP046596).

entire conjugative transfer regions (Figure 3A). Meanwhile, the *tet*(X6)-positive unclassified plasmid pYH12068-2 (CP094557) carrying plasmid transfer modules was transferred from *Acinetobacter* spp. YH12068 to *A. baylyi* ADP1 with a similar efficiency mentioned above. MICs of all transconjugants against tetracyclines increased by at least 32-fold when compared with *A. baylyi* ADP1, including tetracycline (≥64 μg/mL), tigecycline (≥4 μg/mL), the newly FDA-approved eravacycline (≥2 μg/mL) and omadacycline (≥8 μg/mL; Table 2). According to previous reports (Wang et al., 2019; Cui et al., 2020), the GR31 plasmid-mediated *tet*(X5) gene (CP040912) was also able to be transferred from human-derived *A. baumannii* to *A. baumannii* 5AB via electro-transformation, whereas the GR31 plasmid co-harboring *tet*(X3) and *tet*(X6) genes (CP044451) was from environmental *A. indicus* to *A. baylyi* ADP1 by natural transformation. The transferability of *tet*(X) genes between *Acinetobacter* species of human, animal and environment origins reminded us to consider the "One Health" approach to prevent mobile tigecycline resistance.

At the same time, the sulfamethoxazole-trimethoprim resistance (320 μg/mL) was transferred with *tet*(X3)-mediated tigecycline resistance from *Acinetobacter* spp. YH16040, YH16056, and YH12068 to *A. baylyi* ADP1, as well as florfenicol resistance (128 μg/mL) from *Acinetobacter* spp. YH16040 and YH12068 and gentamicin resistance (16 μg/mL) from *Acinetobacter* spp. YH16056, which was consistent with

TABLE 2 MICs of *tet*(X)-positive *Acinetobacter* spp. isolates, transconjugants, and plasmid-cured strain.

Strains†	MICs (μg/mL)							
	TET	TGC	ERA	OMA	CIP	GEN	FFC	SXT
Acinetobacter spp. YH16040	128	32	>8	>16	64	0.25	128	>320
Acinetobacter spp. YH16040C	8	1	0.06	0.125	64	0.25	8	20
A. baylyi ADP1 + pYH16040-1	128	8	4	16	0.25	0.25	128	320
Acinetobacter spp. YH16056	128	16	8	>16	64	32	128	>320
A.baylyi ADP1 + pYH16056-1	64	8	4	16	0.25	16	4	320
Acinetobacter spp. YH12068	256	32	>8	> 16	4	16	256	>320
A.baylyi ADP1 + pYH12068-2	64	4	2	8	0.25	0.25	128	320
A. baylyi ADP1	0.5	0.125	≤0.004	≤0.008	0.25	0.25	4	10

†*All of them were susceptible to amikacin, cefotaxime, meropenem, and colistin. TET, tetracycline; TGC, tigecycline; ERA, eravacycline; OMA, omadacycline; CIP, ciprofloxacin; GEN, gentamicin; FFC, florfenicol; SXT, sulfamethoxazole-trimethoprim.*

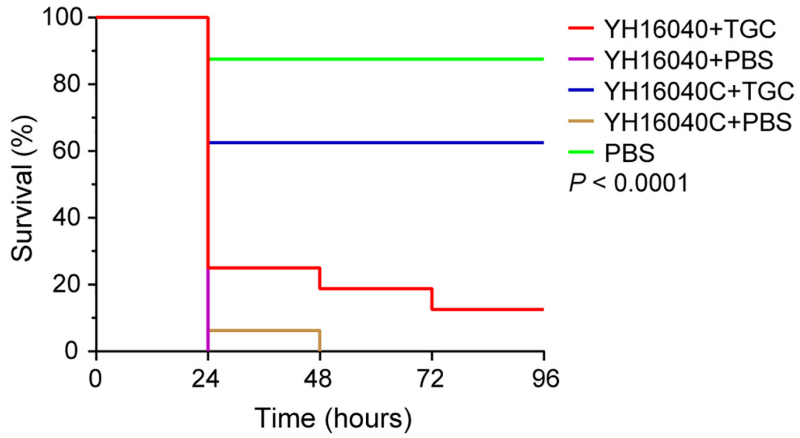

FIGURE 4
Survival curve of *G. mellonella* larvae under the treatment of tigecycline. The *P*-value is calculated by Log-rank (Mantel-Cox) test between GR31 plasmid-mediated *tet*(X3)-positive *Acinetobacter* spp. YH16040 and its plasmid-cured strain YH16040C [*tet*(X3)-negative] using GraphPad Prism version 8.3.0.

the result of plasmid-mediated ARG mining (Table 2 and Figure 1A). Recently, our study has also reported the co-occurrence of mobile *tet*(X)-mediated tigecycline resistance and bla_{NDM-1}-mediated carbapenem resistance between *Acinetobacter* species (Cui et al., 2020). With the co-transfer of multiple ARGs, the continuous application and selection pressures of tetracyclines, sulfonamides, aminoglycosides, β-lactams, and phenicols may promote the spread of *tet*(X) genes, as previously described for resistance determinants *mcr-1 and* bla_{IMP-1} (Wang Y. et al., 2020; Cheng Z. et al., 2021).

In vivo effect of GR31 plasmid-mediated *tet*(X3) gene

To explore the potential effect of GR31 plasmid-mediated *tet*(X3) gene, a plasmid-cured strain YH16040C [*tet*(X3)-negative] was obtained by serially passaging of *tet*(X3)-positive *Acinetobacter* spp. YH16040. For tigecycline, a significant decrease in MIC was detected (1 μg/mL) when compared with the parental isolate YH16040 (32 μg/mL; Table 2). MICs of *Acinetobacter* spp. YH16040C against tetracycline (8 μg/mL), eravacycline (0.06 μg/mL), omadacycline (0.125 μg/mL), florfenicol (8 μg/mL) and sulfamethoxazole-trimethoprim (20 μg/mL) also exhibited at least 16-fold decrease. The result further confirmed the elimination of GR31 plasmid pYH16040-1 (CP094542) that co-harbored resistance genes *tet*(X3), *floR* and *sul2* (Table 2 and Figure 1A).

Subsequently, the *in vivo* effect of pYH16040-1-carrying *tet*(X3) gene was evaluated using a *G. mellonella* model. 96 h later of tigecycline treatment (2 μg/g), the larval mortality rate of *Acinetobacter* spp. YH16040C significantly decreased to 37.5% while *Acinetobacter* spp. YH16040 was 87.5% ($p < 0.0001$; Figure 4). The experiment was performed in triplicate with similar results, indicating the GR31 plasmid-mediated *tet*(X3) gene compromised the clinical effectiveness of tigecycline.

Notably, the infection by *Acinetobacter* spp. YH16040 and *Acinetobacter* spp. YH16040C under the treatment of PBS resulted in a greater larval mortality rate (100%) than PBS only (12.5%) after 48 h ($p < 0.0001$), whereas no significant difference was observed between *Acinetobacter* spp. YH16040 and *Acinetobacter* spp. YH16040C ($p = 0.32$; **Figure 4**). The result suggested virulence genes outside pYH16040-1 remained to be studied. As previously reported (Jiang et al., 2021; Xu et al., 2021), *G. mellonella* models infected by plasmid-mediated *tet*(X6)-positive Enterobacteriaceae bacteria have also been constructed, and therefore *G. mellonella* was available for *in vivo* functional analyses of plasmid-mediated *tet*(X) genes.

Conclusion

Taken together, the data presented in this study highlighted the diverse distribution of *tet*(X)-carrying MDR plasmids in *Acinetobacter* species. Our results classified the *tet*(X)-positive *Acinetobacter* spp. plasmids of Rep_3 superfamily into six homology groups, including two newly assigned GR60 and GR61. To the best of our knowledge, this study first revealed a dominant GR31 plasmid mediating the horizontal transfer of tigecycline resistance gene *tet*(X) across different *Acinetobacter* species and contributed to the failure of tigecycline treatment *in vivo*. Accordingly, more efforts are needed to monitor and prevent the plasmid-mediated *tet*(X)-positive *Acinetobacter* spp. strains.

Data availability statement

The datasets presented in this study can be found in online repositories. The names of the repository/repositories and accession number(s) can be found in the article/**Supplementary material**.

Author contributions

J-LH, Y-HL, and JS designed the study. CC, P-YH, C-YC, and QH performed the experiments. CC and P-YH analyzed the data. CC wrote the draft of the manuscript. All authors reviewed, revised, and approved the final report.

Funding

This study was jointly supported by the Natural Science Foundation of Jiangsu Province of China (BK20210803), the Natural Science Foundation of Jiangsu Higher Education Institutions of China (21KJB230008), the National Natural Science Foundation of China (32172939, 31872493, 31972735), the Taishan Industry Leading Talents Project of Shandong Province (tscy20190113), the Foundation for Innovative Research Groups of the National Natural Science Foundation of China (32121004), and the Local Innovative and Research Teams Project of Guangdong Pearl River Talents Program (2019BT02N054).

Conflict of interest

The authors declare that the research was conducted in the absence of any commercial or financial relationships that could be construed as a potential conflict of interest.

Publisher's note

Supplementary material

The Supplementary Material for this article can be found online at: https://www.frontiersin.org/articles/10.3389/fmicb.2022.974432/full#supplementary-material

References

Aziz, R. K., Bartels, D., Best, A. A., DeJongh, M., Disz, T., Edwards, R. A., et al. (2008). The RAST server: Rapid annotations using subsystems technology. *BMC Genomics* 9:75. doi: 10.1186/1471-2164-9-75

Bertini, A., Poirel, L., Mugnier, P. D., Villa, L., Nordmann, P., and Carattoli, A. (2010). Characterization and PCR-based replicon typing of resistance plasmids in *Acinetobacter baumannii*. *Antimicrob. Agents Chemother.* 54, 4168–4177. doi: 10.1128/AAC.00542-10

Bortolaia, V., Kaas, R. S., Ruppe, E., Roberts, M. C., Schwarz, S., Cattoir, V., et al. (2020). ResFinder 4.0 for predictions of phenotypes from genotypes. *J. Antimicrob. Chemother.* 75, 3491–3500. doi: 10.1093/jac/dkaa345

Brovedan, M. A., Cameranesi, M. M., Limansky, A. S., Moran-Barrio, J., Marchiaro, P., and Repizo, G. D. (2020). What do we know about plasmids carried by members of the *Acinetobacter* genus? *World J. Microbiol. Biotechnol.* 36:109. doi: 10.1007/s11274-020-02890-7

Castro-Jaimes, S., Guerrero, G., Bello-Lopez, E., and Cevallos, M. A. (2022). Replication initiator proteins of *Acinetobacter baumannii* plasmids: An update note. *Plasmid* 119-120:102616. doi: 10.1016/j.plasmid.2021.102616

Chen, C., Cui, C. Y., Wu, X. T., Fang, L. X., He, Q., He, B., et al. (2021). Spread of *tet*(X5) and *tet*(X6) genes in multidrug-resistant *Acinetobacter baumannii* strains of animal origin. *Vet. Microbiol.* 253:108954. doi: 10.1016/j.vetmic.2020.108954

Chen, C., Cui, C. Y., Yu, J. J., He, Q., Wu, X. T., He, Y. Z., et al. (2020). Genetic diversity and characteristics of high-level tigecycline resistance Tet(X) in *Acinetobacter* species. *Genome Med.* 12:111. doi: 10.1186/s13073-020-00807-5

Chen, T., Liu, Y. X., and Huang, L. (2022). ImageGP: An easy-to-use data visualization web server for scientific researchers. *iMeta* 1:e5. doi: 10.1002/imt2.5

Chen, Y., Hu, D., Zhang, Q., Liao, X. P., Liu, Y. H., and Sun, J. (2017). Efflux pump overexpression contributes to tigecycline heteroresistance in *Salmonella enterica* serovar typhimurium. *Front. Cell Infect. Microbiol.* 7:37. doi: 10.3389/fcimb.2017.00037

Cheng, Y., Chen, Y., Liu, Y., Song, J., Chen, Y., Shan, T., et al. (2021). Detection of a new *tet*(X6)-encoding plasmid in *Acinetobacter towneri*. *J. Glob. Antimicrob. Resist.* 25, 132–136. doi: 10.1016/j.jgar.2021.03.004

Cheng, Z., Bethel, C. R., Thomas, P. W., Shurina, B. A., Alao, J. P., Thomas, C. A., et al. (2021). Carbapenem use is driving the evolution of imipenemase 1 variants. *Antimicrob. Agents Chemother.* 65:e01714-20. doi: 10.1128/AAC.01714-20

Clinical and Laboratory Standards Institute [CLSI] (2018). *Performance Standards for Antimicrobial Susceptibility Testing: CLSI supplement M100*, 28th Edn. Wayne, PA: CLSI.

Cui, C.-Y., Chen, C., Liu, B.-T., He, Q., Wu, X.-T., Sun, R.-Y., et al. (2020). Co-occurrence of plasmid-mediated tigecycline and carbapenem resistance in *Acinetobacter* spp. from waterfowls and their neighboring environment. *Antimicrob. Agents Chemother.* 64:e02502-19. doi: 10.1128/aac.02502-19

Dong, C. L., Li, L. X., Cui, Z. H., Chen, S. W., Xiong, Y. Q., Lu, J. Q., et al. (2017). Synergistic effect of pleuromutilins with other antimicrobial agents against *Staphylococcus aureus In Vitro* and in an experimental *Galleria mellonella* model. *Front. Pharmacol.* 8:553. doi: 10.3389/fphar.2017.00553

He, T., Li, R., Wei, R., Liu, D., Bai, L., Zhang, L., et al. (2020). Characterization of *Acinetobacter indicus* co-harbouring *tet*(X3) and bla_{NDM-1} of dairy cow origin. *J. Antimicrob. Chemother.* 75, 2693–2696. doi: 10.1093/jac/dkaa182

He, T., Wang, R., Liu, D., Walsh, T. R., Zhang, R., Lv, Y., et al. (2019). Emergence of plasmid-mediated high-level tigecycline resistance genes in animals and humans. *Nat. Microbiol.* 4, 1450–1456. doi: 10.1038/s41564-019-0445-2

Jiang, L., Cai, W., Tang, F., Wang, Z., and Liu, Y. (2021). Characterization of fitness cost caused by tigecycline-resistance gene *tet*(X6) in different host bacteria. *Antibiotics* 10:1172. doi: 10.3390/antibiotics10101172

Kumar, S., Stecher, G., Li, M., Knyaz, C., and Tamura, K. (2018). MEGA X: Molecular evolutionary genetics analysis across computing platforms. *Mol. Biol. Evol.* 35, 1547–1549. doi: 10.1093/molbev/msy096

Li, R., Peng, K., Xiao, X., Wang, Y., and Wang, Z. (2021). Characterization of novel IS*Aba1*-bounded *tet*(X15)-bearing composite transposon Tn*6866* in *Acinetobacter variabilis*. *J. Antimicrob. Chemother.* 76, 2481–2483. doi: 10.1093/jac/dkab182

Li, Y., Qiu, Y., Fang, C., Dai, X., and Zhang, L. (2022). Coexistence of bla_{OXA-58} and bla_{NDM-1} on a novel plasmid of GR59 from an *Acinetobacter towneri* isolate. *Antimicrob. Agents Chemother.* 66:e0020622. doi: 10.1128/aac.00206-22

Liu, D., Wang, T., Shao, D., Song, H., Zhai, W., Sun, C., et al. (2022). Structural diversity of the IS*CR2*-mediated rolling-cycle transferable unit carrying *tet*(X4). *Sci. Total Environ.* 826:154010. doi: 10.1016/j.scitotenv.2022.154010

Liu, D., Zhai, W., Song, H., Fu, Y., Schwarz, S., He, T., et al. (2020). Identification of the novel tigecycline resistance gene *tet*(X6) and its variants in *Myroides*, *Acinetobacter* and *Proteus* of food animal origin. *J. Antimicrob. Chemother.* 75, 1428–1431. doi: 10.1093/jac/dkaa037

Lu, S., Wang, J., Chitsaz, F., Derbyshire, M. K., Geer, R. C., Gonzales, N. R., et al. (2020). CDD/SPARCLE: The conserved domain database in 2020. *Nucleic Acids Res.* 48, D265–D268. doi: 10.1093/nar/gkz991

Mindlin, S., Beletsky, A., Rakitin, A., Mardanov, A., and Petrova, M. (2020). *Acinetobacter* plasmids: Diversity and development of classification strategies. *Front. Microbiol.* 11:588410. doi: 10.3389/fmicb.2020.588410

Sader, H. S., Castanheira, M., Arends, S. J. R., Goossens, H., and Flamm, R. K. (2019). Geographical and temporal variation in the frequency and antimicrobial susceptibility of bacteria isolated from patients hospitalized with bacterial pneumonia: Results from 20 years of the SENTRY antimicrobial surveillance program (1997–2016). *J. Antimicrob. Chemother.* 74, 1595–1606. doi: 10.1093/jac/dkz074

Salto, I. P., Torres Tejerizo, G., Wibberg, D., Puhler, A., Schluter, A., and Pistorio, M. (2018). Comparative genomic analysis of *Acinetobacter* spp. plasmids originating from clinical settings and environmental habitats. *Sci. Rep.* 8:7783. doi: 10.1038/s41598-018-26180-3

Silva, L., Mourao, J., Grosso, F., and Peixe, L. (2018). Uncommon carbapenemase-encoding plasmids in the clinically emergent *Acinetobacter pittii*. *J. Antimicrob. Chemother.* 73, 52–56. doi: 10.1093/jac/dkx364

Subramanian, B., Gao, S., Lercher, M. J., Hu, S., and Chen, W. H. (2019). Evolview v3: A webserver for visualization, annotation, and management of phylogenetic trees. *Nucleic Acids Res.* 47, W270–W275. doi: 10.1093/nar/gkz357

Sullivan, M. J., Petty, N. K., and Beatson, S. A. (2011). Easyfig: A genome comparison visualizer. *Bioinformatics* 27, 1009–1010. doi: 10.1093/bioinformatics/btr039

Sun, J., Chen, C., Cui, C. Y., Zhang, Y., Liu, X., Cui, Z. H., et al. (2019). Plasmid-encoded *tet*(X) genes that confer high-level tigecycline resistance in *Escherichia coli*. *Nat. Microbiol.* 4, 1457–1464. doi: 10.1038/s41564-019-0496-4

Versalovic, J., Koeuth, T., and Lupski, R. (1991). Distribution of repetitive DNA sequences in eubacteria and application to finerpriting of bacterial genomes. *Nucleic Acids Res.* 19, 6823–6831. doi: 10.1093/nar/19.24.6823

Walker, B. J., Abeel, T., Shea, T., Priest, M., Abouelliel, A., Sakthikumar, S., et al. (2014). Pilon: An integrated tool for comprehensive microbial variant detection and genome assembly improvement. *PLoS One* 9:e112963. doi: 10.1371/journal.pone.0112963

Wang, B., and Sun, D. (2015). Detection of NDM-1 carbapenemase-producing *Acinetobacter calcoaceticus* and *Acinetobacter junii* in environmental samples from livestock farms. *J. Antimicrob. Chemother.* 70, 611–613. doi: 10.1093/jac/dku405

Wang, J., Wang, Y., Wu, H., Wang, Z. Y., Shen, P. C., Tian, Y. Q., et al. (2020). Coexistence of bla_{OXA-58} and *tet*(X) on a Novel Plasmid in *Acinetobacter* sp. From Pig in Shanghai, China. *Front. Microbiol.* 11:578020. doi: 10.3389/fmicb.2020.578020

Wang, L., Liu, D., Lv, Y., Cui, L., Li, Y., Li, T., et al. (2019). Novel plasmid-mediated *tet*(X5) gene conferring resistance to tigecycline, eravacycline, and omadacycline in a clinical *Acinetobacter baumannii* isolate. *Antimicrob. Agents Chemother.* 64:e01326-19. doi: 10.1128/AAC.01326-19

Wang, Y., Xu, C., Zhang, R., Chen, Y., Shen, Y., Hu, F., et al. (2020). Changes in colistin resistance and *mcr-1* abundance in *Escherichia coli* of animal and human origins following the ban of colistin-positive additives in China: An epidemiological comparative study. *Lancet Infect. Dis.* 20, 1161–1171. doi: 10.1016/S1473-3099(20)30149-3

Wick, R. R., Judd, L. M., Gorrie, C. L., and Holt, K. E. (2017). Unicycler: Resolving bacterial genome assemblies from short and long sequencing reads. *PLoS Comput. Biol.* 13:e1005595. doi: 10.1371/journal.pcbi.1005595

Wong, D., Nielsen, T. B., Bonomo, R. A., Pantapalangkoor, P., Luna, B., and Spellberg, B. (2017). Clinical and pathophysiological overview of *Acinetobacter* infections: A century of challenges. *Clin. Microbiol. Rev.* 30, 409–447. doi: 10.1128/CMR.00058-16

Xu, Y., Liu, L., Zhang, H., and Feng, Y. (2021). Co-production of Tet(X) and MCR-1, two resistance enzymes by a single plasmid. *Environ. Microbiol.* 23, 7445–7464. doi: 10.1111/1462-2920.15425

Zheng, X. R., Zhu, J. H., Zhang, J., Cai, P., Sun, Y. H., Chang, M. X., et al. (2020). A novel plasmid-borne *tet*(X6) variant co-existing with bla_{NDM-1} and bla_{OXA-58} in a chicken *Acinetobacter baumannii* isolate. *J. Antimicrob. Chemother.* 75, 3397–3399. doi: 10.1093/jac/dkaa342

Zhu, W., Clark, N., and Patel, J. B. (2013). pSK41-like plasmid is necessary for Inc18-like *vanA* plasmid transfer from *Enterococcus faecalis* to *Staphylococcus aureus in vitro*. *Antimicrob. Agents Chemother.* 57, 212–219. doi: 10.1128/AAC.01587-12

frontiers | Frontiers in Microbiology

TYPE Original Research
PUBLISHED 19 October 2022
DOI 10.3389/fmicb.2022.1010387

OPEN ACCESS

EDITED BY
Eun-Jeong Yoon,
Korea National Institute of Health,
South Korea

REVIEWED BY
Hui Li,
Beijing Center for Disease Prevention and Control (Beijing CDC), China
Chaoyue Cui,
Wenzhou Medical University,
China

*CORRESPONDENCE
Zhiqiang Wang
zqwang@yzu.edu.cn

†These authors have contributed equally to this work

SPECIALTY SECTION
This article was submitted to Antimicrobials, Resistance and Chemotherapy, a section of the journal Frontiers in Microbiology

RECEIVED 03 August 2022
ACCEPTED 26 September 2022
PUBLISHED 19 October 2022

CITATION
Xiao X, Liu Z, Chen X, Peng K, Li R, Liu Y and Wang Z (2022) Persistence of plasmid and *tet*(X4) in an *Escherichia coli* isolate coharboring bla_{NDM-5} and *mcr-1* after acquiring an IncFII *tet*(X4)-positive plasmid. *Front. Microbiol.* 13:1010387. doi: 10.3389/fmicb.2022.1010387

Persistence of plasmid and *tet*(X4) in an *Escherichia coli* isolate coharboring bla_{NDM-5} and *mcr-1* after acquiring an IncFII *tet*(X4)-positive plasmid

Xia Xiao[1,2†], Ziyi Liu[1,2†], Xiaojun Chen[1,2], Kai Peng[1,2], Ruichao Li[1,2,3], Yuan Liu[1,2,3] and Zhiqiang Wang[1,2*]

[1]College of Veterinary Medicine, Yangzhou University, Yangzhou, Jiangsu, China, [2]Jiangsu Co-Innovation Center for Prevention and Control of Important Animal Infectious Diseases and Zoonoses, Yangzhou, Jiangsu, China, [3]Institute of Comparative Medicine, Yangzhou University, Yangzhou, Jiangsu, China

The prevalence of plasmid-mediated tigecycline resistance gene *tet*(X4) is presenting an increasing trend. Once *tet*(X4)-bearing plasmids are captured by multidrug-resistant bacteria, such as bla_{NDM} and *mcr*-coharboring bacteria, it will promote bacteria to develop an ultra-broad resistance spectrum, limiting clinical treatment options. However, little is known about the destiny of such bacteria or how they will evolve in the future. Herein, we constructed a multidrug-resistant bacteria coharboring *tet*(X4), bla_{NDM-5}, and *mcr-1* by introducing a *tet*(X4)-bearing plasmid into a bla_{NDM-5} and *mcr-1* positive *E. coli* strain. Subsequently, the stability of *tet*(X4) and the plasmid was measured after being evolved under tigecycline or antibiotic-free circumstance. Interestingly, we observed both *tet*(X4)-bearing plasmids in tigecycline treated strains and non-tigecycline treated strains were stable, which might be jointly affected by the increased conjugation frequency and the structural alterations of the *tet*(X4)-positive plasmid. However, the stability of *tet*(X4) gene showed different scenarios in the two types of evolved strains. The *tet*(X4) gene in non-tigecycline treated strains was stable whereas the *tet*(X4) gene was discarded rapidly in tigecycline treated strains. Accordingly, we found the expression levels of *tet*(X4) gene in tigecycline-treated strains were several times higher than in non-tigecycline treated strains and ancestral strains, which might in turn impose a stronger burden on the host bacteria. SNPs analysis revealed that a myriad of mutations occurred in genes involving in conjugation transfer, and the missense mutation of *marR* gene in chromosome of tigecycline treated strains might account for the completely different stability of *tet*(X4)-bearing plasmid and *tet*(X4) gene. Collectively, these findings shed a light on the possibility of the emergence of multidrug resistant bacteria due to the transmission of *tet*(X4)-bearing plasmid, and highlighted that the antibiotic residues may be critical to the development of such bacteria.

KEYWORDS

bla_{NDM-5}, *mcr-1*, *tet*(X4)-bearing plasmid, plasmid stability, *tet*(X4) stability

Introduction

Currently, the emergence of plasmid-mediated tigecycline high-level resistance gene *tet*(X) and its variants complicates the antimicrobial resistance (AMR) issue, which means that the use of several critical antibiotics, such as carbapenems, polymyxins, and tigecycline in clinical settings, has been restricted by their corresponding epidemic AMR genes. Generally, AMR genes conferring resistance to carbapenems, polymyxins, and tigecycline simultaneously present in a single pathogen is unusual. Now, however, the situation has begun to deteriorate. The isolate coharboring *tet*(X4) and bla_{NDM} has been described in *E. coli* (Sun et al., 2021), *Acinetobacter* spp. (Cui et al., 2020), *Proteus cibarius* (Li Y. et al., 2020), *K. aerogenes* (Hirabayashi et al., 2021), and *E. cloacae* (Li et al., 2022). Furthermore, the coexistence of *tet*(X4), *mcr-1*, and bla_{NDM-5} in a single *E. coli* isolate has been identified as well (Lu et al., 2022), highlighting these bacteria are constantly evolving. Nevertheless, there is a lack of relevant studies that systematically evaluate the possibility, evolutionary trend, and destiny of bla_{NDM}, *mcr-1*, and *tet*(X4) in a single strain.

Plasmids play an indispensable role in spreading AMR genes and driving its rapid development (Rozwandowicz et al., 2018). Despite plasmids confer benefits to host, they also pose an extra burden (fitness cost) on the host (San Millan and MacLean, 2017). Fitness cost is one of the most important factors that affects plasmid persistence (Carroll and Wong, 2018). However, plasmids or host could alleviate the fitness cost by compensatory evolution under different circumstances, thereby improving the stability of plasmids. For example, large multidrug resistance plasmids could improve their stability through deleting the expensive region to offset fitness cost (Porse et al., 2016; Dorado-Morales et al., 2021). Single nucleotide substitution in the IncP-1 plasmid replication gene *trfA* increased plasmid stability and enhanced adaptation to new hosts (Sota et al., 2010). Mutations in the *uvrD* gene encoding helicase and β-subunit *rpoB* gene encoding RNA polymerase reduced host-plasmid replication protein interactions, which promoted the plasmid stability (Loftie-Eaton et al., 2017). Moreover, many studies demonstrated that the plasmid-host coevolution enhanced their mutual adaption, resulting in the plasmid persistence (Millan et al., 2014; Yano et al., 2016; Hall James et al., 2017). Given that *tet*(X4) gene is a newly identified AMR gene in recent years, and its transmission is predominantly mediated by plasmids. Hence, it is of great significance to investigate the fitness cost and compensatory evolution induced by *tet*(X4)-positive plasmids in host bacteria. Our previous study revealed that the *tet*(X4)-harboring IncFII plasmid showed the lowest fitness cost in TOP10 compared with other type of plasmids carrying *tet*(X4) (Tang et al., 2022). Besides, *E. coli* N31 carrying bla_{NDM-5} and *mcr-1* was isolated from swine feces in our early research project (data not published). Based on this background, we transferred the conjugative *tet*(X4)-positive IncFII plasmid pF65-*tet*(X4) into *E. coli* N31 to evaluate the possibility and the evolution pattern of the superbug carrying these three important AMR genes, and further verified whether positive selection would favor the stability of the plasmid and *tet*(X4) gene.

Materials and methods

Bacterial strains, plasmids, and media

E. coli N31 and *E. coli* F65 used in this study were isolated from pig farm and porcine slaughterhouse, respectively. The *tet*(X4)-positive IncFII plasmid pF65-*tet*(X4) (The original article was labeled as pRF65-1_113k_*tet*X) carried by F65 was regarded as the focal plasmid (Li R. et al., 2020), whereas *E. coli* N31 with *mcr-1* on chromosome, bla_{NDM-5} on IncX3 plasmid served as the recipient strain. The transconjugant CN31-pF65-*tet*(X4) was obtained through conjugation assay. All strains and plasmids used in this study were listed in Table 1. All strains were grown in the LB medium at 37°C.

Evolution experiment

Serial passage was conducted using the transconjugant CN31-pF65-*tet*(X4). Briefly, the ancestral strain was propagated in 5 ml LB broth with or without tigecycline (2 mg/l) at 37°C. Every 12 h, 5 μl of each culture was transferred into 5 ml fresh corresponding LB broth. Each passaging was defined as one generation evolution. The evolution experiment lasted 50 days to yield 100 generations. At the end of evolution, the populations passaged with and without tigecycline were plated on Maconkey agar medium containing tigecycline and meropenem (2 mg/l) to randomly select five evolved clones containing *tet*(X4) gene. These selected strains were named as CN31-pF65-*tet*(X4)-E100$^{+T\text{-}1/-2/-3/-4/-5}$ and CN31-pF65-*tet*(X4)-E100$^{-T\text{-}1/-2/-3/-4/-5}$, respectively.

Plasmid and *tet*(X4) loss frequency assays

To investigate the stability of the plasmid and *tet*(X4) gene, the selected evolved strains (CN31-pF65-*tet*(X4)-E100$^{+T\text{-}1/-2/-3/-4/-5}$, CN31-pF65-*tet*(X4)-E100$^{-T\text{-}1/-2/-3/-4/-5}$) were further passaged in antibiotic-free LB broth using the same strategy described in the evolution experiment. After 60 generations, the cultures were diluted and streaked on antibiotic-free LB plates and incubated for 12 h at 37°C. The strains containing plasmid- or *tet*(X4)-containing were determined by randomly selecting 50 single colonies to perform PCR with specific primers. The primers for IncFII were forward (FV)5′-GGCGAAATCAAAACGGGAGG and reverse (RV) 5′-CGATGCATGTGATGATGGGC. The primers for *tet*(X4) were forward (FV)5′-TGAACCT GGTAAGAAGAAGTG and reverse (RV) 5′-CCGACA ATATCAAGGCATCCA. Plasmid and *tet*(X4) loss rates were determined by dividing the clones without a specific primer band by the 50 clones.

TABLE 1 Basic information of bacteria and plasmids used in this study.

Name	Description	Source/Reference
Strains		
E. coli N31	As a recipient strain, in which *mcr-1* located on chromosome, whereas bla_{NDM-5} located on IncX3 plasmid. The remaining plasmids replicon type were IncFIB (K), IncFIB (AP001918), ColE10, and IncFIA (HI1).	Pig farm
E. coli F65	As a donor strain, in which *tet*(X4) located on IncFII plasmid. The remaining plasmid replicon type were IncFIB (K), IncFIA (HI1), and IncX1.	Porcine slaughterhouse (Li R. et al., 2020)
CN31-pF65-*tet*(X4)	N31 corresponding transconjugant carrying pF65-*tet*(X4).	In this study
CN31-F65-*tet*(X4)-E100^{-T}-1/−2/−3/−4/−5	Five evolved clones selected from 100th generation populations evolved without tigecycline.	In this study
CN31-F65-*tet*(X4)-E100^{+T}-1/−2/−3/−4/−5	Five evolved clones selected from 100th generation populations evolved with tigecycline (2 mg/l).	In this study
Plasmids		
pCN31-F65-*tet*(X4)	The ancestral plasmid from F65.	In this study
pCN31-F65-*tet*(X4)-E100^{-T} − 1/−2/−3/−4/−5	Five plasmids from the evolved strains without tigecycline.	In this study
pCN31-F65-*tet*(X4)-E100^{+T} − 1/−2/−3/−4/−5	Five plasmids from the evolved strains with tigecycline.	In this study

MIC determination

The MICs of tigecycline against the ancestral strain (CN31-pF65-*tet*(X4)) and evolved strains (CN31-pF65-*tet*(X4)-E100$^{+T\text{-}1/-2/-3/-4/-5}$, CN31-pF65-*tet*(X4)-E100$^{-T\text{-}1/-2/-3/-4/-5}$) were determined using the broth microdilution method according to the Clinical and Laboratory Standards Institute (CLSI) guidelines (Zatyka et al., 1997) and interpreted following the criteria of European Committee on Antimicrobial Susceptibility Testing (Version 11.0).[1] *E. coli* ATCC25922 was used as the quality control strain.

Time killing curve

The ancestral strain (CN31-pF65-*tet*(X4)) and evolved strains (CN31-pF65-*tet*(X4)-E100$^{+T\text{-}1/-2/-3/-4/-5}$ and CN31-pF65-*tet*(X4)-E100$^{-T\text{-}1/-2/-3/-4/-5}$) were added with tigecycline at the concentration of 0, 4, 8, 16, 24, 32 mg/l and cultured at 37°C with shaking at 200 rpm. An aliquot of 100 μl mixtures were taken out after being cultured for 4, 12, 24 h, and then were tenfold serially diluted and plated on LB plates to calculate the colony-forming units (CFUs) after incubation at 37°C for 24 h.

Plasmid conjugation assay

To investigate the transferability of ancestral and evolved strains, conjugation assay was performed as described previously (Li Y. et al., 2020). Briefly, the ancestral strain (CN31-pF65-*tet*(X4)) and evolved strains (CN31-pF65-*tet*(X4)-E100$^{+T\text{-}1/-2/-3/-4/-5}$ and CN31-pF65-*tet*(X4)-E100$^{-T\text{-}1/-2/-3/-4/-5}$) were served as the donor strains and *E. coli* C600 (resistant to rifampin) as the recipient strains. Cultures of donor and recipient strain with a density of 0.5 McFarland were mixed at a ratio of 1:4, respectively. Subsequently, 0.1 ml of the mixed cultures was applied onto a sterile filtration membrane. The membrane was cultured in LB agar plates at 37°C for 12 h. Following the bacteria on the membrane was collected and diluted with sterile saline, and then plated on the LB plates containing 300 mg/l rifampin or 2 mg/l tigecycline and 300 mg/l rifampin. The number of transconjugants carrying *tet*(X4) were calculated after incubation at 37°C for 24 h. The presence of *tet*(X4) in transconjugants was confirmed by PCR. Conjugation frequencies were calculated by the number of transconjugants per recipient cell.

Gene expression analysis

The RNA isolater Total RNA extraction Reagent (Vazyme, Nanjing, China) was used to extract total RNA of the ancestral strain (CN31-pF65-*tet*(X4)) and evolved strains (CN31-pF65-*tet*(X4)-E100$^{+T\text{-}1/-2/-3/-4/-5}$ and CN31-pF65-*tet*(X4)-E100$^{-T\text{-}1/-2/-3/-4/-5}$). The extracted RNA was reverse transcribed into cDNA using a HiScript III RT Supermix for qPCR (+g DNA wiper) (Vazyme. Nanjing, China). Real-time quantitative PCR (qPCR) was used to quantify gene expression. The expression levels of *tet*(X4) gene, conjugative transfer regulatory genes *traJ*, *traY*, *traM*, and *traI*, conjugative transfer protein genes *traD*, *trbB*, *trbI*, and *virD2*, conjugative pilus assembly genes *traB*, *traC*, *traG*, *traE*, *traW*, *traP*, *traH*, *traV*, and *traX* were determined using ChamQ SYBR color qPCR master Mix (Vazyme, Nanjing, China) in triplicate. 16S rRNA was used as the internal control. Primer sequences are listed in Supplementary Table S1. The qPCR primers

1 http://eucast.org/clinical_breakpoints/

were synthesized by Tsingke Biotech Co., Ltd. (Nanjing, China), and qPCR was performed using a LineGene 9600 Plus real time PCR detection system (Bioer, Hangzhou, China).

DNA sequencing and bioinformatics analysis

Genomic DNA of the ancestral strain (CN31-pF65-*tet*(X4)) and evolved strains (CN31-pF65-*tet*(X4)-E100$^{+T\text{-}1/-4/-5}$ and CN31-pF65-*tet*(X4)-E100$^{-T\text{-}1/-2/-3}$) were extracted using the TIANamp bacterial DNA kit (TianGen, Beijing, China) and subjected to short-read sequencing (2 × 150 bp) with the Illumina HiSeq 2500 platform. Short-read Illumina raw sequences of ancestral and evolved strains were separately assembled using SPAdes (Bankevich et al., 2012), and contigs less than 500 bp were discarded. SNP analysis was performed using Snippy (4.0.2) against the genome sequences of the ancestral strain.[2]

The plasmids of the ancestral strain and selected evolved strains CN31-pF65-*tet*(X4)-E100$^{+T\text{-}1}$ and CN31-pF65-*tet*(X4)-E100$^{-T\text{-}2}$ were extracted using Qiagen Plasmid Midi-Kit (Qiagen, Hilden, Germany). Subsequently, the plasmids were sequenced with the Oxford Nanopore Technologies MinION long-read platform. The Nanopore long-read MinION sequences of plasmids were subjected to *de novo* assembly with the Flye tool (Kolmogorov et al., 2019). Easyfig was used to describe the structural diversity of the ancestral and the evolved plasmids (Sullivan et al., 2011).

Statistical analyses

GraphPad Prism 8.3.2 was used for data analyses. Data are expressed as mean ± standard deviation. Significant differences were assessed using a two-way analysis and *t* test, with $p < 0.05$ considered as statistically significant.

Results

The IncFII *tet*(X4)-positive plasmid imposes fitness cost in *Escherichia coli* N31

To investigate the fitness cost of the IncFII *tet*(X4)-positive plasmid in wild-type multidrug-resistant *E. coli* N31 carrying $bla_{NDM\text{-}5}$ and *mcr-1*, the plasmid was transferred into strain N31 by conjugation. The transconjugant was resistance to meropenem and colistin with the MICs value of 64 and 2 mg/l, respectively. Pairwise competitions results showed that the relative fitness of transconjugant was less than 1, suggesting the introduction of the plasmid weakened the competitiveness of N31 (Figure 1A). In terms of bacterial growth, there was no significant difference of the bacteria growth between the transconjugant and N31, yet the generation time of N31 was shorter than that of the transconjugant (Figure 1B). These findings indicated that the *tet*(X4)-positive plasmid incurred the fitness cost in N31. To get further insights into the stability of the IncFII *tet*(X4)-positive plasmid in N31, the transconjugant was passaged for 100 generations with or without tigecycline. We randomly selected five *tet*(X4)-positive single clones from the 100th generation population passaged with and without tigecycline, hereafter named CN31-pF65-*tet*(X4)-100$^{+T\text{-}1/-2/-3/-4/-5}$ and CN31-pF65-*tet*(X4)-100$^{-T\text{-}1/-2/-3/-4/-5}$, respectively for further explorations.

Plasmid and *tet*(X4) gene stability of evolved strains in the presence or absence of tigecycline

The evolved strains in the presence or absence of tigecycline were subjected to serial passage in antibiotic-free LB broth for 30 days. PCR targeting the plasmids and *tet*(X4) genes revealed that both the plasmid and *tet*(X4) gene in CN31-pF65-*tet*(X4)-100^{-T} were stable (the retention rate for the plasmid was 100, 75, 100, 90, and 100%, and *tet*(X4) gene was 77, 75, 95, 93, and 85% in CN31-pF65- *tet*(X4)-100$^{-T\text{-}1/-2/-3/-4/-5}$, respectively), while the plasmid in partial CN31-pF65-*tet*(X4)-100^{+T} (3/5) was stable but the *tet*(X4) gene was readily lost and independent of the plasmid (the retention rate for the plasmid was 96, 56, 0, 98, and 88%, and *tet*(X4) gene was 0, 0, 0, 0, and 10% in CN31-pF65- *tet*(X4)-100$^{+T\text{-}1/-2/-3/-4/-5}$, respectively: Figure 2). Notably, we did not observe the loss of native plasmids in N31 during passaging, indicating that these plasmids and host bacteria have perfectly adapted to each other.

The underlying mechanisms resulting in the low retention rate of *tet*(X4) in strains evolved with tigecycline

In order to evaluate the tigecycline resistance levels between the two types of evolved strains, we performed antimicrobial susceptibility testing for tigecycline. The MIC value of tigecycline was 16 μg/ml for ancestral strains (5/5), 8 μg/ml for CN31-pF65-*tet*(X4)-100^{-T} (4/5), and 32 μg/ml for CN31-pF65-*tet*(X4)-100^{+T} (5/5) (Figure 3A). Additionally, the killing curve of tigecycline demonstrated that CN31-pF65-*tet*(X4)-100^{-T} was more susceptible to tigecycline with a 4–$\log_{10}$ reduction at tigecycline concentration of 16 μg/ml while tigecycline only exhibit a bacteriostatic effect even at concentration of 32 μg/ml against CN31-pF65-*tet*(X4)-100^{+T} (Figures 3B–D). These results indicated that the instability of *tet*(X4) in evolved strains under tigecycline pressure may attribute to its high expression level. To verify the hypothesis, we measured the mRNA expression of *tet*(X4). The *tet*(X4) expression levels were 20-fold higher in CN31-pF65-*tet*(X4)-100^{+T} compared to the ancestral strain, yet the *tet*(X4) expression was significantly suppressed in

2 http://github.com/tseemann/snippy

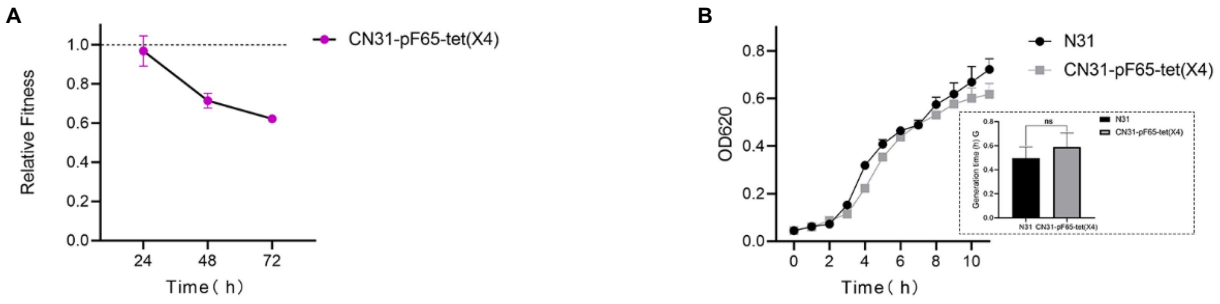

FIGURE 1
tet(X4)-positive plasmid imposes fitness cost on *E. coli* N31. **(A)** Relative fitness of *tet*(X4)-positive plasmid-carrying strains versus isogenic plasmid-free strains *in vitro*. **(B)** Comparison of growth curve and generation time (lower right corner) between *tet*(X4)-positive plasmid-carrying and plasmid-free strains.

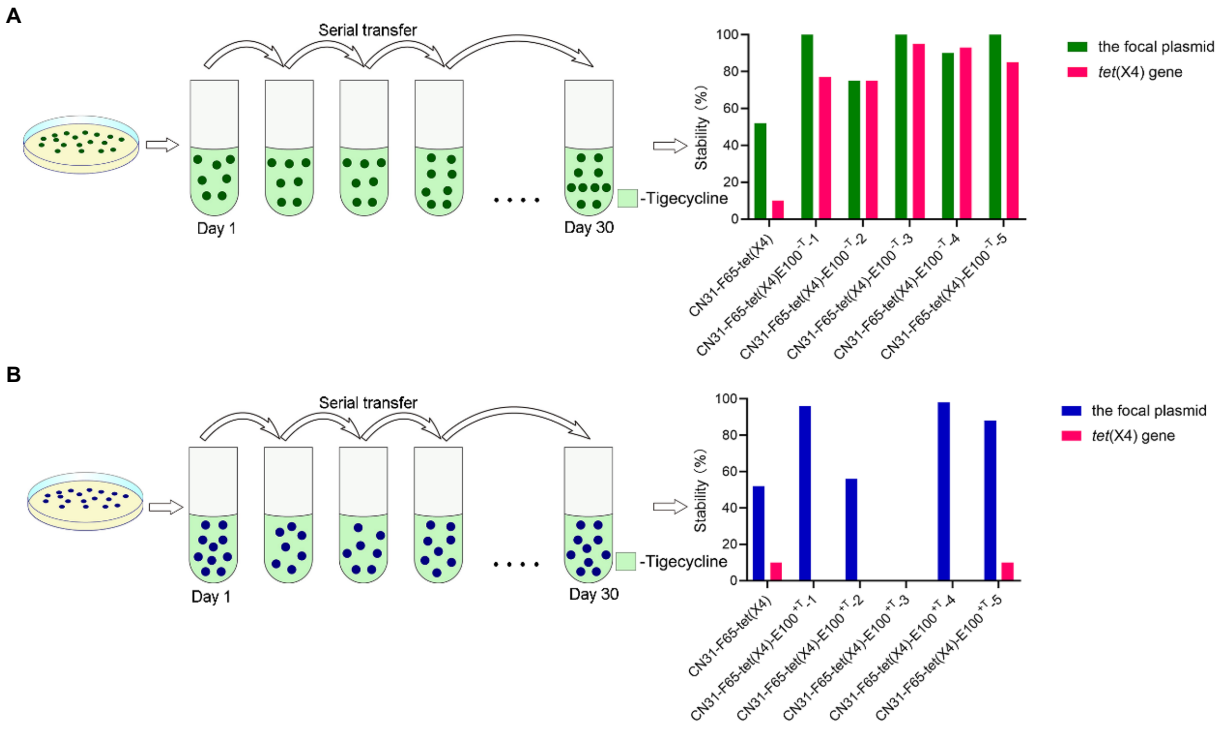

FIGURE 2
Stability of the focal plasmid and *tet*(X4) gene. **(A)** Stability of the focal plasmid and *tet*(X4) gene in five selected strains evolved in antibiotic-free broth and the ancestral strain at the 30th day. **(B)** Stability of the focal plasmid and *tet*(X4) gene in five selected strains evolved in tigecycline containing broth and the ancestral strain at the 30th day.

CN31-pF65-*tet*(X4)-100^{-T} (Figure 3E), suggesting the evolution under the tigecycline pressure would improve the expression of *tet*(X4) gene which in turn enhanced the resistance level to tigecycline. Accordingly, the high expression of *tet*(X4) gene supposed to impose high burden on the cell and led to low retention rate of *tet*(X4). However, the scenario was totally different in the strain evolved without tigecycline.

Changes in conjugation frequency of the focal plasmid during evolution

It was reported that the stability of plasmids could be improved through high conjugation rate (Carroll and Wong, 2018). Thus, the conjugation frequencies of evolved strains were examined to gain insight into plasmid evolution. Interestingly, the conjugation

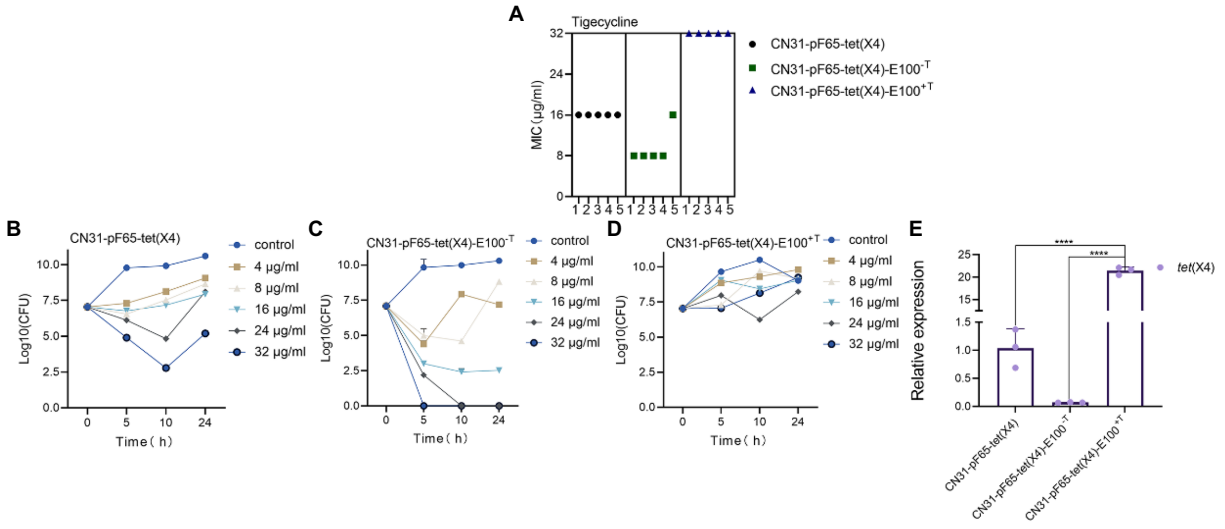

FIGURE 3
Evolved strains with different resistance levels to tigecycline under selective and non-selective pressure. **(A)** Comparison of MIC of tigecycline between ancestral and evolved strains. **(B–D)** Time-kill curve of tigecycline for the ancestral strain **(B)**, evolved strains without tigecycline **(C)**, and evolved strains with tigecycline **(D)**. **(E)** Comparison of the expression levels of *tet*(X4) gene between ancestral and evolved strains.

rate of *tet*(X4)-positive plasmid increased significantly in both tigecycline and non-tigecycline evolved strains (Figure 4A), as the conjugation frequency of the plasmid increased from $2\times10^{-3}\pm0.001914$ (average in the ancestral strains) to $3.93\times10^{-2}\pm0.032495$ (average in the evolved strains without tigecycline) and $9.13\times10^{-2}\pm0.081851$ (average in the evolved strains with tigecycline). Additionally, the conjugative transfer regulatory genes *traJ*, *traY*, *traM*, and *traI* were upregulated in both evolved strains, promoting transcription of downstream genes encoding conjugative-related genes such as pilus assembly genes, T4SS secretion system genes, and others (Figures 4B–D).

Deletion of multidrug resistance regions promotes plasmid stability

To further analyze the structural basis responsible for the enhancement of plasmid stability, we sequenced the evolved plasmid pF65-*tet*(X4)-$100^{-T\text{-}2}$ without tigecycline and the evolved plasmid pF65-*tet*(X4)-$100^{+T\text{-}1}$ with tigecycline. Compared with the ancestral plasmid, a consistent segment of approximately 22 kb was discarded in the two evolved plasmids, and no obvious structural differences were found between them, suggesting they experienced the same evolutionary trajectory, despite evolved in different circumstances. The deleted region contained two fragments, one of which carried *floR* and *erm*(42), whose loss was mediated by homologous recombination of IS*CR2*, whereas the deletion of the other fragment harboring *qnrS1* and $bla_{LAP\text{-}2}$ may be attributed to the IS*26* activity (Figure 5).

In order to verify the stability of structural reorganized plasmids in other strains, we transformed the ancestral and evolved plasmids into the engineering strain TOP10. As predicted, the stability of evolved plasmids was significantly improved, which is much higher than that of the ancestral plasmid in TOP10. Moreover, the retention rates of *tet*(X4) gene were also improved in evolved plasmids (Supplementary Figure S1A), suggesting the stability of *tet*(X4) may also be influenced by genetic characteristics of the host bacteria. Furthermore, the conjugation frequencies of the evolved plasmid were increased in different extent compared to the ancestral plasmids in TOP10 (Supplementary Figure S1B). These results illustrated that such structural alterations may influence on the horizontal transfer and stability of the plasmid.

SNP analysis revealed the mutations of chromosome and plasmid may co-drive the evolutionary process

The accumulations of genomic mutations were powerful evidences to reveal the mechanism of bacterial evolution, hence we sequenced the whole-genomes of the ancestral strain, three evolved bacteria in the absence of tigecycline, and three evolved bacteria in the presence of tigecycline. All SNPs occurring in coding sequences were listed in Supplementary Table S2. Strikingly, the single nucleotide polymorphisms (SNPs) in the plasmid were found in genes involving in the conjugative transfer and antibiotic resistance. Mutations in plasmid *tra* genes were observed, which are conjugative transfer-related genes that play an important role in conjugation transfer by encoding transfer proteins, transfer regulatory, and transfer surface exclusion protein genes. Other SNPs on the plasmid included the *adeQ* gene, which encodes adenine permease, and *floR* gene, conferring florfenicol resistance (Figure 6A). For the chromosome, a missense mutation of *marR* which encoded a multiple antibiotic

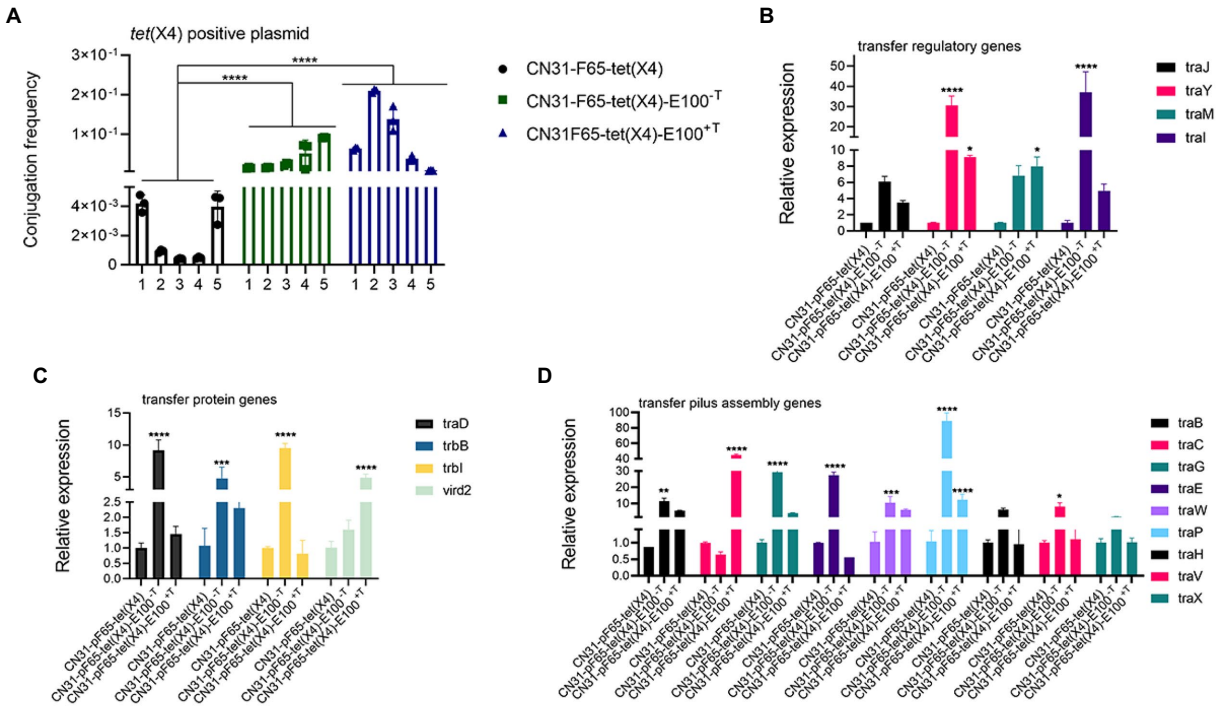

FIGURE 4
Improved conjugation frequencies observed in the evolved strains. **(A)** Comparison of *tet*(X4)-positive plasmid conjugation frequency between ancestral and evolved strains. **(B)** Comparison of the expression levels of conjugative transfer regulatory-related genes between ancestral and evolved strains. **(C)** Comparison of the expression levels of conjugative transfer genes between ancestral and evolved strains. **(D)** Comparison of the expression levels of conjugative transfer pilus assembly genes between ancestral and evolved strains.

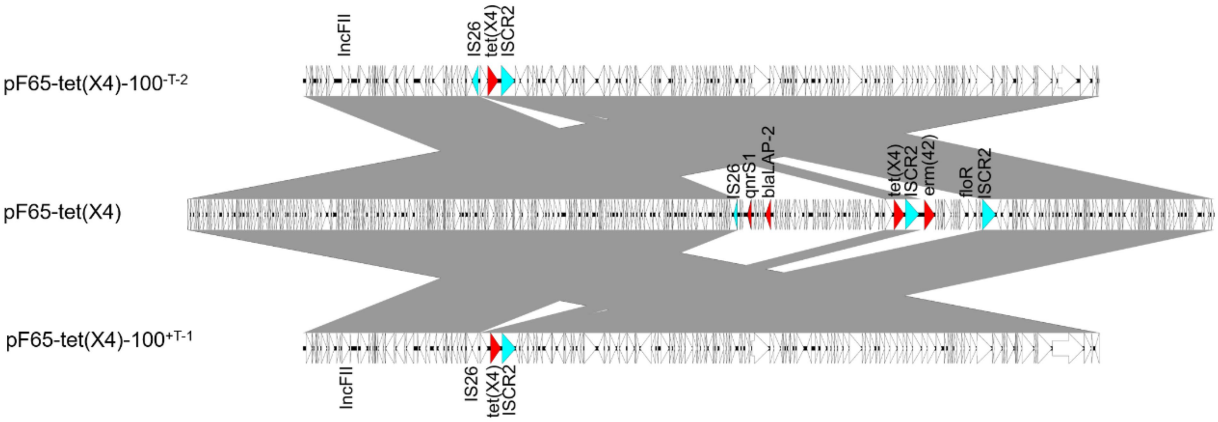

FIGURE 5
Linear comparison among pF65-*tet*(X4) and two evolved plasmids. Two segments were discarded during evolution, and the AMR genes and insertion sequences in deleted regions were marked in red and blue, respectively.

resistance suppressor was identified in all strains evolved with tigecycline (Figure 6B). Functional prediction *via* PROVEAN suggested the altered residue may has deleterious effect on protein functions (Choi et al., 2012). Collectively, the mutations observed in the chromosome and plasmid of evolved strains indicated that the shift of phenotype in evolved strains may due to the plasmid-host coevolution.

Discussion

The emergence and prevalence of multidrug-resistant (MDR) bacteria threaten the efficacy of antibiotics. Conjugative plasmids, which could transfer antimicrobial resistance (AMR) genes among bacteria, played a major role in MDR bacteria formation (Frost et al., 2005; Soucy et al., 2015; Mccollister et al., 2016).

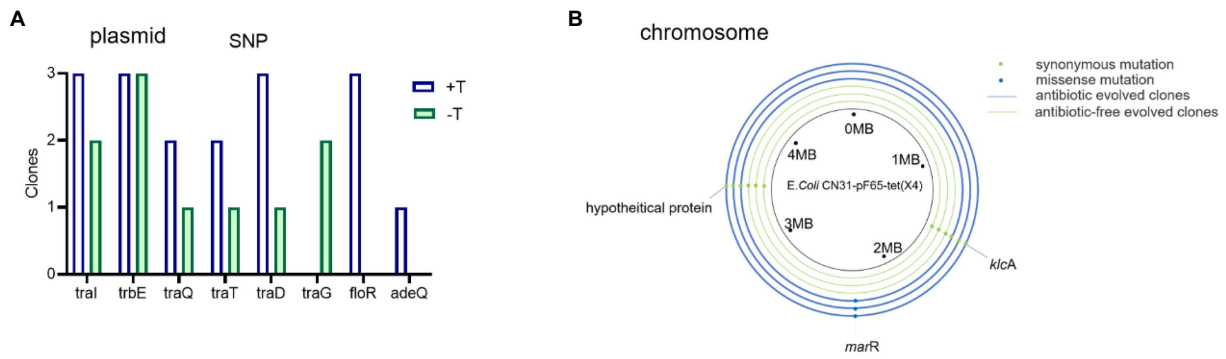

FIGURE 6
Genomic mutations associated with conjugative transfer-related genes and antibiotic resistance genes on plasmid and chromosome. **(A)** Mutations observed on plasmid of evolved clones. **(B)** Mutations observed on chromosome of evolved clones. Blue rings represent the antibiotic evolved clones and the green rings represent the antibiotic-free evolved clones. Dots represent the mutations.

Nevertheless, the acquisition of exogenous plasmids or AMR genes may cause fitness cost to host, and expect to go extinct. Thus, the persistence of plasmids and AMR genes in host cell was critical for the formation and prevalence of MDR bacteria. It was reported that positive selection would favor the maintenance of plasmid (Stevenson et al., 2018). However, little was known about whether it would favor the stability AMR genes. The emergence and dissemination of bla_{NDM}, *mcr*, and *tet*(X4), have seriously undermined the effectiveness of "the last resort antibiotics" in clinical settings (He et al., 2019a,b; Zhi et al., 2020; Mm et al., 2021; Sun et al., 2021a). To evaluate whether "superbugs" co-bearing *tet*(X4), *mcr-1*, and bla_{NDM-5} genes will prevalent in clinical settings, a *tet*(X4)-positive IncFII plasmid, a main prevalence type in China (Li et al., 2021), was introduced into a wide-type MDR *E.coli* N31 carrying *mcr-1* and bla_{NDM-5} genes.

Fitness cost and plasmid transfer rate are key parameters for predicting plasmid persistence. Initially, we observed the focal plasmid entailed a substantial burden in N31, and rapid plasmid extinction was found after 20th generation (data not shown). As fitness cost of plasmids could be alleviated either under non-selection or selection pressure (Porse et al., 2016; Wein et al., 2019), we passaged the strain in the absence or presence of tigecycline. Surprisingly, the stability of both plasmid and *tet*(X4) gene in strains evolved without tigecycline was significantly elevated, whereas the stability of the plasmid in three out of five strains evolved with tigecycline was elevated. However, *tet*(X4) gene harbored by these strains was discarded rapidly, which implied the presence of tigecycline may adversely affect the stability of *tet*(X4) gene. This interesting phenomenon may be collectively caused by the combination of boosted expression of *tet*(X4), increased conjugation frequency, structural alterations of the *tet*(X4)-positive plasmid, and mutations of chromosomal and plasmid genes in evolved strains under tigecycline.

First, we observed the high expression of *tet*(X4) gene in tigecycline treated strains, which may directly contribute to the instability of *tet*(X4). However, the expression level of *tet*(X4) in non-tigecycline treated strains was significantly suppressed. This sharp contrast implied that the high-level expression of *tet*(X4) may arise biosynthetic burden for host bacteria. Previous study has demonstrated the expression of *tet*(X6) exerted high fitness cost in *E. coli* as well (Jiang et al., 2021), suggesting the expression of *tet*(X) variants may be positively correlated with fitness cost. Second, an elevated conjugation frequency was observed in both evolved strains, and the expression of genes involving in the conjugative process was increased as well. It is generally accepted that conjugation is energy-intensive process and reduces the host bacterial fitness (Ilangovan et al., 2015), thus the relationship between bacteria and plasmid should evolve towards lower plasmid costs rather than the high conjugation rate (Hall James et al., 2017). However, the focal plasmid belongs to IncFII type, which represents one of the most prevalent plasmid types in the dissemination of AMR genes (Muthuirulandi Sethuvel et al., 2019). It has perfect conjugation transfer system, partitioning system, *psiB* gene encoding SOS inhibitor protein, and *ssb* encoding DNA-binding protein, which may allow the plasmid to maximize their transfer function (Al Mamun et al., 2021). In addition, it was proved that if the plasmid transfer rate was high enough, it was sufficient to compensate for the loss of plasmids due to plasmid segregation and growth disadvantage and favor the persistence of plasmid (Stewart and Levin, 1977; Dionisio et al., 2002). Third, sequencing of both evolved plasmids revealed that the elevated plasmid stability was also achieved by a large-scale sequence deletion event. Such evolution strategy occurring in plasmids, especially multidrug resistant plasmids, was common. For example, a 73 kb conjugative multidrug resistance plasmid could delete a 25 kb costly region to expand its host range and improve its stability (Porse et al., 2016). Moreover, it was reported that plasmid could compensate its fitness cost to the host through losing 12.8 kb multidrug resistance region (Dorado-Morales et al., 2021). This series of deletion events may be caused by the burden of these genes in transcription, translation and subsequent interactions between these proteins and cellular network, and the loss of these regions may promote the maximum survival of plasmids (Ilangovan et al., 2015; San Millan and

MacLean, 2017). Finally, the SNPs of evolved strains showed consistency. Missense mutation in *marR* gene occurred in chromosome of all strains evolved in tigecycline. The *marR* gene is a member of multiple antibiotic resistance repressor (MarR) family, which acts as a regulator to modulate the multidrug resistance efflux pump (Barbosa and Levy, 2000; Lisa et al., 2020). As previously reported, *marR* regulates the AcrAB multidrug efflux pump through regulation of *marA*, enabling cellular resistance to many structurally unrelated antibiotics, including *tet*racycline, ampicillin, and chloramphenicol (Sato et al., 2018). Moreover, the inactivation mutations in the *marR* gene often associate with a significant fitness cost (Praski Alzrigat et al., 2021). Combining with our results, we hypothesize the mutation of *marR* may be another reason for the increased level of tigecycline resistance and improved plasmid stability in addition to the change of *tet*(X4) expression. Furthermore, plenty of SNPs occurred in conjugation-related genes in the *tet*(X4)-positive plasmids of all evolved strains, probably leading to the high expression of conjugation-related genes. However, further studies were needed to confirm this hypothesis.

In conclusion, this study found that antibiotic-free evolution can improve the stability of *tet*(X4) positive plasmid in $bla_{\text{NDM-5}}$ and *mcr-1* positive *E. coli* by increasing their conjugation frequency and losing large costly fragments. However, the retention rate of *tet*(X4) was reduced through evolution under tigecycline, which was probably caused by the high expression of *tet*(X4). The results of the study provided a theoretical basis for further exploration of the formation of multidrug resistant bacteria and the dissemination of antibiotic resistance.

Data availability statement

The datasets presented in this study can be found in online repositories. All available sequences have been submitted to the Figshare database (https://doi.org/10.6084/m9.figshare.20325096.v1).

Author contributions

XX and ZW designed this study. XX, ZL, and XC did the experiment. KP, RL, and YL analyzed the data. XX and XC wrote the paper. ZL and ZW revised the paper. All authors contributed to the article and approved the submitted version.

Funding

The project was supported by the Priority Academic Program Development of Jiangsu Higher Education Institutions (PAPD), China.

Conflict of interest

The authors declare that the research was conducted in the absence of any commercial or financial relationships that could be construed as a potential conflict of interest.

Publisher's note

All claims expressed in this article are solely those of the authors and do not necessarily represent those of their affiliated organizations, or those of the publisher, the editors and the reviewers. Any product that may be evaluated in this article, or claim that may be made by its manufacturer, is not guaranteed or endorsed by the publisher.

Supplementary material

The Supplementary material for this article can be found online at: https://www.frontiersin.org/articles/10.3389/fmicb.2022.1010387/full#supplementary-material.

References

Al Mamun, A. A. M., Kishida, K., and Christie, P. J. (2021). Protein transfer through an F plasmid-encoded type IV secretion system suppresses the mating-induced SOS response. *MBio* 12:e0162921. doi: 10.1128/mBio.01629-21

Bankevich, A., Nurk, S., Antipov, D., Gurevich, A. A., Dvorkin, M., Kulikov, A. S., et al. (2012). SPAdes: a new genome assembly algorithm and its applications to single-cell sequencing. *J. Comput. Biol.* 19, 455–477. doi: 10.1089/cmb.2012.0021

Barbosa, T. M., and Levy, S. B. (2000). Differential expression of over 60 chromosomal genes in Escherichia coli by constitutive expression of MarA. *J. Bacteriol.* 182, 3467–3474. doi: 10.1128/JB.182.12.3467-3474.2000

Carroll, A. C., and Wong, A. (2018). Plasmid persistence: costs, benefits, and the plasmid paradox. *Can. J. Microbiol.* 64, 293–304. doi: 10.1139/cjm-2017-0609

Choi, Y., Sims, G. E., Murphy, S., Miller, J. R., and Chan, A. P. (2012). Predicting the functional effect of amino acid substitutions and indels. *PLoS One* 7:e46688. doi: 10.1371/journal.pone.0046688

Cui, C. Y., Chen, C., Liu, B. T., He, Q., Wu, X. T., Sun, R. Y., et al. (2020). Co-occurrence of plasmid-mediated Tigecycline and Carbapenem resistance in Acinetobacter spp. from waterfowls and their neighboring environment. *Antimicrob. Agents Chemother.* 64:e02502-19. doi: 10.1128/AAC.02502-19

Dionisio, F., Matic, I., Radman, M., Rodrigues, O. R., and Taddei, F. (2002). Plasmids spread very fast in heterogeneous bacterial communities. *Genetics* 162, 1525–1532. doi: 10.1093/genetics/162.4.1525

Dorado-Morales, P., Garcillán-Barcia, M., Lasa, I., and Solano, C. (2021). Fitness cost evolution of natural plasmids of Staphylococcus aureus. *MBio* 12:e03094-20. doi: 10.1128/mBio.03094-20

Frost, L. S., Leplae, R., Summers, A. O., and Toussaint, A. (2005). Mobile genetic elements: the agents of open source evolution. *Nat. Rev. Microbiol.* 3, 722–732.

Hall James, P. J., Brockhurst, M. A., Dytham, C., and Harrison, E. (2017). The evolution of plasmid stability: are infectious transmission and compensatory evolution competing evolutionary trajectories? *Plasmid* 91, 90–95. doi: 10.1016/j.plasmid.2017.04.003

He, T., Wang, R., Liu, D., Walsh, T. R., and Wang, Y. (2019a). Emergence of plasmid-mediated high-level tigecycline resistance genes in animals and humans. *Nat. Microbiol.* 4:1. doi: 10.1038/s41564-019-0445-2

He, T., Wei, R., Li, R., Zhang, L., Sun, L., Bao, H., et al. (2019b). Co-existence of *tet*(X4) and mcr-1 in two porcine Escherichia coli isolates. *J. Antimicrob. Chemother.* 3, 764–766. doi: 10.1093/jac/dkz510

Hirabayashi, A., Dao, T. D., Takemura, T., Hasebe, F., Trang, L. T., Thanh, N. H., et al. (2021). A transferable IncC-IncX3 hybrid plasmid Cocarrying *bla*NDM-4, *tet*(X), and tmexCD3-toprJ3 confers resistance to Carbapenem and Tigecycline. *mSphere* 6:e0059221. doi: 10.1128/mSphere.00592-21

Ilangovan, A., Connery, S., and Waksman, G. (2015). Structural biology of the gram-negative bacterial conjugation systems. *Trends Microbiol.* 23, 301–310. doi: 10.1016/j.tim.2015.02.012

Jiang, L., Cai, W., Tang, F., Wang, Z., and Liu, Y. (2021). Characterization of fitness cost caused by Tigecycline-resistance gene *tet*(X6) in different host bacteria. *Antibiotics (Basel)* 10:1172. doi: 10.3390/antibiotics10101172

Kolmogorov, M., Yuan, J., Lin, Y., and Pevzner, P. A. (2019). Assembly of long, error-prone reads using repeat graphs. *Nat. Biotechnol.* 37, 540–546. doi: 10.1038/s41587-019-0072-8

Li, R., Li, Y., Peng, K., Yin, Y., Liu, Y., He, T., et al. (2021). Comprehensive genomic investigation of Tigecycline resistance gene *tet*(X4)-bearing strains expanding among different settings. *Microbiol. Spectr.* 9:e0163321. doi: 10.1128/spectrum.01633-21

Li, R., Liu, Z., Li, Y., Xiao, X., and Wang, Z. (2022). Characterization of *bla*NDM-positive Enterobacteriaceae reveals the clonal dissemination of Enterobacter hormaechei coharboring *bla*NDM and *tet*(X4) along the pork production chain. *Int. J. Food Microbiol.* 372:109692. doi: 10.1016/j.ijfoodmicro.2022.109692

Li, R., Lu, X., Peng, K., Liu, Z., Li, Y., Liu, Y., et al. (2020). Deciphering the structural diversity and classification of the Mobile Tigecycline resistance gene *tet*(X)-bearing Plasmidome among bacteria. *mSystems* 5:e00134-20. doi: 10.1128/mSystems.00134-20

Li, Y., Wang, Q., Peng, K., Liu, Y., Li, R., and Wang, Z. (2020). Emergence of Carbapenem- and Tigecycline-resistant Proteus cibarius of animal origin. *Front. Microbiol.* 11:1940. doi: 10.3389/fmicb.2020.01940

Lisa, P. A., Huseby, D. L., Gerrit, B., and Diar Ma Id, H. (2020). Resistance/fitness trade-off is a barrier to the evolution of MarR inactivation mutants in Escherichia coli. *J. Antimicrob. Chemother.* 1, 77–83. doi: 10.1093/jac/dkaa417

Loftie-Eaton, W., Bashford, K., Quinn, H., Dong, K., and Top, E. M. (2017). Compensatory mutations improve general permissiveness to antibiotic resistance plasmids. *Nat. Ecol. Evol.* 1, 1354–1363. doi: 10.1038/s41559-017-0243-2

Lu, X., Du, Y., Peng, K., Zhang, W., Li, J., Wang, Z., et al. (2022). Coexistence of *tet*(X4), mcr-1, and *bla*NDM-5 in ST6775 Escherichia coli isolates of animal origin in China. *Microbiol. Spectr.* 10:e0019622. doi: 10.1128/spectrum.00196-22

Mccollister, B., Kotter, C. V., Frank, D. N., Washburn, T., and Jobling, M. G. (2016). Erratum for McCollister et al., whole-genome sequencing identifies in vivo acquisition of a *bla*CTX-M-27-carrying IncFII transmissible plasmid as the cause of ceftriaxone treatment failure for an invasive salmonella enterica Serovar typhimurium infection. *Antimicrob. Agents Chemother.* 61:7224. doi: 10.1128/AAC.00009-17

Millan, A. S., Pena-Miller, R., Toll-Riera, M., Halbert, Z. V., Mclean, A. R., and Cooper, B. S. (2014). Positive selection and compensatory adaptation interact to stabilize non-transmissible plasmids. *Nat. Commun.* 5:et al.:5208. doi: 10.1038/ncomms6208

Mm, A., Bh, B., Wmb Sm, B., Rl, C., Sa, A., Ks, D., et al. (2021). Emergence of plasmid-mediated tigecycline resistance *tet*(X4) gene in Escherichia coli isolated from poultry, food and the environment in South Asia. *Sci. Total Environ.* 787:147613

Muthuirulandi Sethuvel, D. P., Anandan, S., Devanga Ragupathi, N. K., Gajendiran, R., Kuroda, M., Shibayama, K., et al. (2019). IncFII plasmid carrying antimicrobial resistance genes in Shigella flexneri: vehicle for dissemination. *J. Glob. Antimicrob. Resist.* 16, 215–219. doi: 10.1016/j.jgar.2018.10.014

Porse, A., Schonning, K., Munck, C., and Sommer, M. O. (2016). Survival and evolution of a large multidrug resistance plasmid in new clinical bacterial hosts. *Mol. Biol. Evol.* 33, 2860–2873.

Praski Alzrigat, L., Huseby, D. L., Brandis, G., and Hughes, D. (2021). Resistance/fitness trade-off is a barrier to the evolution of MarR inactivation mutants in Escherichia coli. *J. Antimicrob. Chemother.* 76, 77–83. doi: 10.1093/jac/dkaa417

Rozwandowicz, M., Brouwer, M. S. M., Fischer, J., Wagenaar, J. A., Gonzalez-Zorn, B., Guerra, B., et al. (2018). Plasmids carrying antimicrobial resistance genes in Enterobacteriaceae. *J. Antimicrob. Chemother.* 73, 1121–1137. doi: 10.1093/jac/dkx488

San Millan, A., and Maclean, R. C. (2017). Fitness costs of plasmids: a limit to plasmid transmission. *Microbiol. Spectr.* 5. doi: 10.1128/microbiolspec.MTBP-0016-2017

Sato, Y., Unno, Y., Ubagai, T., and Ono, Y. (2018). Sub-minimum inhibitory concentrations of colistin and polymyxin B promote Acinetobacter baumannii biofilm formation. *PLoS One* 13:e0194556. doi: 10.1371/journal.pone.0194556

Sota, M., Yano, H., Hughes, J. M., Daughdrill, G. W., and Top, E. M. (2010). Shifts in the host range of a promiscuous plasmid through parallel evolution of its replication initiation protein. *ISME J.* 4, 1568–1580. doi: 10.1038/ismej.2010.72

Soucy, S. M., Huang, J., and Gogarten, J. P. (2015). Horizontal gene transfer: building the web of life. *Nat. Rev. Genet.* 16, 472–482. doi: 10.1038/nrg3962

Stevenson, C., Hall, J. P. J., Brockhurst, M. A., and Harrison, E. (2018). Plasmid stability is enhanced by higher-frequency pulses of positive selection. *Proc. Biol. Sci.* 285:20172497. doi: 10.1098/rspb.2017.2497

Stewart, F. M., and Levin, B. R. (1977). The population biology of bacterial plasmids: a PRIORI conditions for the existence of conjugationally transmitted factors. *Genetics* 87, 209–228. doi: 10.1093/genetics/87.2.209

Sullivan, M. J., Petty, N. K., and Beatson, S. A. (2011). Easyfig: a genome comparison visualizer. *Bioinformatics* 27, 1009–1010. doi: 10.1093/bioinformatics/btr039

Sun, H., Zhai, W., Fu, Y., Li, R., and Bai, L. (2021). Co-occurrence of plasmid-mediated resistance genes *tet*(X4) and *bla*NDM-5 in a multidrug-resistant Escherichia coli isolate recovered from chicken in China. *J. Glob. Antimicrob. Resist.* 24, 415–417. doi: 10.1016/j.jgar.2021.02.010

Tang, F., Cai, W., Jiang, L., Wang, Z., and Liu, Y. (2022). Large-scale analysis of fitness cost of *tet*(X4)-positive plasmids in Escherichia coli. *Front. Cell. Infect. Microbiol.* 12:798802. doi: 10.3389/fcimb.2022.798802

Wein, T., Hulter, N. F., Mizrahi, I., and Dagan, T. (2019). Emergence of plasmid stability under non-selective conditions maintains antibiotic resistance. *Nat. Commun.* 10:2595. doi: 10.1038/s41467-019-10600-7

Yano, H., Wegrzyn, K., Loftie-Eaton, W., Johnson, J., Deckert, G. E., Rogers, L. M., et al. (2016). Evolved plasmid-host interactions reduce plasmid interference cost. *Mol. Microbiol.* 101, 743–756. doi: 10.1111/mmi.13407

Zatyka, M., Jagura-Burdzy, G., and Thomas, C. M. (1997). Transcriptional and translational control of the genes for the mating pair formation apparatus of promiscuous IncP plasmids. *J. Bacteriol.* 179, 7201–7209. doi: 10.1128/jb.179.23.7201-7209.1997

Zhi, R., Jia, H., Chen, H., Wu, J., He, F., and Feng, Y. (2020). Co-existence of plasmid-mediated tigecycline and colistin resistance genes *tet*(X4) and mcr-1 in a community-acquired Escherichia coli isolate in China. *J. Antimicrob. Chemother.* 11, 3400–3402. doi: 10.1093/jac/dkaa317

frontiers | Frontiers in Microbiology

TYPE Original Research
PUBLISHED 22 November 2022
DOI 10.3389/fmicb.2022.1043736

OPEN ACCESS

EDITED BY
Seok Hoon Jeong,
Yonsei University,
South Korea

REVIEWED BY
Abbas Yadegar,
Shahid Beheshti University of Medical Sciences, Iran
Andrei Nicoli Gebieluca Dabul,
University of São Paulo, Brazil

*CORRESPONDENCE
Lijiang Chen
29340442@qq.com
Tieli Zhou
wyztli@163.com

SPECIALTY SECTION
This article was submitted to Antimicrobials, Resistance and Chemotherapy, a section of the journal Frontiers in Microbiology

RECEIVED 14 September 2022
ACCEPTED 07 November 2022
PUBLISHED 22 November 2022

CITATION
Zeng W, Zhang X, Liu Y, Zhang Y, Xu M, Wang S, Sun Y, Zhou T and Chen L (2022) *In vitro* antimicrobial activity and resistance mechanisms of the new generation tetracycline agents, eravacycline, omadacycline, and tigecycline against clinical *Staphylococcus aureus* isolates. *Front. Microbiol.* 13:1043736. doi: 10.3389/fmicb.2022.1043736

In vitro antimicrobial activity and resistance mechanisms of the new generation tetracycline agents, eravacycline, omadacycline, and tigecycline against clinical *Staphylococcus aureus* isolates

Weiliang Zeng[1], Xiaotuan Zhang[1], Yan Liu[1], Yi Zhang[2], Mengxin Xu[1], Sipei Wang[1], Yao Sun[1], Tieli Zhou[1]* and Lijiang Chen[1]*

[1]Key Laboratory of Clinical Laboratory Diagnosis and Translational Research of Zhejiang Province, The First Affiliated Hospital of Wenzhou Medical University, Wenzhou, China, [2]School of Laboratory Medicine and Life Science, Wenzhou Medical University, Wenzhou, China

In this study, we investigated the *in vitro* activity and resistance mechanisms of the new generation tetracycline agents, namely eravacycline, omadacycline, and tigecycline, against *Staphylococcus aureus* isolates. A total of 1,017 non-duplicate *S. aureus* isolates were collected and subjected to susceptibility testing against eravacycline, omadacycline, and tigecycline using the broth microdilution method. Tetracyclines-resistant (eravacycline/omadacycline/tigecycline-resistant) isolates were selected to elucidate the resistance mechanisms using polymerase chain reaction (PCR), cloning experiment, efflux pump inhibition, and quantitative real-time PCR. The results of the antibacterial susceptibility testing showed that compared with omadacycline, eravacycline and tigecycline had superior antibacterial activity against *S. aureus* isolates. Among 1,017 *S. aureus*, 41 tetracyclines-resistant isolates were identified. These resistant isolates possessed at least one tetracycline resistance gene and genetic mutation in the MepRAB efflux pump and 30S ribosome units. A frameshift mutation in *mepB* was detected in most tetracyclines-resistant strains (except for JP3349) compared with tetracyclines-susceptible (eravacycline/omadacycline/tigecycline-susceptible) strains. This was first shown to decrease susceptibility to omadacycline, but not to eravacycline and tigecycline. After treatment with eravacycline, omadacycline or tigecycline, overexpression of *mepA*, *tet38*, *tet*(K) and *tet*(L) was detected. Moreover, multi-locus sequence typing showed a major clonal dissemination type, ST5, and its variant ST764 were seen in most tetracyclines-resistant strains. To conclude, eravacycline and tigecycline exhibited better activity against *S. aureus* including tetracycline-resistant isolates than omadacycline. The resistance to these new generation tetracyclines due to an accumulation of many resistance mechanisms.

KEYWORDS

eravacycline, omadacycline, tigecycline, *Staphylococcus aureus*, antimicrobial activity, resistance mechanisms

Introduction

Staphylococcus aureus is an important nosocomial pathogen that is associated with various infections, such as skin and skin structure infections, endocarditis, and bloodstream infections (Pérez-Montarelo et al., 2018). *S. aureus* is one of the major and most fatal causes of bacteremia, and has a mortality rate of almost 20%. Almost half of the patients with *S. aureus* bacteremia will develop complicated bacteremia (Guimaraes et al., 2019). Recently, the emergence of multidrug-resistant (MDR) superbugs, such as methicillin-resistant and vancomycin-resistant *S. aureus*, has become a significant threat to public health (Gasch et al., 2014; McGuinness et al., 2017). The methicillin-resistant *S. aureus* (MRSA) is considered a prioritized nosocomial pathogen by the World Health Organization (WHO; Serral et al., 2021). Overall, *S. aureus* infections are considered a significant clinical challenge.

The tetracycline class of antimicrobial agents has been clinically used for more than 60 years (Roberts, 2003). And they are continued to treat various serious infections caused by Gram-positive and-negative pathogens, including MRSA (Grossman, 2016). With their extensive use in clinical settings, resistance to old tetracyclines, especially doxycycline and tetracycline, is increasing worldwide (Roberts, 2003, 2005; Grossman, 2016). New generation tetracycline agents, such as eravacycline, omadacycline, and tigecycline, can be used as a treatment option for bacterial infections owing to their broad-spectrum antimicrobial activity.

Tigecycline is a semisynthetic glycylcycline with broad-spectrum antimicrobial agents (Doan et al., 2006). In 2005, it was approved by the US Food and Drug Administration (FDA) approval for the treatment of various serious infections, such as adults with complicated intra-abdominal infections and community-acquired bacterial pneumonia (Noskin, 2005). Eravacycline and omadacycline with modifications at the C-9 position are newer generation tetracycline agents similar to tigecycline. They were approved by the FDA in 2018 for the treatment of polymicrobial MDR infections (Solomkin et al., 2019; Morrissey et al., 2020; Zhanel et al., 2020). Similar to other tetracyclines, these new generation tetracycline agents inhibit bacterial protein synthesis by binding to the 30S ribosomal subunit. Eravacycline, omadacycline and tigecycline have broad-spectrum antibacterial activity against Gram-positive and Gram-negative microorganisms. However, the antimicrobial activity of these tetracyclines against *S. aureus* has not been comprehensively studied.

Many mechanisms of underlying tetracyclines resistance have been proposed. The resistance is mostly due to the acquisition of tetracycline resistance genes and mutation of ribosomal protection proteins (Nguyen et al., 2014; Beabout et al., 2015; Grossman, 2016; Linkevicius et al., 2016). Overexpression of efflux pumps has been reported both in Gram-positive and Gram-negative pathogens (Truong-Bolduc et al., 2015; Fiedler et al., 2016; Zhanel et al., 2016). Mutations or overexpression of the MepRAB efflux pump contributes to the decreased susceptibility to tigecycline (McAleese et al., 2005; Fang et al., 2020). Recent studies have revealed that a branched-chain amino acid transport system II carrier protein affects eravacycline and omadacycline susceptibility in *S. aureus* (Bai et al., 2019; Wang et al., 2020). Moreover, a recent study revealed a novel *tet*(L) efflux pump that confers resistance to eravacycline and tigecycline resistance in *Staphylococcus* (Wang et al., 2021). However, the potential contribution of these resistance factors of tetracyclines to the development of resistance to eravacycline and omadacycline in *S. aureus* is not completely known. In addition, multi-locus sequence typing (MLST), which was first established by Maiden et al. (1998), is now the most frequently used method to monitor epidemiology and investigate evolution of pathogens due to its high discriminatory power and comparability (Li T. et al., 2022). The distribution of sequence types (STs) profiles was unclear in tetracyclines-resistant (eravacycline/omadacycline/tigecycline-resistant) *S. aureus* Taken together, the results of this study will give insight into the prevalence and molecular epidemiology characteristics of tetracyclines-resistant *S. aureus* using MLST method.

In this study, we investigated and compared the *in vitro* antimicrobial efficacy of eravacycline, omadacycline, and tigecycline against 1,017 clinical *S. aureus* isolates. Resistance determinants and STs profiles of the tetracyclines-resistant isolates were further investigated using polymerase chain reaction (PCR). Furthermore, genetic mutations in the MepRAB efflux pump and 30S ribosome units and expression of *mepA*, *tet38*, *tet*(K) and *tet*(L) were also determined by sequencing, cloning experiment, efflux pump inhibition and quantitative real-time PCR (RT-qPCR).

Materials and methods

Bacterial isolates and plasmids

This study used strains obtained from the First Affiliated Hospital of Wenzhou Medical University. The First Affiliated Hospital of Wenzhou Medical University of institutional ethics committee did not require the study to be reviewed or approved by an ethics committee as this study, which was of observational nature, mainly focused on bacteria and did not involve any interventions to the patients.

From January 2018 to December 2020, a total of 1,017 non-duplicate clinical *S. aureus* isolates, including 577 tetracycline-resistant and 440 tetracycline-susceptible strains, were obtained from the First Affiliated Hospital of Wenzhou Medical University, Zhejiang, China. These bacteria were identified by matrix-assisted laser desorption/ionization time of flight mass spectrometry. *S. aureus* ATCC 29213 and *Escherichia coli* ATCC 25922 were used as quality control strains in antimicrobial susceptibility testing experiments. *E. coli* strain DH5α and pUCP24 plasmid were used as a recipient and vector in cloning experiments (Cheng et al., 2020), respectively.

Antimicrobial susceptibility testing

The minimum inhibitory concentration (MIC) of eravacycline, omadacycline, and tigecycline was determined by the broth microdilution method. The results were interpreted in accordance with a published research (Zhao et al., 2019), and the European Committee on Antimicrobial Susceptibility Testing, and FDA (FDA, 2020). The tetracyclines-resistant isolates were selected to evaluate their resistance mechanisms. Moreover, the resistance spectrum was examined using the agar dilution method among the resistant strains and ten tetracyclines-susceptible (eravacycline/omadacycline/tigecycline-susceptible) strains randomly selected, including ciprofloxacin (CIP), gentamicin (GEN), levofloxacin (LVX), erythromycin (ERY), linezolid (LNZ), oxacillin (OXA), rifampicin (RIF), and vancomycin (VAN). The interpretation criteria of MIC following the CLSI guidelines (CLSI, 2022). Antimicrobial susceptibility testing was repeated in triplicate. Eravacycline and omadacycline were obtained from the MCE company (Med Chem Express, Monmouth Junction, NJ, United States), and other antibiotics were purchased from Kangtai Biotechnology company (Wenzhou, China).

PCR detection of tetracycline resistance genes, MepRAB efflux pump-encoding genes and 30S ribosome subunits mutations

Genomic DNA of tetracyclines-resistant strains, ten tetracyclines-susceptible strains randomly selected, and *S. aureus* ATCC 29213 were extracted using the Biospin Bacterial Genomic DNA Extraction Kit (Bioflux, Tokyo, Japan). The *tet*(K), *tet*(L), *tet*(M), *tet*(O), and *tet*(S) genes were screened by PCR amplification with specific primers (Supplementary Table S1). Mutations in the MepRAB efflux pump-encoding genes (*mepR*, *mepA*, and *mepB*) and 30S ribosome protein (*S3* and *S10*) were detected by PCR, and the positive PCR products were sequenced by the Shanghai Genomics Institute Technology Co. Ltd. Then, genetic mutations were analyzed by comparison with the genome of *S. aureus* ATCC 29213.

Cloning experiments of *mepB*

Based on the PCR data, JP3936 (omadacycline-resistant and eravacycline/tigecycline-susceptible, with a frameshift mutation in *mepB*), JP4612 (tetracyclines-resistant, with a frameshift mutation in *mepB*), and JP4200 (tetracyclines-susceptible, without a frameshift mutation in *mepB* gene) were selected in the experimental and control groups of cloning experiments, respectively. As described in a past study (Cheng et al., 2020), for cloning, *Eco*RI (Takara) and *Xba*I (Takara) restriction endonuclease sites and their protective bases were incorporated into the primers (Supplementary Table S1). Then, *mepB* was amplified from genomic DNA of tested isolates by PCR. The PCR products were digested with restriction endonucleases *Eco*RI and *Xba*I, and then ligated into an expression vector pUCP24 that had been treated with the same restriction endonucleases using the T4 DNA ligase (Takara). The recombinant plasmids were transformed into *E. coli* DH5α, which were grown on Luria-Bertani agar plates supplemented with gentamicin (20 μg/ml), and then further verified by colony PCR and sequencing.

Antimicrobial susceptibility testing for the transformants was performed to verify the function of *mepB* using the broth microdilution method. The recipient *E. coli* DH5α or *E. coli* DH5α carrying the vector pUCP24 (pUCP24/DH5α) was used as the negative control. *E. coli* ATCC 25922 was used as the quality control strain.

Effect of efflux pump inhibitors

According to past study (Zhu et al., 2021), the effect of efflux pump inhibitor carbonyl cyanide m-chlorophenylhydrazone (CCCP, 0.4 μg/ml) on the tetracyclines activity was determined by the broth microdilution method in the presence and absence of the efflux pump inhibitors. The effects of efflux pump inhibitors were interpreted as follows: it was considered as a positive efflux pump phenotype when the MIC of antibiotics decreased to 4-fold or more after the supplementation of the efflux pump inhibitors (Zhang et al., 2018).

Antibiotic treatment and total RNA isolation

To decipher the mechanisms of resistance to tetracyclines, ten tetracyclines-resistant *S. aureus* strains with a positive efflux pump phenotype, a randomly selected equal number of tetracyclines-susceptible strains and *S. aureus* ATCC 29213 were used to measure the transcriptional levels of the efflux pump encoding-genes *mepA*, *tet38*, *tet*(K), and *tet*(L).

First, a single pure colony of *S. aureus* was randomly picked, inoculated into 3 ml of fresh LB broth, and allowed to grow to the logarithmic phase. Then, 30 μl of the overnight culture was transferred into 2.97 ml fresh LB broth without or with 1/2 × MIC (subinhibitory concentrations) of eravacycline, omadacycline, or tigecycline, respectively (Xu et al., 2020). Next, which the cells were harvested, and their total bacterial RNA was extracted by using the Bacterial RNA Miniprep Kit (Biomiga, Shanghai, China) in accordance with the manufacturer's instructions. The extracted RNA was reverse transcribed into cDNA by using the PrimeScript RT Reagent Kit (Takara Bio Inc., Shiga, Japan).

RT-qPCR analysis

RT-qPCR was performed on the CFX-96 TouchTM Real-Time PCR System (Bio-Rad, Hercules, CA, United States) using the TB Green Premix Ex Taq II (Tli RNase H Plus) (2×) (Takara, Japan).

The internal control gene *gyrB* was used to normalize the expression of target genes, and the data were analyzed by using the $2^{-\Delta\Delta Ct}$ method. The relative expression of the target gene was normalized to that of *S. aureus* ATCC 29213. All RT-qPCR were performed in triplicate using 3 independent RNA samples. The RT-qPCR primers were listed in Supplementary Table S1.

Multi-locus sequence typing

MLST was conducted by amplifying and sequencing 7 housekeeping genes (*arcC*, *aroE*, *glpF*, *gmK*, *pta*, *tpi*,and *yqiL*) using specific primers acquired form PubMLST website.[1] The PCR products were sequenced, and the sequences were compared with those available from the MLST database[2] to obtain the allelic numbers, STs and clonal complexes.

Statistical analyses

Statistical analyses of the gene expression levels were performed with the GraphPad Prism 8.0 software using the paired Student's *t*-test, with $p < 0.05$ was considered to be significant.

Results

Antimicrobial activity of new generation tetracyclines against clinical *Staphylococcus aureus* strains

Among 1,017 *S. aureus* isolates, three eravacycline, omadacycline, and tigecycline co-resistant, six omadacycline and tigecycline co-resistant, and 32 omadacycline-resistant strains were screened from tetracycline-resistant strains, but not from tetracycline-susceptible strains. Moreover, eravacycline (resistance rate, 0.29%) showed the lowest resistance rate when comparing the results of omadacycline (resistance rate, 4.03%) and tigecycline (resistance rate, 0.88%). As shown in Table 1, the MIC_{50} and MIC_{90} of eravacycline, omadacycline, and tigecycline against for 1,017 *S. aureus* isolates were 0.12 and 0.25 μg/ml, 0.5 and 1 μg/ml, and 0.12 and 0.25 μg/ml, respectively. In comparison, MIC_{50} and MIC_{90} values of omadacycline against *S. aureus* increased 4-fold when compared with that of eravacycline and tigecycline. Overall, these data indicated that eravacycline and tigecycline had more excellent antimicrobial activity against *S. aureus* strains than omadacycline, including tetracycline-resistant strains.

Out of the 41 tetracyclines-resistant *S. aureus* isolates, most of them possessed two or more tetracycline resistance genes: *tet*(K) ($n = 5$), *tet*(L) ($n = 1$), *tet*(K) + *tet*(L) ($n = 5$), *tet*(K) + *tet*(M) ($n = 10$), *tet*(L) + *tet*(M) ($n = 6$), *tet*(K) + *tet*(L) + *tet*(M) ($n = 14$). None *tet*(O) and *tet*(S) was detected (Table 2). Notably, three different tetracycline resistance genes [*tet*(K) + *tet*(L) + *tet*(M)] were detected simultaneously in the three tetracyclines co-resistant strains (Figure 1).

TABLE 2 Geographic distribution of 41 tetracyclines-resistant *Staphylococcus aureus* isolates.

Tetracycline resistance genes	No. of isolates	Carrier rate (%)
tet(S)	0	0.00
tet(O)	0	0.00
tet(K)	5	12.20
tet(L)	1	2.43
tet(K) + *tet*(L)	5	12.20
tet(K) + *tet*(M)	10	24.39
tet(L) + *tet*(M)	6	14.63
tet(K) + *tet*(L) + *tet*(M)	14	34.15

TABLE 1 Antimicrobial activity of eravacycline, omadacycline and tigecycline against *Staphylococcus aureus* isolates.

Tetracycline agents	Organism group (no. of isolates tested)	No. (cumulative %) of isolates inhibited at MIC (μg/mL) of:							$MIC_{50/90}$ (μg/mL)	Resistance rate (%)
		≤0.06	0.12	0.25	0.5	1	2	≥4		
Eravacycline	TET-R (577)	101	289	158	26	1	1	1	0.12/0.25	0.52
	TET-S (440)	172	254	13	1	0	0	0	0.12/0.12	0
	Total (1,017)	273	543	171	27	1	1	1	0.12/0.25	0.29
Omadacycline	TET-R (577)	0	60	67	282	127	6	35	0.5/1	7.11
	TET-S (440)	13	44	147	213	23	0	0	0.5/0.5	0
	Total (1,017)	13	104	214	495	150	6	35	0.5/1	4.03
Tigecycline	TET-R (577)	61	260	183	64	6	2	1	0.12/0.5	1.56
	TET-S (440)	108	315	15	2	0	0	0	0.12/0.12	0
	Total (1,017)	169	575	198	66	6	2	1	0.12/0.25	0.88

MIC, minimum inhibitory concentration; TET-R, tetracycline-resistant; TET-S, tetracycline-susceptible.

1 http://pubmlst.org/organisms/staphylococcus-aureus/primers

2 http://saureus.mlst.net/

Tetracyclines-resistant *Staphylococcus aureus* isolates presented a MDR phenotype

A total of 41 tetracyclines-resistant strains presented MDR phenotype to commonly used clinical antibiotics, which exhibited a high frequency of antimicrobial resistance to tetracycline, CIP, GEN, LVX, ERY, and OXA (Table 3). However, the MDR phenotype was not observed in tetracyclines-susceptible isolates.

Mutations in the MepRAB efflux pump and 30S ribosome subunits encoding genes

To elucidate the resistance mechanisms of *S. aureus* strains to tetracyclines, genetic mutations of the MepRAB efflux pump and 30S ribosome subunits encoding genes were determined by PCR and sequenced (Table 4; Figure 1). Compared with tetracyclines-susceptible strains and *S. aureus* ATCC 29213, the amino acid mutations L155F and T411A in *mepA* and Y58D in *S10* were frequently found in tetracyclines-resistant strains. Moreover, tetracyclines-resistant *S. aureus* isolates also contained premature stop codon of *mepA* (E130*), *mepB* (Q139*), and *S10* (K3* and Y13*). Interestingly, except for JP3349, almost all tetracyclines-resistant *S. aureus* isolates contained nucleotide deletion in *mepB* (F144fs) that translated Phe at 144 to Leu. Nevertheless, a frameshift mutation in *mepB* was not found among ten tetracyclines-susceptible *S. aureus* isolates. Therefore, we hypothesized that a frameshift mutation in *mepB* may be associated with tetracyclines resistance. In addition, *mepB*

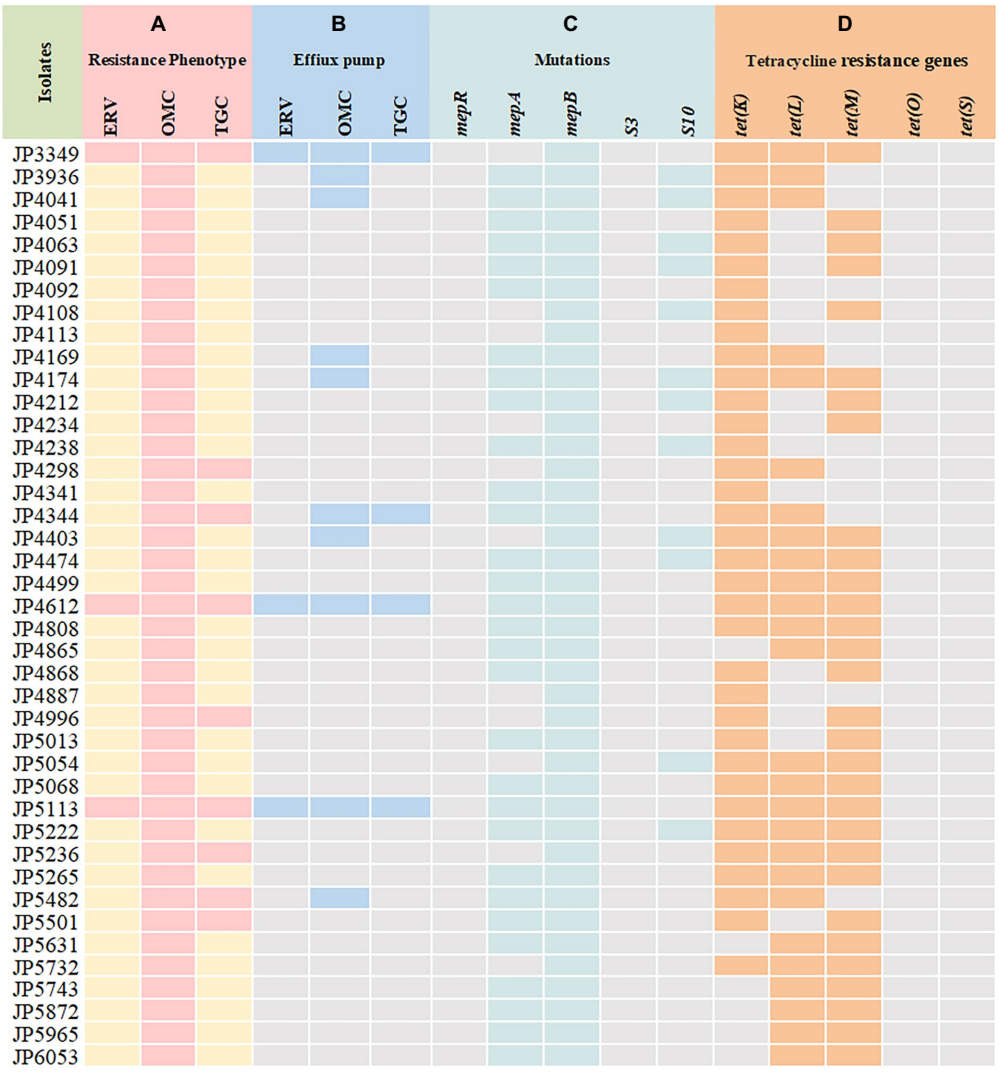

FIGURE 1
Tetracyclines resistance mechanisms determined in the clinical *Staphylococcus aureus* isolates. **(A)** Resistance phenotype of *S. aureus* to tetracyclines; **(B)** carbonyl cyanide 3-chlorophenylhydrazone (CCCP) was used to detect the activity of efflux pumps; **(C)** mutations in MepRAB efflux pump-encoding genes and 30S ribosome subunits; **(D)** PCR detection of tetracycline resistance genes. ERV, eravacycline; OMC, omadacycline; TGC, tigecycline; pink and yellow rectangles indicate resistant and susceptible phenotypes, respectively; Blue rectangles indicate strains with a positive efflux pump phenotype; Green rectangles represent genetic mutations that are only present in the resistant strains; Orange rectangles indicate strains harboring tetracycline resistance genes.

TABLE 3 Characteristics of the resistance spectrum of tetracyclines-resistant and-susceptible *Staphylococcus aureus* isolates.

Isolates	MIC (μg/mL)											
	New tetracycline agents			Commonly used clinical antibiotics								
	ERV	OMC	TGC	TET	CIP	GEN	LVX	ERY	LNZ	OXA	RIF	VAN
JP3349	4^{R}	4^{R}	≥8^{R}	32^{R}	128^{R}	128^{R}	16^{R}	128^{R}	1	≥256^{R}	2	1
JP3936	0.12	2^{R}	0.25	32^{R}	64^{R}	128^{R}	1	0.5	2	≥256^{R}	2	2
JP4041	0.5	4^{R}	0.5	32^{R}	128^{R}	128^{R}	1	0.5	2	≥256^{R}	8^{R}	2
JP4051	0.12	2^{R}	0.5	32^{R}	256^{R}	128^{R}	0.25	1	2	≥256^{R}	2	1
JP4063	0.12	2^{R}	0.5	32^{R}	64^{R}	128^{R}	0.25	1	2	≥256^{R}	2	2
JP4091	0.5	4^{R}	0.5	32^{R}	2	128^{R}	1	0.5	2	≥256^{R}	4^{R}	2
JP4092	0.12	4^{R}	0.5	32^{R}	64^{R}	128^{R}	0.5	0.5	2	≥256^{R}	2	1
JP4108	0.5	4^{R}	0.5	64^{R}	64^{R}	128^{R}	0.25	0.5	2	≥256^{R}	2	2
JP4113	0.25	4^{R}	0.5	64^{R}	256^{R}	128^{R}	0.25	1	2	≥256^{R}	4^{R}	2
JP4169	0.12	4^{R}	0.5	64^{R}	256^{R}	4	32^{R}	64^{R}	2	≥256^{R}	≤0.125	2
JP4174	0.5	4^{R}	0.5	64^{R}	128^{R}	16^{R}	16^{R}	32^{R}	1	≥256^{R}	≤0.125	1
JP4212	0.12	8^{R}	0.5	64^{R}	128^{R}	0.5	32^{R}	64^{R}	1	≥256^{R}	≤0.125	2
JP4234	0.5	8^{R}	0.5	64^{R}	256^{R}	4	32^{R}	128^{R}	1	≥256^{R}	≤0.125	2
JP4238	0.5	4^{R}	0.5	32^{R}	256^{R}	128^{R}	32^{R}	128^{R}	2	≥256^{R}	≤0.125	1
JP4298	0.5	4^{R}	1^{R}	64^{R}	128^{R}	128^{R}	16^{R}	64^{R}	1	≥256^{R}	≤0.125	1
JP4341	0.5	4^{R}	0.5	32^{R}	64^{R}	128^{R}	16^{R}	64^{R}	1	≥256^{R}	≤0.125	1
JP4344	0.5	8^{R}	1^{R}	32^{R}	256^{R}	16^{R}	16^{R}	≥256^{R}	2	≥256^{R}	≤0.125	1
JP4403	0.12	2^{R}	0.5	32^{R}	256^{R}	32^{R}	16^{R}	32^{R}	2	≥256^{R}	≤0.125	2
JP4474	0.5	4^{R}	0.5	32^{R}	128^{R}	128^{R}	16^{R}	64^{R}	2	≥256^{R}	≤0.125	2
JP4499	0.5	4^{R}	0.5	16^{R}	256^{R}	128^{R}	16^{R}	32^{R}	1	≥256^{R}	≤0.125	1
JP4612	2^{R}	4^{R}	2^{R}	64^{R}	64^{R}	≥256^{R}	256	≥256^{R}	1	≥256^{R}	≤0.125	2
JP4808	0.5	8^{R}	0.5	32^{R}	128^{R}	128^{R}	16^{R}	32^{R}	1	≥256^{R}	≤0.125	1
JP4865	0.5	4^{R}	0.5	32^{R}	128^{R}	128^{R}	16^{R}	64^{R}	1	≥256^{R}	≤0.125	2
JP4868	0.5	4^{R}	0.5	32^{R}	256^{R}	128^{R}	16^{R}	64^{R}	2	≥256^{R}	≤0.125	1
JP4887	0.5	4^{R}	0.5	64^{R}	128^{R}	128^{R}	16^{R}	128^{R}	1	≥256^{R}	≤0.125	2
JP4996	0.5	4^{R}	1^{R}	32^{R}	64^{R}	128^{R}	32^{R}	64^{R}	1	≥256^{R}	≤0.125	1
JP5013	0.12	2^{R}	0.25	32^{R}	128^{R}	128^{R}	16^{R}	64^{R}	1	≥256^{R}	≤0.125	1
JP5054	0.5	4^{R}	0.5	64^{R}	256^{R}	128^{R}	16^{R}	32^{R}	1	≥256^{R}	≤0.125	1
JP5068	0.5	4^{R}	0.5	32^{R}	256^{R}	0.5	16^{R}	32^{R}	1	≥256^{R}	≤0.125	1
JP5113	1^{R}	8^{R}	1^{R}	32^{R}	128^{R}	≥256^{R}	16^{R}	32^{R}	1	≥256^{R}	≤0.125	1
JP5222	0.5	4^{R}	0.5	32^{R}	256^{R}	128^{R}	32^{R}	32^{R}	1	≥256^{R}	≤0.125	2
JP5236	0.5	4^{R}	1^{R}	64^{R}	128^{R}	128^{R}	16^{R}	128^{R}	2	≥256^{R}	≤0.125	1
JP5265	0.12	4^{R}	0.5	32^{R}	256^{R}	128^{R}	16^{R}	64^{R}	1	≥256^{R}	≤0.125	2
JP5482	0.12	4^{R}	1^{R}	64^{R}	256^{R}	128^{R}	16^{R}	32^{R}	2	≥256^{R}	≤0.125	1
JP5501	0.5	8^{R}	1^{R}	64^{R}	128^{R}	128^{R}	16^{R}	64^{R}	2	≥256^{R}	≤0.125	1
JP5631	0.5	4^{R}	0.5	16^{R}	128^{R}	128^{R}	16^{R}	64^{R}	2	≥256^{R}	≤0.125	1
JP5732	0.5	8^{R}	0.5	64^{R}	128^{R}	128^{R}	16^{R}	128^{R}	1	≥256^{R}	≤0.125	2
JP5743	0.5	4^{R}	0.5	32^{R}	256^{R}	128^{R}	16^{R}	64^{R}	1	≥256^{R}	≤0.125	2
JP5872	0.5	4^{R}	0.5	32^{R}	256^{R}	128^{R}	32^{R}	32^{R}	2	≥256^{R}	≤0.125	1
JP5965	0.5	4^{R}	0.5	32^{R}	256^{R}	128^{R}	16^{R}	32^{R}	1	≥256^{R}	≤0.125	1
JP6053	0.12	2^{R}	0.5	32^{R}	256^{R}	128^{R}	16^{R}	128^{R}	2	≥256^{R}	≤0.125	2
JP3694	0.12	0.5	0.25	16^{R}	0.25	0.25	0.25	0.5	1	0.5	≤0.125	2
JP3798	0.12	0.5	0.12	32^{R}	0.5	128^{R}	0.25	0.5	2	0.5	≤0.125	0.5
JP4164	0.12	0.5	0.25	16^{R}	0.5	0.5	0.5	≥256^{R}	1	≥256^{R}	≤0.125	0.5
JP4200	0.06	0.5	0.12	32^{R}	0.5	0.25	0.5	≥256^{R}	2	≥256^{R}	≤0.125	1
JP4210	0.12	0.5	0.25	16^{R}	2	0.25	1	≥256^{R}	2	≥256^{R}	≤0.125	1
JP4218	0.06	0.5	0.12	32^{R}	0.5	0.5	0.5	≥256^{R}	1	≥256^{R}	≤0.125	2
JP4389	0.06	0.5	0.12	16^{R}	0.5	0.25	0.25	≥256^{R}	1	≥256^{R}	≤0.125	0.5
JP4697	0.06	0.5	0.12	64^{R}	0.25	0.25	0.25	≥256^{R}	1	≥256^{R}	≤0.125	1
JP5736	0.12	0.25	0.12	16^{R}	0.5	0.25	0.5	1	1	≥256^{R}	≤0.125	1
JP6116	0.12	0.5	0.25	16^{R}	256^{R}	0.5	32^{R}	0.5	1	0.5	≤0.125	1

MIC, minimum inhibitory concentration; ERV, eravacycline; OMC, omadacycline; TGC, tigecycline; TET, tetracycline; CIP, ciprofloxacin; GEN, gentamicin; LVX, levofloxacin; ERY, erythromycin; LNZ, linezolid; OXA, oxacillin; RIF, rifampicin; VAN, vancomycin; Superscript "R" indicates resistance.

TABLE 4 Multi-locus sequence typing and the resistance mechanisms in tetracyclines-resistant and-susceptible *Staphylococcus aureus*.

Isolates	Type	MLST		Resistance mechanisms				
				Mutation of MepRAB efflux pump			Mutation of 30S ribosome protein	
		STs	CCs	*mepR*	*mepA*	*mepB*	*S3*	*S10*
JP3349[a]	R	ST239	CC8	None[c]	None	**Q139***[d]	None	None
JP3936	R	ST5	CC5	None	**L155F**[e], V167I, S332I	**F144fs**[f]	None	**M1L, K3***
JP4041	R	ST5	CC5	None	**E130***	**F144fs**	None	**Y58D**
JP4051	R	ST5	CC5	None	**L155F**, V167I, S332I	**F144fs**	None	K57M
JP4063	R	ST5	CC5	None	**L155F**, V167I, S332I	**F144fs**	None	**Y58D**
JP4091	R	ST5	CC5	None	V167I, S332I,**T411A**	**F144fs**	None	**Y58D**
JP4092	R	ST5	CC5	None	**L155F**, V167I, S332I	**F144fs**	None	K57M
JP4108	R	ST764	CC5	None	V167I, S332I	**F144fs**	None	**Y58D**
JP4113	R	ST764	CC5	None	V167I, S332I	**F144fs**	None	K57M
JP4169	R	ST5	CC5	None	**L155F**, V167I, S332I	**F144fs**	None	K57M
JP4174	R	ST5	CC5	None	**L155F**, V167I, S332I	**F144fs**	None	**Q4K, I6fs**
JP4212	R	ST5	CC5	None	V167I, S332I,**T411A**	**F144fs**	None	**Y58D**
JP4234	R	ST764	CC5	None	V167I, S332I	**F144fs**	None	K57M
JP4238	R	ST5	CC5	None	**E130***	**F144fs**	None	**M1L, K3***
JP4298[b]	R	ST764	CC5	None	None	**F144fs**	None	K57M
JP4341	R	ST5	CC5	None	**E130***	**F144fs**	None	K57M
JP4344[b]	R	ST5	CC5	None	**L155F**, V167I, S332I	**F144fs**	None	K57M
JP4403	R	ST5	CC5	None	**L155F**, V167I, S332I	**F144fs**	None	**Y58D**
JP4474	R	ST5	CC5	None	**E130***	**F144fs**	None	**Y58D**
JP4499	R	ST5	CC5	None	**E130***	**F144fs**	None	K57M
JP4612[a]	R	ST764	CC5	None	**K2Q**, V167I, S332I	**F144fs**	None	K57M
JP4808	R	ST5	CC5	None	V167I, S332I,**T411A**	**F144fs**	None	K57M
JP4865	R	ST5	CC5	None	V167I, S332I,**T411A**	**F144fs**	None	K57M
JP4868	R	ST5	CC5	None	V167I, S332I,**T411A**	**F144fs**	None	K57M
JP4887	R	ST764	CC5	None	V167I, S332I,	**F144fs**	None	K57M
JP4996[b]	R	New1[g]	ND[h]	None	None	**F144fs**	None	K57M
JP5013	R	ST5	CC5	None	**L155F**, V167I, S332I	**F144fs**	None	K57M
JP5054	R	ST764	CC5	None	V167I, S332I	**F144fs**	None	**Y58D**
JP5068	R	ST5	CC5	None	**E130***	**F144fs**	None	K57M
JP5113[a]	R	ST5	CC5	None	**L155F**, V167I, S332I	**F144fs**	None	K57M
JP5222	R	ST5	CC5	None	V167I, S332I,**T411A**	**F144fs**	None	**Y58D**
JP5236[b]	R	ST764	CC5	None	V167I, S332I	**F144fs**	None	K57M
JP5265	R	ST5	CC5	None	V167I, S332I,**T411A**	**F144fs**	None	K57M
JP5482[b]	R	ST5	CC5	None	V167I, S332I,**T411A**	**F144fs**	None	K57M
JP5501[b]	R	ST5	CC5	None	V167I, S332I,**T411A**	**F144fs**	None	K57M
JP5631	R	ST5	CC5	None	V167I, S332I,**T411A**	**F144fs**	None	K57M
JP5732	R	ST764	CC5	None	V167I, S332I	**F144fs**	None	K57M
JP5743	R	ST5	CC5	None	V167I, S332I,**T411A**	**F144fs**	None	K57M
JP5872	R	ST5	CC5	None	V167I, S332I,**T411A**	**F144fs**	None	K57M
JP5965	R	ST5	CC5	None	V167I, S332I,**T411A**	**F144fs**	None	K57M
JP6053	R	ST5	CC5	None	V167I, S332I,**T411A**	**F144fs**	None	K57M
JP3694	S	ST338	CC59	M70I	K93E, T114A, V167I, A307S S332I, A364T	T131R, G133E, K137N	None	K57M
JP3798	S	ST398	CC398	D40G, K74R	V167I, S332I	None	None	None
JP4164	S	ST59	CC59	M70I	V167I, S332I	T131R, G133E, K137N	None	None
JP4200	S	New2	ND	None	V167I, S332I	None	None	None

(Continued)

TABLE 4 (Continued)

Isolates	Type	MLST		Resistance mechanisms				
				Mutation of MepRAB efflux pump			Mutation of 30S ribosome protein	
		STs	CCs	*mepR*	*mepA*	*mepB*	*S3*	*S10*
JP4210	S	ST59	CC59	M70I	K93E, T114A, A307S, A364T	T131R, G133E, K137N	None	None
JP4218	S	New2	ND	None	V167I, S332I	None	None	None
JP4389	S	ST59	CC59	M70I	K93E, T114A, A307S, A364T	T131R, G133E, K137N	None	None
JP4697	S	ST59	CC59	M70I	K93E, T114A, A307S, A364T	T131R, G133E, K137N	None	None
JP5736	S	New3	ND	None	I214V, V167I, S332I, A350D	None	None	None
JP6116	S	ST398	CC398	D40G, K74R	T114A, V167I, S332I, A307S A364T	None	None	None

R, tetracyclines-resistant (eravacycline/omadacycline/tigecycline-resistant) strain; S, tetracyclines-susceptible (eravacycline/omadacycline/tigecycline-susceptible) strain; MLST, multi-locus sequence typing; STs, sequence types; CCs, clonal complexes; [a]means the co-resistant strain of eravacycline, omadacycline and tigecycline; [b]means the co-resistant strain of omadacycline and tigecycline; None[c] means no specific mutation; Q139*[d] means premature stop codon at Gln139; L155F[e] means amino acid substituted at Leu-155; F144fs[f] means frameshift mutation in Phe at 144; New1[g]-New3 means 3 different new ST; ND[h] means not detected. The bold font indicates that the mutation is only present in resistant strains.

TABLE 5 Changes in the MIC of tetracyclines and the information of isolates used in the cloning experiments in this study.

Isolates	MIC (μg/mL)			Description
	ERV	OMC	TGC	
JP3936	0.12	2	0.25	OMC-R and ERV/TGC-S strain, with frameshift mutation of *mepB*
JP4612	2	4	2	Tigecyclines-resistant, with frameshift mutation in *mepB*
JP4200	0.06	0.5	0.12	Tigecyclines-susceptible-S, without frameshift mutation in *mepB*
E. coli ATCC 25922	0.12	1	0.12	Used as a control strain
E. coli DH5α	0.06	0.5	0.12	Used as a host for the PCR product clone
pUCP24/DH5α	0.06	0.5	0.12	*E. coli* DH5α carrying cloning expression vector pUCP24
pUCP24-*mepB*/DH5α-JP3936	0.06	2	0.12	*mepB* of JP3936 was cloned into the expression vector pUCP24 and transformed into *E. coli* DH5 α
pUCP24-*mepB*/DH5α-JP4612	0.06	2	0.12	*mepB* of JP4612 was cloned into the expression vector pUCP24 and transformed into *E. coli* DH5 α
pUCP24-*mepB*/DH5α-JP4200	0.06	0.5	0.12	*mepB* of JP4200 was cloned into the expression vector pUCP24 and transformed into *E. coli* DH5 α

MIC, minimum inhibitory concentrations; ERV, eravacycline; OMC, omadacycline; TGC, tigecycline; OMC-R, omadacycline-resistant; ERV/TGC-S, eravacycline- and tigecycline-susceptible; Tetracyclines-resistant (eravacycline/omadacycline/tigecycline-resistant); Tetracyclines-susceptible (eravacycline/omadacycline/tigecycline-susceptible).

(Q139*), *mepA* (K2Q) + *mepB* (F144fs), and *mepA* (L155F) + *mepB* (F144fs) were detected among three tetracyclines co-resistant strains JP3349, JP4612, and JP5113, respectively. No specific mutations were detected in *mepR* and *S3* genes for tetracyclines-resistant *S. aureus* isolates compared with the tetracyclines-susceptible *S. aureus* isolates.

A frameshift mutation in *mepB* contributed to reduced OMC susceptibility

To verify our hypothesis, *mepB* with and without frameshift mutation was successfully cloned into *E. coli* DH5α. The MIC of tetracyclines against the recombinant strains is shown in Table 5. Compared with negative control strain pUCP24/DH5α, pUCP24-*mepB*/DH5α-JP3936 and pUCP24-*mepB*/DH5α-JP4612 with a frameshift mutation in *mepB* showed increased MIC levels against omadacycline (MIC increased from 0.5–2 μg/ml, 4-fold), but not in pUCP24-*mepB*/DH5α-JP4200 without frameshift mutation in *mepB*. Besides, the MICs of eravacycline and tigecycline did not change compared with that of pUCP24/DH5α among these recombinant strains, regardless of whether the *mepB* they carried underwent frameshift mutation. These data suggested that a frameshift mutation in *mepB* contributed to reduce omadacycline susceptibility.

Efflux pump phenotype assay

The effect of efflux pump inhibitor on the MIC of tetracycline agents was evaluated. As shown in Figure 1 and Supplementary Table S2, among 41 tetracyclines-resistant strains, ten omadacycline-resistant, three eravacycline-resistant and four tigecycline-resistant strains showed positive efflux pump phenotype, including. These results suggested the possible effect of efflux pumps on the occurrence of tetracyclines resistance. Therefore, these strains with a positive efflux pump phenotype were further selected to detect of the expression of efflux pump-encoding genes.

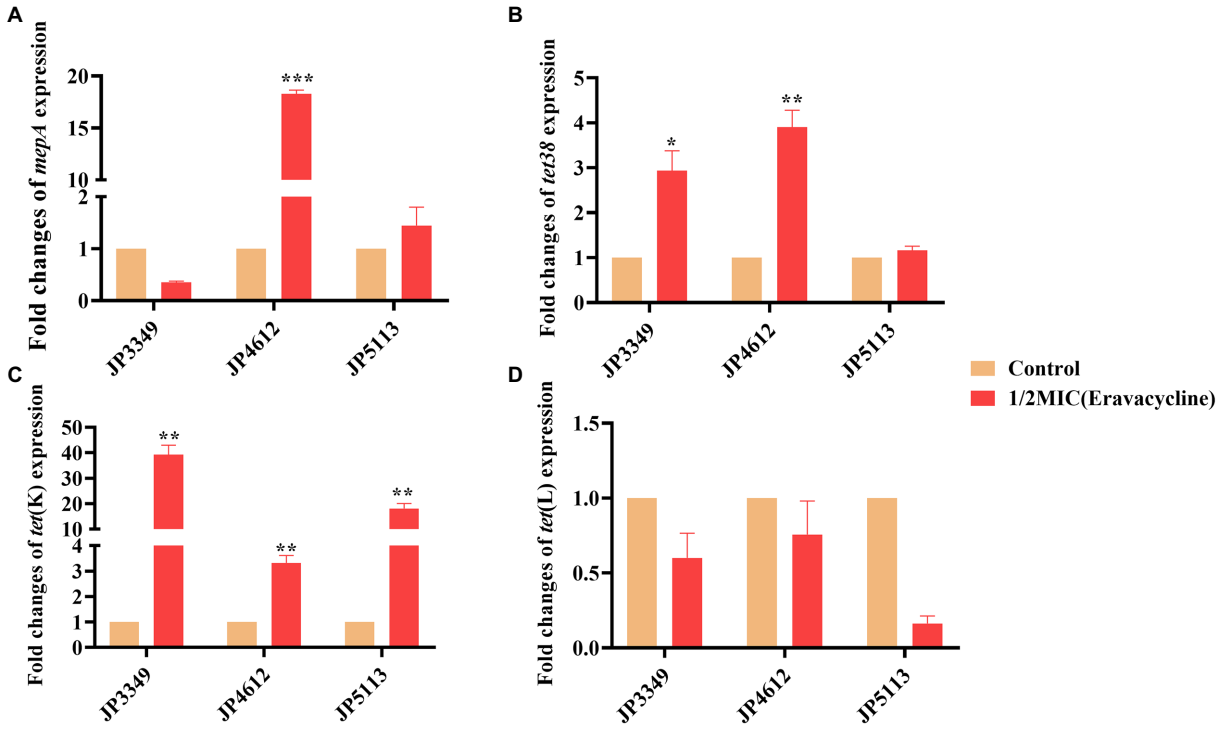

FIGURE 2
Fold changes in the expression of efflux pump-encoding genes in eravacycline-resistant *Staphylococcus aureus* exposed to 1/2×MIC eravacycline concentrations. **(A–D)** The expression levels of *mepA*, *tet38*, *tet*(K), and *tet*(L) genes. The values were normalized based on the internal control gene, *gyrB*. Data from the resistant strain with untreated 1/2×MIC eravacycline were normalized to 1 to allow the comparison of data across different samples. Data represented the mean values from 3 independent experiments with error bars indicating standard deviations, and asterisks denoted the significance of differences in the expression by paired Student's *t*-test (**p<0.01; ***p<0.001).

Expression analysis of efflux pump-encoding genes

The transcriptional levels of the efflux pump-encoding genes *mepA*, *tet38*, *tet*(K), and *tet*(L) were determined in the presence of the tetracycline agents with 1/2×MIC concentrations (Supplementary Table S3). The expression of *mepA*, *tet38*, and *tet*(K) increased significantly in the three eravacycline-resistant strains treated with 1/2×MIC eravacycline than in the control strains (0 MIC; Figure 2). An increased expression of efflux pump-encoding genes was observed in different omadacycline-resistant strains after exposure to 1/2×MIC omadacycline (Figure 3). Furthermore, the expression of *mepA*, *tet38*, *tet*(K), and *tet*(L) was upregulated in the four tigecycline-resistant strains after stimulation with 1/2×MIC tigecycline, (Figure 4). To summarize, different efflux pump genes were upregulated to varying degrees after the resistant strains were exposed to 1/2×MIC tetracycline agents.

Relationship of STs with tetracyclines susceptibility

Totally six STs and three different new STs were found by the MLST analysis in the tested *S. aureus* isolates. The distribution of these STs between the tetracyclines-resistant and-susceptible *S. aureus* was not the same. As shown in Table 4, MLST results showed that one tetracyclines-resistant and three-susceptible strains belonged to the new STs. The phylogenetic tree showed tetracyclines-resistant and-susceptible isolates were divided into two major branches. ST5 (n=30), ST764 (n=9), and ST239 (n=1) were seen in the tetracyclines-resistant isolates, and ST59 (n=4), ST398 (n=2), and ST338 (n=1) were observed in tetracyclines-susceptible isolates (Figure 5; Supplementary Figure S1).

Discussion

Studies have shown that eravacycline, omadacycline, and tigecycline are broad-spectrum antibiotics, which act on several Gram-positive and-negative organisms (Zhanel et al., 2018; Dowzicky and Chmelařová, 2019; Xiao et al., 2020). Consistent with previously published studies (Li et al., 2020; Xiao et al., 2020), an excellent antimicrobial activity of these tetracycline agents was observed against the 1,017 *S. aureus* isolates. In the present study, we compared the antimicrobial effects of them, the results showed that eravacycline and tigecycline, especially eravacycline, had more power antimicrobial effect than omadacycline against tested *S. aureus*. Furthermore, out of the 1,017 *S. aureus*, we successfully

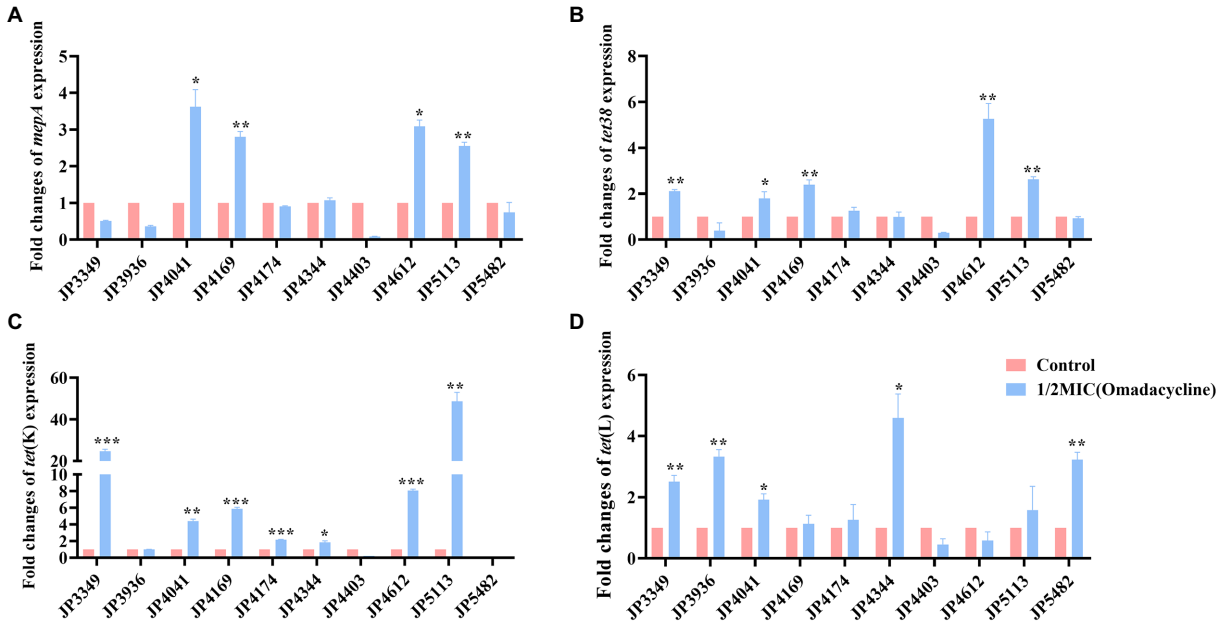

FIGURE 3
Fold changes in the expression of efflux pump-encoding genes in omadacycline-resistant *Staphylococcus aureus* exposed to 1/2×MIC omadacycline concentrations. **(A–D)** The expression levels of *mepA*, *tet38*, *tet*(K), and *tet*(L) genes. The values were normalized based on the internal control gene, *gyrB*. Data from the resistant strain with untreated 1/2×MIC omadacycline were normalized to 1 to allow the comparison of data across different samples. Data represented the mean values from 3 independent experiments with error bars indicating standard deviations, and asterisks denoted the significance of differences in the expression by paired Student's *t*-test (*p<0.05; **p<0.01; ***p<0.001).

screened 41 tetracyclines-resistant isolates. Three tetracyclines co-resistant strains were observed among them, revealing a cross-resistance toward eravacycline, omadacycline, and tigecycline in the clinical *S. aureus* isolates, which was also observed in *Streptococcus agalactiae* (Li et al., 2020; Li G. et al., 2022). Hence, it is important to monitor and detect the resistance of tetracyclines, in order to prevent their cross-resistance leading to treatment failure. We will focus on the cross-resistance mechanism of these new generation tetracycline agents in future studies.

New generation tetracycline agents can overcome the resistance mechanisms of tetracycline and also exhibit antibacterial activity against strains containing tetracycline resistance genes, including *tet*(K), *tet*(L), *tet*(M), *tet*(O), and *tet*(S) (Nguyen et al., 2014; Linkevicius et al., 2016; Zhanel et al., 2018). In this study, eravacycline and tigecycline exhibited great antibacterial activity against clinical *S. aureus* isolates harboring the tetracycline resistance genes. However, eravacycline, omadacycline, or tigecycline were not able to against the isolates (JP3349, JP4612 and JP5113) harboring *tet*(K) + *tet*(L) + *tet*(M). The finding implies that the coexistence of multiple tetracycline resistance genes may be related to the resistance to new generation tetracycline agents in *S. aureus* isolates, which is similar to the findings of Boukthir *et al.* in enterococci (Boukthir et al., 2020). Furthermore, among the 41 tetracyclines-resistant isolates, strains harboring *tet*(K) alone or in combination with other tetracycline resistance genes were predominant. Therefore, the effect of *tet*(K) on tetracyclines susceptibility needs further studied. Consistent with previous studies (Zhang et al., 2018; Bai et al., 2019), *tet*(O) and *tet*(S) were not detected in the tested strains and need further investigation in other *S. aureus* isolates.

The analysis of 41 tetracyclines-resistant isolates showed that the accumulation of several resistance mechanisms resulted in tetracyclines resistance. Accumulating evidence showed that amino acid substitutions at S10 might be associated with reduced tetracyclines susceptibility (Beabout et al., 2015; Bai et al., 2019; Wang et al., 2020). We also detected different mutation sites (such as M1L and Y58D) in S10 in the tetracyclines-resistant isolates. K57M was found in both tetracyclines-resistant and-susceptible strains, suggesting that it was not associated with tetracyclines resistance (Fang et al., 2020). Consistent with the findings of Wang *et al.* (Wang et al., 2020), no mutations were detected in the 30S ribosome protein S3, illustrating that S3 was not the predominant factor contributing to tetracyclines resistance in *S. aureus*.

Another important resistance mechanism is the active efflux pump. The MepRAB efflux pump, a novel MATE family efflux pump, plays a key role in tigecycline resistance in *S. aureus* (McAleese et al., 2005; Fang et al., 2020), however, whether it affects eravacycline and omadacycline resistance is unclear. We first analyzed ta mutation in MepRAB efflux pump-encoding genes. The PCR results showed amino acid substitution mutations and premature termination in *mepA* were found, which might be correlated to tetracyclines resistance. In previous study, *mepR* mutations have already been related to tigecycline resistance in *S. aureus* isolates (Dabul et al., 2018). Conversely, we did not

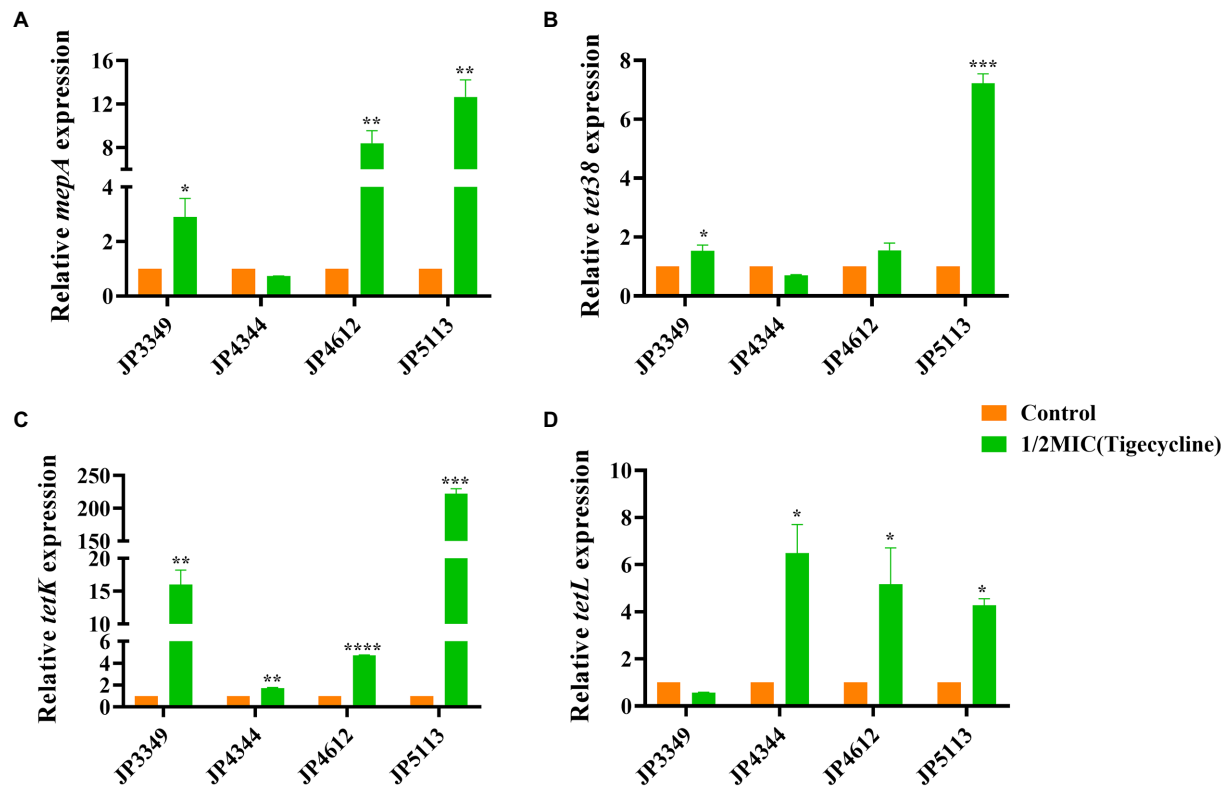

FIGURE 4
Fold changes in the expression of efflux pump-encoding genes in tigecycline-resistant *Staphylococcus aureus* exposed to 1/2×MIC tigecycline concentrations. **(A–D)** The expression levels of *mepA*, *tet38*, *tet*(K), and *tet*(L) genes. The values were normalized based on the internal control gene, *gyrB*. Data from the resistant strain with untreated 1/2×MIC tigecycline were normalized to 1 to allow the comparison of data across different samples. Data represented the mean values from 3 independent experiments with error bars indicating standard deviations, and asterisks denoted the significance of differences in the expression by the paired Student's *t*-test (*p<0.05; **p<0.01; ***p<0.001; ****p<0.0001).

detect mutations in *mepR*, suggesting that it might not affect tetracyclines susceptibility in these tested isolates. Interestingly, the frameshift mutation in *mepB* was observed frequently in tetracyclines-resistant strains but not in tetracyclines-susceptible strains. Cloning experiment further confirmed that a frameshift mutation in *mepB* might contribute to omadacycline resistance in *S. aureus*. MepB has been considered a hypothetical protein with unknown functions until a study by Agah *et al.* revealed that *mepB* played a role in responding to antimicrobials by interacting with nucleic acids (McAleese et al., 2005; Agah et al., 2014). To the best of our knowledge, this is the first study to demonstrate that a frameshift mutation in *mepB* might mediate omadacycline resistance in *S. aureus*. Second, we also comprehensively analyzed the levels of the MepRAB efflux pump in the tetracyclines-resistant strains. We observed that the overexpression of MepRAB efflux pump-encoding genes affected tigecycline, eravacycline and omadacycline resistance.

The isolates were exposure in 1/2 × MIC tetracycline agents to understand the role of different efflux pumps. We found that, different efflux pump-encoding genes, especially *tet*(K), upregulated to varying degrees after the resistant strains were stimulated by 1/2 × MIC tetracyclines, suggesting that the active *tet*(K) efflux pump was primarily responsible for tetracyclines resistance (Bai et al., 2019; Wang et al., 2020). Although previous study showed that tnovel *tet*(L) efflux pump variants affected the susceptibility of eravacycline and tigecycline (Wang et al., 2021), Wang *et al.* and the present study showed that the *tet*(L) overexpression might not confer resistance to eravacycline (Wang et al., 2020), however, it might confer resistance to omadacycline and tigecycline in *S. aureus*. Besides conferring resistance to tetracycline (Chen and Hooper, 2018), our study revealed that the active *tet38* efflux pump might be associated with resistance to eravacycline, tigecycline and omadacycline.

The MLST analyses showed that the most tetracyclines-resistant *S. aureus* belonged to ST5, a globally disseminated and highly pathogenic lineage (Hau et al., 2018), and ST764, a variant of the ST5 lineage.

Combined with drug sensitivity, we found that the ST5 and ST764 clonotype isolates were MDR strains. Previous studies have reported that ST5 and ST764 MRSA strains were hypervirulent and MDR, and dominated *S. aureus* infections in China (Takano et al., 2013; Jian et al., 2021). For the first time, our findings revealed that ST5 and its variant ST764 dominated

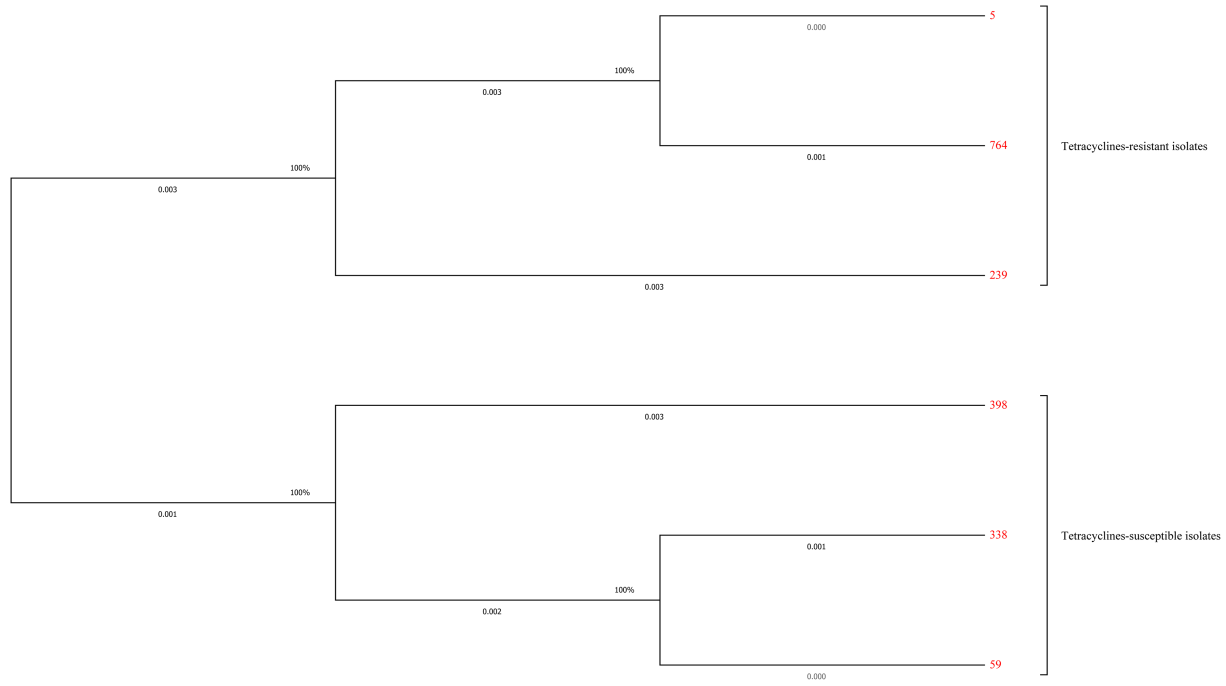

FIGURE 5
Maximum-likelihood trees of 41 tetracyclines-resistant and 10 tetracyclines-susceptible *Staphylococcus aureus* isolates based on the concatenated sequences of MLST. Tetracyclines-resistant and-susceptible isolates were divided into two major branches. ST5 (*n*=30), ST764 (*n*=9), and ST239 (*n*=1) were seen in the tetracyclines-resistant isolates, and ST59 (*n*=4), ST398 (*n*=2), and ST338 (*n*=1) were observed in tetracyclines-susceptible isolates.

tetracyclines-resistant *S. aureus* strains, suggesting that tetracyclines-resistant *S. aureus* strains might pose a serious clinical threat hence more attention should be paid to their prevention and control.

However, our work also has some limitations. Tetracyclines-resistant *S. aureus* strains were only collected from the same hospital, which might lead to deviation in our results. It is necessary to use other pathogen to verify our findings, as the efficacy and resistance mechanisms of tetracyclines and distribution of ST type might be different in different hospital. Besides, the cross-resistance mechanism of these new generation tetracyclines was not illustrated in this work. Thus, the resistance and cross-resistance mechanisms of these new generation tetracyclines should be further investigated.

Conclusion

To conclude, eravacycline and tigecycline showed more excellent antibacterial activity against *S. aureus*, including tetracycline-resistant isolates, than omadacycline did. Tetracyclines resistance resulted from an accumulation of several resistance mechanisms. The coexistence of multiple tetracycline resistance genes may contribute to the emergence of tetracyclines resistance. Moreover, mutations in *mepA* and *S10* might play crucial role in tetracyclines resistance. Importantly, we reported that frameshift mutations in *mepB* contributed to reduced omadacycline susceptibility. Furthermore, *mepA*, *tet38*, *tet*(K) and *tet*(L) overexpression reduced tetracyclines susceptibility. Moreover, a major clonal dissemination type, ST5, and its variant ST764 were determined in most tetracycline-resistant strains, suggesting that these strains might possess the risk of clonal transmission and require further investigation.

Data availability statement

The original contributions presented in the study are included in the article/Supplementary material, further inquiries can be directed to the corresponding authors.

Author contributions

WZ participated in the design of the study, carried out the experiments, analyzed the data, and drafted the manuscript. XZ, YL, and YZ participated in experiments and data analyses. MX and SW provided the analysis of the results. YS participated in analysis and discussions. LC and TZ designed the study, participated in data analyses, and provided critical revisions of the manuscript. All authors contributed to the revision of the manuscript and approved the final version for submission.

Conflict of interest

The authors declare that the research was conducted in the absence of any commercial or financial relationships that could be construed as a potential conflict of interest.

Publisher's note

All claims expressed in this article are solely those of the authors and do not necessarily represent those of their affiliated organizations, or those of the publisher, the editors and the reviewers. Any product that may be evaluated in this article, or claim that may be made by its manufacturer, is not guaranteed or endorsed by the publisher.

Supplementary material

The Supplementary material for this article can be found online at: https://www.frontiersin.org/articles/10.3389/fmicb.2022.1043736/full#supplementary-material

References

Agah, S., Poulos, S., Banchs, C., and Faham, S. (2014). Structural characterization of MepB from *Staphylococcus aureus* reveals homology to endonucleases. *Protein Sci.* 23, 594–602. doi: 10.1002/pro.2438

Bai, B., Lin, Z., Pu, Z., Xu, G., Zhang, F., Chen, Z., et al. (2019). In vitro activity and Heteroresistance of omadacycline against clinical *Staphylococcus aureus* isolates from China reveal the impact of omadacycline susceptibility by branched-chain amino acid transport system II carrier protein, Na/pi cotransporter family protein, and fibronectin-binding protein. *Front. Microbiol.* 10:2546. doi: 10.3389/fmicb.2019.02546

Beabout, K., Hammerstrom, T. G., Perez, A. M., Magalhães, B. F., Prater, A. G., Clements, T. P., et al. (2015). The ribosomal S10 protein is a general target for decreased tigecycline susceptibility. *Antimicrob. Agents Chemother.* 59, 5561–5566. doi: 10.1128/aac.00547-15

Boukthir, S., Dejoies, L., Zouari, A., Collet, A., Potrel, S., Auger, G., et al. (2020). In vitro activity of eravacycline and mechanisms of resistance in enterococci. *Int. J. Antimicrob. Agents* 56:106215. doi: 10.1016/j.ijantimicag.2020.106215

Chen, C., and Hooper, D. C. (2018). Effect of *Staphylococcus aureus* Tet38 native efflux pump on in vivo response to tetracycline in a murine subcutaneous abscess model. *J. Antimicrob. Chemother.* 73, 720–723. doi: 10.1093/jac/dkx432

Cheng, C., Ying, Y., Zhou, D., Zhu, L., Lu, J., Li, A., et al. (2020). RamA, a transcriptional regulator conferring florfenicol resistance in Leclercia adecarboxylata R25. *Folia Microbiol. (Praha)* 65, 1051–1060. doi: 10.1007/s12223-020-00816-2

CLSI (2022). *Performance Standards for Antimicrobial Susceptibility Testing. 32nd Edn.* CLSI, M100. https://clsi.org/

Dabul, A. N. G., Avaca-Crusca, J. S., Van Tyne, D., Gilmore, M. S., and Camargo, I. (2018). Resistance in in vitro selected tigecycline-resistant methicillin-resistant *Staphylococcus aureus* sequence type 5 is driven by mutations in mep R and mepA genes. *Microb. Drug Resist.* 24, 519–526. doi: 10.1089/mdr.2017.0279

Doan, T. L., Fung, H. B., Mehta, D., and Riska, P. F. (2006). Tigecycline: a glycylcycline antimicrobial agent. *Clin. Ther.* 28, 1079–1106. doi: 10.1016/j.clinthera.2006.08.011

Dowzicky, M. J., and Chmelařová, E. (2019). Antimicrobial susceptibility of gram-negative and gram-positive bacteria collected from eastern Europe: results from the tigecycline evaluation and surveillance trial (T.E.S.T.), 2011-2016. *J. Glob. Antimicrob. Resist.* 17, 44–52. doi: 10.1016/j.jgar.2018.11.007

Fang, R., Sun, Y., Dai, W., Zheng, X., Tian, X., Zhang, X., et al. (2020). Mutations in the MepRAB efflux system contribute to the in vitro development of tigecycline resistance in *Staphylococcus aureus*. *J. Glob. Antimicrob. Resist.* 22, 631–636. doi: 10.1016/j.jgar.2020.06.005

FDA Antibacterial Susceptibility Test Interpretive Criteria (2020). Available at: https://www.fda.gov/

Fiedler, S., Bender, J. K., Klare, I., Halbedel, S., Grohmann, E., Szewzyk, U., et al. (2016). Tigecycline resistance in clinical isolates of enterococcus faecium is mediated by an upregulation of plasmid-encoded tetracycline determinants tet(L) and tet(M). *J. Antimicrob. Chemother.* 71, 871–881. doi: 10.1093/jac/dkv420

Gasch, O., Camoez, M., Domínguez, M. A., Padilla, B., Pintado, V., Almirante, B., et al. (2014). Emergence of resistance to daptomycin in a cohort of patients with methicillin-resistant *Staphylococcus aureus* persistent bacteraemia treated with daptomycin. *J. Antimicrob. Chemother.* 69, 568–571. doi: 10.1093/jac/dkt396

Grossman, T. H. (2016). Tetracycline antibiotics and resistance. *Cold Spring Harb. Perspect. Med.* 6:a025387. doi: 10.1101/cshperspect.a025387

Guimaraes, A. O., Cao, Y., Hong, K., Mayba, O., Peck, M. C., Gutierrez, J., et al. (2019). A prognostic model of persistent bacteremia and mortality in complicated *Staphylococcus aureus* bloodstream infection. *Clin. Infect. Dis.* 68, 1502–1511. doi: 10.1093/cid/ciy739

Hau, S. J., Allué-Guardia, A., Rusconi, B., Haan, J. S., Davies, P. R., Frana, T. S., et al. (2018). Single nucleotide polymorphism analysis indicates genetic distinction and reduced diversity of swine-associated methicillin resistant *Staphylococcus aureus* (MRSA) ST5 isolates compared to clinical MRSA ST5 isolates. *Front. Microbiol.* 9:2078. doi: 10.3389/fmicb.2018.02078

Jian, Y., Zhao, L., Zhao, N., Lv, H. Y., Liu, Y., He, L., et al. (2021). Increasing prevalence of hypervirulent ST5 methicillin susceptible *Staphylococcus aureus* subtype poses a serious clinical threat. *Emerg. Microbes. Infect.* 10, 109–122. doi: 10.1080/22221751.2020.1868950

Li, G., Wei, Y., Guo, Y., Gong, H., Lian, J., Xu, G., et al. (2022). Omadacycline efficacy against *Streptococcus agalactiae* isolated in China: correlation between resistance and virulence gene and Biofilm formation. *Comput. Intell. Neurosci.* 2022, 7636983–7636988. doi: 10.1155/2022/7636983

Li, P., Wei, Y., Li, G., Cheng, H., Xu, Z., Yu, Z., et al. (2020). Comparison of antimicrobial efficacy of eravacycline and tigecycline against clinical isolates of *Streptococcus agalactiae* in China: in vitro activity, heteroresistance, and cross-resistance. *Microb. Pathog.* 149:104502. doi: 10.1016/j.micpath.2020.104502

Li, T., Yang, Y., Yan, R., Lan, P., Liu, H., Fu, Y., et al. (2022). Comparing core-genome MLST with PFGE and MLST for cluster analysis of carbapenem-resistant *Acinetobacter baumannii*. *J. Glob. Antimicrob. Resist.* 30, 148–151. doi: 10.1016/j.jgar.2022.06.014

Linkevicius, M., Sandegren, L., and Andersson, D. I. (2016). Potential of tetracycline resistance proteins to evolve tigecycline resistance. *Antimicrob. Agents Chemother.* 60, 789–796. doi: 10.1128/aac.02465-15

Maiden, M. C., Bygraves, J. A., Feil, E., Morelli, G., Russell, J. E., Urwin, R., et al. (1998). Multilocus sequence typing: a portable approach to the identification of clones within populations of pathogenic microorganisms. *Proc. Natl. Acad. Sci. U. S. A.* 95, 3140–3145. doi: 10.1073/pnas.95.6.3140

McAleese, F., Petersen, P., Ruzin, A., Dunman, P. M., Murphy, E., Projan, S. J., et al. (2005). A novel MATE family efflux pump contributes to the reduced susceptibility of laboratory-derived *Staphylococcus aureus* mutants to tigecycline. *Antimicrob. Agents Chemother.* 49, 1865–1871. doi: 10.1128/aac.49.5.1865-1871.2005

McGuinness, W. A., Malachowa, N., and DeLeo, F. R. (2017). Vancomycin resistance in *Staphylococcus aureus*. *Yale J. Biol. Med.* 90, 269–281.

Morrissey, I., Hawser, S., Lob, S. H., Karlowsky, J. A., Bassetti, M., Corey, G. R., et al. (2020). In vitro activity of eravacycline against gram-positive bacteria isolated in clinical laboratories worldwide from 2013 to 2017. *Antimicrob. Agents Chemother.* 64:e01715-15. doi: 10.1128/aac.01715-19

Nguyen, F., Starosta, A. L., Arenz, S., Sohmen, D., Dönhöfer, A., and Wilson, D. N. (2014). Tetracycline antibiotics and resistance mechanisms. *Biol. Chem.* 395, 559–575. doi: 10.1515/hsz-2013-0292

Noskin, G. A. (2005). Tigecycline: a new glycylcycline for treatment of serious infections. *Clin. Infect. Dis.* 41, S303–S314. doi: 10.1086/431672

Pérez-Montarelo, D., Viedma, E., Larrosa, N., Gómez-González, C., Ruiz de Gopegui, E., Muñoz-Gallego, I., et al. (2018). Molecular epidemiology of *Staphylococcus aureus* bacteremia: association of molecular factors with the source of infection. *Front. Microbiol.* 9:2210. doi: 10.3389/fmicb.2018.02210

Roberts, M. C. (2003). Tetracycline therapy: update. *Clin. Infect. Dis.* 36, 462–467. doi: 10.1086/367622

Roberts, M. C. (2005). Update on acquired tetracycline resistance genes. *FEMS Microbiol. Lett.* 245, 195–203. doi: 10.1016/j.femsle.2005.02.034

Serral, F., Castello, F. A., Sosa, E. J., Pardo, A. M., Palumbo, M. C., Modenutti, C., et al. (2021). From genome to drugs: new approaches in antimicrobial discovery. *Front. Pharmacol.* 12:647060. doi: 10.3389/fphar.2021.647060

Solomkin, J. S., Sway, A., Lawrence, K., Olesky, M., Izmailyan, S., and Tsai, L. (2019). Eravacycline: a new treatment option for complicated intra-abdominal infections in the age of multidrug resistance. *Future Microbiol.* 14, 1293–1308. doi: 10.2217/fmb-2019-0135

Takano, T., Hung, W. C., Shibuya, M., Higuchi, W., Iwao, Y., Nishiyama, A., et al. (2013). A new local variant (ST764) of the globally disseminated ST5 lineage of hospital-associated methicillin-resistant *Staphylococcus aureus* (MRSA) carrying the virulence determinants of community-associated MRSA. *Antimicrob. Agents Chemother.* 57, 1589–1595. doi: 10.1128/aac.01147-12

Truong-Bolduc, Q. C., Bolduc, G. R., Medeiros, H., Vyas, J. M., Wang, Y., and Hooper, D. C. (2015). Role of the Tet38 efflux pump in *Staphylococcus aureus* internalization and survival in epithelial cells. *Infect. Immun.* 83, 4362–4372. doi: 10.1128/iai.00723-15

Wang, N., Li, D., Schwarz, S., Qin, S., Yao, H., and Du, X. D. (2021). Novel Tet (L) efflux pump variants conferring resistance to tigecycline and eravacycline in *Staphylococcus* Spp. *Microbiol. Spectr.* 9:e0131021. doi: 10.1128/Spectrum.01310-21

Wang, Z., Lin, Z., Bai, B., Xu, G., Li, P., Yu, Z., et al. (2020). Eravacycline susceptibility was impacted by genetic mutation of 30S ribosome subunits, and branched-chain amino acid transport system II carrier protein, Na/pi cotransporter family protein in *Staphylococcus aureus*. *BMC Microbiol.* 20:189. doi: 10.1186/s12866-020-01869-6

Xiao, M., Huang, J. J., Zhang, G., Yang, W. H., Kong, F., Kudinha, T., et al. (2020). Antimicrobial activity of omadacycline in vitro against bacteria isolated from 2014 to 2017 in China, a multi-center study. *BMC Microbiol.* 20:350. doi: 10.1186/s12866-020-02019-8

Xu, W., Chen, T., Wang, H., Zeng, W., Wu, Q., Yu, K., et al. (2020). Molecular mechanisms and epidemiology of Fosfomycin resistance in *Staphylococcus aureus* isolated from patients at a teaching hospital in China. *Front. Microbiol.* 11:1290. doi: 10.3389/fmicb.2020.01290

Zhanel, G. G., Baxter, M. R., Adam, H. J., Sutcliffe, J., and Karlowsky, J. A. (2018). In vitro activity of eravacycline against 2213 gram-negative and 2424 gram-positive bacterial pathogens isolated in Canadian hospital laboratories: CANWARD surveillance study 2014-2015. *Diagn. Microbiol. Infect. Dis.* 91, 55–62. doi: 10.1016/j.diagmicrobio.2017.12.013

Zhanel, G. G., Cheung, D., Adam, H., Zelenitsky, S., Golden, A., Schweizer, F., et al. (2016). Review of eravacycline, a novel fluorocycline antibacterial agent. *Drugs* 76, 567–588. doi: 10.1007/s40265-016-0545-8

Zhanel, G. G., Esquivel, J., Zelenitsky, S., Lawrence, C. K., Adam, H. J., Golden, A., et al. (2020). Omadacycline: a novel oral and intravenous aminomethylcycline antibiotic agent. *Drugs* 80, 285–313. doi: 10.1007/s40265-020-01257-4

Zhang, F., Bai, B., Xu, G. J., Lin, Z. W., Li, G. Q., Chen, Z., et al. (2018). Eravacycline activity against clinical *S. aureus* isolates from China: in vitro activity, MLST profiles and heteroresistance. *BMC Microbiol.* 18:211. doi: 10.1186/s12866-018-1349-7

Zhao, C., Wang, X., Zhang, Y., Wang, R., Wang, Q., Li, H., et al. (2019). In vitro activities of eravacycline against 336 isolates collected from 2012 to 2016 from 11 teaching hospitals in China. *BMC Infect. Dis.* 19:508. doi: 10.1186/s12879-019-4093-1

Zhu, Y., Wang, C., Schwarz, S., Liu, W., Yang, Q., Luan, T., et al. (2021). Identification of a novel tetracycline resistance gene, tet(63), located on a multiresistance plasmid from *Staphylococcus aureus*. *J. Antimicrob. Chemother.* 76, 576–581. doi: 10.1093/jac/dkaa485

Frontiers in Microbiology

Explores the habitable world and the potential of microbial life

The largest and most cited microbiology journal which advances our understanding of the role microbes play in addressing global challenges such as healthcare, food security, and climate change.

Discover the latest Research Topics

See more →

Frontiers

Avenue du Tribunal-Fédéral 34
1005 Lausanne, Switzerland
frontiersin.org

Contact us

+41 (0)21 510 17 00
frontiersin.org/about/contact